University of Southampton

Faculty of Medicine

Clinical and Experimental Sciences

Natural Killer Cell Responses to Influenza A Virus in the Human Lung

by

Grace Elizabeth Cooper

Thesis for the degree of Doctor of Philosophy

December 2018

University of Southampton

Abstract

Faculty of Medicine

Clinical and Experimental Sciences

Thesis for the degree of Doctor of Philosophy

Natural Killer Cell Responses to Influenza A Virus in the Human Lung

by

Grace Elizabeth Cooper

Influenza infection is a major contributor to global mortality and morbidity, with high potential for pandemic and vaccine evasion. Natural Killer (NK) cells are innate anti-viral effector cells but their functions in respiratory influenza infection are poorly understood. NK cells have been implicated in the control of influenza in mouse models but their regulation in the human respiratory environment is still an area of study. For instance, phenotypically and functionally unique resident NK cell populations have been described in the liver and uterus, but have not yet been explored in the human lung.

The aim of this thesis was to investigate the human lung NK cell phenotype and function during respiratory infection and disease, primarily focusing on influenza infection. To do this, NK cells were characterized from macroscopically normal human lung tissue by multi-parameter cytometry and NK cell function characterized in an *ex vivo* tissue explant model of influenza infection. NK cell function was further characterized by autologous co-culture of peripheral NK cells with influenza-infected monocyte-derived macrophages (MDMs) and primary bronchial epithelial cells (PBECS). Cytotoxic and cytokine responses of NK cells were measured by a combination of flow cytometry and enzyme-linked immunosorbent assay (ELISA). Mechanisms of NK cell activation to IAV-infected macrophages were further explored including activating and inhibitory contact with infected cells and cytokine release.

Both lung and peripheral NK cells were found to mediate strong anti-viral responses to influenza infection; with increased IFN-γ, Gzm-B and measures of degranulation. Furthermore, mechanistic studies demonstrated that physical contact between NK cells and influenza-infected MDMs was essential to NK cell activation, despite a strongly pro-inflammatory environment. However, NKp46 and NKG2D ligands were redundant in stimulating NK cell activation towards infected MDMs, demonstrating complicated and extensive regulation of NK cells activation by infected macrophages. The majority of human lung NK share a phenotype with circulating NK cells, however, this thesis identified novel lung resident NK cell populations. Lung resident (CD49a+) NK cells were found to respond more potently to influenza infection than non-resident (CD49a-) NK cells. This suggests that resident, trained NK cell populations are present in the human lung and may provide early and important control of viral infection. CD49a+ lung NK cells were also increased in donors with more severe COPD, indicating possible modulation of lung resident NK cells in chronic disease.

Overall this thesis presents evidence that NK cells play an important role during human influenza infection through both cytotoxicity and IFN-γ production in the human lung. This work has also highlighted the differences between lung resident and non-resident NK cells in terms of phenotype and function, which may have important implications for understanding mucosal immunity in the lung.

Table of Contents

Table of Tables

Table of Tables

Table of Figures

Table of Figures

Research Thesis: Declaration of Authorship

Print name:	GRACE ELIZABETH COOPER

Title of thesis:	Natural Killer Cell Responses to Influenza A Virus in the Human Lung

I declare that this thesis and the work presented in it are my own and has been generated by me as the result of my own original research.

I confirm that:

1. This work was done wholly or mainly while in candidature for a research degree at this University;
2. Where any part of this thesis has previously been submitted for a degree or any other qualification at this University or any other institution, this has been clearly stated;
3. Where I have consulted the published work of others, this is always clearly attributed;
4. Where I have quoted from the work of others, the source is always given. With the exception of such quotations, this thesis is entirely my own work;
5. I have acknowledged all main sources of help;
6. Where the thesis is based on work done by myself jointly with others, I have made clear exactly what was done by others and what I have contributed myself;
7. Parts of this work have been published as:

Cooper GE, Ostridge K, Khakoo SI, Wilkinson TMA, and Staples KJ, 2018. Human CD49a+ Lung Natural Killer Cell Cytotoxicity in Response to Influenza A Virus. *Front Immunol*. Vol. 9

Signature:		Date:	

Acknowledgements

I'd firstly like to thank my supervisors Dr Karl Staples, Prof Tom Wilkinson and Prof Salim Khakoo for their advice and guidance during the course of my PhD. I also need to thank all members of both the Pulmonary Immunity and NK cell labs who were a constant source of support and scientific knowledge. In particular, I must thank Josh Wallington for the late night banter and trips to M&S, Jodie Ackland for her continuous enthusiasm and support and Joanne Kelly for intense NK cell-based chats. Thanks must also go to Dr Richard Jewell and Carolann McGuire who provided fantastic flow cytometry support. Thanks go to Theresa Hydes for her assistance with flow panels and Pauline Rettman for NK cell advice. Mirella Spalluto was also a fantastic source for all things epithelia and I thank her for her technical advice.

Considerable acknowledgments must go to all the phlebotomists contributed to this study and a special thanks to Ben Johnson, and Carine Fixmer for providing lung tissue throughout the study. Thanks must also go to the surgeons, clinical staff and the rest of the Target Lung team for coordinating lung tissue acquisition and pathological assessment. I'm incredibly grateful to all of the people who donated lung tissue and blood, without whom my research would not have been possible.

Lastly, I'd like to thank my family, including my parents and brothers for their support in all my endeavours. Most of all I must thank Ryan Wood for his contribution to the proof-reading of this thesis and for providing welcome relief during the pressures of a PhD.

Definitions and Abbreviations

ADCC	Antibody Dependent Cellular Cytotoxicity
APC	Antigen Presenting Cell
APC	Allophycocyanin
BAL	Broncho-Alveolar Lavage
BSA	Bovine Serum Albumin
BV	Brilliant Violet
CCL	Chemokine C-C Motif Ligand
CCR	C-C Chemokine Receptor
CD	Classification Determinant
CMV	Cytomegalovirus
cNK	circulating Natural Killer cell
COPD	Chronic Obstructive Pulmonary Disease
CR-PB	Cancer Resection Donor– Peripheral Blood
CTL	Cytotoxic T Lymphocyte
CXCL	Chemokine C-X-C Motif Ligand
CXCR	C-X-C Chemokine receptor
Cy	Cyanine 7
Cy5.5	Cyanine 5.5
DC	Dendritic Cell
DP	Double Positive
Dpi	Days post infection
E:T	Effector cell : Target Cell ratio
ELISA	Enzyme Linked Immunosorbent Assay

EOMES	Eomesodermin
FACS	Fluorescence-Activated Cell Sorting
FAS	FS-7 Associated Surface Antigen
FEV1%	Forced expiratory volume in one second
FITC	Fluorescein isothiocyanate
FSC	Forward Scatter
FVC	Forced vital capacity
GM-CSF	Granulocyte-Macrophage Colony Stimulating Factor
GOLD	Global Initiative for Chronic Obstructive Lung Disease
Gzm-B	Granzyme -B
HA	Hemagglutinin
HCV	Hepatitis C Virus
HIV	Human Immunodeficiency Virus
HLA	Human Leukocyte Antigens
H-PB	Healthy Donor – Peripheral Blood
HSV	Herpes Simplex Virus
IAV	Influenza A Virus
ICS	Inhaled corticosteroids
IFN	Interferon
Ig	Immunoglobulin
IL	Interleukin
ILC	Innate Lymphoid Cell
IQR	Interquartile Range
ISG	Interferon Stimulated Gene

KIR	Killer cell Immunoglobulin-like Receptor
LDH	Lactate Dehydrogenase
LIF	Leukemia Inhibitory Factor
MDMs	Monocyte-derived Macrophages
MHC I	Major Histocompatibility Complex class I
MIC-A/B	Major Histocompatibility Complex class I chain-related protein A and B
MMP1	Matrix Metalloproteinase 1
Ms	Mouse
NA	Neuraminidase
NCAM	Neural Cell Adhesion Molecule
NCR	Natural Cytotoxicity Receptor
NF-κB	Nuclear Factor - κB
NK	Natural Killer
NP-1	Nucleoprotein-1
NT	Not Treated
PAMP	Pathogen-Associated Molecular Patter
PBEC	Primary Bronchial Epithelial Cell
PBMC	Peripheral Blood Mononuclear Cell
PBS	Dulbecco's Phosphate Buffered Saline
PE	Phycoerythrin
PerCP	Peridinin-chlorophyll protein
PFU	Plaque Forming Units
PMA/I	Phorbol-Myristate-Acetate and Ionomycin
PRR	Pattern Recognition Receptor

Definitions and Abbreviations

REC	Research Ethics Committee
RIG-I	Retinoic acid Inducible Gene - I
rNK	resident Natural Killer cell
RPMI	Roswell Park Memorial Institute
RSV	Respiratory syncytial virus
RT	Room Temperature
RV	Rhinovirus
S1P1	Sphingosine 1-Phosphate Receptor
SIGLEC-7	Sialic acid-binding Ig-like lectin 7
sMFI	specific Mean Fluorescence Intensity
SP	Single Positive
SSC	Side Scatter
ssRNA	single-stranded Ribonucleic Acid
TLR	Toll-like Receptor
TN	Triple Negative
TNF	Tumor Necrosis Factor
TP	Triple Positive
TRAIL	Tumor Necrosis Factor-Related Apoptosis-Inducing Ligand
Trm	Resident Memory T cells
t-SNE	t-Distributed Stochastic Neighbor Embedding
TW	Transwell
ULBP	UL16 Binding Protein
UV-X31	UV-irradiated X31
vRNA	viral RNA

Chapter 1 Introduction

1.1 Influenza Virus

1.1.1 Influenza – Global Perspective and Impacts

Each year 20% of the world's population is infected with influenza virus, resulting in 3-5 million cases of severe illness and 250-500 000 deaths worldwide [1]. Temperate climates experience seasonal epidemics during winter months, whereas outbreaks occur more irregularly in tropical regions [1]. Influenza infection causes acute viral syndrome characterised by fever, chills, sore throat, runny nose, cough, myalgia and fatigue [1]. The infection is typically self-resolving after 1-2 weeks in healthy adults but in the young, elderly and those with underlying medical conditions, life-threatening complications can occur [2-5]. Opportunistic bacteria (classically *Streptococcus* species) are thought to take advantage of the impaired immunity and respiratory tract damage caused by influenza infection [2, 6-13]. Thus influenza-related mortality is often attributed to secondary bacterial infections rather than the virus itself [2, 6-13].

The rapid viral transmission, severe illness and high mortality in at-risk groups make seasonal influenza a serious public health problem [1, 14]. Furthermore, viral reassortment and inter-species transmission results in the frequent emergence of new influenza strains and semi-regular human pandemics, such as in 1968, 1957 and most recently in 2009 [15-17]. In 1918 a particularly devastating emergent H1N1 strain killed an estimated 40 million people and the potential for another influenza pandemic of this magnitude is an international concern [15-17]. Lastly, influenza infection exacerbates symptoms of chronic obstructive pulmonary disease (COPD) and is associated with deterioration in lung function in this group [4, 18-21].

1.1.2 Influenza Virus Structure

Influenza virus belongs to the Orthomyxoviridae family and is a small (50-120 nm) enveloped single strand ribonucleic acid (ssRNA) virus [22]. There are four subtypes of this virus, Influenza A, B, C and D which are distinguished by their surface proteins [22]. Only influenza A and B cause human disease, with Influenza A Virus (IAV) the most pathogenic and most commonly associated with viral pandemics [22].

The IAV genome is made up of 8 segments of viral RNA (vRNA) which encodes 9 structural proteins and up to 9 non-structural (NS) proteins, depending on the viral strain [23]. vRNA is packaged inside the influenza virion in complex with nucleoprotein (NP) and polymerase subunits PB1, PB2 and PA [23]. This riboprotein complex is held to the inner surface of the virion by a ring of M1 protein [23]. The outer surface of the virion consists of a lipid membrane containing hemagglutinin (HA), neuraminidase (NA) and M2 proteins [22, 23]. HA is a sialic-acid (N-acetyl-neuraminic acid) binding molecule facilitating viral entry and cellular tropism [24, 25]. Whereas NA cleaves HA-sialic acid linkages, allowing the release of new viral particles from the infected cell [26]. Both HA and NA are highly mutable as they are commonly recognised by the human immune system [27, 28]. These viral proteins undergo both antigenic drift and shift due to the strong selection pressures imposed by host immunity [27, 28]. A phenomenon that has allowed the classification of IAV strains based on the combination of highly variable HA and NA alleles [22, 29, 30].

1.1.3 IAV Replication in the Respiratory Tract

IAV infection is spread through person-to-person transmission of airborne droplets and contaminated surfaces [1]. Once inside the respiratory tract, influenza infects airway epithelial cells and macrophages, co-opting cellular machinery in order to replicate [23]. Influenza primarily enters cells through ligation of viral HA protein with α2-3 and α2-6 linked sialic acid residues on the cell surface [24, 25]. Once bound, influenza is taken up by cells through either clathrin or non-clathrin mediated endocytosis and then enters the endosomal pathway [31-33]. In late endosomes the M2 ion channel allows entry of protons into the viral particles, increasing the acidity within the virion [34, 35]. This drop in pH causes structural change to HA proteins, allowing the fusion of endosomal and virion membranes and release of vRNA into the cytosol [34-37]. vRNA travels to the nucleus, where thousands of new copies are transcribed [38-40]. Translation of vRNA and protein trafficking by the host cell then results in the accumulation of viral protein at the cell membranes [41, 42]. Once this has taken place vRNA is packaged into new virions, which have been found to bud from cell surfaces as early as 6 h after infection [43].

A secondary mechanism of IAV uptake exists in macrophages as the virus can also be bound by the macrophage mannose receptor (Classification Determinant-206; CD206) and macrophage galactose-C type lectin (CD301) receptor [44]. However, there is controversy surrounding the fate of virus entering macrophages this way, as this may represent a mechanism of macrophage phagocytosis [44, 45]. Numerous strains of IAV have been shown to enter macrophages, but all

appear to undergo abortive replication (with the exception of the most pathogenic H5 strains) [46-53]. In the airway macrophage dysfunctional viral protein trafficking and virion assembly may restrict IAV replication [45]. This abortive IAV replication may lead to macrophage apoptosis, potentially facilitating viral control [54].

1.1.4 Anti-Viral Drugs and Influenza Vaccination Strategies

In recent years a number of anti-viral drugs have been developed to target the function of influenza proteins, including NA inhibitors (oseltamivir and zanamivir) and M2 inhibitors (the adamantanes; adamantadine and rimantadine) [43, 55-58]. However the efficacy of these types of drugs are limited as they require early administration to be effective and rapid viral evolution has resulted in drug-resistance [43, 55-58]. For instance, oseltamavir resistance increased from 0.7% of circulating H1N1 in 2006-2007 to 98.5% in 2008-2009 and nearly all circulating strains are amantadine resistant [55-58]. Thus, annual immunisation remains the primary method of disease control [59, 60]. A significant amount of time and resources is invested each year in developing a vaccine, but immunisation efficiency varies from year to year [59-61]. Even in years with high coverage, vaccine efficacy is low in elderly populations [59-61]. Thus it is important to develop better vaccination strategies to control the spread of this virus and reduce the impact of emergent strains [59, 60, 62]. This could potentially be achieved by targeting multiple arms of the immune system, including the innate immune system [63]. The importance of innate immune cells to generating protective adaptive immunity is often overlooked in vaccine design, but may offer opportunities to increase the cross-reactivity of IAV immunisation [63]. The innate immune system is made up of many cellular and protein components, including mucins, collectins, complement, macrophages, neutrophils and natural killer (NK) cells which act together to eliminate influenza infection [64, 65]. Understanding this aspect of human immunity is therefore crucial to manipulating the human immune response during therapeutic intervention and vaccination.

1.2 Influenza and Chronic Obstructive Pulmonary Disease

1.2.1 Overview of COPD Presentation, Pathology and Symptom Management

COPD is a chronic inflammatory disorder of the lung, characterised by progressive irreversible lung obstruction and is the third leading cause of death worldwide [66, 67]. 80% of COPD deaths are related to smoking, representing the largest risk factor for disease development [68, 69]. Air pollution, exposure to biomass fuels and chemical irritants are additional risk factors for COPD, linking environmental insult to dysregulated lung immunity and function [66]. COPD is a clinically heterogeneous syndrome that can manifest as emphysema, chronic bronchitis and small airways disease and is primarily diagnosed by reduced and obstructed lung function [66]. Dysregulated immunity, epithelial apoptosis and microbiome dysbiosis are all key hallmarks of this disease [66, 67, 70-73]. However, the precise interplay between the microbiome, epithelium and immune system are poorly understood [66]. Recent evidence has described a distinct COPD microbiome with non-typeable *Haemophilus influenzae, Streptococcus pneumoniae* and *Moraxella catarrhalis* as the most common colonisers [70, 74-77]. However, the relationship between bacterial colonisation and disease progression is poorly understood. Our prevailing understanding of COPD pathology suggests a defect in bacterial clearance, followed by chronic inflammation and leukocyte infiltration of the airways but the precise mechanism of disease onset remains unknown [66].

COPD symptoms are often managed through the use of bronchodilators and inhaled corticosteroids (ICS) required throughout patient lifetime [78-80]. However neither of these treatments can return original lung function, and not all patients respond to such treatment [78, 79]. In addition, people diagnosed with COPD are more susceptible to persistent bacterial and viral infections, which can result in frequent hospitalisation and require antibiotic treatment [80]. Together this leads to a high cost of disease management and a substantial burden on health care systems [80].

1.2.2 Innate Immune Function in COPD

Wide ranging effects on the immune system have been associated with COPD, including the innate immune system, which acts to provide an early barrier to infection [81-88]. This includes (but is not limited to) suppression of NF-κB and Interferon (IFN) signalling from the epithelium, reduced IgA translocation into the airway lumen, defective macrophage phagocytosis, increased NK cell cytotoxicity, neutrophilia and increased immaturity of dendritic cells in the COPD lung [83-88].

Furthermore, systemic effects on innate immune signalling have also been reported in COPD with reduced cytokine production in response to pathogen-associated molecular pattern (PAMP) stimulation [89]. Many studies on COPD immune function are limited by accessibility to lung tissue and are often carried out in the peripheral blood, thus limiting the conclusions that can be drawn for lung biology [81, 82]. However, there is a strong picture for a reduction in the innate immune control of infection in COPD, possibly resulting in increased destruction to host tissues and disruption to adaptive immune function [82].

1.2.3 Viral Exacerbation of COPD

COPD symptoms undergo periodic exacerbation that are often viral in origin, particularly during winter seasons [90]. Exacerbations are defined as acute deterioration of symptoms and reduction in lung function and can result in hospitalisation and death [90]. Furthermore, the exacerbation process accelerates overall lung function decline, which does not recover to baseline after the infection [19, 90]. Thus exacerbation is considered one of the major costs of COPD patient care [19-21, 80]. A better understanding of this process is essential to reducing hospitalisation and improving quality of life in COPD patients [90, 91].

The mechanisms by which viral infection cause rapid deterioration of lung function are largely unknown but could result from inappropriate immune responses, such as a deficiency in IFN-β, which fails to clear infection [73, 82, 92]. Influenza virus is a major contributor to COPD exacerbations [20, 93-97]. Studies in different countries and cohorts have identified influenza infection in 8.2% - 36% of COPD exacerbations [20, 93-97]. The variation in IAV contribution to COPD exacerbation in these studies may come from the degree of influenza vaccination in the cohort and pathogenicity of circulating IAV strains at the time of study [20, 93-97]. Interestingly the largest detection of IAV in exacerbating COPD patients (36%) was found in a non IAV-vaccinated cohort [94]. IAV vaccination of COPD patients has been shown to have long term effects on patient health, including reduced exacerbations and hospital admissions, suggesting that improved vaccination strategies could improve COPD management [98]. Therefore, a greater understanding of the human immune response to IAV could benefit both seasonal control of this virus and protection of at-risk groups.

1.3 The Innate Immune Response to IAV Infection

IAV may be capable of hijacking cellular protein synthesis machinery but this virus does not go unrecognised by the immune system [99, 100]. IAV infection results in IFN production from infected epithelial cells and macrophages, thus stimulating innate and adaptive immune responses [99, 100]. Adaptive immunity is thought to be essential for influenza clearance, however cytotoxic T Lymphocytes (CTLs) and neutralising antibodies are not detected until 5-7dpi, after peak viral replication [43, 101-104]. Thus innate immunity is critical to early viral control, enabling host survival until adaptive immunity can be generated [43, 64, 65, 102-106]. For instance, innate effector cells such as NK cells respond to influenza infection within the first three days of infection leading to reduced viral titres in mouse (Ms) models of infection [107-113]. In addition, pro-inflammatory signalling from innate immune cells is essential to generating protective Th1 adaptive immunity which aids viral clearance and prevents re-infection [106, 114].

1.3.1 The Epithelial Response to IAV infection

Epithelial cells detect intracellular influenza replication by innate pattern recognition receptors (PRR), such as Toll-like Receptors (TLR) 3 and 7, and Retinoic acid-inducible gene-I (RIG-I) which recognise endosomal and cytosolic vRNA respectively [115, 116]. Activation of these receptors induces intracellular signalling through the Nuclear Factor-κB (NF-κB) pathway and production of pro-inflammatory IFN including type I IFN (IFN-α/β) and type III IFN (IL-28A, IL-28B and IL-29) [115-118]. IFN α/β are potent anti-viral molecules primarily upregulated by IAV infected epithelia and are protective in mouse models of influenza [117, 119]. Type I IFN signalling upregulates hundreds of IFN-stimulated genes (ISG) to inhibit host cell protein synthesis in neighbouring cells, inducing an antiviral state as well as stimulating host immunity through antigen presentation and leukocyte IFN-γ production [100, 120, 121]. Epithelia-derived type III IFN function is less well understood but these cytokines are part of the ISG network and may have similar roles to type I IFN, including restriction of viral replication in the epithelium [122-124]. In addition, IAV infected epithelial cells produce IL-6, IL-1A, IL-1B, IL-23A, IL-17C and IL-32 cytokines and some chemokines including Chemokine C-C Motif Ligands (CCL)-2, 8 and Chemokine C-X-C Motif Ligand-5 (CXCL5) to simulate immune cell recruitment [117, 118, 125]. Thus the epithelium plays a key role in stimulating immune responses to IAV-infection, providing early pro-inflammatory signalling and recruiting immune cells to the site of infection [117, 118, 125].

1.3.2 The Macrophage Response to IAV Infection

Two groups of macrophages are found in the lungs; alveolar macrophages derived from foetal liver cells and interstitial macrophages replenished by the circulation [54]. Airway macrophages are critical to the control of influenza in a number of *in vivo* murine models [53, 126-134]. These cells constantly patrol the epithelia and are likely one of the first immune cells to contact influenza virions in the airway [135, 136]. Thus, macrophages may provide essential early pro-inflammatory signalling to the rest of the immune system [54, 135, 136]. Macrophages share the same innate detection of intracellular virus replication pathways as the airway epithelium and therefore pro-inflammatory signalling is promoted by many of the same mechanisms [54]. However a greater variety of cytokines are upregulated by macrophages during IAV infection including IFN-α/β, Tumour Necrosis Factor (TNF)-α and Interleukins (IL) 1β, 6, 12, 15, 18, 23A and 27 [52, 100, 134-144]. Macrophages also stimulate immune cell recruitment, including monocytes, NK cells and T cells to areas of IAV infection through expression of chemokines such as CXCL8, CCL2, CCL3, CCL4, CXCL9 and CXCL10 [145-148]. Airway macrophages may also support inflammation resolution following influenza clearance through the production of anti-inflammatory IL-10 and TGF-β cytokines [149-151]. Finally, airway macrophages are also important to physical clearance of virus, through both phagocytosis of infected cells and by inducing apoptosis of infected cells through upregulation of TNF-related apoptosis-inducing ligand (TRAIL) [140, 152, 153].

Macrophage efferocytosis of infected cells, phagocytosis of virions and direct infection by IAV are all potential resources of viral protein in these cells and therefore may allow antigen presentation on class I and II HLA molecules on the macrophage surface [154]. As antigen presenting cells (APCs) macrophages provide important stimulation of the adaptive immune system through presentation of such phagocytosed antigens to T and B cells, a function that is shared with airway dendritic cells (DCs) [155]. In fact, airway macrophages and DCs share many functions, including environmental sampling and pro-inflammatory cytokine release [156]. However, whilst macrophages play a more sentinel and homeostatic role in tissues, dendritic cells have specialised role in stimulating adaptive immunity. DCs are essential to generating appropriate T and B cell responses to infection through direct contact with adaptive leukocytes at lymph nodes [156, 157]. In the periphery, activated DCs migrate to secondary lymphoid tissues, allowing T and B cell differentiation via antigen presentation, co-stimulatory contacts and directed release of pro-inflammatory cytokines such as IL-12 and TNF-α [156, 157]. Therefore the dual capacity of airway macrophages to present viral protein and release pro-inflammatory cytokines, suggests that macrophages might also bridge innate and adaptive immune responses during respiratory infection [54, 158].

Although airway macrophages may be essential to influenza control through sentinel signalling and direct clearance of infected cells, they may also contribute to the immunopathology of influenza [53, 126-134, 145, 153, 159]. For instance, the most pathogenic strain of avian influenza (H5N1) has been shown to stimulate a dysregulated and inappropriate cytokine release from macrophages [145]. Macrophage hypocytokinemia and overexpression of TRAIL have both been associated with epithelia damage and IAV lethality in the mouse [153, 159]. Given the importance of macrophages to controlling IAV replication and pathogenicity, it is therefore no surprise that the macrophage is an important target of immunomodulation by influenza virus [53, 126-134]. In fact, IAV has been shown to suppresses both macrophage scavenger receptor expression and phagocytosis *in vitro* [134, 160, 161]. This reduced phagocytic capacity of IAV-infected macrophages might represent an evolutionary adaptation of the virus as it attempts to evade innate immunity. However, reduced macrophage phagocytosis during influenza infection may also enable bacterial colonisation and could explain why secondary bacterial pneumonias are a common cause of influenza-associated death [2, 3, 160, 161].

1.3.3 IAV Modulation of the Host Response

As described in section 1.1.2, IAV replication produces a number of non-structural IAV proteins as a result of frameshifts or alternatively spliced versions of structural protein sequences [162]. Thus far, nine different NS proteins have been identified including NS1, PB1-F2, PA-X, PB2Δ, PB1-N40, PA-N155, PA-N182, M42 and NS3 [162]. NS proteins collectively function to inhibit anti-viral host responses, regulating host cell gene expression and inflammatory signalling cascades [163]. Although there is substantial heterogeneity in NS protein expression between IAV strains, NS1, PA-X and PB1-F2 are strongly conserved, reflecting the importance of these proteins to viral pathogenicity and virulence [162].

IAV NS proteins are multi-functional with many different binding partners in the host cell [162]. For instance, NS1 is thought to bind 79 different host cell proteins, including multiple components of the IFN signalling pathway [163, 164]. This allows NS1 to inhibit many components of the retinoic acid inducible gene I (RIG-I) signalling pathway, thus down-regulating host gene expression and reducing early pro-inflammatory signalling [163]. Other NS proteins also regulate host gene expression, such as PA-X which directly cleaves host cell RNA but maintains viral transcript production [165]. In addition, NS proteins also contribute to IAV pathogenicity as PB1-F2 has strong pro-apoptotic effects, exacerbating secondary bacterial infections in animal models [166, 167].

Taken together these studies demonstrate a substantial capacity of IAV to effect and modulate the host cell response and resulting inflammation [163]. Like HA and NA, NS proteins are fast-evolving to favour IAV replication in the host cell, a feature that is reflected by heterogeneity in NS protein expression between IAV strains [162]. The varied expression of NS protein between IAV strains demonstrates the complex nature of host-pathogen interactions, which will impact on downstream signalling and the extent of subsequent immune response.

Despite the substantial modulation of immune response by IAV proteins, both the airway epithelia and macrophages are still capable of secreting pro-inflammatory molecules following PRR detection of the virus [145-148]. This pro-inflammatory signalling is capable of recruiting antiviral effector cells to sites of IAV infection and these recruited immune cells act together to clear virus from the respiratory tract [145-148]. One such responding cell type is the NK cell, but the nature of NK cell responses to human respiratory infections is not well understood and requires further investigation [168].

1.4 NK Cells

1.4.1 NK Cell Definition and Function

NK cells, defined as CD3-CD56+ lymphocytes are important effectors of innate anti-viral immunity [169-174]. But despite this established role in anti-viral immunity, there is not a full understanding of the NK cell function in pulmonary immunology [169-174]. NK cells have been described as "professional" killer cells as they are densely packed with lytic granules containing Perforin and Granzyme molecules [175, 176]. Following NK cell recognition of a virally infected cell, the contents of NK cell granules are released across an immunological synapse with the target cell [177-179]. Once released from the NK cell, Perforin forms pores in the target cell membrane allowing cytotoxic molecules such as Granzyme-B (Gzm-B) to move into the target cell, cleaving caspase precursors and inducing cellular apoptosis [180-184]. CD107a, a protein on granule membranes is important in Perforin trafficking and granule motility; migrating to the NK cell surface during granule release [185]. CD107a is therefore a commonly used marker of NK cell degranulation and cytotoxicity [185]. NK cells are also capable of initiating cell killing through death receptors such as TRAIL (CD253) and FS-7 Associated Surface Antigen (FAS / CD95), which induce apoptotic programmes in cells expressing their ligands [178, 186-188].

Once activated, NK cells also recruit and stimulate DCs, monocytes, macrophages and T cells to sites of inflammation through the production of chemokines such as CCL3, CCL4, CCL5 and Granulocyte-Macrophage Colony Stimulating Factor (GM-CSF) [189-193]. NK cells also produce other inflammatory and anti-viral cytokines such as TNF-α and IL-6 and are an important early source of IFN-γ [194-196]. IFN-γ coordinates the transition from innate to adaptive immunity through promoting B cell isotype switching and increasing leukocyte extravasation [197]. It is also important in skewing the CD4+ T cell response towards a Th1 response, the most optimal immune response for countering intracellular pathogens such as respiratory viruses [192, 193, 198]. IFN-γ is therefore crucial to promoting an anti-viral immune response during inflammation [197].

In the past few decades NK cells have been associated with the control of many viral species such as Herpes Simplex Virus (HSV), Hepatitis C Virus (HCV), Cytomegalovirus (CMV), and Human Immunodeficiency Virus (HIV) [169-174]. Recent advances in our understanding of how NK cell cytotoxicity is regulated has shed light on the mechanisms in which NK cells contribute to human anti-viral immunity. NK cell activation is controlled through the integration of signalling from a large

arsenal of germ-line encoded inhibitory and activating receptors on the NK cell surface [199]. These receptors include the C-type lectins, Natural Cytotoxicity Receptors (NCR), Leukocyte Immunoglobulin-like Receptors (LIR) and the Killer Cell Immunoglobulin (Ig)-like Receptors (KIR) as shown in Figure 1.1 [200]. NK cell receptors enable constant surveillance of neighbouring cell surfaces and are sensitive to viral protein, "stress" molecules and class I human leukocyte antigen (HLA) expressed on infected cell surfaces [200, 201]. Loss of NK cell inhibition, or engagement of activating receptors induces a directional release of lytic granules, thus ensuring specificity of killing (reviewed in Mace *et al.* 2014 and described in Figure 1.2) [202]. Inhibitory receptor signalling is dominant within NK cells, as activating signalling alone does not stimulate granule release *in vitro* [203, 204].

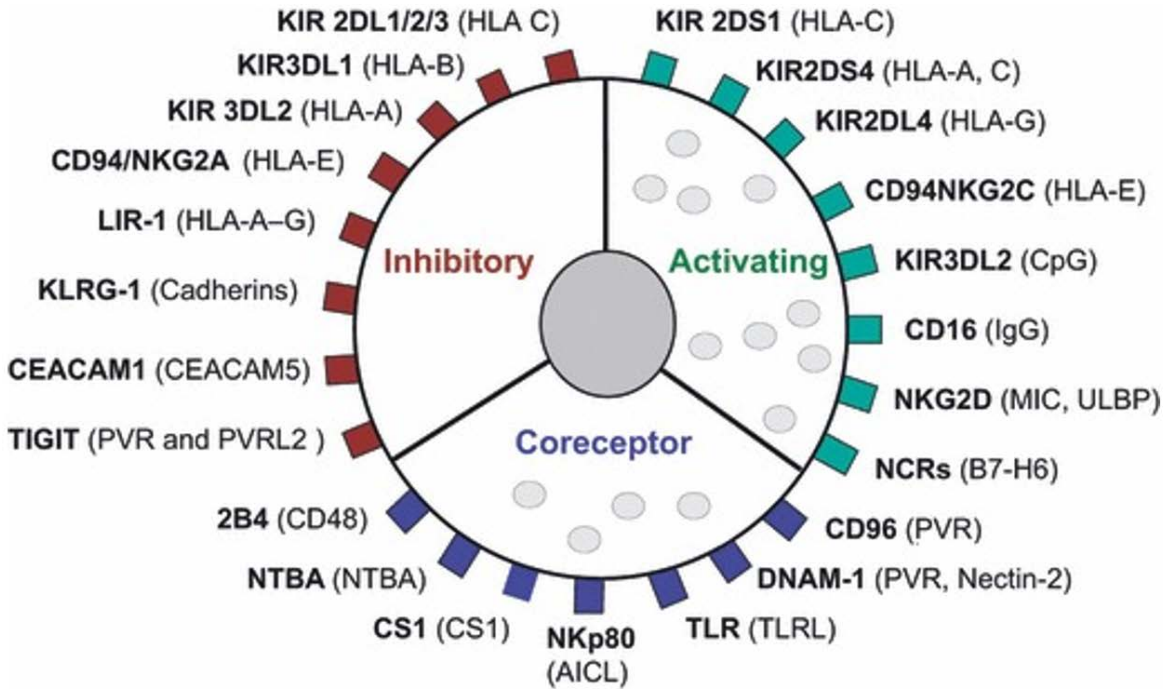

Figure 1.1: NK cell receptors NK cell receptors (in bold) are shown alongside their corresponding ligands (in brackets) and classified based on their functional role. Inhibitory co-receptors CD300, Leukocyte-associated Ig-like Receptor 1 and Sialic Acid-Binding Ig-like Lectin 7 (SIGLEC-7) not shown. Image reproduced from Leung *et al.* 2011 with permission from John Wiley and Sons [205].

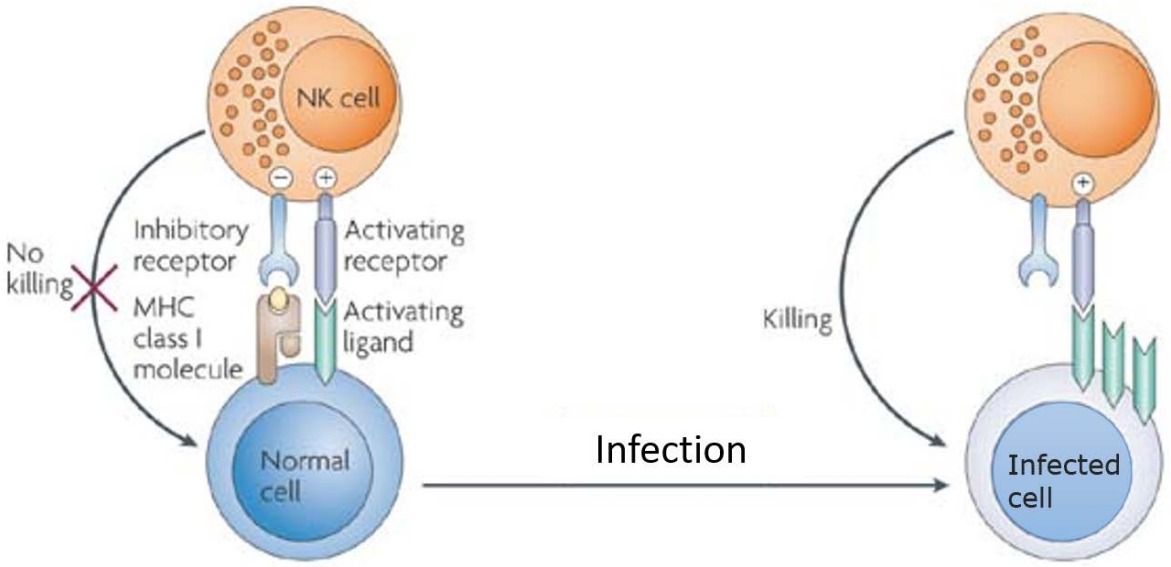

Figure 1.2: NK cell activity is regulated by activating and inhibitory signalling. During viral infection Major Histocompatibility Complex class I (MHC I) ligands are downregulated whilst activating NK cell receptors are engaged. This change to the balance of inhibitory and activating signalling during viral infection or transformation will activate NK cell killing of target cells. Image adapted from Ljunggren *et al*. 2007, with permission from Springer Nature [206].

1.4.2 HLA-dependent Function

NK cells possess many inhibitory HLA-dependent receptors including the LIR, long intracellular chain KIR, and CD94-NKG2A and NKG2E heterodimers [207-213]. However, the most well-known are the KIR family, which are stochastically expressed upon the NK cell surface [199, 200]. There are 15 highly polymorphic KIR genes found with varying frequencies in different populations [214]. This variety in KIR genes creates substantial genotypic variation, but an individual's genotype can often be characterised into one of two KIR haplotypes [214]. Individuals with haplotype A typically possess KIR alleles with a more inhibitory role than those with KIR haplotype B, which has a more activating effect on NK cell function [214]. One of the most important functions of the KIR proteins is to allow NK cell licensing (also known as NK cell education), a process whereby NK cells gain functionality during their development [215-217]. HLA engagement with cognate inhibitory KIR prevents NK cell degranulation [215-217]. Once licensing has occurred NK cells will target and kill cells that do not engage the inhibitory KIR [215-217]. In licensed NK cells the default response is to kill and thus NK cells must experience constant inhibitory signalling from healthy somatic cells [215-221]. These interactions enable NK cells to recognise target cells through the loss of HLA class I (the "Missing Self" hypothesis) an important mechanism of NK cell activation as HLA class I is downregulated in many viral infections and tumours [222, 223]. The avidity and availability of HLA

molecules during licensing is thought to determine the strength of NK cell responsiveness upon the loss of inhibition, although this has been disputed [215, 224, 225].

As the HLA and KIR gene loci are on different chromosomes, KIR alleles may not be inherited with their cognate HLA molecules, thus populations of unlicensed NK cells can exist within individuals. Despite initially being reported as non-responsive, unlicensed NK cells may have an important role in combating viral infection and malignancy, particularly where HLA I expression is increased and licensed NK cells may be switched off [226-228]. For instance, it has been suggested that inflammatory cytokine stimulation may allow afunctional unlicensed NK cells populations to respond to viral infection and cancer [228].

Interestingly, some HLA-dependent receptors deliver activating signals into the NK cell, including short chain KIR and NKG2C-CD94 heterodimers [208, 229]. Activating KIR have largely homologous extracellular regions to their long-chain counterparts and are thought to bind the same HLA alleles at a lower affinity [229, 230]. However, many ligands of the activating KIR are unknown. Activating KIR may be sensitive to changes in the peptide repertoire of HLA molecules, as this has been shown for NKG2A/CD94 complexes with HLA-E- in HIV [231, 232]. Furthermore KIR2DS2 has been shown to be capable of binding conserved sequences in the Non-Structural Protein-3 of Dengue virus, suggesting that activating KIR may directly recognise viral proteins [233]. Finally, some activating KIR have been shown to bind HLA-F open conformers upregulated during inflammation [234].

1.4.3 HLA-independent Function

NK cells also possess several families of HLA-independent inhibitory and activating receptors. For instance the HLA-independent NK cell receptors include SIGLEC-7 (CD328) which binds sialic acid and the CD300 family which bind lipids expressed during apoptosis [235, 236]. HLA-independent activating receptors also include the NCR family (NKp46, NKp44 and NKp30) and C-type lectin receptors, but the ligands for many of these receptors are unknown [204, 230, 237-239]. However, NKp46 (CD335) and NKp44 (CD336) have recently been shown to bind influenza HA *in vitro* [240-242]. In addition some C-type lectin receptors bind cellular molecules such as heparan sulphate proteoglycans and HLA-B-associated transcript 3 and have been shown to be a major mechanism of NK cell mediated tumour killing [239, 243-247]. Other activating NK cell receptors have evolved to recognise markers of cellular stress, such as NKG2D (CD314) and DNAM-1 (CD226) [248-250]. The ligands of these receptors are often upregulated during viral infection and periods of chronic

inflammation [251-254]. Furthermore, damaged or infected cells can be targeted for destruction through antibody-dependent cellular cytotoxicity (ADCC), as NK cells express the low affinity FcγIII receptor, CD16 [255, 256]. Together these studies demonstrate that the extensive repertoire of NK cell germ-line encoded receptors provide a broad specificity and flexibility in the NK cell response to pathogens, stress and inflammation. However, the variety in ligands NK cells can recognise provides a further layer of complexity in elucidating mechanisms of NK cell activation during human infections.

1.4.4 NK cell Development

NK cells derive from CD34+ common lymphoid progenitors in the bone marrow [257-260]. This process is controlled by the expression of several different transcription factors (reviewed by Sun and Lanier 2011) [261]. In the bone marrow the common lymphoid progenitor develops into an early innate lymphoid precursor which gives rise to both NK cells and ILCs [262]. ILCs have a range of functions throughout the body and are important co-ordinators of innate immunity and tissue homeostasis [262]. NK cells are sometimes grouped into an ILC classification as the prototypical member of the ILC 1 family [262]. Further differentiation of progenitor NK cells into mature NK cells corresponds with a gain in cytotoxic potential and is characterised by the sequential gain and loss of surface protein, a process that has largely been investigated in mice but appears to be replicated in humans (Figure 1.3) [259, 263-266]. However, a full understanding of human NK cell development has been hampered by a lack of continuity between mouse and human NK cell receptors.

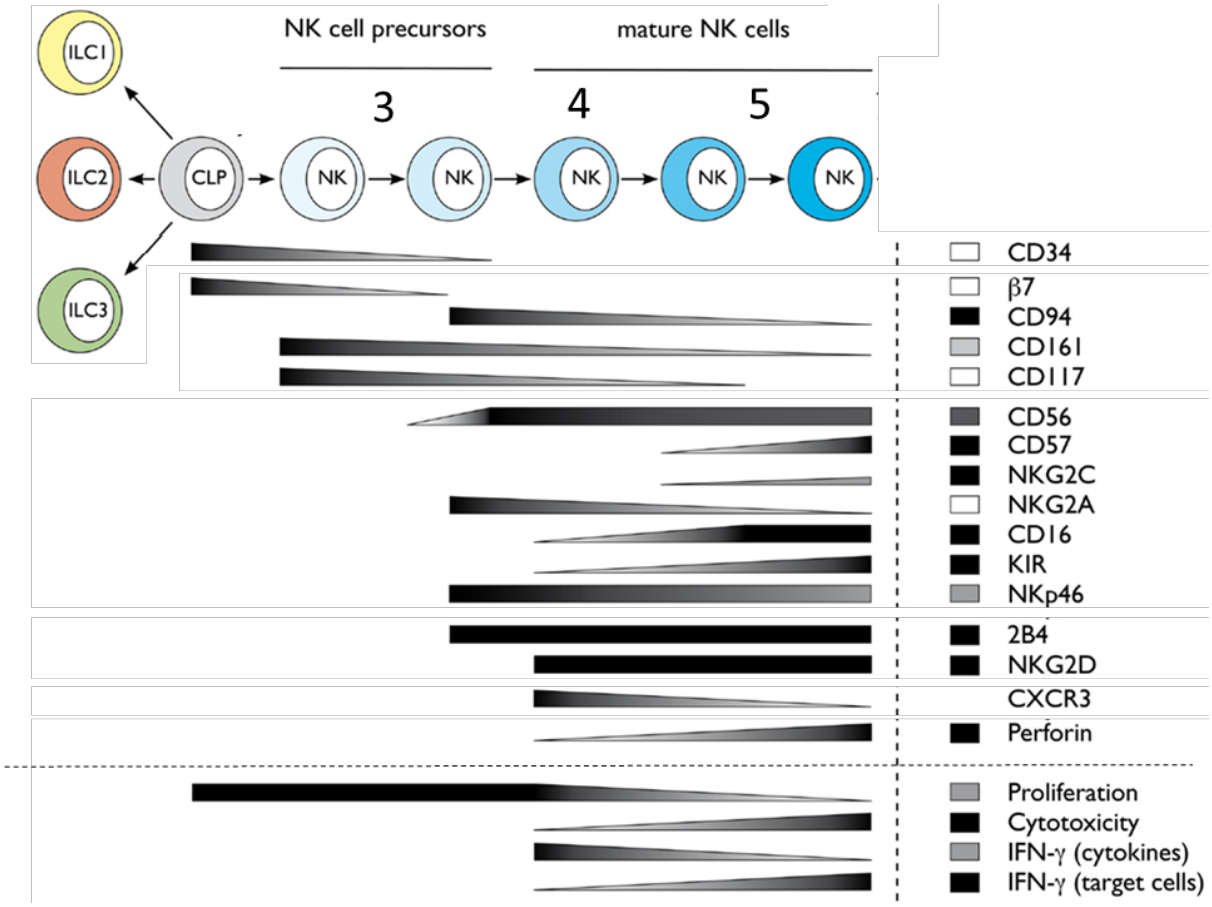

Figure 1.3: Human NK cell maturation is characterised by surface protein. Image adapted from Luetke-Eversloh *et al*. to show key marker expression during NK cell developmental stages 3, 4 and 5 [267]. The change to NK cell functional capacity throughout their developments is summarised beneath. This image is reproduced with permission of Leutke-Eversloh, Killig and Romagnani.

Freud *et al.* divided human NK cell differentiation into stages based on the expression of CD117, CD94 and CD56 expression, as shown in Figure 1.3 and 1.4 [266]. Each NK cell developmental stage is accompanied by change in surface proteins such as CD2, integrin-β7, CD11b, CD43 and CD161 (Figure 1.3) [266]. CD117 binds Stem Cell Factor and is associated with early NK cell progenitors, the loss of this molecule and acquisition of CD94 indicates differentiation into NK cells [266]. Mature NK cells are distinguished from their progenitors by the expression of CD56 in stage 4 of their development [266]. CD56, also known as neural cell adhesion molecule (NCAM) is thought to be important in NK cell adhesion to neighbouring cells, binding other CD56 molecules and Fibroblast Growth Factor 1 [268-270]. Progression into a stage 4 NK cell also corresponds with increased NCR, NKG2D and CD16 expression, a process that is summarised in Figure 1.3 [263, 266]. Stage 4 NK cells are $CD56^{bright}CD16-$ and have low cytotoxic activity but are capable of further maturation to a stage 5 NK cells ($CD56^{dim}CD16+$ cell) which represents the canonical NK cells found in the blood. The

process governing this transition is still being elucidated but T cells have been implicated in $CD56^{bright}$ differentiation and activation through the release of IL-2, a process that may occur in secondary lymphoid organs [271]. Development into a $CD56^{dim}$CD16+ phenotype induces full NK cell cytotoxic potential and coincides with the acquisition of inhibitory KIR molecules, see Figure 1.3 [270, 272, 273]. CD57, a glucuronyl transferase which recognises non-reducing terminal sugars is also upregulated during late-stage NK cell maturation [274, 275]. $CD56^{dim}$CD57+ NK cells have been found to be more responsive and better able to kill targets than $CD56^{dim}$CD57- NK cells, leading to the use of CD57 as a marker of terminal NK cell differentiation [274, 275]. From stage 4 onwards NK cells are capable of circulating in the peripheral blood, however 90% of the peripheral NK cells are $CD56^{dim}$CD16+ cells (stage 5) with 10% of NK cells $CD56^{bright}$ (stage 4) [276]. It is thought that peripheral NK cells slowly self-renew in the steady state and that their survival is dependent on access to IL-2 and IL-15 [277-286].

Historically NK cell development was thought to occur in the bone marrow [257-260]. However, CD117+CD56+/- cells (stage 3 - 4) NK cells have recently been identified in the tonsils and lymph nodes, liver and intestinal lamina propria (summarised in Figure 1.4), suggesting that immature NK cells are capable of leaving the bone marrow and may undergo further differentiation in the periphery [259, 287-291]. In support of this theory NK cell development is also accompanied by a change in chemokine receptor expression, as reviewed by Carrega *et al.* 2012 suggesting that the migrational capacities of NK cells may be altered as they mature [292]. However, the migration of NK cells between the circulation, lymphoid and non-lymphoid organs has not been fully characterised.

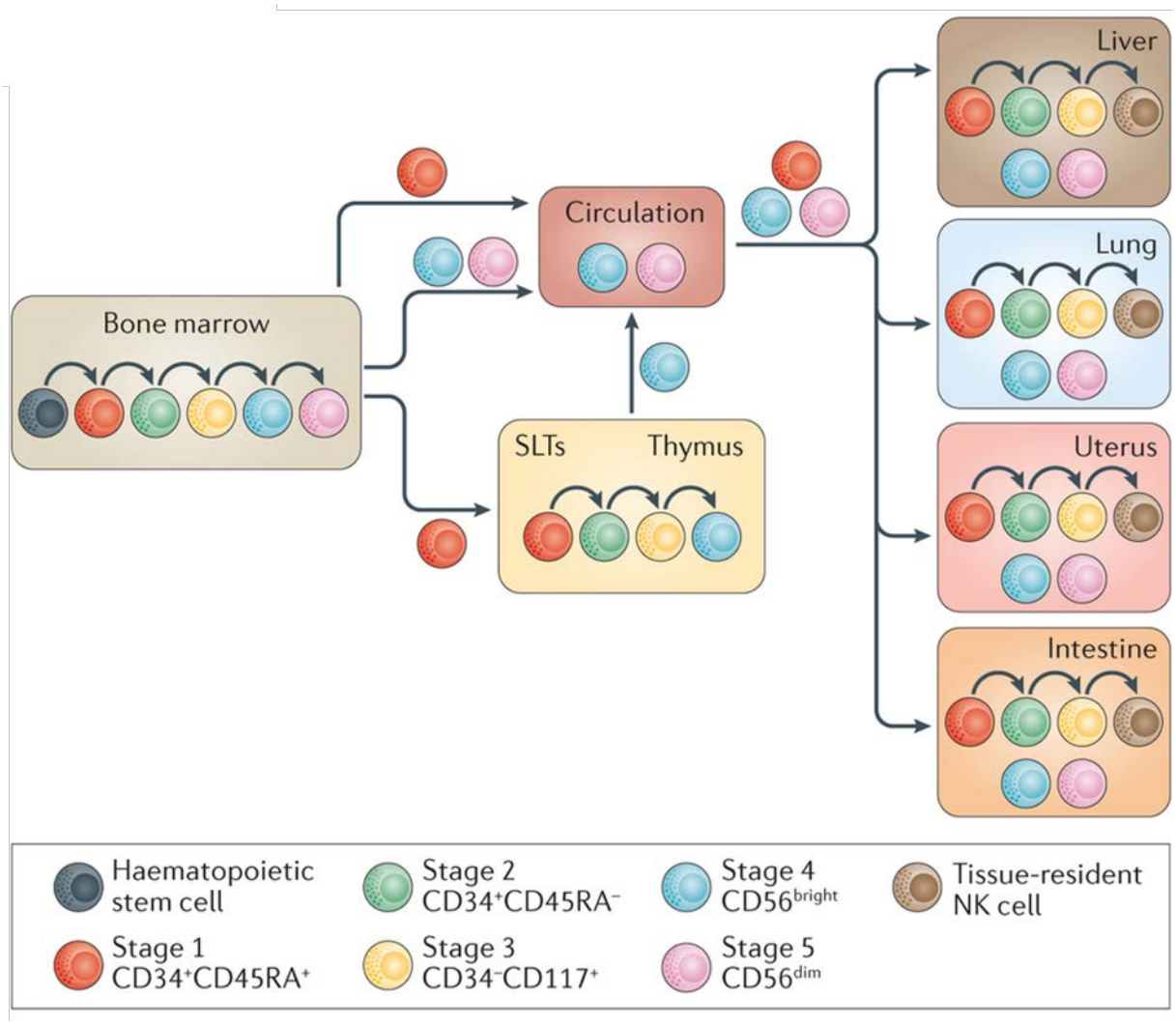

Figure 1.4: A model for NK cell developmentNK cell development occurs in the bone marrow but immature precursors may be capable of continuing their maturation in secondary lymphoid tissues. Image reproduced from Bjorkstrom *et al.* 2016 with permission of Springer Nature [293].

1.4.5 Differences in Mature NK cell Phenotype and Function

$CD56^{bright}CD16$- NK cells are thought to be immature precursors of the canonical $CD56^{dim}CD16$+ NK cells found in the periphery [269, 270, 282, 294, 295]. Indeed, $CD56^{bright}$ and $CD56^{dim}$ NK cells differ in the expression of a number of proteins, including chemokine receptors, KIR and NKG2D, as reviewed in Montaldo *et al* 2013 [296]. $CD56^{dim}CD16$+ NK cells predominate in the peripheral blood and spleen but the more immature $CD56^{bright}$ NK cells predominate in the lymph nodes, tonsils and liver [259, 266, 291, 297]. However, $CD56^{bright}$ NK cells isolated from the lymph node and liver appear phenotypically different to the $CD56^{bright}$ NK cells in the blood [298]. This could suggest a further difference in NK cell maturation between the organs and periphery or may indicate unique phenotypic NK cell population organs [298-301]

Some reports have described distinct functional roles for CD56^{bright} and CD56^{dim} NK cells, for instance CD56^{bright} NK cells produce more cytokines upon *in vitro* stimulation compared to CD56^{dim} NK cells [259, 295, 302-304]. Interestingly, CD56^{bright} NK cells can home to the secondary lymphoid, an anatomical location that may allow influence over other immune cell interactions, a finding that has led some authors to suggest an immunoregulatory role for these cells [190, 271, 297, 302, 305-307] [295]. In addition, CD56^{dim}CD16+ NK cells have been proposed to be more cytotoxic than the CD56^{bright} NK cells, which has been suggested to be due to the acquisition of receptors such as KIR and CD16 [295, 302, 304, 308, 309]. However, "cytotoxic" CD56^{dim} NK cells can also release large-amounts of cytokines upon receptor ligation and CD56^{bright} NK cells become cytotoxic following cytokine stimulation [189, 310-312]. This suggests that the activity of CD56^{bright} and CD56^{dim} NK cells depend on the nature of the *in vitro* stimulation.

CD56^{dim}CD16- NK cells can also be identified in the peripheral blood but are not reported in all studies [313, 314]. There is evidence this phenotype results from CD56 and CD16 protein shedding following NK cell activation and therefore may represent a post-activation phenotype [313-317]. Increases in CD56^{dim}CD16- NK cells have been associated with cancer and can be observed following IAV vaccination, perhaps indicating enhanced NK cell activation in these inflammatory contexts [316, 318-320]. However, the functional roles of CD56^{dim} and CD56^{bright} NK cells are yet to be fully characterised in physiologically relevant models of human infection.

1.4.6 Organ Resident NK cells

The majority of our understanding of human NK cell phenotypes and function come from studies using the peripheral blood. However, with growing access to human tissues new phenotypes and functional roles have been described for NK cells. Recently, tissue-resident NK cell populations (rNK) have been described in the liver, adipose tissue, skin, kidney, salivary glands, uterus and lymph nodes [299-301]. Tissue-resident NK cells have a significant proliferative capacity and retain their phenotype during long-term *in vitro* culture [301]. Tissue-residency has mostly been described for CD56^{bright} NK cells, with the exception of one study which found CD56^{dim} resident NK cells in the nasal mucosa [299-301, 321, 322]. In the liver and uterus NK cell residency has been characterised by the expression of proteins which prevent tissue egress, such as CD69, CD49a and CD103 as well as unique chemokine receptor expression [299-301]. CD69, a C-type lectin-like signalling receptor is important in preventing lymphocyte trafficking from lymphoid tissues [323-327]. CD69 has been found to down-modulate the activity of Spingosine-1-phosphate receptor 1 (S1P1), a protein

important in lymphocyte egress from organs [323-327]. CD49a, also known as the integrin α1 subunit, forms a cell surface receptor for collagen IV and laminin, whereas CD103 (integrin αE) binds E-cadherin [328-330]. These two proteins may therefore play a role in resident NK cell adhesion to the extracellular matrix, as has been observed for resident memory T cells (Trm) [331].

There are substantial differences between rNK cells in the different human organs. For instance in the uterus, integrin-β7 and CD9 have also been associated with tissue residency, whereas in the liver C-X-C chemokine receptor type-6 (CXCR-6) and C-C Chemokine Receptor type-5 (CCR5) are thought to be important to resident NK cell retention [298, 299, 332, 333]. Liver-produced CCL3 and 5 and CXCL16 stimulate selective NK cell migration of CXCR6+ and CCR5+ NK cells into the sinusoidal space [332]. Interestingly, CXCR6 has also been linked to NK cell homing to secondary lymphoid tissues [300].

1.4.6.1 Recruitment and Development of Tissue-Resident NK Cells

A number of models for resident NK cell development and recruitment have been proposed and are currently an area of discussion within the field. One theory is that pre-NK cells are recruited to organs as they egress from the bone marrow, as shown in Figure 1.4 [293]. Interestingly adoptive transfer experiments in the mouse have shown that NK cells adjust their level of activation to the anatomical location, suggesting regulation of NK cell activity at the organ level [334]. This might also implicate the organ microenvironment in shaping NK cell development, phenotypic profile and function [299, 335]. The organ-specific factors controlling NK cell residency are yet to be explored in humans and are likely to be multifactorial. However, TGF-β has been suggested to induce tissue-residency markers CD103 and CD9 in the human uterus, implicating a role for this cytokine in NK cell residency [299].

Lymphoid tissue-resident CD69+CXCR6+ NK cell do not express immaturity markers such as CD117 or late stage markers such as KIR and CD57, suggesting a developmental intermediate between stage 4 and 5, based on the differentiation model described above. However, tissue-resident NK cells may represent developmentally distinct populations from the NK cells found in circulation. This hypothesis is supported by transcriptomic analysis of uterine NK cells which found extensive differences between uterine $CD56^{bright}$ NK cells and peripheral blood $CD56^{bright/dim}$ NK cells [321]. Different transcription factors have been found in each group with liver rNK cells controlled by T-

bet rather than EOMES in peripheral blood NK cells [336-338]. Furthermore, a recent lineage tracing study identified an ILC precursor which could also give rise to a an “NK-cell-like phenotype” in the organs which could represent rNK cells, however this progenitor did not produce circulating NK cells (cNK) [339]. This suggests that although ILC and NK cells share a developmental pathway from the common lymphocyte progenitor resident NK cell precursors and circulating NK cells may have different developmental lineages [339].

1.4.6.2 Function of Tissue-Resident NK Cells

The discovery of NK cell populations unique to human organs raise important questions about how these NK cells may contribute to human immunity [299-301]. The unique phenotypic profiles of organ-resident NK cells hints at different functional roles of NK cells in different organs [293, 340]. For example, hepatic CD49a+ NK cells express high levels of inflammatory cytokines such as TNF-α, GM-CSF and IL-2 but degranulate poorly when stimulated with phorbol 12-myristate 13-acetate/Ionomycin (PMA/I), potentially indicating an immunoregulatory role for rNK cells in the liver [301, 338, 341]. In addition, salivary gland resident NK cells are thought to prevent autoimmunity by eliminating activated T cells [342]. However, tissue resident NK cells have also been associated with promoting inflammation in adipose tissue [343]. These data suggest that rNK cells may have a variety of functions in the human body, acting to maintain organ homeostasis and moderate immune responses much like the ILC populations [293, 340]. However, rNK cell function has not been fully explored in human infection and disease [344].

1.4.6.3 NK cell Memory and Organ Residency

Interestingly, the surface proteins associated with NK cell residency have also been linked to memory-like features in these cells, suggesting that these two phenotypes may be related [301, 345]. In contrast with adaptive memory, which requires genetic recombination, innate immunological memory most likely reflects fine-tuning of signalling pathways and epigenetic remodelling in innate immune cells [344]. As a relatively new concept, the mechanisms governing innate immunological memory are not well understood, but the feature has been clearly demonstrated for NK cells in a number of models. NK cell memory was first identified in a murine hapten-challenge model, where NK cells mediated potent hapten-specific responses upon secondary challenge [346, 347]. Long-lived, virus-specific NK cell memory has also been observed in Simian Immunodeficiency Virus infection of macaques and murine CMV [348-350]. Human

vaccination has also been shown to induce NK cell memory responses in a number of contexts including influenza infection [345, 351, 352].

"Memory" NK cells in the hapten-challenge model were found exclusively in the liver and were Ly49C/I, CD90, CXCR6 and CD49a positive [336, 345, 347]. CXCR6 is thought to play a critical role in NK cell memory to hapten and is important to the persistence of memory NK cells to vaccine antigens [345]. Furthermore, the human equivalents of hepatic memory/resident NK cells (CD49+CD69a+CXCR6+ cells) show features of clonal expansion of an NKG2C+ NK cell subset, a phenomenon observed in the mouse [301, 350]. Indeed, there is increasing evidence of long-term expansion of NKG2C+ memory-like NK cells during human CMV infection [349, 353-356].

The mechanism by which a more potent secondary NK cell response is generated is unclear, although epigenetic modification has been implicated in this process [357]. It has also been suggested that altered intracellular signalling pathways may enable easier bypass of the dominant inhibitory signalling from receptors engaging the HLA class I, which may also enable enhanced responsiveness [345]. Inflammatory cytokine signalling may be responsible for this change in signalling pathways and has also been found to be key to the generation of memory NK cells in murine CMV [358]. Furthermore memory-like human NK cells can be produced *in vitro* with IL-12, IL-15 and IL-18 stimulation [358-360].

1.5 NK Cells in the lung

1.5.1 The Lung NK cell Phenotype

As discussed in section 1.4.6 a range of NK cell phenotypes have been reported in human organs, however there has been less research into the lung NK cell phenotype [293]. NK cells represent 10-30% of lymphocytes in the human lung and are predominantly stage 5 $CD56^{dim}CD16+$ cells, similar to the peripheral blood [307, 361, 362]. Recently, Marquardt *et al* reported that the majority of NK cells in the lung are circulating NK cells [362]. NK cells make up 5 – 15% of peripheral blood mononuclear cells (PBMCs) and thus are constantly passing through lung tissue during steady state [276, 362]. However, steady state lung tissue expresses chemokines, such as CXCL2, CXC3CL1, CCL4, CXCL9, CXCL10 and CXCL12, capable of recruiting $CD56^{dim}$ and $CD56^{bright}$ NK cells which suggests NK cells could be recruited to lung tissue from the periphery [307, 363]. Marquardt *et al* also identified CD69 expression on approximately 75% of $CD56^{bright}$ lung cells, which could indicate tissue residency in the lung [362]. However, CD69 expression alone is not a definitive marker for NK cell residency and other markers of NK cell residency have not been explored in the human lung [293].

Despite this predominantly mature, cytotoxic ready phenotype, NK cells isolated from the lungs appear to be functionally impaired in both mice and humans [362, 364-366]. Stimulation by susceptible cancer lines, cytokines, LPS and PMA/I found a reduced lung NK cell response relative to the peripheral blood and spleen [362, 364-366]. This research led to the description of lung NK cells as hypofunctional in the lung environment [362, 364-366]. The findings from such studies suggest that NK cell activation could be tightly regulated in the pulmonary environment, a mechanism that may prevent unchecked cytotoxicity from damaging tissue architecture and compromising lung function [364-366]. Broncho-alveolar lavage (BAL) and alveolar macrophages have both been implicated in the suppression of lung NK cell cytotoxicity [364-366]. As the whole lung NK cell population is affected by the respiratory environment, NK cell function is most likely to be controlled through the action of soluble mediators, although direct cell contact cannot be excluded as a mechanism of regulation [365-367]. Signals from macrophages may serve to dampen NK cell sensitivity as they pass through the lungs during circulation. However, the mechanism by which this takes place remains to be elucidated. Interestingly NK cells isolated from the mouse lung have altered receptor profiles compared to the peripheral blood and spleen, with increased expression of inhibitory receptors and decreased activating receptors [364, 365]. Furthermore, Marquardt *et al*. 2016 demonstrate increased expression of self-recognising KIR on NK cells isolated from the lung parenchyma compared to the blood [362]. These observations suggest that reduced

pulmonary NK cell cytotoxicity may be due to an altered balance of activating and inhibitory signalling into the NK cell.

1.5.2 NK Cells in IAV Infection

NK cells have an essential anti-viral role within the body, however it is unclear how NK cells may contribute to lung health and disease in humans. A number of murine models have implicated NK cells in the immune response to influenza, but data conflict as to the role described for these cells [107-113, 227]. The majority of studies describe a protective role for NK cells in murine influenza infection and even suggest that NK cells could stimulate epithelial regeneration following viral clearance [107-110, 227]. Furthermore, treatments that enhance NK activity, such as prophylactic IL-12 administration and post-infection poly-gamma glutamate, protect against influenza in mice [368, 369]. However, some studies using a high dose influenza challenge ($5x10^3$ plaque forming units (PFU) or 5 Hemagglutinating Units) report detrimental effects of NK cells during murine influenza infection [111, 112]. In contrast, Zhou 2016 performed high dose ($1x10^6$ PFU) infection but reported a protective effect of NK cells. This may be due to the use of the 129 mouse line in Zhou *et al* compared to the C57BL/6 background in other reports [113]. Different mouse strains have significant differences in their immunological function therefore influenza infection may differentially affect C57BL/6 and 129 backgrounds [370]. Although contradictory, these studies all describe a role for NK cells in both the resolution and lethality of influenza infection in mice [107-113, 227, 371, 372].

Most studies of human NK cells in influenza infection rely on human peripheral blood for infection models, *in vitro* binding studies or measure NK cell function during IAV vaccination [203, 241, 254, 373-377]. These studies have all indicated that NK cells recognise and respond to IAV-infected cells but are not representative of the cells that are infected *in vivo* i.e. the lung epithelia and alveolar macrophage [23]. The development of more physiologically relevant models of human infection is important to understanding the biology of NK cells during human lung health and disease. Understanding this aspect of innate immunity may present novel opportunities for developing vaccination strategies and therapies as these cells provide such early innate signalling to the rest of the immune system [197, 200].

1.5.2.1 NK Cell Recognition of IAV Infected Cells

So far, two activating NK cell receptors have been shown to directly bind influenza-infected human cells; NKp46 and NKG2D [254, 376, 378, 379]. NKG2D belongs to the C-type Lectin family and NKp46 the NCR family, both are constitutively expressed on human NK cells [249, 250, 380]. NKG2D binds HLA I related molecules such as Major Histocompatibility Complex class I Chain-related protein-A/B (MIC-A/B) and UL16 Binding proteins-1/2/3/4/5/6 (ULBP1-6), which are upregulated after pathogen invasion and TLR signalling [251-254]. Whereas NKp46 directly binds influenza HA through its sialic acid residues [240, 241, 381]. Furthermore, NKp46 co-receptors 2B4 and NTB-A, have also been implicated in HA binding [373, 377]. An *in vivo* role for NKp46 in IAV infection has been indicated by knockout of the murine homolog of the NKp46 receptor (Ncr1) which is lethal following influenza infection [379, 382]. NKp46 expression is also increased on NK cells in the lungs of influenza-infected pigs and high expression was associated with areas of detectable influenza nucleoprotein [372].

In addition the HLA-C genotype has been shown to influence NK cell activation to influenza-infected monocytes, implicating HLA-dependent NK cell receptors in the NK cell response to this virus [383]. Two *in vitro* studies have investigated the role of the KIR family of receptors on the control of the 2009 H1N1 influenza strain, yet there was little consensus between these studies. Aranda-Romo *et al* 2012 associated KIR3DS1, KIR2DS5 and KIR2DL5 with increased influenza severity [384]. However, La *et al.* 2011 linked KIR2DL2/3 and functional HLA-C1 interactions with symptom severity but suggested that KIR3DL1/S1 and KIR2DL1 may be protective in HLA-C2 haplotypes [385]. However, both of these studies were underpowered as the allelic and genotypic diversity in both the KIR and HLA requires much larger cohorts to enable assessment of clinical associations between KIR/HLA haplotypes and influenza severity [384, 385]. Thus the extent to which KIR signalling is altered in human influenza infection remains to be explored. Interestingly, unlicensed NK cells (those without functional binding between HLA and KIR, as discussed in section 1.4.2) were shown to be protective in murine influenza infection when licensed NK cells were not [227]. A finding that implies a detrimental role of KIR signalling for NK cell activation to influenza [227]. Influenza infected cells upregulate HLA I expression and greater HLA clustering occurs at the surface of infected cells [203, 227]. Therefore the increased expression and altered membrane organisation of HLA may increase the inhibitory signalling experienced by an NK cell in contact with an IAV-infected cell and thus may enable influenza evasion of NK cell cytotoxicity [203, 227]. However, so far only KIR2DL2 has been shown to functionally bind the surface of human IAV infected cells [240].

Finally, NK cells may also recognise influenza infected cells following the generation of a protective B cell response, whereby IAV-specific antibodies induce NK cell ADCC, as described in section 1.4.1 [319, 386-388]. This process may be important during later stages of viral clearance following the generation of adaptive immunity and prevention of re-infection [319, 387, 389-392].

1.5.3 NK cell Recruitment and Regulation during Influenza Infection

NK cell numbers are increased in mouse and pig lungs following influenza infection, suggesting these cells are recruited to IAV infection [112, 364, 372, 382, 393, 394]. Carlin *et al* recently demonstrated that NK cell recruitment to mice lungs are dependent on chemotactic signalling through CXCR3 and CCR5 [168]. Ligands for these receptors include CXCL9, CXCL10, CXCL11, CCL3, CCL4 and CCL5 [395]. A number of cells may be responsible for this recruitment of NK cells in IAV infection, including macrophages (which express CCL3, CCL4, CXCL9 and CXCL10) and epithelia (which express CCL5) [145-148].

In addition, the pro-inflammatory signalling induced by IAV-infected lung epithelium and sentinel macrophages may play an important role in regulating the NK cell response to this infection [54]. Cytokine exposure has a large effect on NK cell development, cytotoxicity, cytokine production and receptor expression [396]. For instance, type I and III IFNs upregulate NK cell production of IFN-γ and cytotoxic effector functions [254, 397-403]. It therefore follows that IFN-α/β priming of NK cell activity has been shown to be important for NK cell activation in murine influenza infection [404, 405]. Furthermore, IL-12, IL-15, IL-18, cytokines important in NK cell maturation and activation are some of the first cytokines to be produced in the respiratory tract following IAV infection, and are most likely produced by macrophages and DCs [254, 406-408]. Different combinations of cytokines induce unique cytokine profiles from NK cells, suggesting that the inflammatory milieu the NK cell encounters during viral infection may shape the resulting NK cell cytotoxicity and cytokine production [396]. This may be an important aspect in understanding how NK cells may function in the lung environment. Interestingly, many inflammatory cytokines suppress NK cell killing *in vitro,* promoting cytokine production instead [396]. This suggests that “helper-type” NK cells may be generated by extensive cytokine contact and therefore could occur during IAV-induced hypercytokinemia [396].

1.5.3.1 Macrophage and NK cell cross-talk

There is an emerging role for macrophage and NK cell cross talk as a major front line defence against pathogens, particularly at mucosal surfaces [409, 410]. Recent work has suggested that macrophages may have a crucial intermediary role in NK cell activation through cell-cell contact and cytokine secretion [411-418]. NK cell ligands including CD40, CD48, ULPB1-3, MIC-A/B and C-Type Lectin Domain Family 2 Member B have been shown to be expressed by macrophages in various models of infection [133, 247, 253, 378, 419-421]. Furthermore, cytokines produced by the alveolar macrophage such as IL-2, IL-6, IL-12, IL-15 and TNF-α activate NK cells in models of bacterial infection [412, 415, 417, 420, 422]. In addition, macrophages have been shown to play an important role in NK cell regulation in the lung microenvironment as these cells suppress NK cell cytotoxicity at the steady state [366]. Therefore, the relationship between lung macrophages and NK cells may have important implications for NK cell function in infections, particularly as airway macrophages are critical sentinel cells responding to IAV infection [53, 126-134]. There is a lack of knowledge about how these two innate cell types may interact during IAV infection. However, extensive inflammatory signalling from the macrophage could stimulate NK cell cytotoxicity towards IAV-infected cells and have further downstream effects on NK cell cytokine production [254, 423-425].

1.5.4 NK Cell Memory to Influenza

There is some evidence that memory NK cells could be generated in response to influenza infection [345, 352, 426]. For instance murine liver CD49a+ NK cells generated during influenza infection were protective following adoptive transfer and subsequent influenza infections [426]. In addition, murine influenza vaccination has been shown to generate modestly protective NK cell responses following secondary challenge [345]. This may also occur in humans as the functional response of human NK cells to IAV-infection were enhanced post influenza vaccination [352]. However lung CD49a+ NK cells generated in a murine model of IAV were not found to be protective upon secondary IAV challenge [426]. It therefore remains to be seen whether human lung NK cells are capable of recalling past infections with IAV and what impact this may have on infection outcome.

1.5.5 Lung NK cells in COPD

A greater understanding of the role NK cells play during respiratory infection and insult will contribute to our understanding of how these cells function during exacerbation of inflammatory diseases such as COPD. Previous studies have shown that baseline NK cell function is altered in COPD, as NK cells exhibit increased cytotoxicity against lung epithelial cells and have been implicated in lung tissue destruction and emphysema onset [86, 361]. This dysregulated NK cell function may have consequences for viral clearance from the lung but has not yet been investigated.

Finch *et al* demonstrated that increased lung NK cell cytotoxicity in COPD was mediated by enhanced priming of NK cells with IL-15 presented by lung DCs [86]. Although Finch *et al* demonstrated substantial enhanced function through this cytokine priming, NK cell cytotoxicity requires direct recognition of target cells to release NK cell degranulation from intracellular inhibitory signalling (discussed in section 1.4) [199]. However, the signals governing NK cell recognition of COPD epithelial cells are unknown [86]. One candidate is the "stress" ligand MIC-A/B as these proteins are increased on the COPD lung epithelium and have been found to correlate with reduced lung function [361]. MIC-A/B is recognised by the activating NKG2D receptor and could stimulate NK cell activation in the COPD lung, particularly given the primed status of the NK cells [86, 361]. Therefore the increased cytokine stimulation of NK cells by COPD DCs may facilitate a greater responsiveness and destruction of stressed structural cells in the lung [86, 361]. Interestingly, cigarette smoke-induced murine NKG2D ligands have been suggested to prime NKG2D-mediated NK cell activation to virus [427]. Therefore the enhanced cytotoxicity of NK cells in COPD may be further enhanced by viral infections, contributing to greater cellular destruction in COPD exacerbations [427]. Thus, a greater mechanistic understanding of how NK cells are altered in COPD has the capacity to aid development of new interventions and treatments for chronic lung disease.

1.6 Summary

NK cells play an important role in human anti-viral immunity, removing infected cells and producing cytokines important in stimulating adaptive immunity [169-174]. In the past few decades new functional roles for NK cells have been described across the human body [293]. Complex NK cell biology has now been elucidated, including mechanisms of education, integration of receptor signalling and innate memory [199]. Furthermore, unique populations of NK cells have been described in the human uterus, liver and secondary lymphoid, which may have important implications for local immune function in these organs [340].

Despite this advance in understanding NK cell biology, the function of these cells in the human lung is poorly understood. The first bona fide description of the human lung NK cell phenotype was published in 2017, describing highly differentiated but functionally impaired NK cells in this organ [362]. However, the early and potent production of IFN-γ, as well as the capacity for cellular destruction suggest that NK cells could play important roles in controlling respiratory infection [199, 293]. Despite this the NK cell responses to human respiratory virus', such as influenza, have not been fully characterised. In addition, airway macrophages have important roles in regulating NK cells in the lung environment and coordinating innate immune responses to viral infection, but NK cell interactions with this cell type are poorly understood [144]. Finally, it is not currently known if resident NK cell populations exit in the lungs, nor what their functional contribution to lung immunity might be.

1.7 Hypothesis and Aims

The primary hypothesis of this thesis is that NK cells contribute to the anti-influenza immune response in human lung through the production of pro-inflammatory cytokines and destruction of infected cells. Secondly, I hypothesise that resident NK cell populations are present within the human lungs, with distinct roles in human lung infection and diseases, such as COPD.

Therefore, the specific aims of this project are to:

1. Explore the NK cell phenotype in the human lung through characterisation of markers of maturity, homing and activation, drawing comparisons with the peripheral blood.
2. Characterise resident NK cell populations in the lung through the expression of CD49a, CD103 and CD69 and chemokine receptors.
3. Investigate whether resident NK cell populations are altered in lung tissue from COPD patients compared to tissue from controls.
4. Determine whether human resident and non-resident lung NK cells respond to IAV-infection using a model of *ex vivo* infected human lung tissue. Effector functions of NK cells will be confirmed including the production of pro-inflammatory cytokines and measures of degranulation.
5. Develop models of epithelial cell and macrophage IAV infection using primary bronchial epithelia cells (PBECs) and monocyte-derived macrophages (MDMs) to determine the effects of NK cell activation.
6. Characterise the expression of NK cell activating ligands and HLA class I on IAV-infected cells.
7. Characterise the expression of IAV-recognising NK cell receptors, NKp46 and NKG2D, on NK cells during IAV infection.
8. Understand the functional roles of NKp46 and NKG2D in the NK cell response to influenza-infected macrophages.
9. Explore the cross-talk between macrophages and NK cells during influenza infection, including pro-inflammatory cytokine and chemokine production.

To achieve these research aims NK cells from human lung parenchyma will be isolated and characterised by multi-parameter flow cytometry. Flow cytometric measures of NK cell activation will be developed in an established *ex vivo* model of IAV infected human lung tissue [428, 429]. This will be used to explore the function of different lung NK cell populations during influenza infection. Findings from the *ex vivo* model of human IAV infection will be taken forward into *in vitro* models of infection, developing autologous co-culture models to explore NK cell effector function in response to IAV-infected macrophages and epithelial cells. The macrophage is the preferred target for investigating NK cell function in this thesis as these cells show considerable functional contributions to IAV infection and NK cell regulation. Therefore, NK cell receptor ligation will be blocked in the MDM-NK cell co-cultures to assess the functional contribution of activating and inhibitory signalling to NK cells. Finally, the release of cytokines and chemokines from both NK cells and IAV-infected macrophages will be investigated by multiplex ELISA to further explore the cross-talk between these two cell types.

Chapter 2 Materials and Methods

2.1 Ethics and Donor Recruitment

Fresh peripheral blood from healthy volunteers was collected with ethical approval from the Hampshire A Research Ethics Committee (REC) 13/SC/0416 and the South Central Oxford REC 15/SC/0528. Recruitment criteria required individuals to be healthy and aged 18-65. Individuals that had a respiratory infection within one month of recruitment or immunomodulatory drug use were excluded. The demographic information for healthy peripheral blood cohorts are reported in Tables 3.1 and 3.2 respectively.

Lung tissue samples were obtained at Southampton General Hospital from patients undergoing cancer resection surgery. After pathologist assessment, macroscopically normal lung tissue was taken distal to the tumour site and was approved by the Southampton and South West Hampshire REC 08/H0502/32. 27mL of peripheral blood was taken from lung donors immediately prior to surgery. Demographic information for the cancer resection patients is reported Table 3.1. Lung donor COPD was also diagnosed and classified on the basis of a predicted Forced Expiratory Volume (FEV1%) below 80%, according to the Global Initiative for Chronic Obstructive Lung Disease (GOLD) guidelines and the demographic differences of these lung donors are summarised in Table 4.2.

Lastly, undifferentiated human PBMC and matched PBEC were obtained from bronchial brushings of healthy controls with ethical approval of from the South Central Oxford REC (REC 15/SC/0528). All peripheral blood and lung donors gave written consent and a recent medical history.

2.2 Isolation of Peripheral NK cells and Monocyte-Derived Macrophages

120mL of venous human blood was collected from healthy donors and diluted ~1:1 in Dulbecco's phosphate buffered saline (PBS, Sigma-Aldritch, Poole, UK). The diluted blood was then layered over 20 mL of Ficoll-Pacque (GE Healthcare, Little Chalfont, UK) and centrifuged for 35 min at 800 g, 20^{o}C until a visible interface layer formed. PBMCs were then harvested from the PBS-Ficoll interface. To isolate both NK cells and monocytes from PBMCs, magnetic-associated cell sorting (MACS) was performed. PBMCs were washed with 40mL of PBS and resuspended in ice-cold 80 µL Monocyte Isolation Buffer (MIB) per 1x10^{7} cells (MIB; 2 mM EDTA (Sigma-Aldritch) and 0.5% (v/v)

Bovine Serum Albumin (BSA, Sigma-Aldritch) in PBS). All centrifugation steps were performed at 4°C, 400g for 5 min. 10 µL per $1x10^7$ cells of CD14-binding microbeads were then added to the resuspended PBMCs (Miltenyi Biotec, Bergisch Gladbach, Germany). The cells were then incubated on ice for 20 min before washing in 10 mL of ice-cold MIB. Cells were resuspended in 500 µL MIB per $1x10^8$ cells and passed through an LS column (Miltenyi Biotech) suspended in a magnet. Bead-bound CD14+ PBMCs were retained in the column by the magnetic field. The column was then washed three times with 3mL of MIB to ensure CD14+ cell purity. CD14+ monocytes were removed from the column by flushing with 5mL MIB. The extruded monocytes were resuspended in complete Roswell Park Memorial Institute (RPMI)-1640 Medium (Sigma-Aldritch) with 10% (v/v) heat-inactivated foetal calf serum (FCS) and 2 ng/mL GM-CSF (R&D Systems, Minneapolis, USA). Complete RPMI consisted of basal RPMI medium supplemented with 2 mg/mL L-glutamine (Sigma-Aldritch), 0.05 IU/mL Penicillin (Sigma-Aldritch), 50 µg/mL Streptomycin (Sigma-Aldritch), and 0.25 µg/mL Amphotericin B (Sigma-Aldritch). The monocytes isolated during this procedure had been found to be >95% pure in previously published work [430]. Purified monocytes were seeded into either 96 or 48 well plates at a density of either $1.25x10^5$ or $0.5x10^6$ cells/well respectively. Monocytes were then cultured for 12 days at 5% CO_2, 37^0C in a humid environment. MDM culture medium was replaced every 2-3 days. This previously published protocol has been shown to induce a "lung-like" macrophage phenotype, modelling that of human alveolar macrophage in terms of receptor expression and phagocytosis [85, 423, 431, 432]. Thus these cells are described as monocyte-derived macrophages (MDMs) in all subsequent sections.

NK cells were also extracted from PBMCs by MACS, this time with negative selection using the Miltenyi NK cell isolation kit (Miltenyi Biotech). Using this reagent, the remaining CD14- PBMCs were labelled with antibodies against T cells, B cells, stem cells, dendritic cells, monocytes, granulocytes and erythroid cells. To do this, CD14- PBMCs were first resuspended in 40µL of ice-cold MIB and 10µL of Biotin-Antibody Cocktail per 10^7 cells (Miltenyi Biotech). The cells were then incubated on ice for 5 min. A further 30µL of MIB and 20µL of the Microbead cocktail (Miltenyi Biotech) was added per 10^7 cells and cells incubated for another 10 min on ice. The labelled PBMCs were then applied to another LS-column. All non-NK cells remained bound to the column, whilst NK cells were washed through with 3mL of MIB. This protocol achieved a high level of NK cell purity as 94.28 ± 1.43% of isolated cells were CD56+CD3- (N=4, Figure 2.1). MACS isolated NK cells were frozen in 10% Dimethyl sulfoxide (DMSO) / FCS at -80^oC until use.

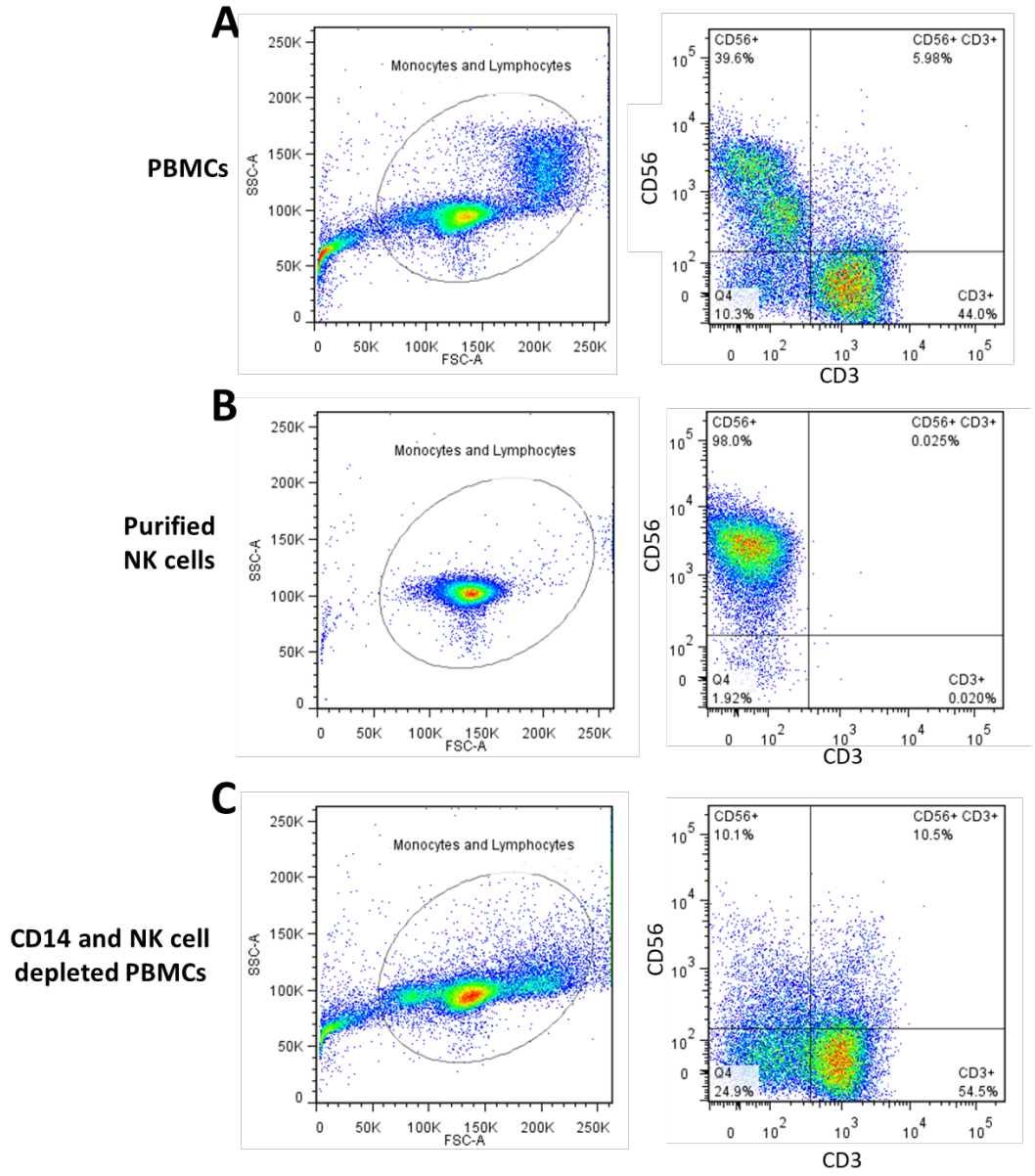

Figure 2.1: Purification of circulating NK cells from human peripheral blood. NK cells were extracted from PBMCs using MACS. The proportion of NK cells in the PBMCs was compared with MACS purified NK cells and cells unlabelled by the MACS process (CD14 and NK cell depleted PBMCs). NK cell purity was assessed by flow cytometry with NK cells defined as CD3-CD56+ cells.

2.3 IAV infection of MDMs

Fully differentiated MDMs were incubated with 1000 PFU/mL of a 2012 stock of live and UV-irradiated X31 virus in 0.1% FCS (v/v) complete RPMI for 2 h, as described previously [423, 429, 433]. UV-irradiated X31 was created by exposing live X31 to UV light for 2 h on ice. Extracellular IAV was removed by washing three time with basal RPMI and viral replication allowed to continue for a further 22 h. The extent of IAV infection was measured by flow cytometry detection of intracellular IAV NP-1. To do this MDMs were detached from well surfaces by incubation with 200µL of non-enzymatic cell dissociation solution (Sigma-Aldritch) for 20 min at 37°C. Suspended MDMs were then collected and stained for flow cytometry as described in section 2.8.

2.4 Generating Submerged PBEC Cultures

Human PBEC cultures were grown out of bronchial brushings taken during bronchoscopy of healthy volunteers (REC 15/SC/0528). Epithelial cells removed from the bronchial surface were cultured in a collagen–coated T75 flask in 10 mL of complete PBEC culture medium. Complete PBEC media consisted of Pneumacult ^{TM}-Ex Basal Medium (Stemcell Technologies, Vancouver, Canada) supplemented with a 1:50 dilution of Pneumacult^{TM}Ex Plus supplement (Stemcell Technologies), 0.48µg/mL hydrocortisone (Stemcell Technologies), 0.25 µg/mL Amphotericin B (Sigma-Aldritch) and 0.05mg/mL Gentamycin (Thermofisher Scientific, Massachusetts, USA). All culture vessels were pre-treated with 60 µg/mL type I bovine collagen (PureCol^{TM}, Advanced Biomatrix, California, USA) in dH_2O for at least 30 min at 37°C prior to use. Once PBECs covered 70-80% of the flask surface, cells were frozen at -80°C, with long-term storage in liquid nitrogen. To remove PBECs from the culture vessel, culture media was discarded and the adherent cells rinsed with 10mL of PBS. The cells were then incubated with 0.5 mL of 50mg/mL of trypsin and 20mg/mL EDTA (Sigma-Aldritch) at 37°C for 10 min or until cells became spherical. Cells were removed from the flask surface by agitation and 10mL of 10% FCS in complete pneumocult added to the flask. The PBEC cell suspension was collected, centrifuged at 400g for 5 min and frozen in 10% (v/v) DMSO / 20% (v/v) FCS / 70% (v/v) complete Pneumocult medium at $0.5x10^6$ cells/mL. To resuscitate frozen PBECs the cells were thawed and immediately added to complete Pneumocult with 10% (v/v) FCS. Cells were then seeded over collagen coated T75 flasks at a density of $5x10^4$ cells/mL and cultured in 10mL of complete Pneumocult media (Stemcell Technologies) at 37°C, 5% CO_2 in a humidified environment. PBEC culture media was replaced every 2-3 days until cells reached 70-80% confluency (approx. 2-3 weeks).

2.5 IAV Infection of PBECs

To infect PBECs with X31, cells were first seeded into a 24-well plate at a density of 100, 000 cells/well. Seeded PBECs were allowed to adhere to well surfaces for 16 h prior to IAV infection before washing with PBS. Culture media was then replaced with starvation media to prevent PBEC replication during IAV infection. Starvation media consisted of Pneumacult^{TM}-ex Basal Medium with 0.3% (v/v) of BSA (Sigma-Aldritch) and a 1:100 dilution of Insulin-Transferrin-Selenium solution (Sigma-Aldritch, working concentration; 10µg/mL insulin, 5.5µg/mL transferrin and 5ng/mL sodium selenite). PBECs were allowed to adjust to starvation media for one hour before addition of 57, 000 IU/mL of a 2017 stock of live or UV-irradiated X31. X31 dose was titrated in the PBEC monolayer to achieve infection of 30% of the cells, in keeping with the MDM infection model (Figure 6.18). PBECs were incubated with X31 for 2 h before extracellular virions were removed by washing in PBS and the cells incubated for a further 22 h. To assess IAV replication and PBEC viability the cells were detached from well surfaced by treatment with 0.2 mL of 50mg/mL of trypsin and 20mg/mL EDTA (Sigma-Aldritch) for 5 min at 37°C. Suspended PBECs were then centrifuged at 400 g for 5 min before undergoing flow cytometry staining as described in section 2.8. PBECs which had experienced 2-3 sets of passage were used in these experiments.

2.6 NK Cell Culture with IAV-Infected MDMs and PBECs

IAV-infected MDMs and PBECs were cultured with autologous NK cells to measure NK cell functional responses. Prior to NK cell addition MDM and PBEC culture medium was removed by washing three times with PBS and replaced with 400µL of 0.1% (v/v) FCS in complete RPMI. Autologous NK cells had been stored at -80°C prior to use and were first brought to room temperature (RT). The thawed NK cells were then added drop wise into 10% FCS (v/v) complete RPMI, pre-warmed to 37^{o}C. To remove toxic DMSO, the cells were centrifuged at 400g for 5min and washed with 10 mL of basal RPMI before resuspending in 0.1% FCS (v/v) RPMI. NK cells were counted in a haemocytometer and adjusted to an appropriate concentration. 100µL of thawed NK cells were then added to MDM and PBEC cultures at an appropriate effector to target cell ratios (E:T). For MDM-NK cell co-culture this was 1:5 and for PBEC-NK cell co-culture it was 1:10 (unless otherwise stated). Dead NK cells were excluded from the calculation of E:T through trypan blue staining.

For PBEC-NK cell co-cultures, autologous PBMCs from each donor had been stored at -80°C. Therefore, the PBMCs were defrosted and washed in 10mL of PBS as described previously. The

PBMCs were then resuspended in ice-cold MIB and NK cells isolated by MACS prior to co-culture (as described in section 2.2). The MACS-isolated NK cells were washed again in 10mL of PBS, resuspended in 0.1% FCS (v/v) RPMI and adjusted to an appropriate concentration following counting in a haemocytometer.

NK cells were incubated with infected target cells for 6 h, with 2 µM of monensin (eBiosciences) added 1 h after the addition of NK cells. As a positive control for NK cell activation, uninfected MDMs were also stimulated with 1.34 µM Phorbol Myristate Acetate and 81 nM Ionomycin (Cell Stimulation Cocktail, eBiosciences, Hatfield, UK) according to manufacturer's instructions. Non-adherent cells were then harvested from co-cultures and NK cell functional markers analysed by flow cytometry (described in section 2.8). Culture supernatants were also collected for analysis by ELISA and Luminex, in which case monensin was not added to co-cultures. Culture supernatants for ELISA were centrifuged at 800 g for 5 min, aliquoted and stored at -80° until use.

2.7 Transwell Separated Co-cultures and Blocking Experiments

Physical contact between MDMs and NK cells was prevented through culturing in a transwell (TW) system (Corning, New York, USA) with 0.4µM pores. NK cells were cultured in the top compartment with MDMs beneath. Transwell cultures were carried out at the same volume and cellular concentrations of the co-cultures described in section 2.6. In addition, NKG2D and NKp46 ligands were also blocked on MDM surfaces with chimeric receptor Ig fusion construct (R&D systems). In which case 10µg/mL of NKG2D receptor Fc and 5 µg/mL of NKp46 receptor Fc was incubated with MDMs for 20min at 37°C, 5%CO_2 prior to the addition of NK cells. MDM HLA class I was also blocked from binding NK cells through incubation of MDMs with 20 µg/mL of low endotoxin, azide-free αHLA-A/B/C antibody (W6/32; Biolegend).

2.8 Flow Cytometry

Cells collected for flow cytometry analysis were washed with 2mL of PBS and centrifuged at 4°C, 400 g for 5 min (as for all subsequent centrifugation steps). All staining steps were carried out in the dark. For functional analyses cellular viability staining was performed, in which case the cells were resuspended in 100µL PBS and incubated with a 1:100 dilution of Zombie-Violet (Biolegend,

San Diego, USA) amine binding dye for 30 min on ice. The cells were then washed in 1mL of PBS prior to flow cytometry staining of cell surfaces. For surface staining cells were resuspended in 100µL Fluorescence-Activated Cell Sorting (FACS) buffer consisting of 2 mM EDTA (Sigma-Aldritch), 0.5% BSA, Sigma-Aldritch) in PBS. In addition, 2 mg/mL human IgG (Sigma-Aldritch) was included in the FACS buffer to block cell surfaces. Cells were then incubated with antibodies against NK, epithelial and macrophage cell markers for 30min on ice, or alternatively with isotype controls, as listed in Tables 2.1 and 2.2. The antibodies for key NK cell proteins and functional markers were titrated for co-culture experiments, as shown in Figure 2.2 and reported in Table 2.1.

Following incubation with antibodies, the cells were washed in 1mL of FACS buffer and fixed with 2% paraformaldehyde (Sigma-Aldritch) in FACS buffer. Alternatively, for analysis of intracellular molecules, cells were treated with 200µL of Cytofix/Cytoperm (BD) for 20 min on ice and resuspended in 100 µL of Permwash (BD) to permeabilise cells. Antibodies against intracellular antigens were then incubated with the cells for 30 min on ice. Following staining NK cells were washed, resuspended in 200µL FACS buffer and analysed with the FACSaria II (BD Biosciences, Oxford, UK), FACSDiva software (BD Biosciences) and FlowJo v7.6.5 software (Tree Star, Ashland, USA). Boolean gating was performed based on negative straining from isotype controls. specific MFI (sMFI) was calculated by subtraction of baseline fluorescence in isotype controls from positive staining.

To detect NK cell receptor ligands on MDM surfaces receptor fusion constructs were used in place of antibodies. To do this, MDMs were first blocked with 2 mg/mL human IgG (Sigma-Aldritch) in FACS buffer for 15 min at RT. Receptor fusion constructs or appropriate non-binding controls (R&D systems, Minneapolis, USA) were then added to the cells and incubated for 45 min on ice. 10µg/mL of NKG2D and 5µg/mL NKp46 Fc were used for staining unless otherwise stated. MDMs were then washed in 1mL of FACS buffer and resuspended in 100µL of FACS buffer. Fusion construct binding was detected through incubation with 5 µL of α-human IgG-PE-Cy7 (Ms IgG2aκ, clone HP6017, Biolegend) for 30 min on ice.

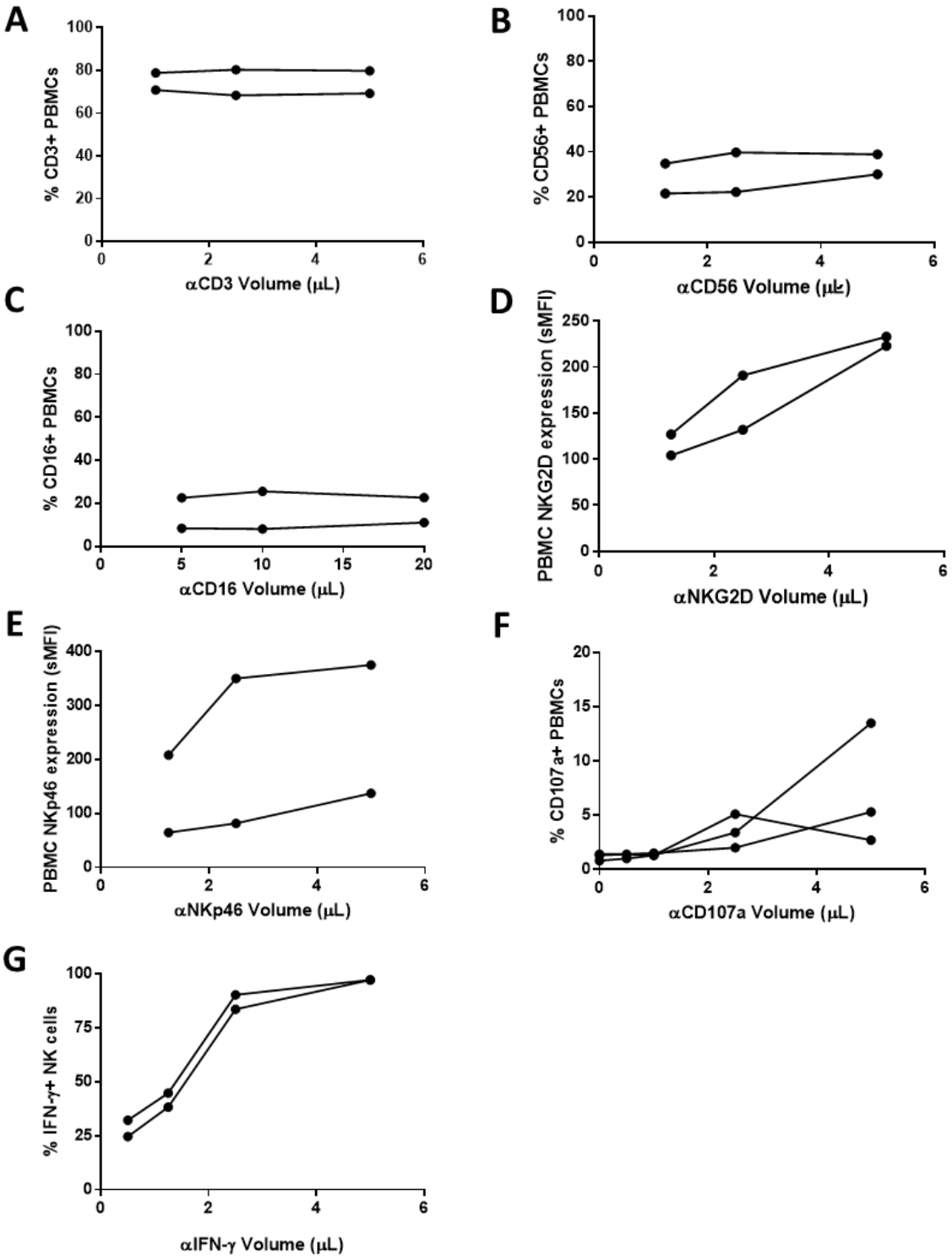

Figure 2.2: Antibody volumes for staining peripheral blood NK cells. Antibodies against NK cell surface proteins and functional markers were diluted from manufacturer recommended volumes against $1x10^6$ PBMCs (N=2, except αCD107a N=3). (**F, G**) IFN-γ and CD107a expression was stimulated by treatment with PMA/I for 4hr and monensin for 3hr, as described in section 2.7. (**G**) αIFN-γ antibody was titrated against $1x10^6$ MACS purified NK cells.

Antigen	Fluorophore	Isotype	Clone	Volume (µL)	Company
Phenotyping:					
CD3	PerCP	MsIgG1κ	UCHT1	5 *(1)*	Biolegend
CD16	FITC	MsIgG1κ	3G8	20 *(5)*	BD Biosciences
CD45	BV510	MsIgG1κ	HI30	5	BD Biosciences
CD49a	PE	MsIgG1κ	SR84	20	BD Biosciences
CD56	PE-Cy7	MsIgG1κ	HCD56	5 *(2.5)*	Biolegend
CD57	Pacific Blue	MsIgM	HCD57	5	Biolegend
CD69	BV421	Ms IgG1κ	FN50	5	Biolegend
CD103	APC	Ms IgG1κ	Ber-ACT8	5	Biolegend
CD117	PECF594	MsIgG1κ	YB5.B8	5	BD Biosciences
CD158b	PE	MsIgG2b	CH-L	20	BD Biosciences
NKG2C (CD159c)	APC	Human recombinant	REA205	5	R&D Systems
CXCR3 (CD184)	APC-Cy7	MsIgG1κ	G025H7	5	Biolegend
CXCR6 (CD186)	PE-DAZZLE	MsIgG2a	56811	5	Biolegend
CCR5 (CD195)	PE-DAZZLE	Rat IgG2b	J418F1	5	Biolegend
NKG2D (CD314)	APC-Cy7	MsIgG1κ	1D11	5	Biolegend
NKp46 (CD335)	PE / BV421	MsIgG1κ	9E2	5 *(1.25)*	Biolegend
Functional Studies:					
CD3	APC	Ms IgG1κ	UCHT1	5	Biolegend
CD45	APC-CY7	MsIgG1κ	HI30	5	BD Biosciences
CD107a	BV510	Ms IgG1κ	H4A3	5	Biolegend
EpCAM (CD326)	PerCP-Cy5.5	Ms IgG1κ	EBA-1	20	BD Biosciences
Gzm-B	APC	Ms IgG1κ	QA16A02	5	Biolegend
HLA-DR	APC-Cy7	Ms IgG2a κ	L243	5	BD Biosciences
IFN-γ	PerCP-Cy5.5	Ms IgG1κ	4S.B3	5	Biolegend
MIC-A/B	APC	Ms IgG2a κ	6D4	5	Biolegend
NP1	FITC	Ms IgG1κ	431	1	Abcam

Table 2.1: Flow cytometry antibodies. The antibodies used to explore NK cell phenotype and function are listed along with clone and volumes used in experiments. The reported volume of antibody was added per 20 lung tissue fragments or $1x10^6$ cells. Some antibody volumes were reduced in the NK-MDM or NK-PBEC co-culture experiments following antibody titration (see Figure 2.2) in which case the alternative volume shown italicised and in brackets. Ms = mouse, FITC = Fluorescein isothiocyanate, PerCP = Peridinin-chlorophyll protein, PE = phycoerythrin, APC = Allophycocyanin, BV421 = Brilliant violet 421, BV510 = Brilliant Violet 510, Cy5.5 =cyanine 5.5 Cy7 = cyanine 7.

Isotype	Fluorophore	Clone	Volume (µL)	Company
Ms IgG1κ	APC	MOPC-21	5	Biolegend
Ms IgG1κ	APC/Cy7	MOPC-21	5	Biolegend
Ms IgG1κ	BV421	MOPC-21	5 *(1.25)*	Biolegend
Ms IgG1κ	BV510	X40	5	BD Biosciences
Ms IgG1κ	FITC	MOPC-21	20 *(1)*	BD Biosciences
Ms IgG1κ	PE	MOPC-21	20	BD Biosciences
MsIgG1κ	PECF594	X40	5	BD Biosciences
Ms IgG1κ	PE-Cy7	MOPC-21	5 *(2.5)*	BD Biosciences
Ms IgG1κ	PerCP	MOPC-21	5 *(1)*	Biolegend
Ms IgG1κ	PerCP-Cy5.5	P3.6.2.8.1	5	eBiosciences
Ms IgG2a	APC	MOPC-21	5	Biolegend
Ms IgG2aκ	APC-Cy7	MOPC-21	5	Life Tech
Ms IgG2aκ	PE-DAZZLE	MOPC-21	5	Biolegend
Ms IgG2bκ	PE	MOPC-21	5	Biolegend
Ms IgM	Pacific Blue	MM-30	5	Biolegend
Rat IgG2bκ	PE-DAZZLE	RTK4530	5	Biolegened
REA Control	APC	REA293	5	Miltenyi Biotech

Table 2.2: Isotype controls for flow cytometry. Isotype species and antigen are reported alongside antibody volumes. The reported volume of antibody was added per 20 lung tissue fragments or $1x10^6$ cells. Some antibody volumes were reduced in the NK-MDM or NK-PBEC co-culture experiments following antibody titration, in which case the alternative volume is italicised and in brackets. Ms = mouse, FITC = Fluorescein isothiocyanate, PerCP = Peridinin-chlorophyll protein, PE = Phycoerythrin, APC = Allophycocyanin, BV421 = Brilliant violet 421, BV510 = Brilliant Violet 510, Cy5.5 =cyanine 5.5 Cy7 = cyanine 7.

2.9 ELISA

IFN-γ ELISA MAX (Biolegend), and Granzyme B Duoset ELISA (R&D Systems) were performed on the culture media from both infected lung tissue and NK-MDM co-cultures. Co-culture supernatants were diluted 1:2 for both IFN-γ and Gzm-B analysis. Whereas for IFN-γ analysis of lung tissue, culture supernatants were diluted 1:3 when hpi > 6 and analysed neat in Gzm-B ELISAs. Individual protocols and antibody working concentrations can be found in the manufacturer's instructions, however the following general protocol was used for both assays.

MaxiSorp ELISA plates (Biolegend) were coated with 100 µL of capture antibody at the required concentration at either 4°C or RT 24 h prior to running the ELISA. ELISA plates were then washed three times with PBS-0.05% (v/v) Tween (washing buffer), as were all subsequent wash steps. The ELISA plates were then blocked with 200 µL PBS-1% (v/v) BSA solution (or equivalent buffer) for 1 h at RT. The blocking buffer was then removed through repeated washes in washing buffer. Culture media was diluted if required and 50 µL added to the plate in duplicates. A series of protein standards were also included on each ELISA plate. Samples were incubated on the plates for 2 h at RT before further washing and addition of 100 µL of detection antibody. Plates were incubated for 2 h at RT, washed and then incubated with 100 µL of streptavidin-horse radish peroxidase for 30 min at RT. The plates were washed a final time before addition of 3,3',5,5'-tetramethylbenzidine substrate in the dark. The enzymatic reaction was stopped by the addition of 50 µL of 1M H_2SO_4 and the degree of colour change measured by a microplate reader at 450 nm with a 550 nm correction (Multiskan Ascent, Agilent Technologies, Wokingham, UK). Molecule concentrations were determined by a four-parameter logistic curve-fit analysis of the absorbance reading to known standard concentrations.

2.10 Lactate Dehydrogenase (LDH) Release Assay

MDM-NK cell co-culture media was also assessed for extracellular LDH as a measure of cell death. This was performed with the CytoTox 96 Non-Radioactive Cytotoxicity Assay (Promega, Madison, USA). 100µL of culture supernatants were added to each well of a 96-well plate followed by 50µL of the CytoTox 96 Reagent. Plates were then incubated in the dark for 30 min at RT before the addition of 50µL of stop solution. Absorbance at 490nm was then measured on a microplate reader (Multiskan Ascent, Agilent Technologies).

2.11 Luminex Assay

Luminex analysis of MDM-NK cell supernatants was performed using a premixed 28-plex panel with a magnetic bead system, according to manufacturer instructions (R&D systems). In brief 50µL of the microparticle cocktail was added to a 96-well plate, followed by 50µL of neat culture supernatant or pre-prepared standards. The Luminex plate was incubated with agitation for 2 h at RT and the plate washed three times with 100µL of wash buffer (R&D systems). Microparticles were held to the bottom of the plate during wash steps with a Bio-Plex Handheld Magnetic Washer (Bio-Rad, California, USA). 50µL of Biotin Antibody cocktail was added to each well and the plate incubated with agitation for 1 h in the dark. Antibody was removed through three washes with wash buffer and 50µL of Streptavidin-PE added (R&D systems). The plate was washed three times and microparticles resuspended in 100µL of wash buffer. The magnitude of the PE-derived signal was analysed for each bead using a Bio-Plex 200 System (Bio-Rad) and analyte concentrations calculated based on the detection of known standard concentrations.

2.12 Analysis of human lung NK cells

2.12.1 Isolating Mononuclear Cells from Human Lung Parenchyma

Following removal from the body lung parenchyma was cut into 1-5mm fragments whilst submerged in cold RPMI (Sigma-Aldritch). Lung tissue fragments were washed extensively in PBS to remove contaminant blood. The lung tissue was then rested for 16 h in complete RPMI-10% (v/v) FCS (Sigma-Aldritch) at 37°C, 5% CO_2 in a humidified environment. Lung fragments were then agitated in 0.5 mg/mL collagenase (Sigma-Aldritch) in basal RPMI for 15 min at 37^{o}C to break up the tissue. The collagenase-digested tissue was then applied to 0.7 µm filters to remove the remaining tissue fragments. The filtered lung cells were then washed in 10mL PBS and centrifuged at 400 g for 5 min before resuspension in 3 mL PBS. The resuspended cells were then layered over 2 mL of Ficoll-Pacque (GE Healthcare) and centrifuged for 35 min at 800 g, 20^{o}C until a visible interface layer of mononuclear cells formed. These cells were harvested and washed in 20mL of PBS prior to flow cytometry staining described in section 2.8. Density gradient centrifugation was also used to isolate PBMCs from the peripheral blood of lung donors. 27mL of peripheral blood was collected just prior to resection surgery, diluted ~1:1 in PBS and layered over 20 mL of Ficoll-Pacque.

2.12.2 Flow Cytometry Analysis of the Lung NK Cell Phenotype

Mononuclear cells isolated from human lung and matched peripheral blood underwent flow cytometry straining of cell surfaces, as described in section 2.8. The phenotyping antibodies and corresponding isotype controls used in this analysis are listed in Tables 2.1 and 2.2 respectively. NK cells were defined as CD45+CD3-CD56+ cells, and further divided into $CD56^{bright}$CD16-, $CD56^{dim}$CD16+ and $CD56^{dim}$CD16- populations, as shown in Figure 2.3. A median of 410,676 ± 153,226 CD45+ leukocytes were isolated per resection sample, according to flow cytometry analysis. The median total events in the NK cell gate was 10,011 ± 9,073 with a minimum value of 2,760 (N=8). For the rarer $CD56^{bright}$ CD49a+ NK cells the median number of events fell to 940 ± 194 with a minimum value of 130. To be included in the analysis a minimum 100 events in this gate was required of any cell type.

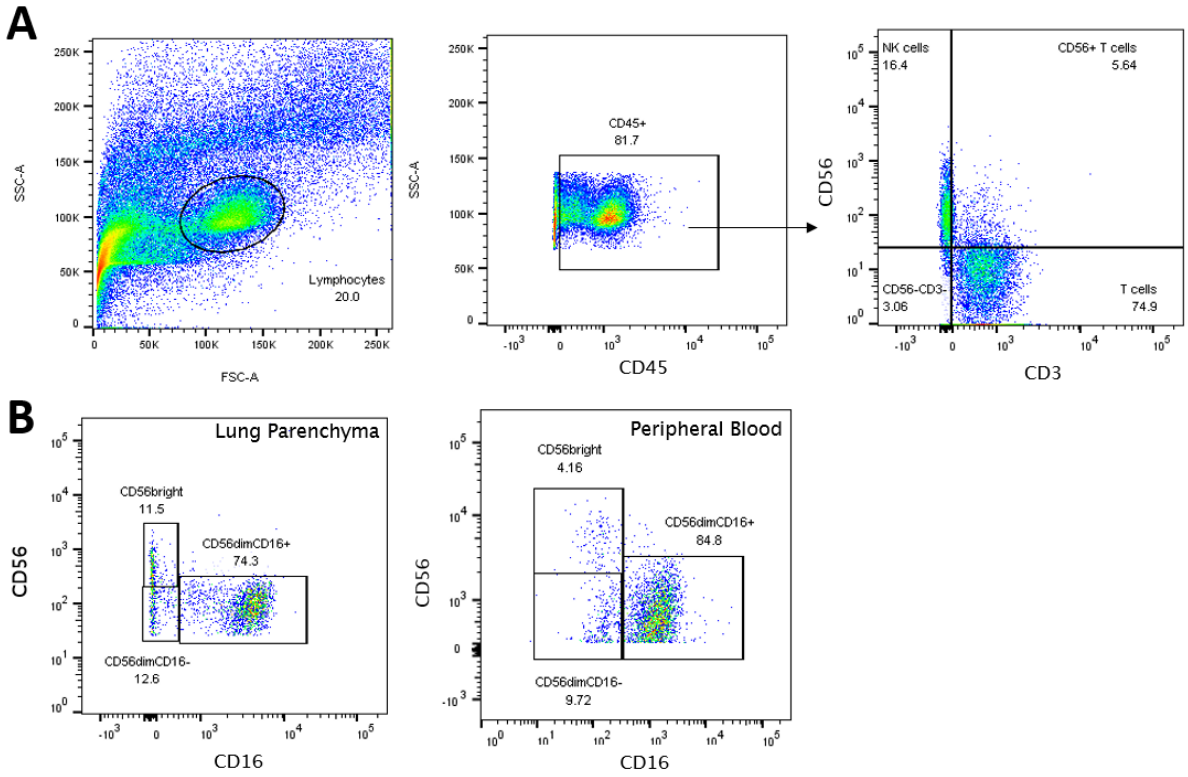

Figure 2.3: Gating strategy to define NK cells in the peripheral blood and lung. (A) NK cells were defined as CD45+CD3-CD56+ lymphocytes. Representative flow cytometry gating on lung cells is shown. $CD56^{bright}$CD16-, $CD56^{dim}$CD16+ and $CD56^{dim}$CD16- NK cells were further distinguished in the lung parenchyma **(B)** and peripheral blood **(C)** as shown.

2.13 IAV Infection of Human Lung Explants

Lung tissue was cut into 4-6mm^2 pieces with 6 fragments/well placed in a 24-well plate and washed thoroughly with cold RPMI to remove contaminant blood. The lung explants were then infected with live or UV-irradiated X31 (H3N2) Influenza A Virus (Virapur, San Diego, USA) in 0.1% FCS (v/v) complete RPMI, as published previously [423, 429].

To infect lung tissue X31 virus was incubated with the explants for 2 h at 37°C, 5% CO_2 before extracellular virions were removed by washing three times in 500µL of PBS. The lung explants were then cultured in fresh media for a further 22h. As a positive control for lymphocyte activation uninfected lung explants were also treated with 1.34 µM Phorbol Myristate Acetate and 81 nM Ionomycin (Cell Stimulation Cocktail, eBiosciences, Hatfield, UK). Each treatment was performed in quadruplicate and pooled before digestion. Following a total incubation time of 24 h lung leukocytes were released from the tissue by incubation in 0.5 mg/ml collagenase (Sigma-Aldritch) in basal RPMI at 37°C under agitation. Lung digests were then filtered to remove any large tissue fragments and the remaining cells stained for flow cytometry (described in section 2.8). Flow cytometry antibodies against key functional markers were first titrated in lung mononuclear cells to confirm saturation of antigens on NK cells, as shown in Figure 2.4. The median number of events for CD56^{bright}CD49a+ NK cells in X31-infected explants was 1,035 ± 1,024 with a minimum value of 164 (N=5). This was typical of both untreated and UV-irradiated X31 treated explant tissue. Culture supernatants were also collected, centrifuged at 800 g for 5 min and stored at -80°C prior to assessment by ELISA (described in section 2.9).

To investigate NK cell degranulation and HLA class I expression on infected cells 200,000 PFU/mL of a 2012 stock of X31 was used. However, a 2017 stock of X31 was used to investigate IFN-γ production. The 2017 stock of X31 was titrated in the lung tissue to give an equivalent level of infection to the 2012 X31 stock (Figure 2.4) and 3.15x10^7 IU/mL used to infect lung tissue. IAV replication was confirmed in the lung tissue through detection of intracellular viral Nucleoprotein-1 (NP-1) expression by flow cytometry (section 2.8). To measure the accumulation of IFN-γ in lung lymphocytes, 2µM Monensin Solution (eBiosciences) was added to lung explants 16 hpi and the explants incubated for a further 24h, giving a total experiment time of 40 h for this measure.

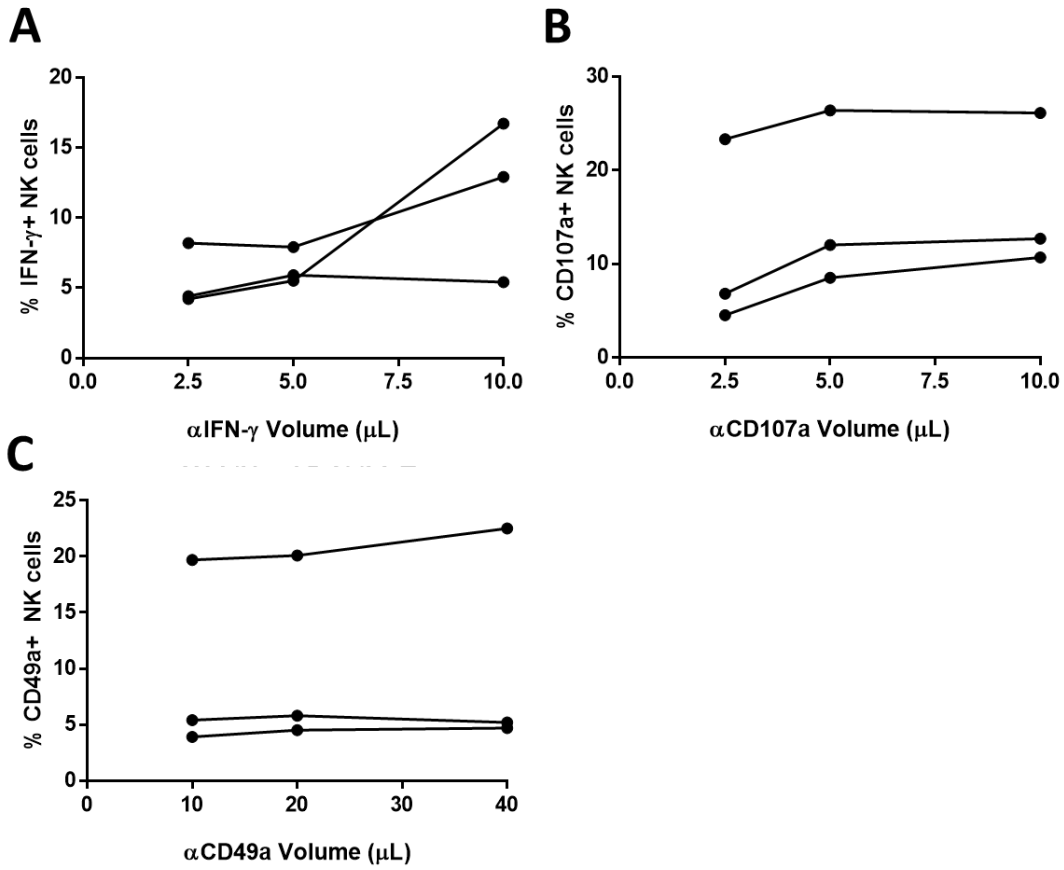

Figure 2.4: Antibody titrations against mononuclear cells isolated from human lung tissue. Antibodies against IFN-γ, CD107a and CD49a were diluted from manufacturer recommended volumes and titrated against mononuclear cells isolated from human lung tissue. IFN-γ and CD107a expression was stimulated by treatment with PMA/I for 6 h and monensin for 5 h.

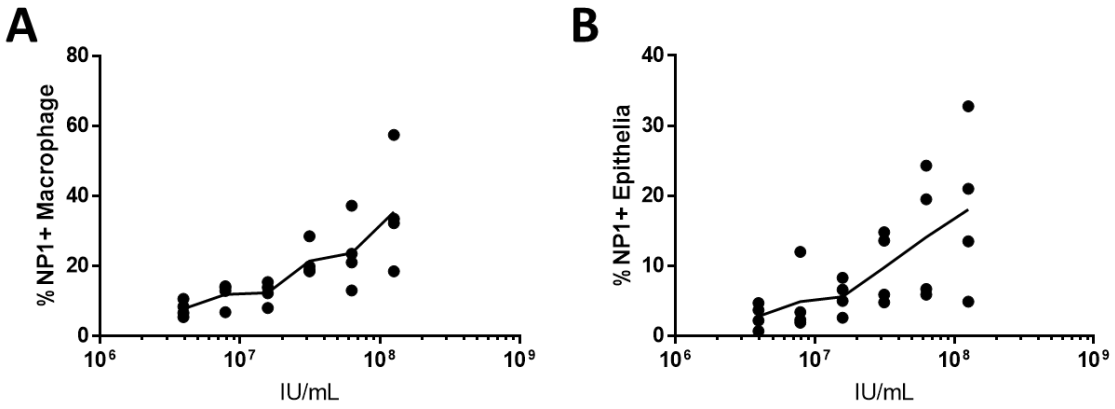

Figure 2.5: **2017 X31 stock titration in human lung explants.** Human lung was incubated with a 2017 stock of X31 IAV for 2 h before extracellular virus was removed. The tissue was then incubated for a further 22 h before collagenase digestion. IAV replication was measured in airway macrophages (**A**) and epithelial cells (**B**) by intracellular IAV NP-1 expression.

2.14 Statistical Analysis

In general the data in this thesis was considered non-parametric as the number of repeats (typically N=6) is too small for accurate normality testing [434]. Even in the larger phenotyping data sets of N=15 or N=22 the data was considered non-parametric due to high heterogeneity in human sampling and a clear skew in some data sets. Thus the data is presented as medians and interquartile range (IQR) and statistical analyses were performed using either a Chi-squared test, Fisher's test, Wilcoxon's matched-pairs signed-rank test, Mann-Whitney U test and Kruskal-Wallis or Friedman's test with Dunn's multiple comparison testing, as appropriate. All statistical analysis was performed with GraphPad Prism v7.0 (GraphPad Software Inc., San Diego, USA). Results were considered significant if $P<0.05$.

Chapter 3 Assessing the Phenotype of Peripheral Blood NK Cells

3.1 Introduction

NK cells are important effectors of anti-viral immunity, providing a source of early IFN-γ and removing infected cells by targeted cytotoxicity [169-174]. As described in section 1.4.5 human NK cells can be divided into subsets based on the expression of CD56 and CD16. In the blood ~90% of NK cells are $CD56^{dim}$CD16+ cells and ~10% are $CD56^{bright}$ [276]. $CD56^{bright}$ NK cells are a more immature precursor to $CD56^{dim}$ NK cells, with differential expression of NK cell receptors [270, 272, 273, 275, 296]. $CD56^{dim}$CD16+ NK cells are thought to have a strong cytotoxic potential whereas $CD56^{bright}$ NK cells are more potent producers of cytokines [259, 295, 302-304, 308, 309]. However, these proposed functional differences have been disputed [189, 310-312]. In addition $CD56^{dim}$CD16- NK cells have also been identified in the peripheral blood, possibly representing a post-activation NK cell phenotype [313-317, 320]. Recently, a number of studies have described NK cells isolated from human organs as phenotypically distinct from the peripheral blood, with different proportions of $CD56^{bright}$ and $CD56^{dim}$ NK cells [190, 271, 293, 302, 305, 307]. However, there is limited information on the NK cell phenotype in the lung.

One of the aims of this thesis was to investigate the phenotype and function of NK cells from resected human lung compared to the circulation. However, NK cells are rapid innate responders to change and infection within the body and their phenotype and functions are plastic [435, 436]. Removal from the body, purification and extraction from lung tissue involves *in vitro* handling which may affect the phenotypic measurements in this study. Furthermore, cancer resection patients are typically older and commonly ex-smokers (Table 3.1) which could also impact on the reported NK cell phenotype [362]. Therefore, this chapter will investigate how *in vitro* manipulation and donor demographics affect the NK cell phenotypes reported in this thesis. To do this, PBMCs from healthy donors were cultured *in vitro,* purified and stored at -80°C. The expression of NK cell CD56, CD16, CD57, CD158b and activating receptors were measured by flow cytometry. In addition, the peripheral NK cell phenotype will be compared between healthy donors and lung tissue donors to examine any disease-specific effects on NK cells. Finally, the impact of donor age, gender and smoking status is explored to understand how these variables may affect the lung NK cell phenotype presented in this study.

3.2 Results

3.2.1 Culturing Peripheral Blood NK cells *in vitro*

Understanding how culture conditions affect primary human NK cells is important to ensure the development of physiologically relevant models and results. To investigate whether short-term *in vitro* culture may affect the phenotype and viability of NK cells, PBMCs from healthy donors (REC 13/SC/0416) were cultured for 24h in complete RPMI (Figure 3.2). NK cells were defined as CD45+CD3-CD56+, as shown in Figure 2.3. $CD56^{bright}$, $CD56^{dim}CD16+$ and $CD56^{dim}CD16-$ NK cells were all identified by flow cytometry. Small increases in the proportion of $CD56^{dim}CD16-$ and $CD56^{bright}$ NK cells were detected following *in vitro* culture compared to freshly isolated PBMCs ($CD56^{dim}CD16-$ 5.8% vs 13.3% and $CD56^{bright}$ 3.4% vs 7.2% respectively, N=3, Figure 3.2). This corresponded with a slight reduction of $CD56^{dim}CD16+$ cells from 88.8% to 79.2% after culture (N=3, Figure 3.2). Therefore, i*n vitro* conditions appeared to slightly alter the proportions of $CD56^{bright}$ and $CD56^{dim}$ subsets but largely maintained the existing phenotype, although a larger sample size is required for statistical testing.

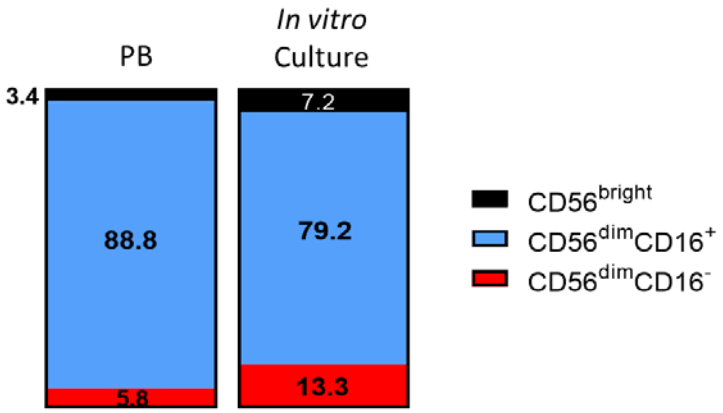

Figure 3.1: The effect of in vitro culture on the proportion of NK cell subsets. NK cell subsets were measured in freshly isolated PBMCs (N=10). PBMCs were then cultured for 24h at $1x10^6$ cells/mL in FCS containing-RPMI (N=3). The surface expression of CD56 and CD16 on peripheral NK cells was analysed by flow cytometry.

The FCS component of culture media has been suggested to alter the phenotype of lung epithelial cells and therefore was also assessed for effects on NK cells [437]. FCS was removed from the culture media of freshly isolated PBMCs for 24h and cellular viability measured through increased permeability detected by amine-binding dye (Figure 3.2). Without FCS NK cell recovery and viability was reduced (Figure 3.3 A and B) and the proportions of NK cell subsets altered (Figure 3.3 C, E and G). The percentage of $CD56^{dim}CD16+$ NK cells was reduced from 79.2% to 69.9% whilst proportions of $CD56^{bright}$ and $CD56^{dim}CD16-$ NK cells increased when FCS was removed from culture media (7.2 to 8.4% and 13.3% to 18.4% respectively). Thus it appeared that media lacking FCS exacerbated the change to NK cell subset proportions observed after *in vitro* culture (Figure 3.2 and 3.1).

The loss of CD16 from NK cell surfaces may be linked to NK cell viability, as $CD56^{dim}CD16-$ NK cells were the least viable in culture conditions, compared with $CD56^{bright}$ and $CD56^{dim}CD16+$ NK cells (63.8% vs 96.1 and 99% respectively Figure 3.2 D, F and H). $CD56^{dim}CD16-$ viability was also the most affected by removal of FCS, dropping by 20.2% whilst $CD56^{bright}$ and $CD56^{dim}CD16+$ viability only reduced by 0.5% and 2.2% respectively. In previous reports CD56 and CD16 downregulation has been associated with NK cell activation and activation-induced apoptosis, which may explain the findings in Figure 3.2 [314, 316, 317]. It is unclear whether this phenotypic change in CD56 and CD16 results from NK cell activation or from NK cell death. However, as activated NK cells undergo controlled apoptosis, the two phenomena may be intrinsically linked [438]. Removal of FCS from the culture media most likely resulted in less optimal culture conditions and more NK cell death, causing in an increase in $CD56^{dim}CD16-$ NK cells (Figure 3.2). Although, the expansion or loss of certain subsets during culture time cannot be excluded as an alternative explanation for this finding. Taken together, these results show that the inclusion of FCS in the culture media is essential to maintaining NK cell viability and subset proportions.

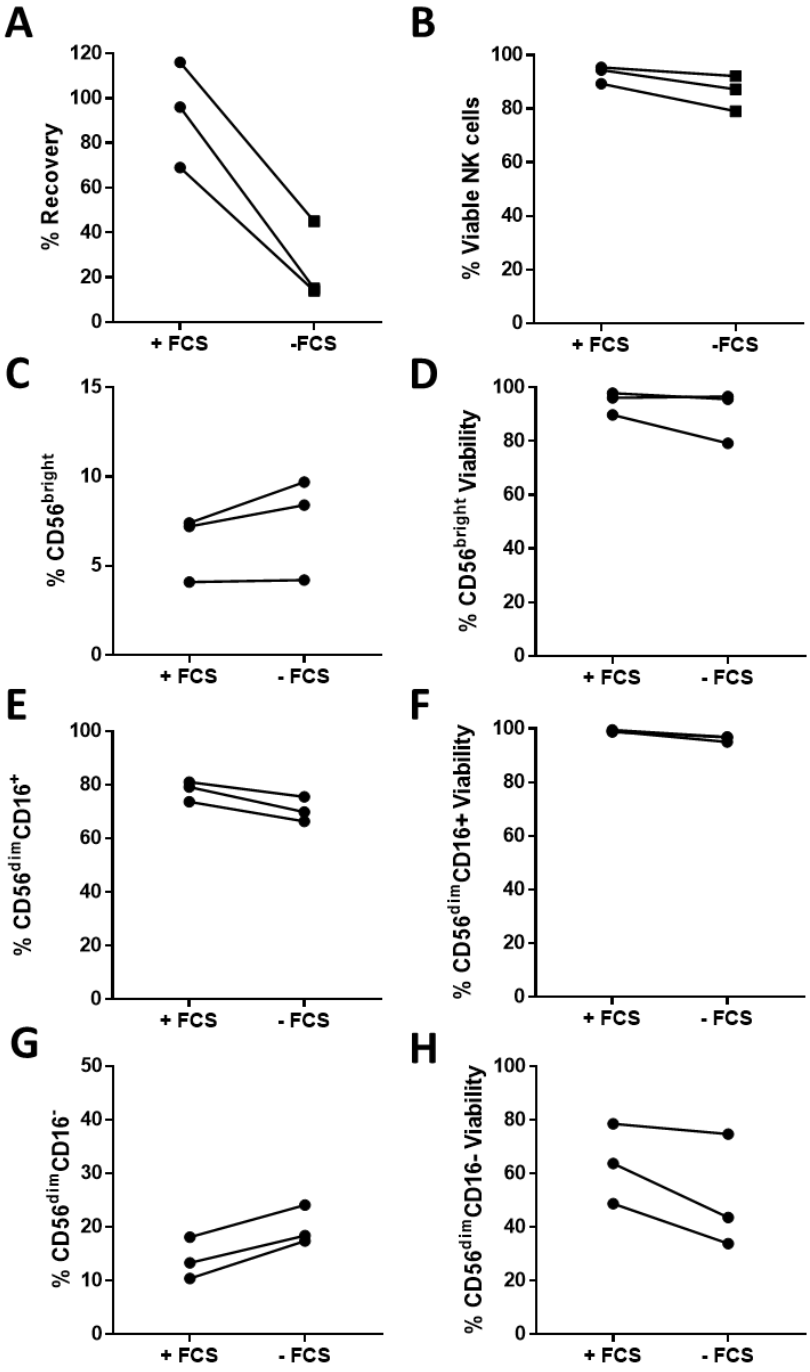

Figure 3.2: FCS maintains NK cell viability and NK cell subset proportions. PBMCs were cultured in RPMI with or without 10% (v/v) FCS for 24 h. (**A**) Percentage recovery was determined by trypan count of live cells after 24h culture relative to cell number seeded. (**B**) NK cell viability (as a percentage of total NK cells) was measured by flow cytometry in a mixed PBMC culture with or without FCS. The effect of FCS on the proportion of NK cell subsets (**C, E, G**) and the viability of each of these subsets (**D, F, H**) was also measured. Lines denote individual donors.

3.2.2 Isolating and Storing Primary Human NK Cells

The further investigate the effect of *in vitro* handling on NK cells, the NK cell phenotype was analysed after purification and cryopreservation. NK cells were purified from the peripheral blood by density-gradient centrifugation and magnetic-activated cell sorting (MACS). A slight, non-significant increase in $CD56^{dim}CD16+$ (P=0.0625, Figure 3.1 B) and corresponding decreased in CD56dimCD16- (P=0.0625, Figure 3.1 C) NK cells were found after MACS purification, with no effect on CD56 bright NK cells (P=0.1875, Figure 3.1 A). This could suggest a lack of collection of CD56dimCD16- NK cells by the MACS process but is more likely to result in the death of these cells during the purification process, which involves several centrifugation steps and elution through a matrix of ferromagnetic spheres (described in section 2.2). Purified NK cells were then stored at -80°C in 10% (v/v) FCS/DMSO and thawed to check NK cell viability and maintenance of surface receptor associated phenotypes. Cryopreservation of MACS purified NK cells was found to maintain cellular viability as 85.5% of NK cells were viable following thaw. There was a slight, non-significant reduction in $CD56^{dim}CD16+$ NK cells and a corresponding increase in $CD56^{dim}CD16-$ NK cells, which may indicate a small amount of NK cell activation as a result of NK cell storage ($CD56^{dim}CD16+$; P=0.0625, and $CD56^{dim}CD16-$; P=0.125, Figure 3.3 B and C). However, this process largely maintained subset proportions with no significant difference in the proportion of $CD56^{bright}$ NK cells ($CD56^{bright}$; P=0.1875, Figure 3.1 A). Indeed, the proportions of CD56bright and CD56dim NK cells after purification and storage still closely mirrored that of the peripheral blood (Figure 3.3). Furthermore, NK cells were functionally responsive to PMA/I treatment after freeze-thaw (P=0.0313 Figure 3.3 D). Thus both MACS isolation and cryopreservation maintained NK cell phenotype and function.

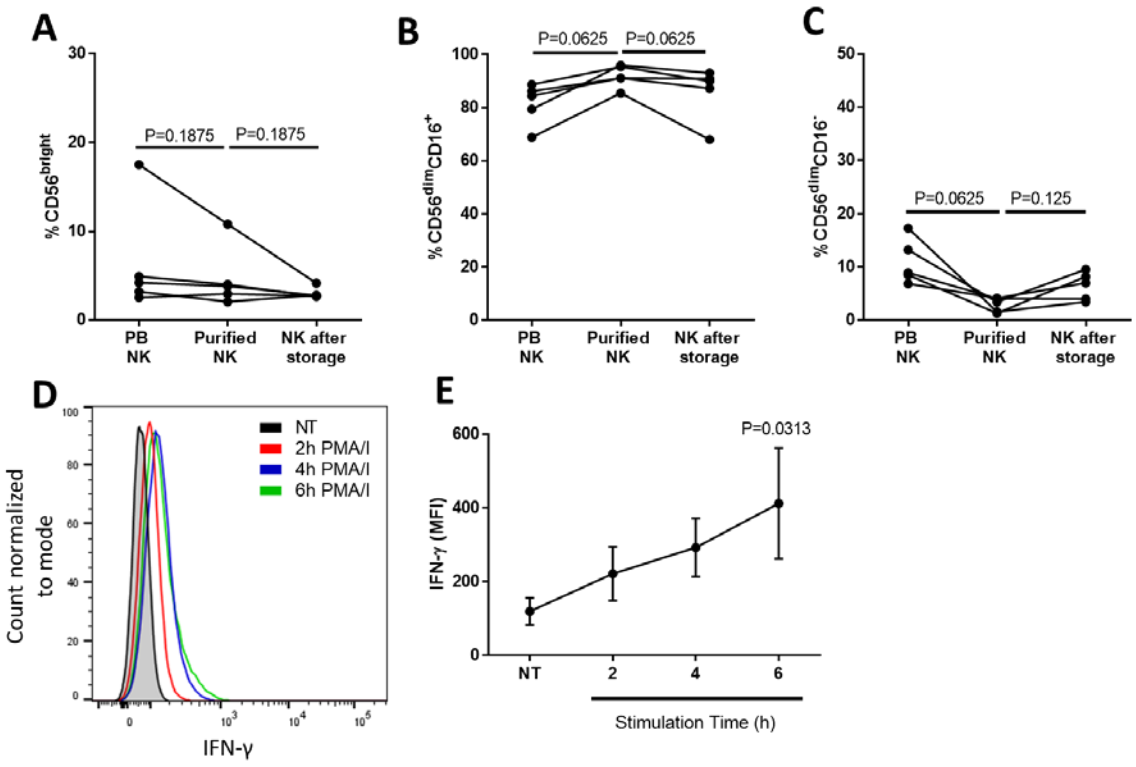

Figure 3.3: **The effect of MACS isolation and cryopreservation on the phenotype and function of peripheral NK cells.** The proportion of $CD56^{bright}$ (**A**) $CD56^{dim}CD16+$ (**B**) and $CD56^{dim}CD16-$ (**C**) NK cells was measured following isolation from PBMCs and storage at -80^{o} for 12 d. Statistical analysis was performed by Wilcoxon signed-rank test. (**D**) Purified peripheral NK cells were treated with PMA/I for 1-6h and intracellular IFN-γ measured by flow cytometry (N=5). A representative plot of the intracellular IFN-γ expression of NK cells over 6h of stimulation is shown. Intracellular cytokine was captured through the addition of monensin to cultured cells 1h after stimulation. (E) Mean IFN-γ response and standard error of the mean are shown for PMA/I stimulated NK cells. Comparison of IFN-γ expression between 6h PMA/I stimulation with NT NK cells by Wilcoxon signed-rank test.

3.2.3 Comparing Peripheral Blood NK cells from Cancer Resection Patients and Healthy Controls

In the analyses presented in Chapters 4 and 5, macroscopically normal human lung tissue was obtained from cancer resection patients. However, to control for any disease-related effects on the NK cell phenotype, peripheral NK cells from the cancer resection donors (CR-PB; REC 15/SC/0528) were compared to that of healthy peripheral blood (H-PB; REC 13/SC/0416 and). Recruitment to these two studies is described in section 2.1 and cohort demographics are summarised in Table 3.1. Data for the total lung resection cohort is shown in Table 3.1, however some samples were used for functional analysis in subsequent chapters and are not included in this section. Only the peripheral blood used for phenotyping studies (N=23) are compared against healthy peripheral blood (N=15) in this chapter.

	Lung resection	Healthy control	P-value
Number of donors	35	15	
Median Age	70 *(9.75)*	24 *(8)*	<0.0001[1]
M/F	21/14	10/5	0.7570 [2]
Smoking status, never/ex/current/unknown	5/22/7/1	10/4/1/0	0.0013 [3]
Pack-years of smoking	40 *(33.75)*	NA	NA
FEV1%	86 *(28.5)*	NA	NA
FEV1/FVC ratio	0.65 *(0.15)*	NA	NA
Resection Location, LUL/LLL/RUL/ RML/RLL	8/7/11/3/3 *1 RUL+LUL *1RUL+RML *1 Left pneumonectomy	NA	NA

Table 3.1: Cohort demographics for resection donors and healthy controls. Median values are shown with interquartile range italicised and in brackets. NA = Data not available. * indicates additional locations of resection surgeries. [1] Two-tailed Mann Whitney Test [2] Fisher's Test [3] Chi-square Test

PBMCs were isolated from whole blood following density gradient centrifugation and NK cell phenotypes assessed by flow cytometry. The proportion of NK cells in peripheral CD45+ lymphocytes was consistent in both H-PB and CR-PB cohorts (11.9% vs 11.1%, P=0.3397, Figure 3.4 A). CD45 is a pan-leukocyte marker, used to define lung lymphocytes in Chapters 4 and 5 (as shown in Figure 2.3). $CD56^{bright}$ NK cells were found in the same proportions between the two cohorts (P=0.7505, Figure 3.4 B) but $CD56^{dim}$CD16+ NK cells were reduced by 7% in CR-PB (P=0.0305, Figure 3.4 C) and $CD56^{dim}$CD16- NK cells were increased from 5.9% in CR-PB to 14.6% (P=0.009, Figure 3.4 D). This change in $CD56^{dim}$ NK cells may suggest a greater level of NK cell activation in the peripheral blood of resection patients. This may be related to disease status in the CR-PB cohort but there are also other significant demographic differences between the two cohorts, including cohort age (P<0.0001) and smoking status (P=0.0013, Table 3.1) which could account for these differences.

The NK cell maturation state was also analysed in H-PB and CR-PB. The terminal differentiation marker, CD57 was detected on ~60% of peripheral NK cells and was equivalent between H-PB and CR-PB NK cells (P=0.3410, Figure 3. 5A and C) [275]. $CD56^{dim}$CD16+ NK cells were found to express the most CD57 (72% in H-PB) with a small amount of CD57 expression on $CD56^{dim}$CD16- NK cells (7.9% in H-PB) and minimal expression on $CD56^{bright}$ NK cells (1.6% in H-PB). CD57 expression did not differ on any of the $CD56^{bright}$ or $CD56^{dim}$ NK cell subsets between H-PB and CR-PB ($CD56^{bright}$ P=0.865, P>0.9999 for both $CD56^{dim}$CD16+ and $CD56^{dim}$CD16- NK cells, Figure 3.5 D).

NK cell maturity was also assessed through the expression of CD158b (KIR2DL2/L3/S2) as KIR proteins are gradually acquired throughout NK cell development (summarised in section 1.4.4 and Figure 1.3) [266, 439]. Measuring CD158b expression does not evaluate the expression of all KIR alleles which vary across individuals, but it includes KIR from both haplotypes (discussed in section 1.4.5) [440]. CD158b expression was also found to be equivalent between peripheral NK cells of healthy donors and those undergoing cancer resection (P=0.4199, Figure 3.5 E and D). Likewise, no difference in CD158b expression was found on $CD56^{bright}$ or $CD56^{dim}$ subsets ($CD56^{bright}$ P=0.3830 and P>0.9999 for $CD56^{dim}$CD16+ and $CD56^{dim}$CD16- NK cells, Figure 3.5 F). Consistent with the literature CD158b was also mostly expressed by $CD56^{dim}$CD16+ NK cells (38.2% of H-PB) with little to no expression on either $CD56^{bright}$ or $CD56^{dim}$CD16- NK cells [266]. Thus the maturation state of the peripheral NK cells was not found to differ between cancer resection patients and healthy controls.

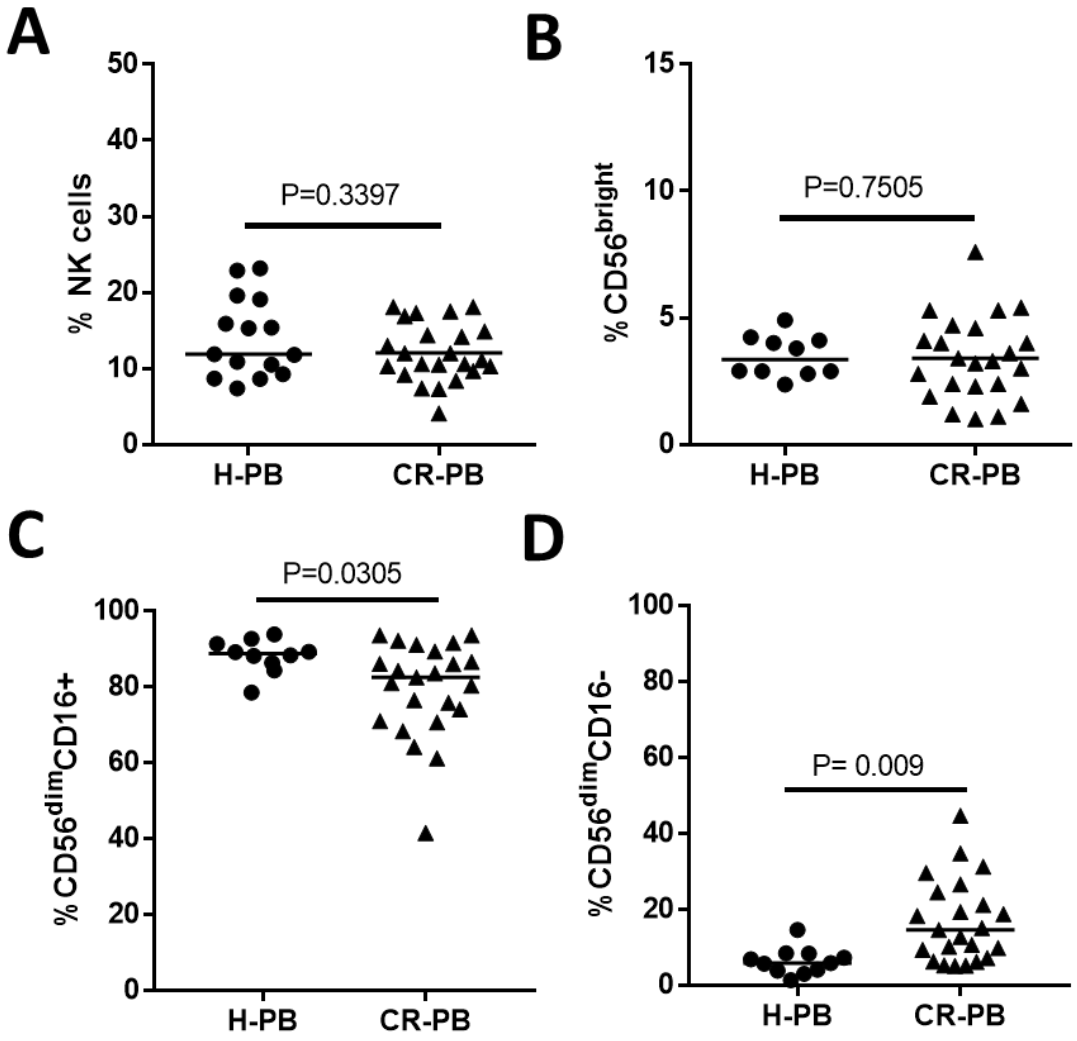

Figure 3.4: NK cell subsets in the peripheral blood of lung tissue donors (CR-PB) and healthy controls (H-PB). (**A**) Quantification of CR-PB (N=23) and H-PB (N=10) NK cells as a percentage of CD45+ lymphocytes. (**B, C, D**) Proportions of $CD56^{bright}$ (**B**), $CD56^{dim}CD16+$ (**C**) and $CD56^{dim}CD16-$ (**D**) NK cells in the peripheral blood of healthy controls and lung donors. Lines describe medians, statistical analysis by Mann-Whitney U test.

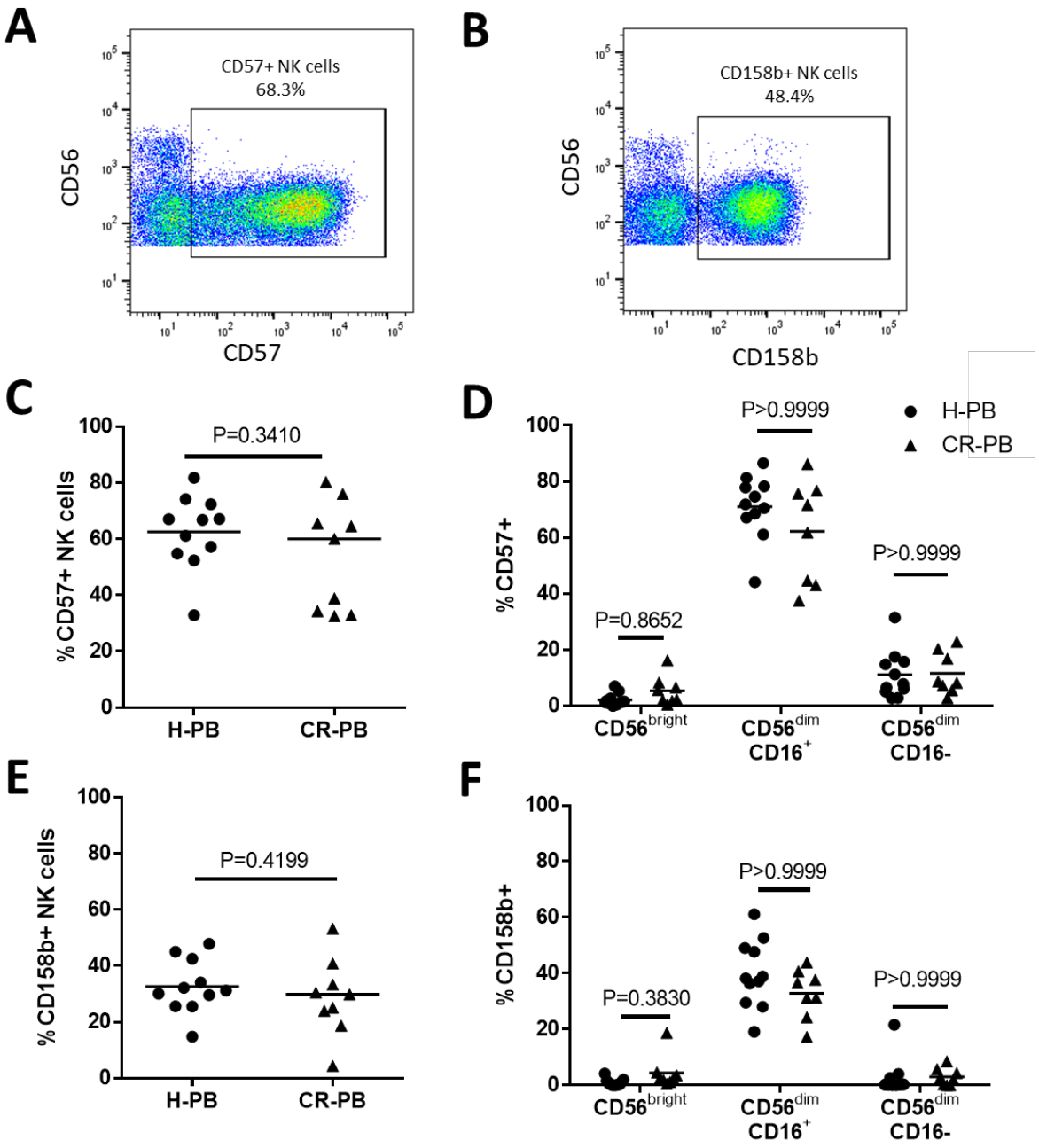

Figure 3.5: CD57 and CD158b expression on peripheral blood NK cells from healthy controls (H-PB) and cancer resection patients (CR-PB). (**A, B**) Representative flow cytometry plots of CD57 (**A**) and CD158b (**B**) expression on NK cells from a H-PB donor. Gates were set based on negative staining with isotype controls. Quantification of CD57 (**C**) and CD158b (**E**) expression on peripheral NK cells in CR-PB (N=9) and H-PB (N=11). Lines describe medians, statistical analysis by Mann Whitney U test. **(D, F**) CD57 and CD158b expression on $CD56^{bright}$, $CD56^{dim}CD16+$ and $CD56^{dim}CD16-$ NK cell subsets from the blood and lung. Statistical analysis by Kruskal-Wallis test with Dunn's multiple comparison correction. Lines describe medians.

3.2.4 The Effect of Age and Gender on the Peripheral Blood NK Cell Phenotype

Age related changes to the NK cell repertoire have been described, including altered $CD56^{bright}$/$CD56^{dim}$ proportions and receptor expression [317, 441-444]. Although the precise effect of age on the NK cell phenotype is inconsistently reported in the literature, an immunosenescent phenomenon is generally agreed upon [317, 441-444]. As the age of the lung resection cohort is significantly greater than that of the healthy blood donors (P<0.0001, Table 3.1), the effect of age on the NK cell phenotypes was assessed in healthy peripheral blood. To do this, blood was taken from healthy controls aged 22-72 yr (REC 15/SC/0528; donor demographics in Table 2.3). This age range covers the median age of both the healthy control group (24 ± 8), and lung resection cohort (70 ± 9.75) and was used to assess potential age-related differences between the two cohorts. PBMCs were isolated from healthy donors by density gradient centrifugation and stored at -80^{0}C until use. The cells were then defrosted and stained for flow cytometry (see section 2.8).

	Healthy controls
Number of donors	22
Median Age	57 *(33.25)*
M/F	8/14
Smoking status, never/ex/current	12/9/1
Pack-years of smoking	0 *(4.5)*
FEV1%	100 *(15.75)*
FEV1/FVC ratio	0.79 *(0.068)*

Table 3.2: Cohort demographics for healthy peripheral blood donors used to assess the effect of age and gender on peripheral NK cells. Median values are shown with the interquartile range italicised and in brackets.

The relationship between age and proportion of peripheral NK cells was assessed but no correlation was found between the two variables (P=0.3016, Figure 3.6 A). Likewise, the proportions of $CD56^{bright}$, $CD56^{dim}$CD16+ and $CD56^{dim}$CD16- subsets did not correlate with donor age (P=0.3630, P=0.2174 and P=0.3287 respectively, Figure 3.6 B, C and D). NK cell differentiation was analysed through expression of CD57 (Figure 3.7 D) but this NK cell protein was also not found to correlate with age (Figure 3.7 D P=0.31944).

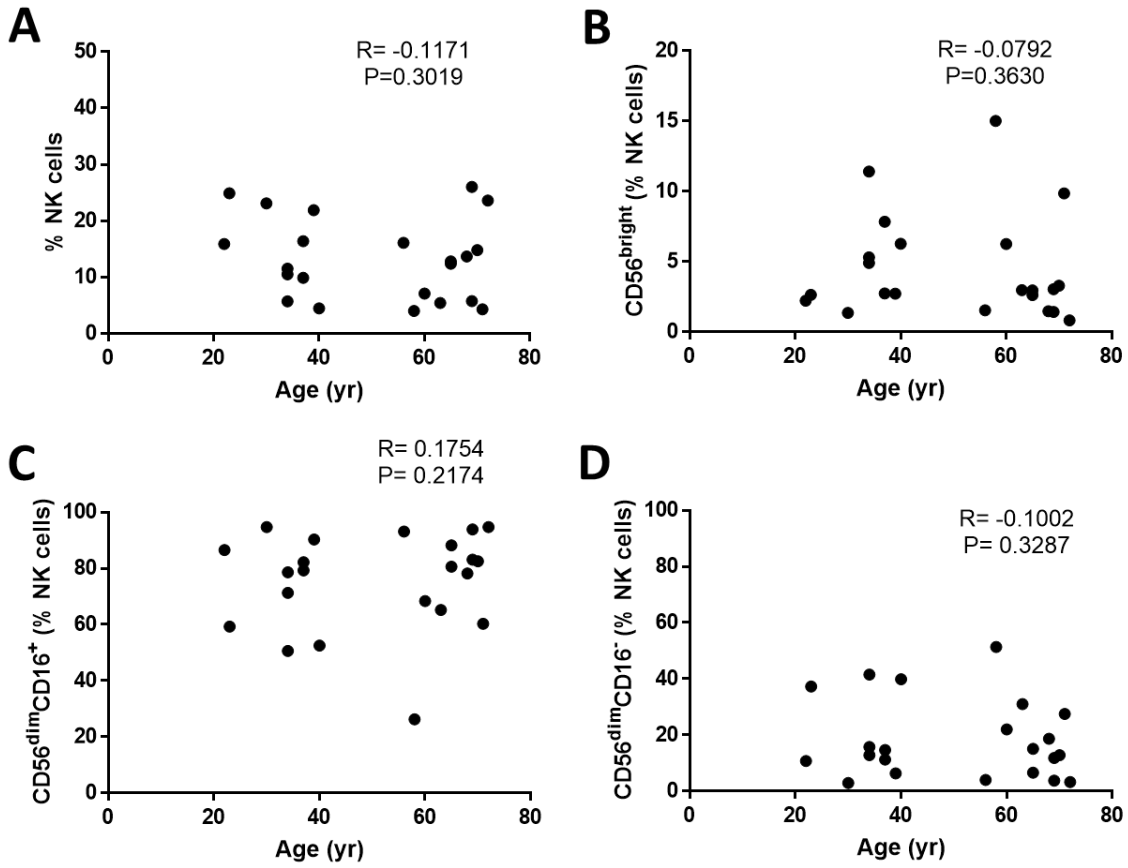

Figure 3.6: The effect of age on peripheral blood NK cells. PBMCs from healthy volunteers were analysed by flow cytometry and phenotypic measures correlated with donor age. The relationship between the proportion of NK cells or NK cell subpopulations with donor age was analysed by one-tailed Spearman's correlation, N=22. The rank-order correlation coefficient and statistical significance are shown on the graphs. (**A**) The proportion of NK cells within CD45+ lymphocytes correlated with donor age (**B, C, D**) $CD56^{bright}$, $CD56^{dim}CD16^{+}$ and $CD56^{dim}CD16^{-}$ as a percentage of NK cells in the peripheral blood correlated with age.

The effect of donor age on the expression of NK cell activating receptors was also analysed (Figure 3.7). Activating receptor expression has been linked to recognition of virus' and will be analysed on the lung NK cell populations in Chapter 4. However, there is some controversy over the effect of age on NK cell receptor expression in the literature [442, 443, 445]. Therefore, to exclude the effect of age on the phenotypes described in section 4.2.4, NK cell expression of NKG2C, NKp46 and NKG2D were compared based on donor age. As NKp46 and NKG2D are constitutively expressed by NK cells (shown in Figure 3.7 B and C), the surface expression of these proteins was analysed by MFI. Neither NKp46 or NKG2D expression was found to be affected by donor age in this cohort (Figure 3.7 F and G, P=0.2866 and P=0.1991 respectively). However, there was a moderate positive correlation between NKG2C expression and donor age (P=0.0202, Figure 3.7 A and E).

The increase in NK cell NKG2C expression in older blood donors demonstrates the importance of considering age-specific differences between cohorts. However, the data in this chapter excludes age difference as a reason for the increased peripheral $CD56^{dim}CD16$- NK cells in CR-PB donors compared with healthy controls. These findings also validate the comparison of NK cell maturity between CR-PB and H-PB donors, as age was not found to affect this aspect of NK cell biology.

Gender is another biological variable which can affect readouts from immune cells, predominantly due to hormonal differences between the two sexes [446, 447]. Environmental factors such as nutrition and the microbiome also differentially affect immune functioning in males and females [446, 447]. To control for this in our study the effect of gender on the NK cell phenotypes of interest was assessed. To do this, peripheral NK cell phenotypes in healthy controls were stratified based on gender. However, no differences in the proportions of NK cells or NK cell subsets were found (NK cells P=0.1825, $CD56^{bright}$ P=0.0633, $CD56^{dim}CD16$+ P=0.1791 or $CD56^{dim}CD16$- P=0.2573, Figure 3.8). Furthermore, the expression of CD57 and activating receptors on NK cells was unaffected by donor gender (CD57 P=0.2847, NKG2C P=0.188, NKp46 P=0.1059 and NKG2D P=0.2733, Figure 3.9). Therefore, the gender of lung tissue donors is unlikely to impact the lung NK cell phenotype examined in Chapter 4.

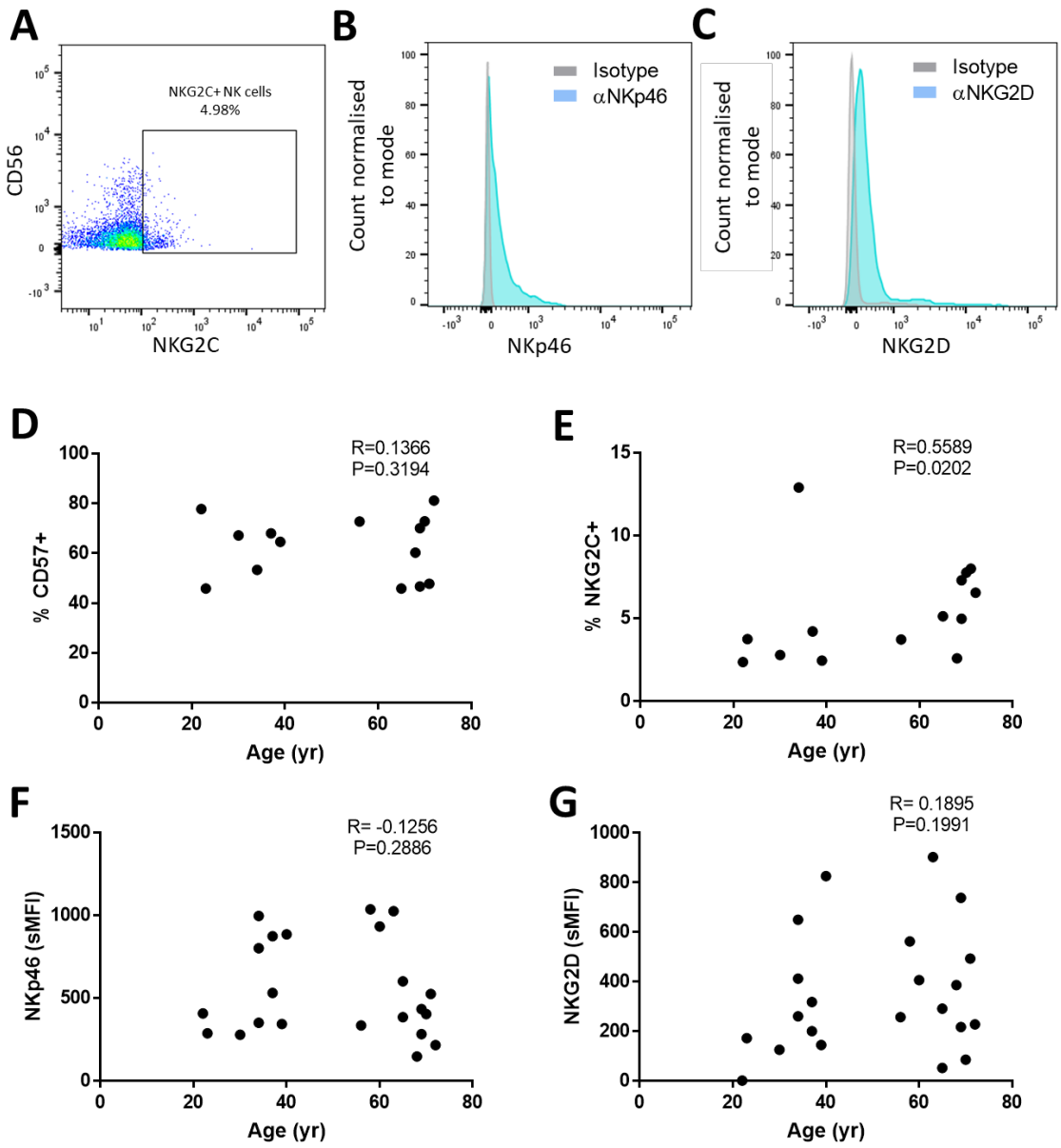

Figure 3.7: The effect of age on NK cell receptor expression. PBMCs collected from healthy volunteers were analysed by flow cytometry. Maturity markers and activating receptor expression were measured and correlated with donor age. (**A, B, C**) Representative flow cytometry plots of NK cell activating receptor expression in healthy peripheral blood. NKG2C (**A**), NKp46 (**B**) and NKG2D (**C**) are shown. NKp46 and NKG2D are constitutively expressed and are therefore presented as histograms. NK cell counts are presented normalised to the mode due to differences in numbers of acquired cells. NKG2C gating was set from negative staining with an isotype control. (**D**) NK cell CD57 expression correlated with donor age (N=14). NKG2C (N=14) (**E**), NKp46 (N=22) (**F**) and NKG2D (N=22) (**G**) expression on NK cells correlated with age. (**D, E, F, G**) The relationships between age and NK cell surface proteins were assessed by one-tailed Spearman's correlation. The rank-order correlation coefficient and statistical significance are shown on the graphs.

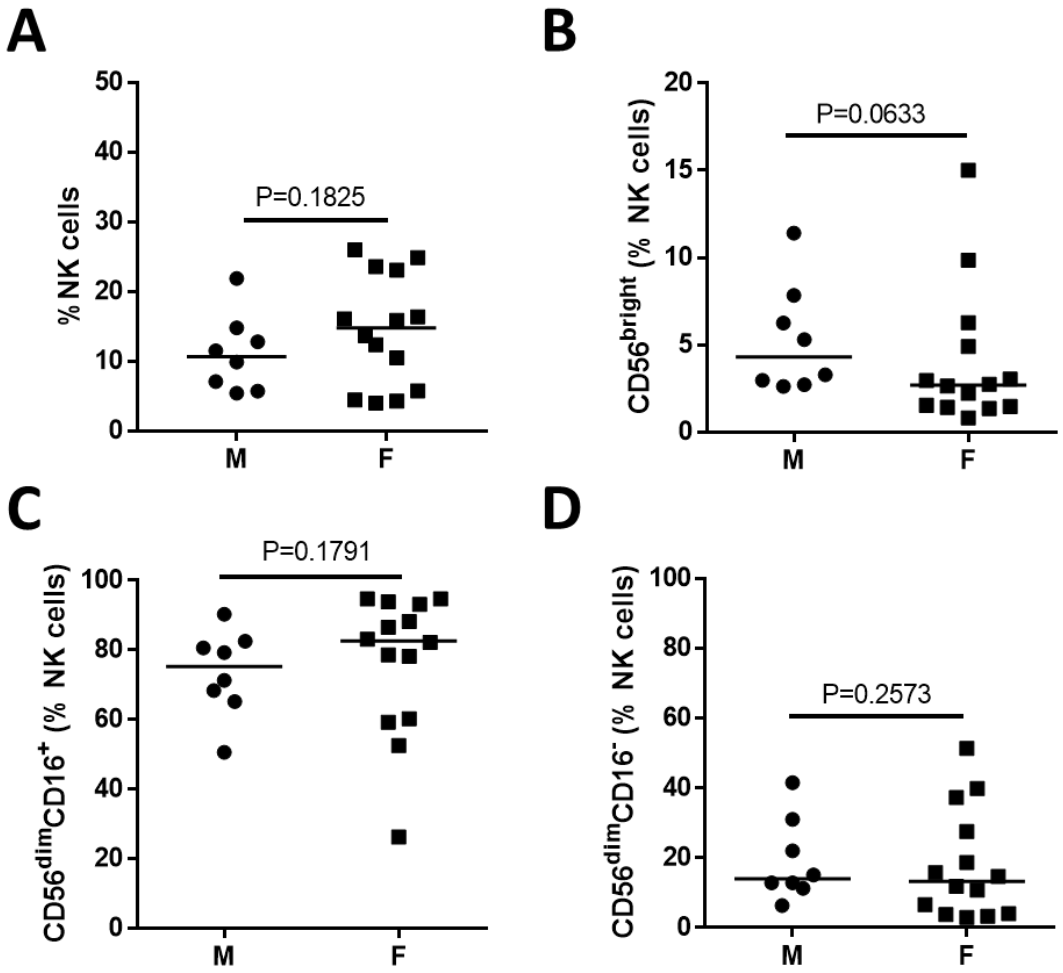

Figure 3.8: **The effect of gender on peripheral blood NK cells.** PBMCs from healthy volunteers were analysed by flow cytometry. (**A**) The proportion of NK cells within CD45+ lymphocytes stratified by gender. (**B, C, D**) The effect of gender on the proportion of $CD56^{bright}$, $CD56^{dim}CD16^{+}$ and $CD56^{dim}CD16^{-}$ NK cells in the peripheral blood. Lines describe medians. All statistical analysis carried out by Mann Whitney U test.

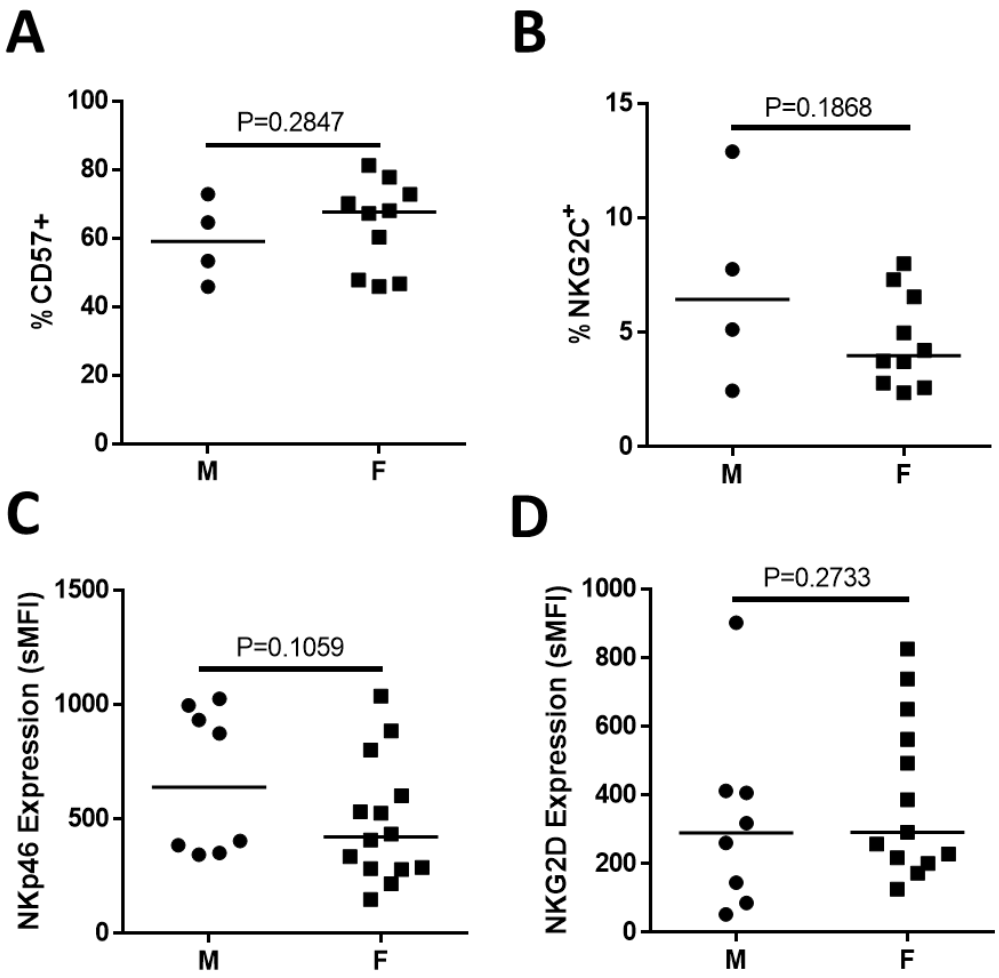

Figure 3.9: The effect of gender on NK cell receptor expression. Healthy donor PBMCs were analysed for change in CD57 (**A**) and activating receptor expression (**B, C, D**) on NK cells. Activating receptors included NKG2C (**B**), NKp46 (**C**) and NKG2D (**D**). Lines describe medians. All statistical analysis carried out by one-tailed Mann Whitney U test.

3.2.5 The Effect of Smoking Status on the Peripheral NK Cell Phenotype

Donor smoking status was also found to differ between CR-PB and H-PB cohorts (P=0.0013, Table 2.1) with more current and ex-smokers in those undergoing cancer resection compared to healthy controls. A current smoking status has been linked to increased NK cell activation, which may explain the increased proportion of $CD56^{dim}$CD16- NK cells identified in CR-PB. Unfortunately, the lack of current smokers in the healthy control cohort (N=1, Table 2.1) precludes analysis of the effect of smoking on the healthy peripheral NK cell phenotype. However, the proportion of NK cells and NK cell subsets in the CR-PB cohort were stratified based on smoking status (never smoker N=3, ex-smoker N=15 and current smoker N=5) as shown in Figure 3.10. This analysis did not show any difference in the proportion of NK cells or $CD56^{bright}$/$CD56^{dim}$ subsets between groups of current, ex

and never smokers (Figure 3.10). This included CD56^{dim}CD16- NK cells, which were found at comparable proportions in current and ex-smokers (P>0.9999, Figure 3.10 D) and when compared to never smokers (current vs never P=0.4451, ex-smoker vs never P>0.9999, Figure 3.10 D). Thus it is unlikely that the smoking status of our cohorts is an explanation for the increases percentage of CD56^{dim}CD16- NK cells in CR-PB donors. However, this analysis is limited by the sample size of never and current smokers; increasing the sample size would enhance the validity of these findings.

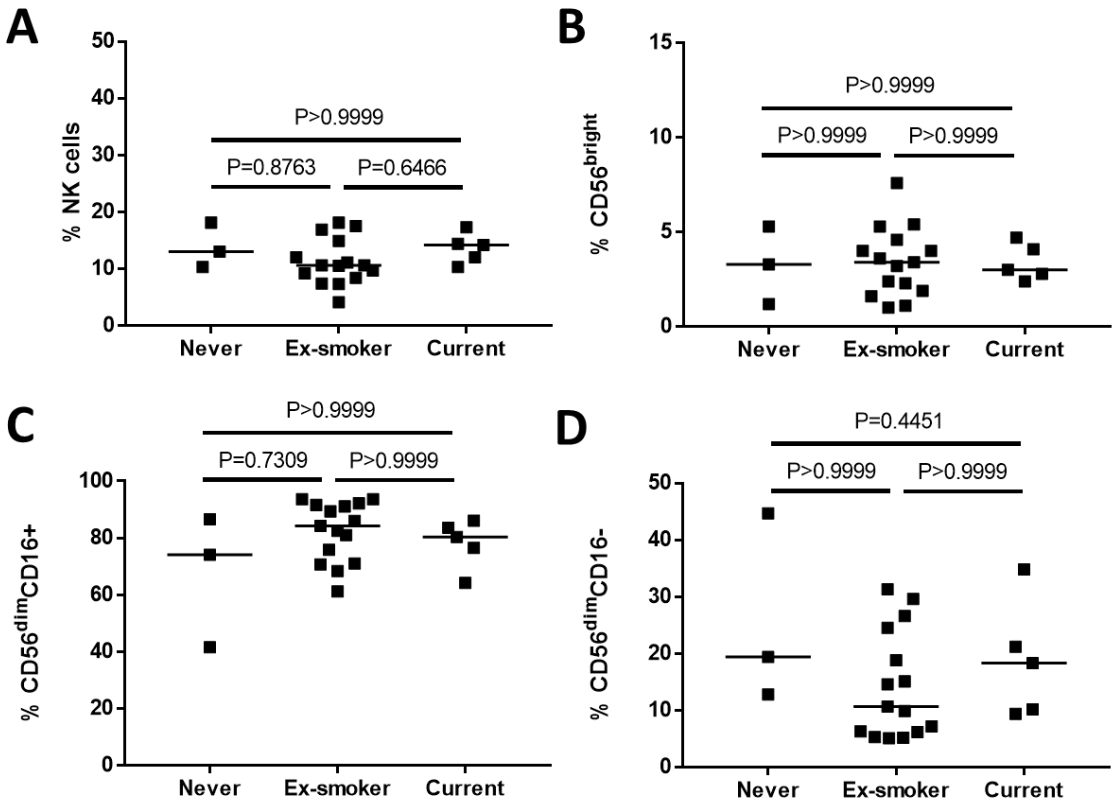

Figure 3.10: The effect of smoking status on peripheral blood NK cells. PBMCs from cancer resection patients were isolated before flow cytometry staining for NK cells. NK cell phenotypes were stratified based on smoking status. Never smokers N=3, Ex-smokers N=15 and current smokers N=5 were analysed. (**A**) Proportion of NK cells as CD45+ lymphocytes (**B, C, D**) The proportion of CD56^{bright} (**B**) CD56^{dim}CD16+ (**C**) and CD56^{dim}CD16- (**D**) NK cells. Lines describe medians. All statistical analysis carried out by Kruskal-Wallis test with Dunn's multiple comparison correction.

3.3 Discussion

3.3.1 Culturing Primary Human NK Cells

Together the experiments presented in this chapter show that NK cells can be successfully isolated from human blood, cultured and stored with a preserved phenotype and minimal activation. In addition, this work has explored potential demographic effects on reported NK cell phenotypes, including age, gender and smoking status and are summarised in Table 3.3.

Figure	Comparison	Result
3.1	Freshly isolated NK cells were compared to NK cells cultured for 24h	*In vitro* culture largely maintains NK cell subpopulations with a small increase in $CD56^{dim}CD16^{-}$ cells
3.2	The NK cells phenotype was compared between *in vitro* culture with and without FCS	FCS preserves NK cell viability and sub populations
3.3	NK cell subpopulations were compared following MACS isolation and cryopreservation	Peripheral NK cell subpopulations are preserved during both MACS isolation and freeze-thaw.
3.4	Peripheral NK cell subpopulations from healthy donors versus cancer resection donors	More $CD56^{dim}CD16^{-}$ NK cells were identified in cancer resection donor blood. Non-significant reduction in $CD56^{dim}CD16^{+}$ cells and no change to $CD56^{bright}$ cells
3.5	Peripheral NK cell maturity was compared in healthy donors and cancer resection donors	Maturation markers; CD57 and CD158b were equivalent between H-PB and CR-PB NK cells
3.6	NK cell subpopulations correlated with donor age	No effect of this age range on peripheral NK cell subpopulations
3.7	NK cell receptor expression correlated with donor age	No effect of this age range on CD57, NKp46 or NKG2D expression. NKG2C was increased on NK cells in older donors
3.8	Comparison of NK cell subpopulations between genders	No effect of gender on peripheral NK cell subpopulations
3.9	Comparison of NK cell receptor expression between genders	No effect of gender on CD57, NKG2C, NKp46 or NKG2D expression
3.10	Peripheral NK cells from cancer resection donors were compared based on donor smoking status	No effect of smoking status on peripheral NK cell subpopulations

Table 3. 1 Summary of the key results in Chapter 3. The comparisons made in each Figure are summarised alongside the main findings of this chapter.

This work reported 11.9% ± 7.62 NK cells from the blood of healthy controls (N=15) with 4 % ±2 $CD56^{bright}$, 88.2% ± 15.45 $CD56^{dim}CD16^{+}$ and 6.86 % ± 14.55 $CD56^{dim}CD16^{-}$ NK cells, consistent with findings from the literature (Figure 3.4) [276]. $CD56^{dim}CD16^{-}$ NK cells are not always reported in the peripheral blood but have been described by Amand *et al.* and Romee *et al.* [313, 314, 320]. It has been suggested that contaminating CD56+CD3+ cells could account for the reported $CD56^{dim}CD16^{-}$ phenotype, however strong staining for the CD3 protein, as shown in Figure 2.3, allowed T cell exclusion from the analysis in this chapter [316]. Furthermore, the $CD56^{dim}CD16^{-}$ NK cell phenotype has been associated with NK cell activation, possibly through CD56 and CD16 shedding following the action of metalloproteases on the cell surface [314, 316, 317, 320]. The loss of CD16 from the

immunological synapse in this way has been suggested to loosen NK cell binding with target cells to allow increased serial engagement of targets, promoting NK cell function [448].

NK cell culture *in vitro* resulted in a 7.5% increase in $CD56^{dim}CD16$- NK cells (Figure 3.1) which was exacerbated by removal of FCS (Figure 3.2). This indicates that NK cells could be slightly activated by *ex vivo* culture. This may be because NK cells are responding to PBMCs that have become stressed or activated during the isolation process [449]. Other i*n vitro* stressors could include NK cell exposure to plastic, heparin and Ficoll [450-452]. $CD56^{bright}$ NK cell proportions were also found to rise fractionally from 3.4% to 7.2% which may be related to the death of $CD56^{dim}$ NK cells following *in vitro* activation [314, 316, 317, 320, 438, 453]. In support of this $CD56^{dim}CD16$- NK cells were found to be the least viable in culture conditions (Figure 3.2H).

$CD56^{dim}CD16$- NK cell have also been reported to be increased by cryopreservation protocols, a result most likely due to cellular activation or stress [315]. However, the cryopreservation protocol in this thesis (section 2.6) was not found to alter the proportion of $CD56^{dim}CD16$- NK cells (P=0.125, Figure 3.8). In fact, storage of frozen peripheral NK cells in FCS and 10% DMSO allowed the recovery of viable cells and preserved NK cell subpopulations (Figure 3.3). Taken together these results suggest that careful handling of primary human NK cells is essential to preserving *in vivo* NK cell phenotypes. Short *in vitro* culture and minimal manipulation should be favoured in protocols to assess their function.

3.3.2 Peripheral NK cells from Healthy Controls and Resection Donors are Phenotypically Comparable

In chapters 4 and 5 macroscopically normal lung tissue taken from cancer resection surgeries will be used to interrogate the lung NK cell phenotype and function. To validate the use of this material and to exclude disease-specific effects on the NK cell phenotype, the peripheral blood from cancer resection donors (CR-PB) was compared to a healthy control group (H-PB). The proportion of NK cells was found to be equivalent between the two groups, as were $CD56^{bright}$ NK cells (P=0.3397 and P=0.7505 respectively, Figure 3.4 A and B). However, CR-PB was found to contain more $CD56^{dim}CD16$- NK cells and fewer $CD56^{dim}CD16$+ NK cells (P=0.009 and P=0.0305 and respectively, Figure 3.4 C and D). As $CD56^{dim}CD16$- NK cells are thought to represent an activated and dying

phenotype this might suggest that CR-PB NK cells are more activated than those from healthy controls [314, 316, 317, 320].

It is possible that the increase in $CD56^{dim}CD16$- NK cells in CR-PB may be a cancer-related effect. $CD56^{dim}CD16$- NK cells have been identified in the blood and tumour sites of breast cancer patients and have been shown to degranulate when exposed to tumour targets [316, 318]. Interestingly, CD56 and CD16 downregulation have also been observed in disease contexts where the immune system is activated [318-320]. For instance, CD16 was reduced on $CD16^{high}CD57+$ ($CD56^{dim}CD16+$) NK cells following influenza vaccination and this change was associated with NK cell degranulation in the blood of vaccinated individuals [319]. However, the demographic differences between resection donors and healthy controls could also explain the reported difference in $CD56^{dim}$ NK cells. For instance, there are significant differences between healthy blood donors and those undergoing cancer resection, including age and smoking status (Table 2.1).

Smoking status has been reported to affect lung and blood NK cell cytotoxicity against K562 targets, with reduced degranulation in current smokers compared to ex-smokers [362]. Unfortunately, the effect of smoking status could not be assessed in healthy controls due to a limited number of current and ex-smokers in this cohort (Table 2.1). However, analysis of NK cell and subset proportions in CR-PB did not yield any differences based on donor smoking status (Figure 3.10), including the proportion of $CD56^{dim}CD16$- NK cells. Although limited by a small sample size of never and current smokers these results indicate that the difference in $CD56^{dim}$ NK cell proportions between CR-PB and H-PB is unlikely to be explained by smoking status. Gender has also been found to affect immune cell function but this was also not found to affect either proportions of $CD56^{bright}$ and $CD56^{dim}$ NK cells or receptor expression in this study (Figure 3.8 and Figure 3.9) [446, 447].

3.3.3 NK cells and Ageing

Age has been reported to alter $CD56^{bright}$:$CD56^{dim}$ ratios in the blood and could explain the difference in $CD56^{dim}CD16$- NK cell populations observed between these two cohorts (Figure 3.4 D) [317, 441-443, 445, 454, 455]. However, age effects on the NK cell phenotype are inconsistently reported in the literature [317, 441-443, 445, 454, 455]. Different study inclusion criteria, preparations of peripheral blood NK cells and experiment duration confound our understanding of NK cell functionality in the elderly. As the healthy blood donors recruited in this study significantly

differed in age to lung tissue donors (P<0.0001, 24 ± 8 yr vs 70 ± 9.8 yr) the effect of this age difference was investigated in the peripheral blood. To do this the NK cell phenotype was analysed on donors between the ages of 22 and 72 (see section 2.1 and Table 3.2 for cohort demographics). However, no differences were observed in the proportion of total NK cells or $CD56^{bright}$ and $CD56^{dim}$ subsets based on age (Figure 3.6). This conflicts with several reports which have described increased proportions of NK cells in >65yr cohorts with decreased $CD56^{bright}$ and increased $CD56^{dim}$ NK cells [317, 441-443, 445, 454, 455]. Although differences in cohort demographics make it difficult to compare studies, it is possible that any change in the proportion of $CD56^{bright}$ and $CD56^{dim}$ NK cells during ageing may be too subtle to be observed in our study at its current size. However, Le Garff-Tavernier *et al.* 2010 analysed cohorts of ages similar to the groups described here and described no difference in the proportion of blood NK cells between adult (18-60yr) and elderly (60-80yr) cohorts, with increased proportions of peripheral blood NK cells only observed in the 80-100yr group [442]. In addition Hayhoe *et al*. 2010 describes a very gradual increase in the $CD56^{dim}$:$CD56^{bright}$ ratio with age that becomes more marked past the age of 50 [455].

Although CD57 expression has consistently been shown to be increased in cohorts of 50-80 yr when compared to younger age groups, no difference in CD57 expression was observed between 22 and 72 in this thesis (Figure 3.7 A) [442, 445, 456]. NKp46 expression also appeared steady between the age groups in our analysis (Figure 3.7 C), a finding that is also supported by Le Garff-Tavernier *et al.* 2010 [442]. However, this is a subject of controversy in the literature with some authors describing decreased NKp46 during aging [443, 445]. NKG2D expression was also statistically comparable between ages (Figure 3.7 D), a finding consistent with previous reports [442, 445]. Interestingly, increased NKG2C expression was identified on peripheral NK cells from older donors (P=0.0202, Figure 3.7 B). This may relate to donor CMV status as NKG2C+ NK cells have been found to expand during CMV, a common systemic virus which will infect 80% of the UK population by the time they're 65 [457]. CMV infection is life-long and the likelihood that a person is carrying this virus increases with age [457, 458]. Therefore the positive correlation between NK cell NKG2C expression and age found in this thesis could be related to CMV-mediated expansion of NKG2C+ NK cells throughout life-time [349, 353-356, 442, 459]. This finding highlights the importance of considering age-related effects on the immune phenotype, particularly given the advanced age of the lung tissue donors in this study. However, the results from this chapter indicate that age of lung tissue donors in this thesis would not affect the gross NK cell phenotype, maturation state or expression of the activating receptors NKp46 and NKG2D. Furthermore, these results exclude both age, gender and smoking status as a reason for the observed increase in $CD56^{dim}$CD16- NK cells in CR-PB compared to healthy controls.

3.3.4 Summary

The results described here demonstrate the effects of isolation, culture and storage on NK cells taken from human peripheral blood. These data indicate that primary NK cells can be isolated, cultured and stored with minimal changes to phenotype whilst maintaining function. Small changes in the $CD56^{bright}$/$CD56^{dim}$ ratio were observed following *in vitro* culture with increases in $CD56^{dim}$CD16- NK cells. This is most likely due to a small amount of activation during isolation and culture. These data indicate that prompt and minimal handling of NK cells is required to preserve the NK cell phenotype. Furthermore, the NK cell phenotype in the periphery of cancer resection patients was mostly unchanged compared to healthy controls with the exception of a raised proportion of $CD56^{dim}$CD16- NK cells and decreased $CD56^{dim}$CD16+ NK cells. This change suggests a greater level of NK cell activation in CR-PB and may be a cancer-related effect or due to smoking status, as $CD56^{bright}$ and $CD56^{dim}$ subsets were not affected by age. Thus the presence of cancer minimally affected the peripheral NK cell phenotype. Finally, this chapter has reported a validated flow cytometry panel for the assessment of NK cell phenotype, which can now be applied to cells from the human lung.

Chapter 4 The NK Cell Phenotype in the Human Lung

4.1 Introduction

An analysis of the human lung NK cell phenotype was first reported by Marquardt *et al.* in 2017, who found that NK cells comprised 10-30% of lymphocytes and were predominantly mature canonical $CD56^{dim}CD16+$ NK cells [362]. Despite this cytotoxic phenotype, lung NK cells are hypofunctional in response to K562 targets, PMA and cytokine stimulation [364-366]. Thus the lung environment appears to exert a repressive effect on NK cells, suggesting that there is unique regulation of NK cells in this setting [365-367]. Despite their key role in early innate immune defense, NK cell biology in human lungs is poorly understood. Characterizing the phenotypic features of lung NK cells may shed light on NK cell function, regulation, trafficking and residency within the lung environment.

Therefore, in this chapter the human lung NK cell phenotype was analyzed in terms of maturity, activating receptor expression and residency. Resident NK cell populations have been identified in many human organs including the liver, adipose tissue, skin, kidney, salivary glands, uterus and lymph nodes but have yet to be identified in the lungs [293, 340]. To investigate the lung NK cell phenotype a previously published method of lung resident T cell isolation was validated for the extraction of NK cells [428, 429, 460]. Human lung tissue was obtained from cancer resection surgeries taking place at Southampton General Hospital (REC 08/H0502/32) and the NK cell phenotype analysed by flow cytometry. Macroscopically normal lung tissue, distal from tumour sites was taken for analysis. As described in section 3.3.2, minimal change to the peripheral NK cell phenotype was found in cancer resection donors compared to healthy controls, giving confidence in the analysis of lung tissue from these patients. As a further control for disease effects, the lung NK cell phenotype was compared to matched peripheral blood. Finally, many lung tissue donors had underlying pathology in the form of COPD. This chronic inflammatory disorder has been associated with dysregulated NK cell function, as discussed in section 1.5.5 [361, 461]. Therefore, the NK cell phenotype was also examined relative to the obstructive lung disease status of tissue donors.

4.2 Results

4.2.1 Isolating NK Cells from Human Lung Tissue

To isolate NK cells lung parenchyma was cut into 2-3mm^2 portions and washed thoroughly in RPMI to remove contaminant peripheral blood. The lung tissue was then rested in 10% (v/v) FCS RPMI for 16h, as this was found to support NK cell survival (Figure 3.2). The connective tissue was disrupted by 0.5mg/mL collagenase treatment for 15min at 37°C, as described in section 2.12.1. This method avoided erythrocyte lysis and minimised enzymatic treatment to preserve *in vivo* cellular phenotypes. The yield of NK cells was compared following tissue rest and collagenase digestion (Figure 4.1).

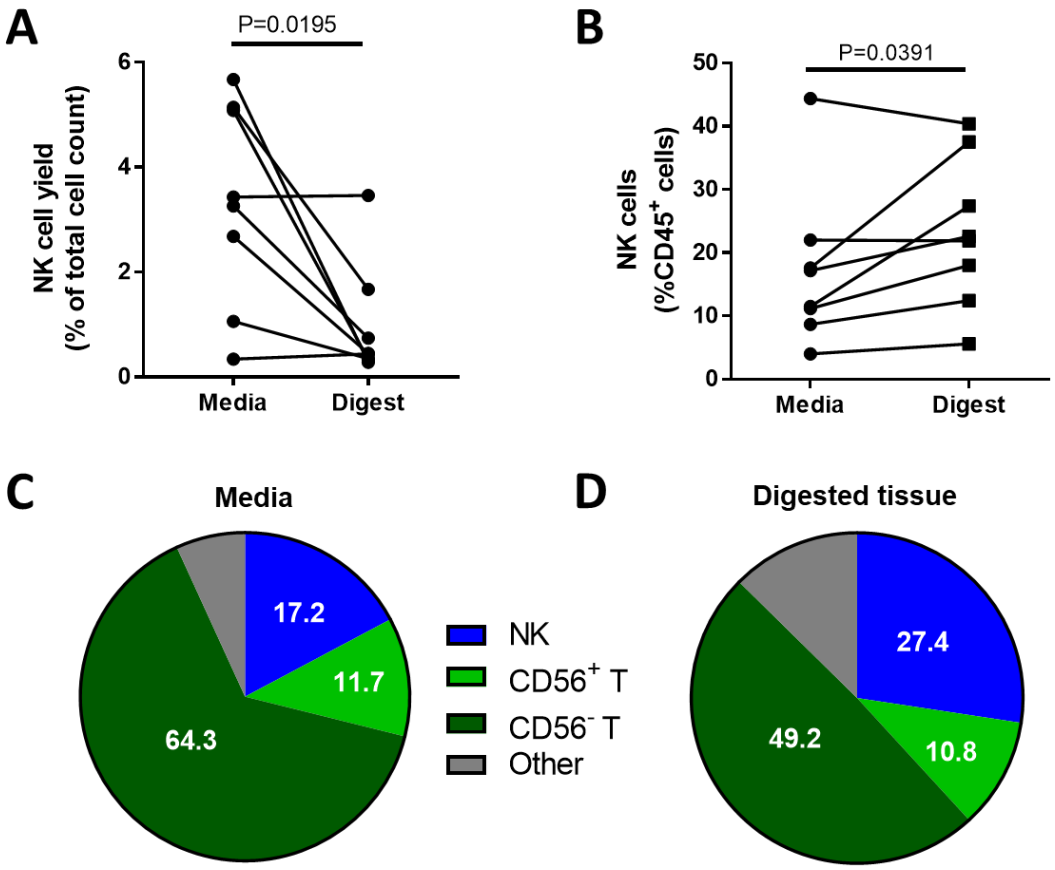

Figure 4.1: The NK cell yield from digested lung tissue. (A, B) The yield of NK cells from lung tissue allowed to rest in media for 16 h and then digested with collagenase for 15 min at 37°C. The yield from each protocol stage in compared, lines denote individuals. (**A**) NK cell yield was calculated based on the number of CD3-CD56+ cells detected by flow cytometry normalised to total cell counts. (**B**) NK cells as a fraction of CD45+ lymphocytes. Statistical analysis performed by one-tailed Wilcoxon test. Lines denote individual donors. (**C, D**) Summary of lymphocyte populations isolated from rested tissue (media) (**C**) and after collagenase digestion (**D**).

NK cells were identified in both the culture media used to rest lung tissue and following collagenase digestion of the lung pieces (Figure 4.1). The yield of NK cells from the lung tissue varied extensively, ranging between 0.34% and 5.67% of cells in the culture media and 0.28% to 3.46% in collagenase-digested tissue (Figure 4.1 A). Consistently fewer NK cells were measured after collagenase-digestion than in the culture media (P=0.0195, Figure 4.1 A). However, NK cells made up a greater proportion of the CD45+ lymphocytes recovered from the digested tissue than the culture media (27.4% vs 17.2% respectively, P=0.0391 Figure 4.1 B). CD56- T cells and other lymphocytes made up a bigger proportion of the lymphocytes isolated from the culture media (Digest CD56- T cells; 64.3, culture media CD56- T cells; 49.2%, Figure 4.1 C and D). The median number of NK cell events in digested lung tissue was 10,011 ± 9,073 with a minimum value of 2,760 (N=8), thus demonstrating a sufficient yield for flow cytometry analysis.

To exclude any effect of collagenase treatment on the detection of cell surface protein, human PBMCs were treated with or without 0.5mg/mL collagenase for 15 min at 37°C and analysed by flow cytometry. This treatment with collagenase enzyme did not affect measures of NK cell defining proteins such as CD45, CD3, CD56 or CD16 (Figure 4.2 A, B, C and D). Neither were other phenotypic markers affected, including CD69, CD103 and CCR5 (Figure 4.2 E, F and G). CD49a resistance to collagenase had been previously validated [462]. Unfortunately, collagenase digestion was found to reduce the detection of CXCR3 on PBMCs and therefore this marker could not be analysed in digested tissue explants (Figure 4.2 H).

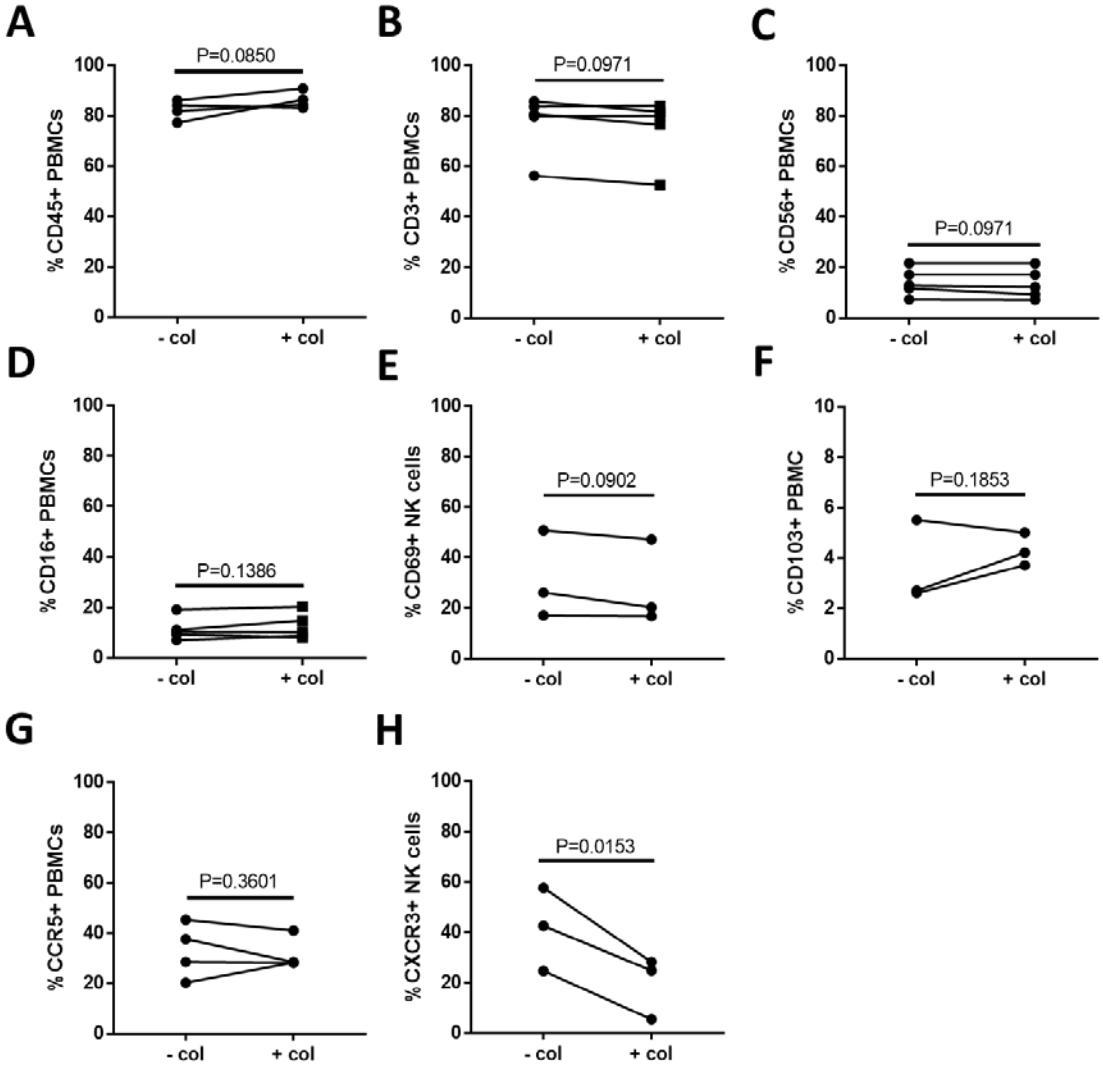

Figure 4.2: Treatment in collagenase does not affect antibody binding or detection. 1x10^6 PBMCs from healthy controls were treated with 0.5µg/mL collagenase for 15min at 37°C and antibody binding measured by flow cytometry (**A, G** N=4) (**B, C, D** N=5) (**E, F, H** N=3). Where N numbers are small statistical analysis was performed by one-tailed T test. Lines denote individual donors.

$CD56^{bright}$, $CD56^{dim}$CD16+ and $CD56^{dim}$CD16- NK cells could all be identified in human lung tissue (Figure 4.3 A). $CD56^{dim}$CD16- NK cells were found to be increased in collagenase-digested tissue compared to the culture media (10.7% vs 23.5% respectively, P=0.0156, Figure 3.3 D). There was a non-significant trend for reduced $CD56^{bright}$ NK cells in the collagenase digested fraction indicating that these cells may have become activated (digest; 16% vs media; 11.6%, P=0.1484 Figure 3.6 B) as there was no difference in the proportion of $CD56^{dim}$CD16+ NK cells (media; 67.5% vs digest; 52.9% respectively, P=0.3828, Figure 4.3 C).

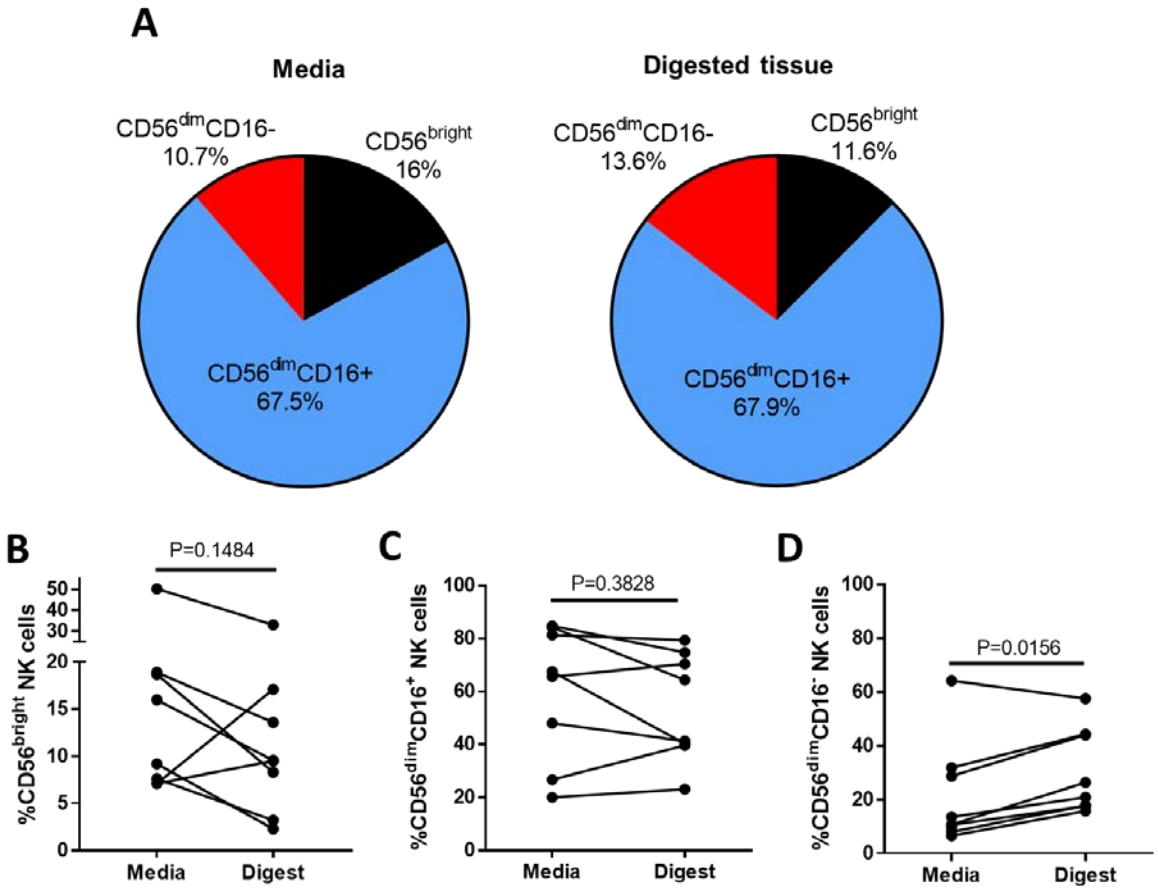

Figure 4.3: CD56^{bright} and CD56^{dim} NK cells isolated from the human lung. (**A**) Summary of the percentage of CD56^{bright}, CD56^{dim}CD16+ and CD56^{dim}CD16- NK cell isolated from human lung parenchyma following non enzymatic isolation (media) and collagenase digestion (N=8). Median proportions are shown. (**B, C, D**) Direct comparison of CD56^{bright} (**B**), CD56^{dim}CD16+ (**C**) and CD56^{dim}CD16- (**D**) proportions from lung tissue were rested in media and then digested. Lines describe individual donors (N=8). Data was interrogated by a two-tailed Wilcoxon test as this was not a hypothesis driven statistical analysis.

Previous work assessing lung T cells suggests that collagenase digested tissue is more relevant to the aims of this thesis as this fraction was found to entirely contain Trm cells [429, 460]. Therefore the digested lung tissue is more likely to include lymphocytes embedded within the parenchyma and therefore those most influenced by the pulmonary environment [429, 460]. In contrast the culture media is more likely to contain lymphocytes easily removed from the tissue and therefore may contain more circulating NK cells [460]. For this reason, collagenase-digested tissue was used to derive the lung NK cell phenotype in the following experiments.

4.2.2 Human Lung NK cells are highly differentiated

Having validated a protocol for NK cell isolation from parenchymal human lung tissue, the expression of NK cell surface proteins was analysed from the lung and matched peripheral blood (CR-PB) by flow cytometry. Demographic information for this cohort is provided in Table 3.1. Direct comparisons were made between the lung and blood of the same donor to control for donor heterogeneity. However, the peripheral blood from cancer resection patients was found to closely mirror that of healthy controls (section 3.3.2).

NK cells were found to make up a substantial proportion of CD45+ lymphocytes isolated from the human lung parenchyma (median of 10.85 % ±14.98, N=22, Figure 4.4 B and C). In four lung donors NK cells represented >40% of lung CD45+ cells. However, the average lung NK cell population was found at a similar proportion to lymphocytes in the peripheral blood (CR-PB; median 11.1% ± 4.65, N=22, Figure 4.4 A and C). The majority of lung-associated NK cells were canonical cytotoxic $CD56^{dim}CD16+$ cells (69.25%) with a minority population of $CD56^{bright}$ NK cells (8.6%), similar to the phenotype of the peripheral blood (Figure 4.4 and Figure 3.4). However, the proportion of $CD56^{bright}$ NK cells was increased in the lung parenchyma compared to peripheral blood (lungs 8.6% vs blood 3.3%, $P<0.0001$, Figure 4.4D). There was a corresponding trend for reduced $CD56^{dim}CD16+$ NK cells in the lungs, although this did not reach significance (69.25% vs 82.5% respectively $P=0.0522$). The proportion of $CD56^{dim}CD16-$ NK cells was equivalent between the lungs and blood of resection donors ($CD56^{dim}CD16+$, $CD56^{dim}CD16-$ 14.6% vs 9.55% respectively $P=0.1488$, Figure 4.4 E and F).

To further evaluate the maturity of lung NK cells, the expression of CD57 and CD158b was analysed [274, 275]. CD57 was expressed on 62.7% of lung NK cells and predominantly found on $CD56^{dim}CD16+$ NK cells, much like the peripheral blood (79.55% lung $CD56^{dim}CD16+$ vs 66.75% blood, $P>0.9999$ Figure 4.5 A and B). In contrast, only 21.8% of $CD56^{dim}CD16-$ and 8% of $CD56^{bright}$ lung NK cells expressed CD57 (Figure 4.5 B). Lung NK cells were also strongly (36.4%) CD158b positive, a slight non-significant increase relative to the blood (29.9%, $P=0.0742$, Figure 4.5 C). CD158b was mainly expressed on lung $CD56^{dim}CD16+$ NK cells with a 5% increase in expression relative to the peripheral blood (lung 38.9% vs blood 33.95%, $P>0.9999$, Figure 4.5 D), although this was not found to be a statistically significant difference. A small amount of CD158b was expressed on $CD56^{bright}$ (9.65%) and $CD56^{dim}CD16-$ (11.55%) lung NK cells, with small but non-significant increases in CD158b expression compared to the peripheral blood (4.5 C and E). The apparent high

maturation of lung NK cells was further confirmed through the lack of CD117 expression (N=8, 0% CD117+ lung NK cells), a protein which defines immature NK cell progenitors.

To further explore the differentiation state of CD158b (KIR2DL2/L3/S2) expressing NK cells, the co-expression of CD57 on CD158b+ cells was analysed, as shown in Figure 4.5. CD57 was equivalently distributed through CD158b positive and negative NK cells and the co-expression of CD158b and CD57 on lung NK cells was equivalent to matched blood ($P>0.9999$ for each analysis, Figure 4.5 F). Taken together these results indicate that lung NK cells are predominantly mature and terminally differentiated with a potently cytotoxic phenotype, strongly mirroring the phenotype of the peripheral blood [275].

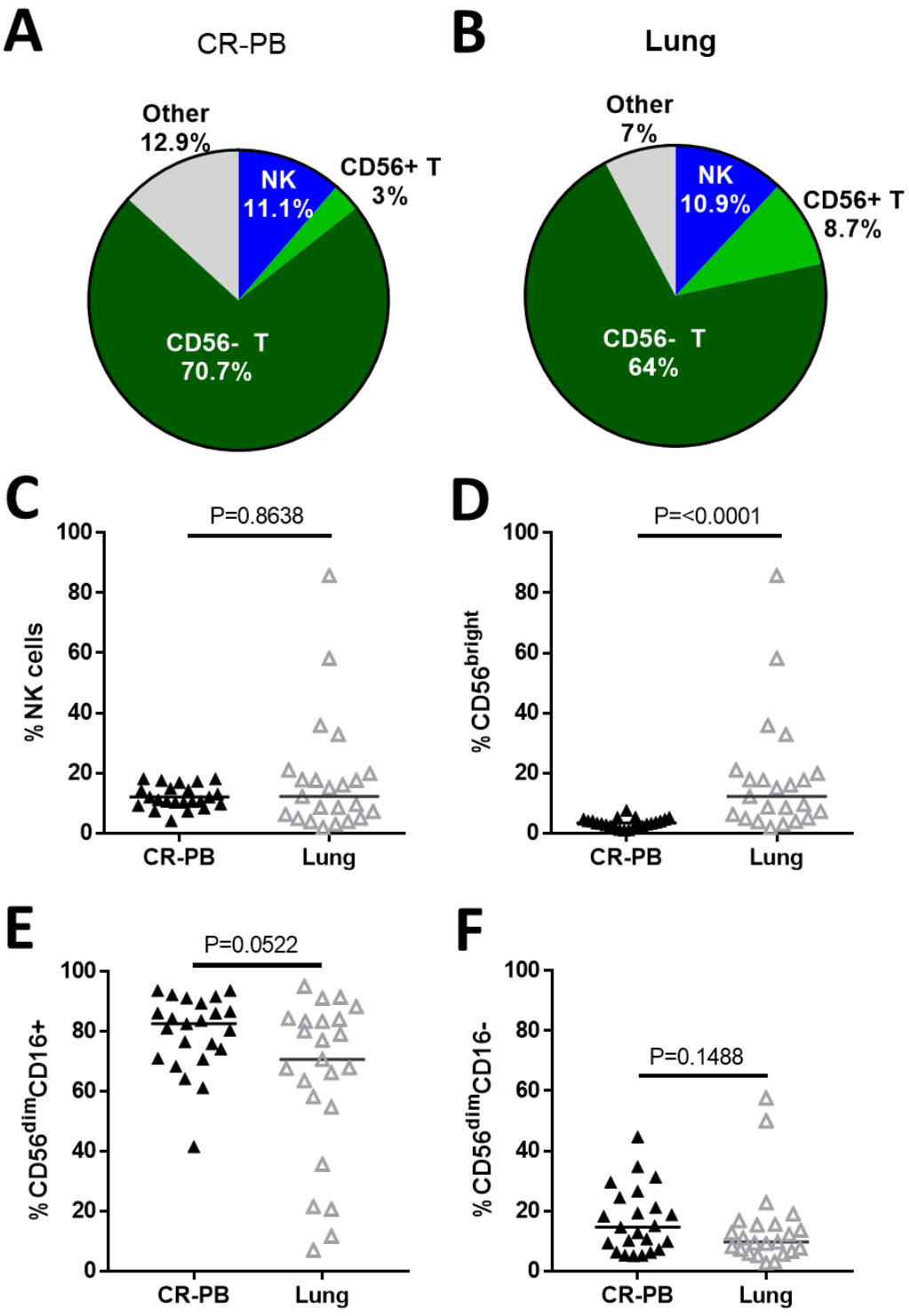

Figure 4.4: NK cells are found at similar proportions in matched blood (CR-PB) and lung. (**A, B**) Quantification of CR-PB and lung CD45+ lymphocyte populations, N=22. (**C**) NK cells as a percentage of CD45+ lymphocytes in matched blood and lung (N=22) (**D, E, F**) Proportions of $CD56^{bright}$, $CD56^{dim}CD16+$ and $CD56^{dim}CD16-$ NK cells in lung tissue and matched blood (N=22). Lines describe medians, statistical analysis by Wilcoxon signed-rank test.

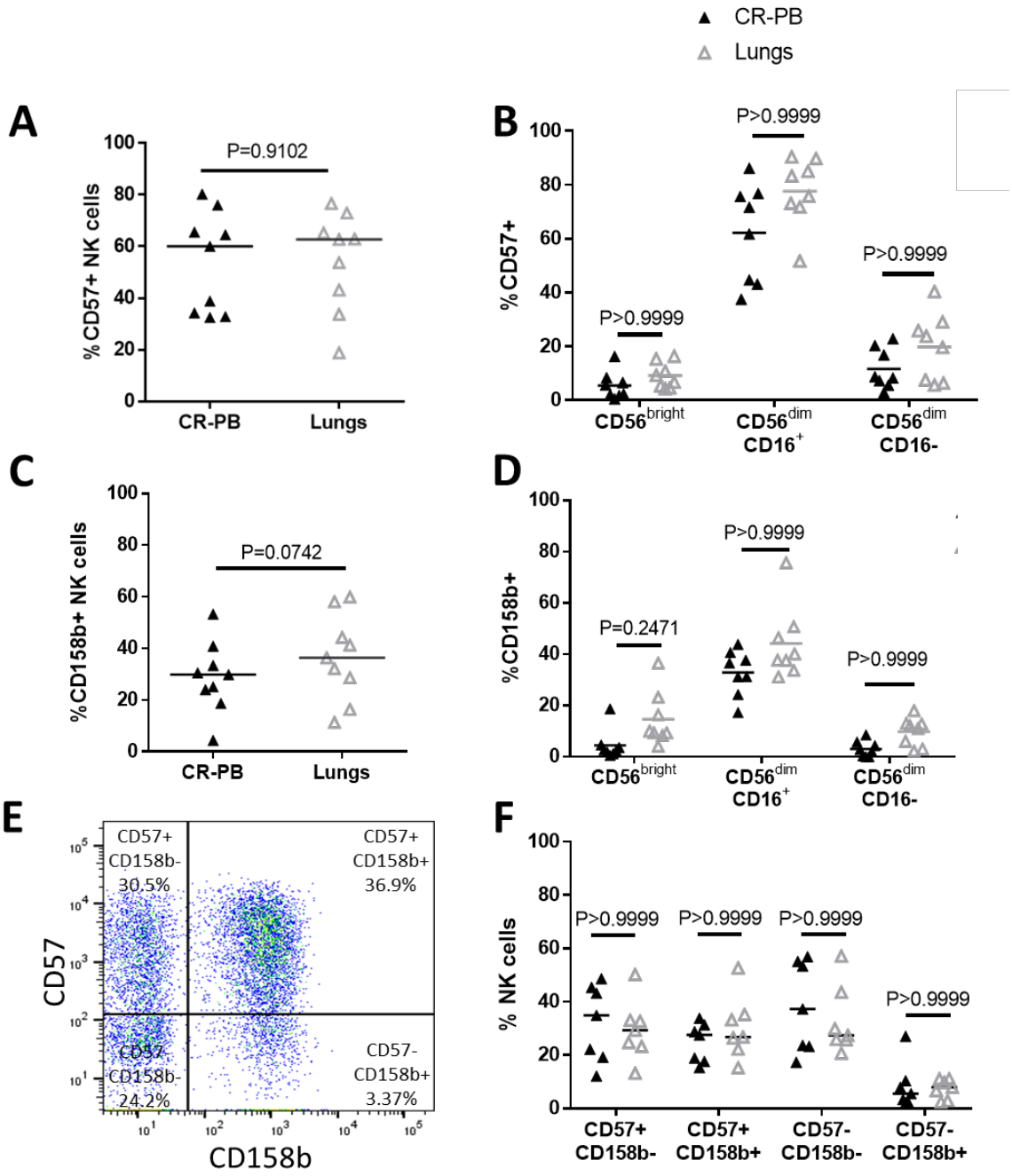

Figure 4.5: CD57 and CD158b expression on lung and blood NK cells. CD57 (**A**) and CD158b (**C**) expression on NK cells in the peripheral blood (CR-PB) and lung of cancer resection patients (N=9). Lines describe medians, statistical analysis by Wilcoxon signed-rank test. **(B, D**) CD57 and CD158b expression on CD56^{bright}, CD56^{dim}CD16+ and CD56^{dim}CD16- NK cell subsets from the blood and lung. Statistical analysis by Friedman's test with Dunn's multiple comparison correction. (**E**) Representative flow cytometry plot describing lung NK cell CD57 and CD158b co-expression. Gates were set based on negative staining with isotype controls. (**F**) CD57 and CD158b expression on NK cells from the lung and matched blood (CR-PB (N=7). Statistical analysis by Friedman's test with Dunn's multiple comparison correction. **NK Cell Activating Receptor Expression in the Blood and Lung**

As discussed in section 1.4.3, the activating receptors NKp46, NKG2D and NKG2C can stimulate NK cell cytotoxicity towards virally infected cells, including IAV [254, 353, 354]. The expression of these activating receptors was therefore measured on NK cells isolated from the lungs and analyzed relative to the peripheral blood. AS NKp46 and NKG2D are constitutively expressed by NK cells the surface expression of these proteins are presented as sMFI.

Consistent with the reported peripheral blood phenotype, NKp46 was strongly expressed on $CD56^{bright}$ NK cells and only weakly on $CD56^{dim}$ NK cell subsets (Figure 4.6 B). This pattern of expression was also found on lung NK cells. NKp46 expression did not differ between the blood and lungs at the gross NK cell level (P=0.2769, Figure 4.3 A) or when stratified based on CD56 and CD16 expression (P>0.9999 for all analyses, Figure 4.6B). NKG2C was also expressed similarly between the blood and lung (6.4% vs 10.5%, P=0.8906 Figure 4.6 E). The proportions of NKG2C+ $CD56^{bright}$, $CD56^{dim}$CD16+ and $CD56^{dim}$CD16- NK cells were all equivalent between the lungs and blood (P=0.7789, P=0.4214 and P=0.779 respectively, Figure 4.6 F).

Interestingly, NKG2D expression was significantly increased on lung NK cells compared to the blood, however the difference in average sMFI was small (135.5 vs 93.5 P=0.0488, Figure 4.3 C) with outliers in the lung group. Interestingly, this increase in NKG2D expression was only found on the lung $CD56^{dim}$CD16- NK cells (P=0.0362, Figure 4.6 D). No statistical differences were found in the expression of NKG2D on $CD56^{bright}$ or $CD56^{dim}$CD16+ NK cells between the lung and blood (P>0.9999 for both subsets, Figure 4.6D). Taken together these results show that in general lung NK cells do not differ from the blood in their expression of these three key anti-viral activating receptors, with the exception of a slight increase in lung $CD56^{dim}$CD16- expression of NKG2D.

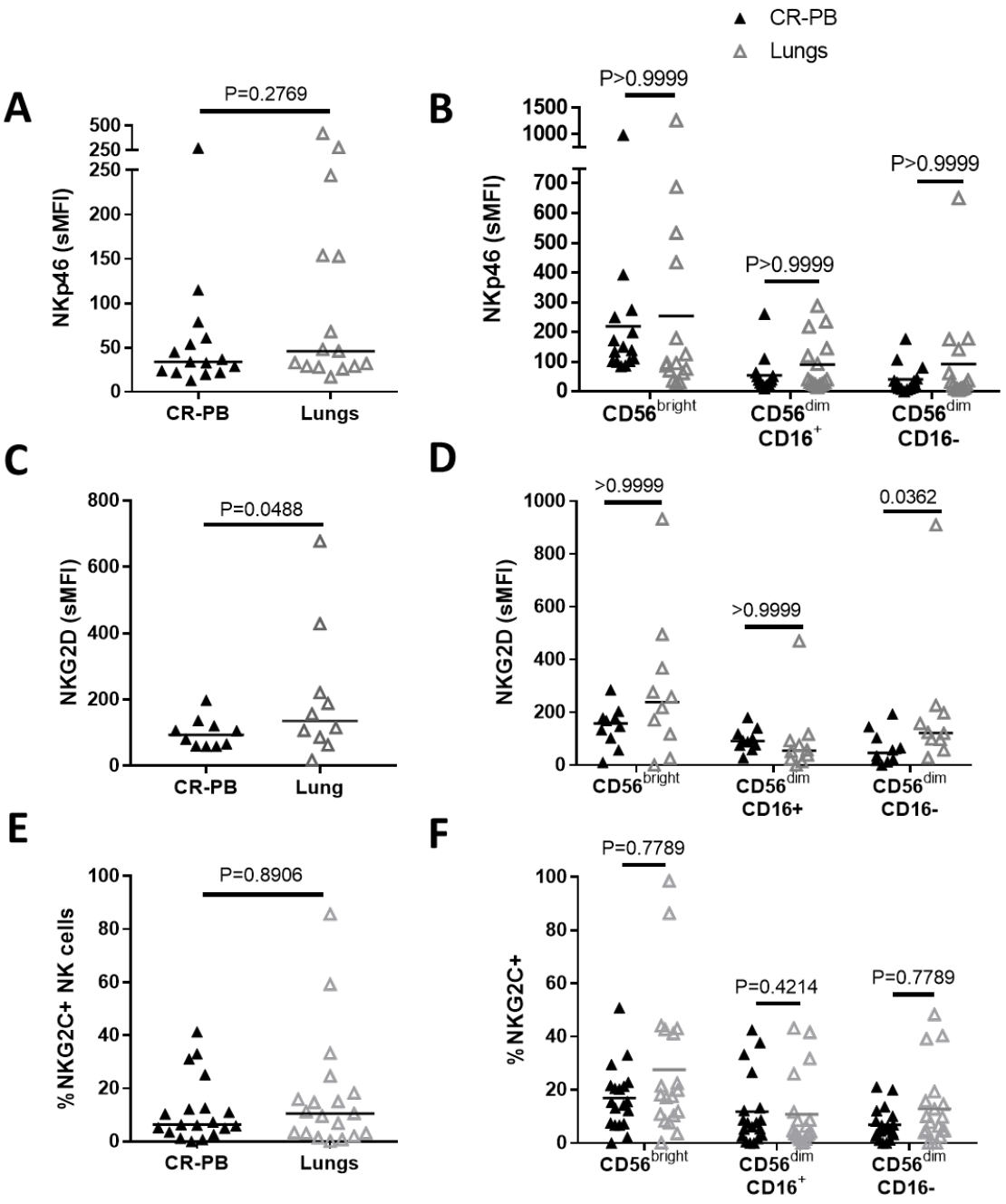

Figure 4.6: **Activating receptor expression on lung and blood NK cells.** (**A, C, E**) NKp46 (N=15), NKG2D (N=11) and NKG2C (N=19) expression on NK cell subsets in peripheral blood (CR-PB) and lungs of resection donors. Lines describe medians, statistical analysis by Wilcoxon signed-rank test. **(B, D, F**) NKp46, NKG2D and NKG2C expression on $CD56^{bright}$, $CD56^{dim}CD16+$ and $CD56^{dim}CD16-$ NK cells from the blood and lung. Statistical analysis by Friedman's test with Dunn's multiple comparison correction.

4.2.4 Residency Markers on NK cells of the Human Lung

Thus far, NK cells of the lung appear very phenotypically similar to the peripheral blood. To investigate unique pulmonary NK cell populations the expression of the residency markers, CD49a, CD103 and CD69 were investigated. As shown in Figure 4.7 a distinct CD49a+ NK cell population was identified in the lung parenchyma and not found in the circulation (P<0.0001). CD49a+ NK cells made up 13.3% ±11 of the total lung NK cell population and were primarily $CD56^{bright}$CD16- and $CD56^{dim}$CD16- NK cells (44.2% and 27.3% respectively, Figure 4.7 A and 4B). Negligible amounts of CD49a were detected on $CD56^{dim}$CD16+ lung NK cells (3.8%) and none detected in the peripheral blood. Other markers of residency, CD69 and CD103 were also identified in the lung parenchyma. A small proportion of lung NK cells (3.65% ±7.65) expressed CD103, a protein not found on blood NK cells (P=0.016, Figure 4.7 C). The expression of CD103 on NK cell $CD56^{bright}$ and $CD56^{dim}$ subsets mirrored that of CD49a, with most CD103 expressed on $CD56^{bright}$ NK cells (31.7%) and a smaller expression on $CD56^{dim}$CD16- NK cells (8.35%, Figure 4.7 D). Minimal CD103 expression (0.05%) was found on lung $CD56^{dim}$CD16+ NK cells.

In contrast, CD69 was not found to be expressed differently between the blood and lung at the whole NK cell level (22.1 vs 22.75% respectively P=0.9453, Figure 4.7 E). CD69 was also found to be expressed equivalently by lung and blood $CD56^{dim}$CD16+ and $CD56^{dim}$CD16- NK cells (P=0.33 and 0.18 respectively). However, CD69 was increased on lung $CD56^{bright}$ cells (lung 67.25% vs blood 21.2%, P=0.0015, Figure 4.7 F).

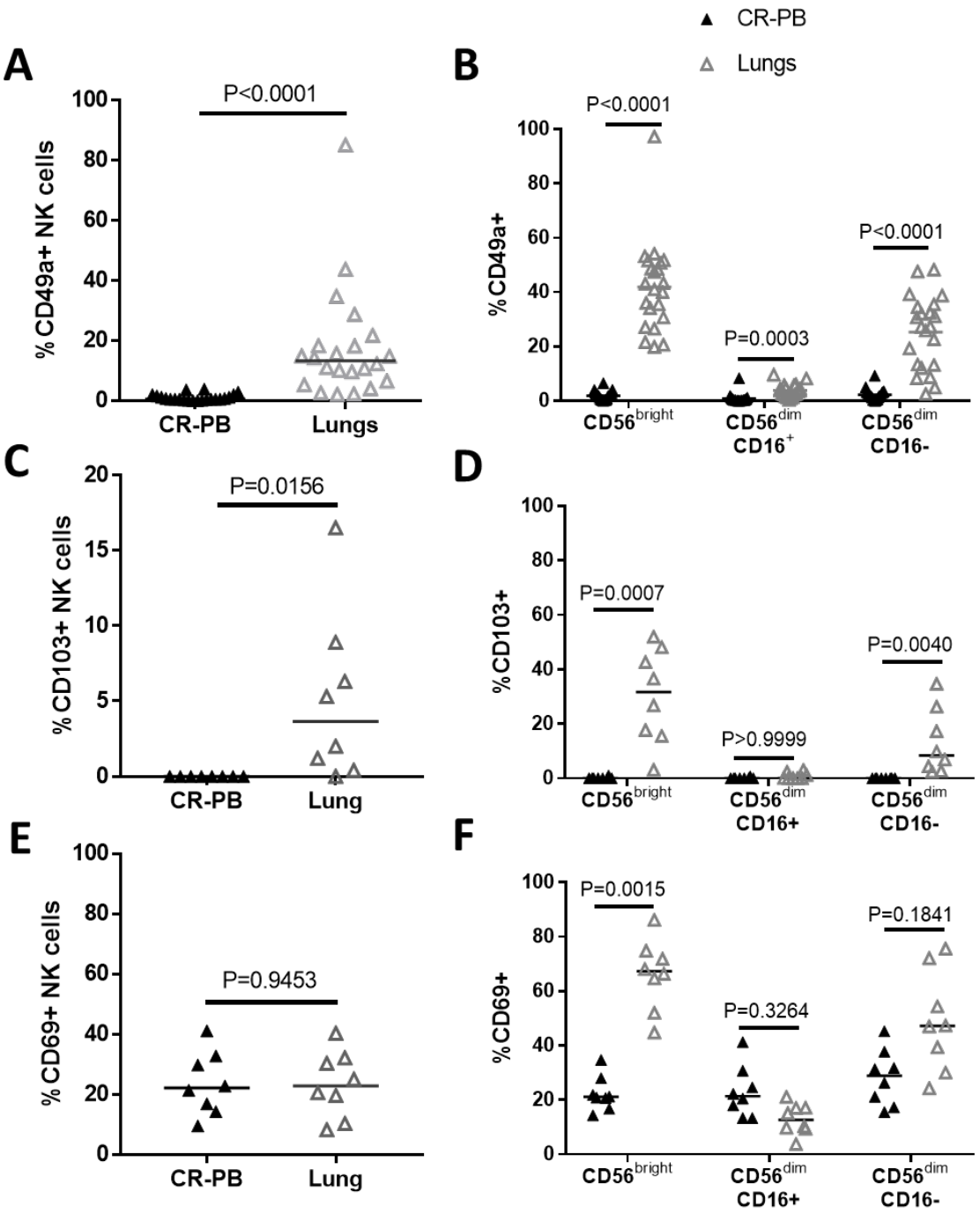

Figure 4.7: Distinct NK cell populations are present in the lung, but not the blood. (**A, C, E**) Flow cytometric analysis of CD49a (N=22), CD103 (N=8) and CD69 (N=8) expression on lung and blood NK cells. Statistical analysis performed by Wilcoxon signed-rank test. Lines describe medians. (**B, D, F**) Residency marker expression on $CD56^{bright}$ and $CD56^{dim}$ NK cell subsets. Statistical analysis by Friedman's test with Dunn's multiple comparison correction.

To visualise the co-expression of CD49a, CD69 and CD103, CD56^{bright} NK cells were analysed as shown in Figure 4.8 A and B. A t-distributed stochastic neighbour embedding (t-SNE) analysis of CD56^{bright} NK cells was performed based on the expression of the three residency markers (Figure 4.8 C). Lung CD56^{bright} NK cells clustered together and appear distinct to CD56^{bright} of matched peripheral blood (Figure 4.8C). Strong individual heterogeneity can be observed in this analysis as each individual was represented as a distinct cluster. This same technique was used to visualise the expression of CD49a, CD103 and CD69 on CD56^{bright} NK cells in the lung (Figure 4.8 D). CD56^{bright} lung NK cells consisted of single positive, double positive and triple positive populations for CD49a, CD103 and CD69. CD69 and CD103 were strongly co-expressed by CD49a positive CD56^{bright} NK cells compared to CD49a negative cells (P=0.0496, Figure 4.8E). CD49a+CD103+CD69+ cells made up one of the largest populations (20.9% ±12.66) of lung CD56^{bright} NK cells (Figure 4.8 F and G). Interestingly single positive CD49a+ NK cells were positioned together with triple and double positive CD56^{bright} NK cells in the t-SNE analysis (Figure 4.8 C). In contrast only CD69 was detected in the peripheral blood (Figure 4.8 G). CD69 single positive CD56^{bright} NK cells were also identified in the lungs and found at a similar proportion to the blood (CR-PB; 22.8% of CD56^{bright} NK cells vs lung; 25.7%).

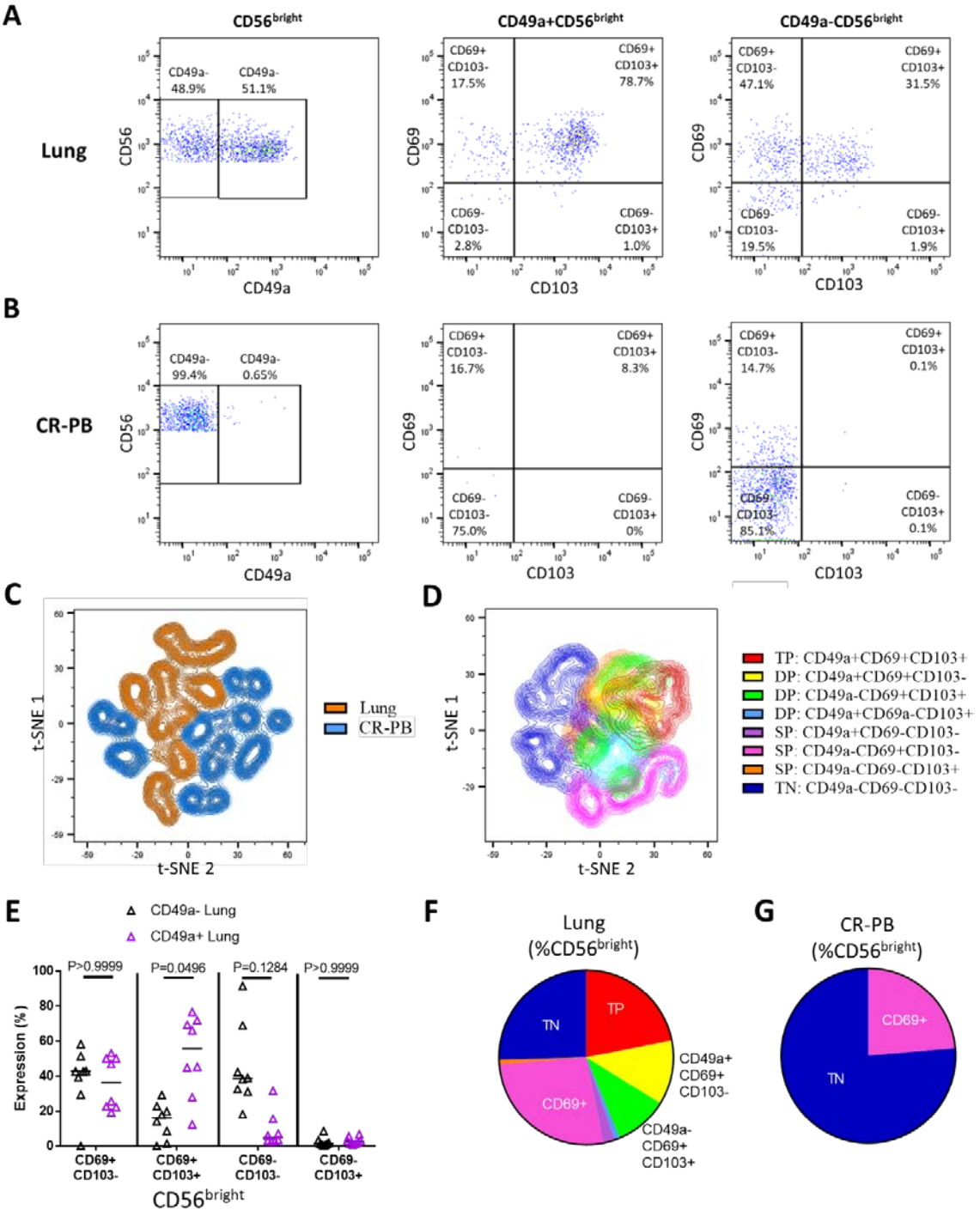
A
CD56bright
CD49a+CD56bright
CD49a-CD56bright
Lung
CD49a- 48.9%
CD49a- 51.1%
CD56
CD49a
CD69+ CD103- 17.5%
CD69+ CD103+ 78.7%
CD69- CD103- 2.8%
CD69- CD103+ 1.0%
CD69
CD103
CD69+ CD103- 47.1%
CD69+ CD103+ 31.5%
CD69- CD103- 19.5%
CD69- CD103+ 1.9%
B
CR-PB
CD49a- 99.4%
CD49a- 0.65%
CD69+ CD103- 16.7%
CD69+ CD103+ 8.3%
CD69- CD103- 75.0%
CD69- CD103+ 0%
CD69+ CD103- 14.7%
CD69+ CD103+ 0.1%
CD69- CD103- 85.1%
CD69- CD103+ 0.1%
C
t-SNE 1
t-SNE 2
Lung
CR-PB
D
TP: CD49a+CD69+CD103+
DP: CD49a+CD69+CD103-
DP: CD49a-CD69+CD103+
DP: CD49a+CD69a-CD103+
SP: CD49a+CD69-CD103-
SP: CD49a-CD69+CD103-
SP: CD49a-CD69-CD103+
TN: CD49a-CD69-CD103-
E
CD49a- Lung
CD49a+ Lung
P>0.9999
P=0.0496
P=0.1284
P>0.9999
Expression (%)
CD69+ CD103-
CD69+ CD103+
CD69- CD103-
CD69- CD103+
CD56bright
F
Lung (%CD56bright)
TP
TN
CD69+
CD49a+ CD69+ CD103-
CD49a- CD69+ CD103+
G
CR-PB (%CD56bright)
CD69+
TN

Figure 4.8: CD56^{bright} CD49a+ lung NK cells co-express CD69 and CD103. (**A**) Gating strategy to define co-expression of CD69 and CD103 on CD49a+ and CD49a- populations of CD56^{bright} NK cells isolated from the lung (**A**) and blood (CR-PB) (**B**). (**C**) t-SNE plot of CD56^{bright} NK cells in matched blood (blue) and lung (orange) based on CD49a, CD69 and CD103 expression (N=16, 8 individuals). From each sample 300 events were randomly selected. Perplexity=20, 1000 iterations. (**D**) t-SNE plot of CD56^{bright} NK cells isolated from the lungs based on CD49a, CD69 and CD103 expression (N=6). Cells are coloured according to expression of each marker, showing single-positive (SP), double-positive (DP) and triple-positive (TP) populations. 600 events were randomly selected from each sample. Perplexity=20, 1000 Iterations. A singlet gate based on Forward Scatter (FSC)-A versus FSC-W was included for the cells in this analysis. (**E**) Quantification of CD69 and CD103 expression on CD49a+ and CD49a- NK cell populations of the lung and blood. Lines described medians, statistical analysis by Friedman's test with Dun's multiple comparison correction (N=8). Overall P value <0.001 (**F, G**) Quantification of residency marker expression on CD56^{bright} NK cells of matched blood (**F**) and lung (**G**). Key as shown in **D**. TP = triple positive, DP = double positive, SP= single positive and TN= triple negative.

A similar analysis was conducted for CD56^{dim}CD16- NK cells, as this subset of NK cells was also found to express CD49a and CD103, albeit at a lower level to CD56^{bright} NK cells (Figure 4.7). The co-expression of residency markers on lung CD56^{dim}CD16- NK cells was similar to that seen for CD56^{bright} NK cells (Figure 4.9). The same triple, double and single positive populations of NK cells were observed as in the CD56^{bright} subset (Figure 4.9 A, C and D) and most double positive and single positive populations were found in similar proportions to CD56^{bright} NK cells (Table 4.1). Furthermore, CD69 and CD103 were also strongly co-expressed with CD49a on this subset (P=0.0089, Figure 4.9 B). This is visualised by t-SNE analysis of CD56^{dim}CD16- residency marker expression as CD56^{dim}CD16- CD49a+ cells clustered closely with CD49a+CD103+CD69+ cells (Figure 4.9 A). Whereas single positive CD69 NK cells made up a cluster distinct from other residency marker expressing cells.

There were some differences between residency marker expression in CD56^{bright} and CD6^{dim}CD16- NK cells. For instance, triple positive CD69+CD49a+CD103+ cells made up a significantly smaller proportion of the CD56^{dim}CD16- subset compared to CD56^{brigh}t (4.4% vs 20.9% respectively P=0.0234, Table 4.1). There was also a smaller proportion of CD49a-CD69+CD103+ cells in CD56^{dim}CD16- NK cells (CD56^{dim}CD16- 4.25% vs CD56^{bright} 9.45%, P=0.0391, Table 4.1). Finally, NK cells single positive for CD69 were increased in CD56^{dim}CD16- NK cells relative to CD56^{bright} NK cells

(P=0.0078, Table 4.1) suggesting that lung CD56^{dim}CD16- NK cell subset may be more activated than the CD56^{bright} NK cells. Residency marker expression on both CD56^{bright} and CD56^{dim}CD16- cells and their comparison is summarised in Table 4.1.

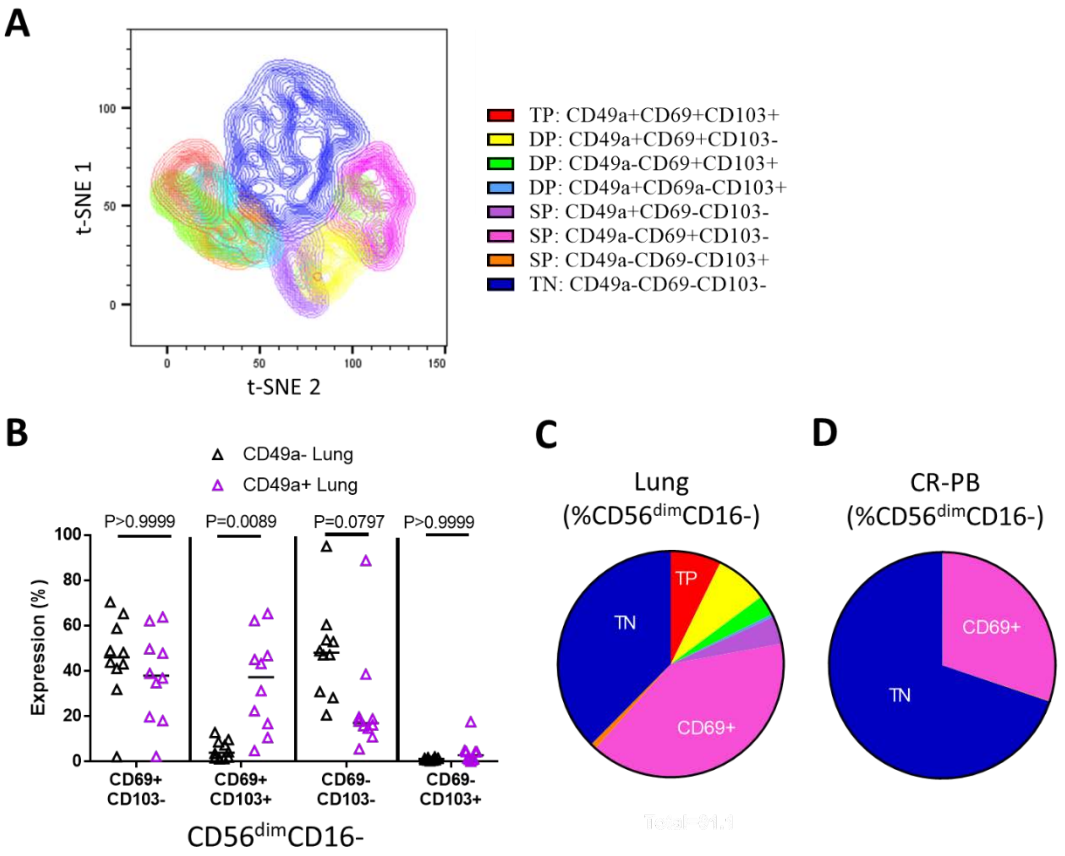

Figure 4.9: CD56^{dim}CD16- CD49a+ lung NK cells co-express CD69 and CD103. (**A**) t-SNE plot of CD56^{dim}CD16- NK cells isolated from the lungs based on CD49a, CD69 and CD103 expression (N=6). Cells are coloured according to expression of each marker, showing single-positive (SP), double-positive (DP) and triple-positive (TP) populations. From each sample 1000 events were randomly selected. Perplexity=20, 1000 iterations. (**B**) Quantification of CD69 and CD103 co-expression of CD49a+ and CD49a- CD56^{dim}CD16- NK cell populations of the lung and blood. Lines describe medians, statistical analysis by Friedman's test with Dun's multiple comparison correction (N=10). (**C, D**) Residency marker expression on CD56^{bright} NK cells of matched blood (**D**) and lung (**C**). Key as shown in **A**. TP = triple positive, DP = double positive, SP= single positive and TN= triple negative.

	CD56^{bright}	CD56^{dim}CD16-	P-value
TP: CD49a+CD69+CD103+	20.9 (20.8)	4.4 (10.9)	0.0234
DP: CD49a+CD69+CD103-	11.4 (5.1)	6.45 (3.6)	0.0547
DP: CD49a-CD69+CD103+	9.45 (6.0)	2.25 (4.7)	0.0391
DP: CD49a+CD69-CD103+	0.95 (1.2)	0.25(0.6)	0.2969
SP: CD49a+CD69-CD103-	2.05 (2.7)	4.4 (4.5)	0.2344
SP: CD49a-CD69+CD103-	25.65 (5.8)	36 (16)	0.0078
SP:CD49a-CD69-CD103+	0.8 (0.7)	0.7 (0.6)	0.8750
TN: CD49a-CD69-CD103-	24.3 (7.9	34.2 (14.8)	0.3125

Table 4.1: Summary of the percentage expression of residency markers CD49a, CD103 and CD69 on CD56^{bright} and CD56^{dim}CD16- lung NK cells. Median values and italicized interquartile range are shown. TP = triple positive, DP = double positive, SP= single positive and TN= triple negative. Statistical analysis by Wilcoxon signed-rank test.

Resident CD49a+ NK cell populations have been associated with a memory phenotype, as CD49a+ cells mediate an enhanced NK cell response to secondary challenge with hapten [336]. How this innate memory may be generated remains a mystery, but one possible explanation is an altered balance of inhibitory and activating receptors on the NK cell surface [344]. For instance CMV infection has been associated with expanded populations of NKG2C+ NK cells [349, 353-356]. Therefore, the expression of activating receptors, NKp46, NKG2D and NKG2C was compared between CD49a+ and CD49a- NK cells after stratified based on CD56 and CD16 expression (Figure 4.10). Within CD56^{bright} NK cells, NKp46 expression was reduced on CD49a+ cells compared to CD49a- cells (P=0.0254, Figure 4.10A). In contrast NKG2D and NKG2C expression was increased on CD56^{bright} NK CD49a+ cells (P=0.0078 and P=0.0049 respectively, Figure 4.10 B and C). A similar trend for reduced NKp46 expression on CD49a+ cells was observed in CD56^{dim}CD16- NK cells (P=0.0640, Figure 4.10 D) and an increase in NKG2D expression was also measured on CD49a+ CD56^{dim}CD16- NK cells (P=0.0420, Figure 4.10 E). However, NKG2C was not differentially expressed by CD49a+ and CD49a- CD56^{dim}CD16- NK cells (P=0.1602, Figure 4.10 F). Taken together these results show a distorted expression of activating receptors on CD56^{bright}CD49a+ cells, indicating that activating signaling might be amplified in this NK cell population. Similar trends were found in the activating receptor profiles of resident CD56^{dim}CD16- NK cells but the differences were not as clear.

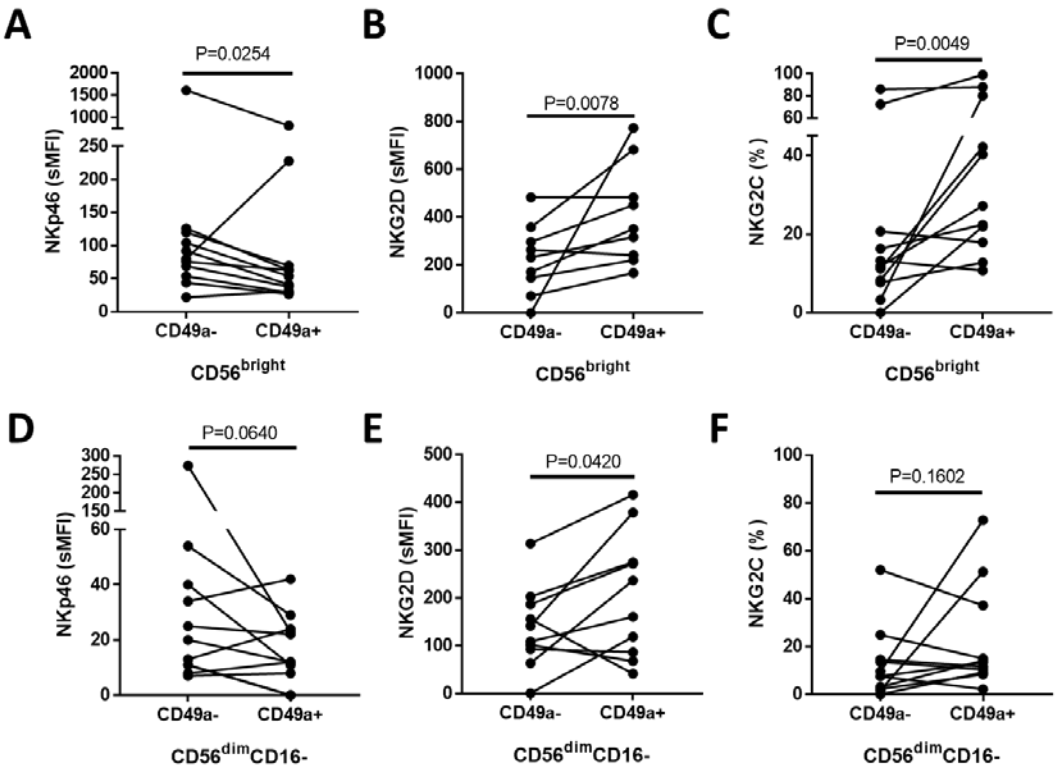

Figure 4.10: Activating receptors are expressed differentially on CD49a+ and CD49a- NK cells of the lung. (**A, B, C**) NKp46 (N=11) (**A**)**,** NKG2D (N=9) (**B**) and NKG2C (N=11) (**C**) expression on $CD56^{bright}$ CD49a+ and CD49a- NK cells isolated from the lungs. (**D, E, F**) NKp46 (**D**)**,** NKG2D (**E**) and NKG2C (**F**) expression on $CD56^{dim}$CD16- CD49a+ and CD49a- NK cells isolated from the lungs. Statistical analysis by Wilcoxon signed rank test, lines denote individual donors.

4.2.5 CCR5 is enriched on Human Lung NK Cells

The novel identification of a resident NK cell population in the lungs raises questions about how NK cells traffic through the lungs. The hypothesis of this thesis is that $CD56^{bright}$ CD49a+CD69+CD103+ NK cells are recruited to the lungs via CCR5 as this receptor involved in maintaining liver rNK cells, [332]. Therefore, this receptor was measured on CD49a+ and CD49a- NK cells in the lung. CXCR6 and CXCR3 have also been linked to the recruitment of resident NK cells to the liver, lymph node and spleen [300, 332, 333]. Unfortunately, CXCR6 could not be detected in the lungs due to technical issues with high tissue autofluorescence whilst CXCR3 detection was inhibited by collagenase digestion (Figure 4.2).

CCR5 expression was first analysed on the whole NK cell population and was detected on 16.9% ± 10 of lung NK cells but only on 3.75% ± 1.6 of NK cells in the peripheral blood (P=0.0020, Figure 4.11 A). Interestingly, CCR5 was predominantly found on lung CD56^{dim}CD16- NK cells (39.85%) with a smaller degree of expression on CD56^{bright} (27.35%) and CD56^{dim}CD16+ (6.55%) NK cells. Furthermore, CCR5 was significantly increased on lung CD56^{dim}CD16- cells relative to the peripheral blood, in which only 7.1% of CD56^{dim}CD16- NK cells were positive for CCR5 (P=0.0046, Figure 4.11B). There was also a trend for increased CCR5 expression on CD56^{bright} lung NK cells but this did not reach significance (lung 27.35% vs blood 11.5% P=0.1675, Figure 4.11 B). Only a small proportion (6.55%) of lung CD56^{dim}CD16+ NK cells expressed CCR5 and this was comparable with the blood (4.25%, P=0.7685, Figure 4.11 B).

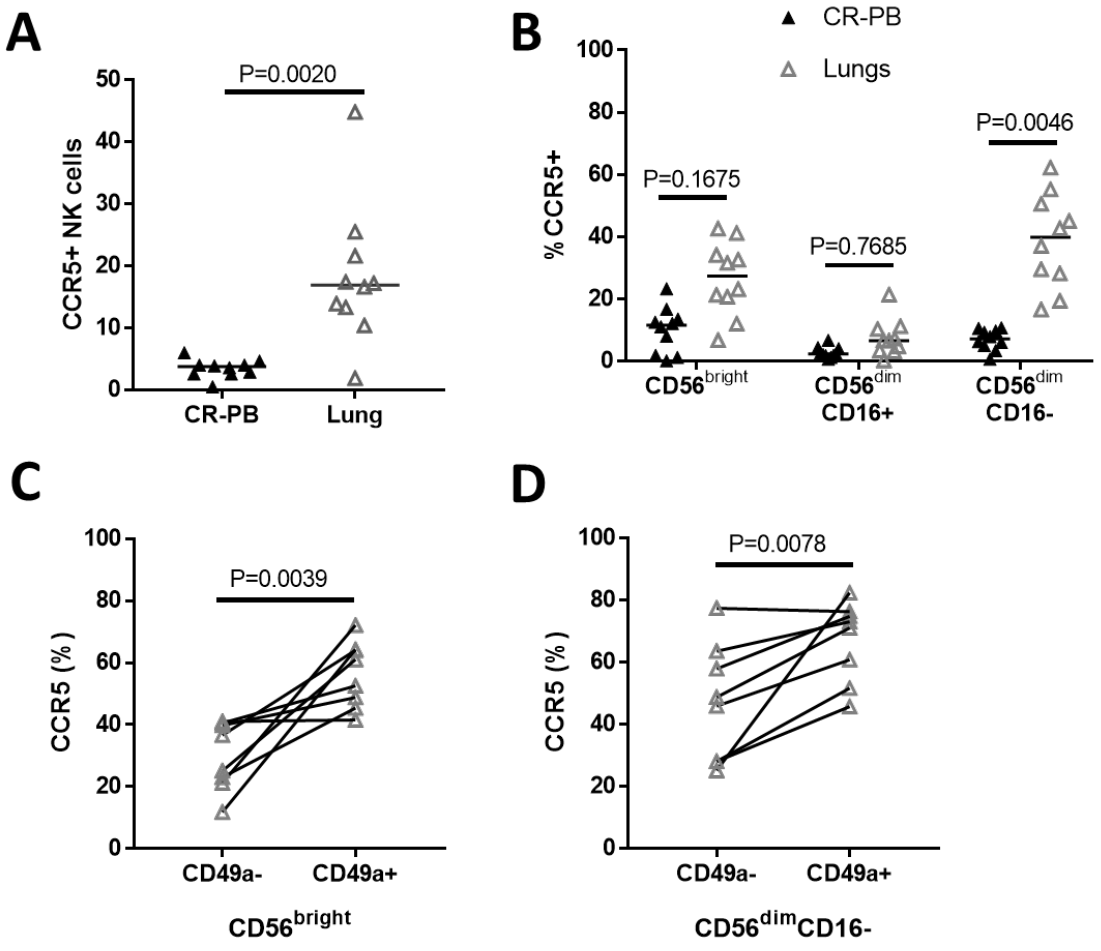

Figure 4.11: Lung NK cells express greater levels of CCR5 than in the periphery. (**A**) Expression of CCR5 on matched blood and lung NK cells. Statistical analysis by two-tailed Wilcoxon signed rank test. Lines describe medians. (**B**) CCR5 expression on CD56^{bright} and CD56^{dim} NK cell subsets of the peripheral blood and lung. Statistical analysis by Friedman's test with Dun's multiple comparison correction. (**C, D**) CCR5 expression on lung CD49a+ and CD49a- NK cells. NK cells were first stratified based into CD56^{bright} (**C**) and CD56^{dim}CD16- (**D**) subsets. Statistical analysis by Wilcoxon signed-rank test.

The expression of CCR5 was compared on CD49a positive and negative NK cells, as shown in Figure 4.11 C and D. In both $CD56^{bright}$ and $CD56^{dim}$CD16- NK cells CCR5 expression was enriched on CD49a+ NK cells (P=0.0039 and P=0.0078 respectively, Figure 4.11 C and D). A median of 56.8% of $CD56^{bright}$ CD49a+ cells expressed CCR5 compared to 30.9% of CD49a- cells. Similarly, 72% of $CD56^{dim}$CD16- CD49a+ cells were CCR5 positive with only 47.3% of CD49a- expressing this chemokine receptor (Figure 4.11D). These results show that CCR5 is differentially expressed by CD49a positive NK cells and these cells may therefore be more sensitive to CCR5-based chemotaxis in the lungs. However, CCR5 expression was still greater on CD49a- lung NK cells compared with CD49a- peripheral blood NK cells ($CD56^{bright}$ P=0.0078 and $CD56^{dim}$CD16- P=0.0039) showing that CCR5 is generally increased on lung NK cells, including the non-resident populations. Taken together these results suggest that CCR5 might play a role in NK cell homing to the lung and could represent a potential mechanism for CD49a+ NK cell retention in this organ.

4.2.6 The Lung NK cell Phenotype in COPD

COPD is a chronic inflammatory disease of the lung, during which lung NK cell cytotoxicity increased [361, 461]. COPD is a common comorbidity of lung cancer and 15 of the lung tissue donors had been diagnosed with this disease. Therefore, to investigate whether the NK cell phenotype is altered in COPD, phenotyping data was stratified based on a diagnosis of COPD (Table 4.2). In section 4.2.5 unique CD49a+ NK cell populations were identified in the human lung which may have as yet undiscovered roles in pulmonary health and disease. To explore this aspect of lung NK cell biology in COPD the expression of CD49a on lung NK cells were also stratified based on COPD status.

Within the lung tissue donors diagnosed with COPD, four individuals had been diagnosed with mild disease, ten with moderate COPD and one with severe COPD, based on GOLD classifications (Table 4.2). Lung donors with COPD had reduced lung function compared to those without COPD, with a FEV1% value of 70 ± 16.5 compared to 89 ± 21 in non-COPD donors (P=0.001, Table 4.2). The COPD cohort also had increased donor smoking, including a greater pack year history (COPD; 45 ± 22.5 vs non-COPD; 20 ± 35, P=0.0087, Table 4.2) and more current and ex-smokers at the time of resection (P=0.0337, Table 4.2). Otherwise lung tissue donors with and without COPD were equivalent in terms of age, gender and location of resection surgery (P=0.6575, P=0.7051 and P=0.2230 respectively, Table 4.2).

	Non-COPD	COPD	P-value
Number of patients	13	15	
Age (yr)	70 *(11.25)*	70 *(9)*	0.6575[1]
M/F	6/7	9/6	0.7051[2]
Smoking status, never/ex/current/unknown	4/8/1/0	0/10/5/0	0.0337[3]
Pack-years of smoking	20 *(35)*	45 *(22.5)*	0.0087[1]
FEV1%	89 *(21)*	70 *(16.5)*	0.0010[1]
FEV1/FVC ratio	0.75 *(0.11)*	0.62 *(0.155)*	0.0004[1]
Resection Location, LUL/LLL/RUL/RML/RLL	4/1/3/3/1 *1 RUL+LUL	3/3/7/0/2	0.2230[3]
COPD Severity Mild / Moderate / Severe	NA	4/10/1	NA
ICS +/-	0/13	7/8	0.0069

Table 4.2: Cohort demographics for lung tissue donors with and without COPD. Median values and italicised interquartile range are shown. * indicates additional locations of resection surgeries. COPD severity was classified based on GOLD recommendations; Mild COPD where FEV1% > 80%, Moderate COPD with FEV1% between 50 and 80 and severe disease with FEV1% < 50. NA = Data not available. FEV1% = FEV1 / (FEV1/FVC) x 100. FVC= Forced Vital Capacity. ICS = Inhaled corticosteroids. [1] Two-tailed Mann Whitney Test [2] Fisher's Test [3] Chi-square Test.

Analysis of the proportion of NK cells in the lung lymphocytes did not show any difference between COPD and non-COPD lung donors (P=0.3686), nor in the proportion of lung $CD56^{bright}$, $CD56^{dim}CD16+$ or $CD56^{dim}CD16-$ NK cells (P=0.6094, P=0.3105 and P=0.01413 respectively, Figure 4.12). Furthermore, the expression of CD49a by both $CD56^{bright}$ and $CD56^{dim}CD16-$ NK cells was equivalent between donors with and without COPD (P=0.7938 and P=0.6948 respectively, Figure 4.12 E and F).

FEV1% predicted, a measure of lung function is used to diagnose COPD, with a cut off of 80% indicating disease in association with an obstructed FEV1/FVC ration of <0.7. Further reduction in FEV1% predicted enables the categorization into mild, moderate and severe disease. Therefore, NK cell phenotypes were analyzed based on donor FEV1% predicted within the whole cohort of lung tissue donors, as shown in Figure 4.13. As with the categorical distinction of COPD and non-COPD (Figure 4.12) there was no significant correlation between FEV1% and the proportion of NK cells (P=0.3042, Figure 4.14 A). However, there was a moderate negative correlation between the proportion of $CD56^{bright}$ lung NK cells and lung function (R= -0.5459, P=0.0020, Figure 4.14 B). Likewise, these was a corresponding trend for an increased proportion of $CD56^{dim}CD16+$ with donor FEV1%, but this did not reach significance (R=0.3089, P=0.0623, Figure 4.13 C). However, no relationship was found between donor FEV1% and the proportion of $CD56^{dim}CD16-$ NK cells

(R=0.1779, P=0.1923, Figure 4.13 D). Interestingly, the percentage of CD49a+ CD56^{bright} NK cells was also found to negatively correlated with FEV1% (R=-0.4107, P=0.0322 Figure 4.13 E) whilst CD49a+ CD56^{dim}CD16- NK cells did not (R=-0.2536, P=0.1288, Figure 4.13 F).

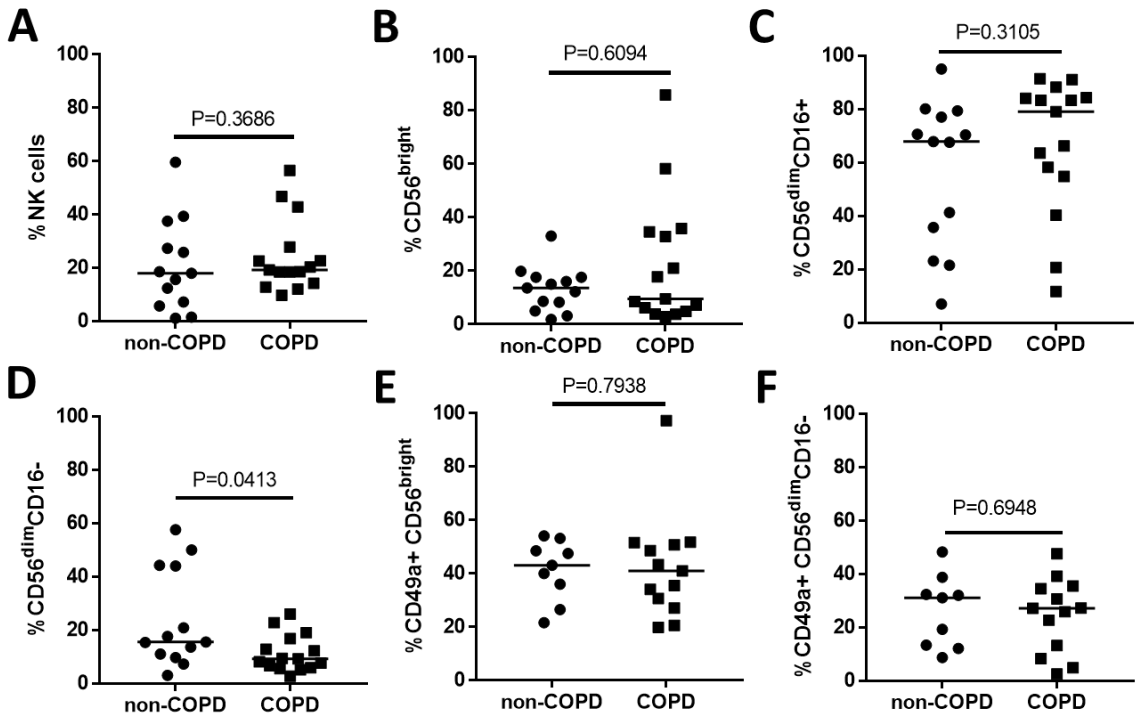

Figure 4.12: Total lung NK cells and NK cell subset proportions are not affected by COPD. (**A**) The proportion of NK cells as a percentage of CD45+ lymphocytes in donors with (N=15) and without COPD (N=13). (**B, C, D**) Proportions of CD56^{bright}, CD56^{dim}CD16+ and CD56^{dim}CD16- NK cell subsets in donors. (**E, F**) Proportions of CD56^{bright} CD49a+ (**E**) and CD56^{dim}CD16- CD49a+ (**F**) NK cells with (N=13) and without COPD (N=9). Statistical analysis by two-tailed Mann-Whitney U test. Lines describe medians.

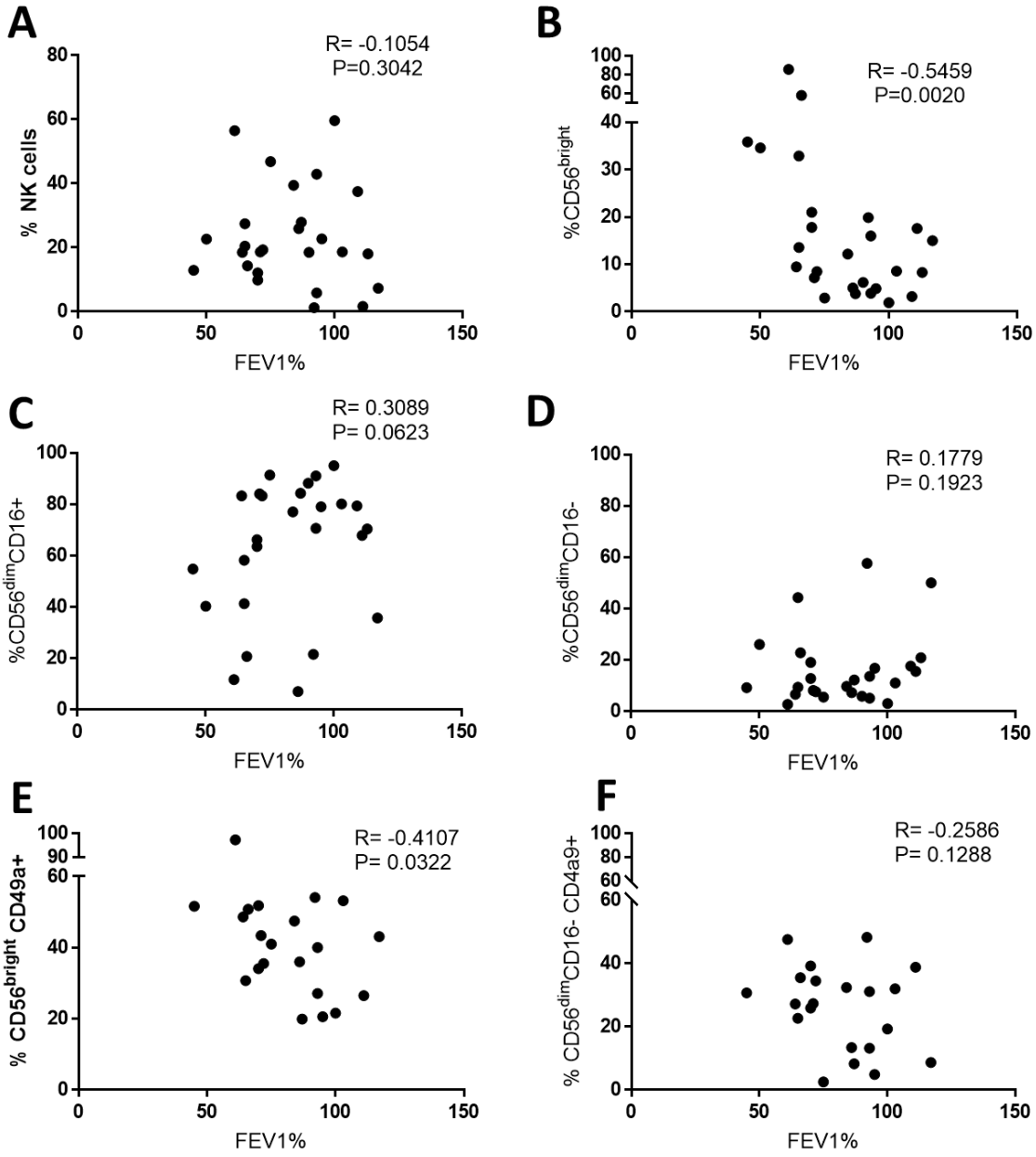

Figure 4.13: The NK cell phenotype of lung tissue donors correlated with FEV1%. (**A**) The proportion of NK cells as a percentage of CD45+ lymphocytes correlated with FEV1%. FEV1% = FEV1 / (FEV1/FVC) x 100 (**B, C, D)** $CD56^{bright}$ and $CD56^{dim}$ NK cell subsets correlated with FEV1%. (**E, F**) Percentage of CD49a expression on $CD56^{bright}$ (**E**) and $CD56^{dim}$CD16- (**F**) lung NK cells correlated with FEV1%. Spearman's correlation coefficient and significance are reported (N=26).

The results of Figure 4.13 demonstrate some phenotypic distortion of NK cells in donors with worsening lung function. Therefore, lung tissue donors with COPD were stratified based on disease severity, including donors with mild and moderate disease (Figure 4.14). Mild COPD is defined based on an FEV1% value greater than 80% and moderate COPD between 50 and 80. In this analysis the proportion of NK cells in CD45+ lung lymphocytes were unaltered between mild and moderate COPD (P=0.1588, Figure 4.14 A). However, there was an increased proportion of $CD56^{bright}$ NK cells with increased disease severity (mild; 4.4% vs moderate; 19.4%, P=0.0120, Figure 4.14 B) and a corresponding reduction in $CD56^{dim}$CD16+ NK cells (mild; 86.25% vs moderate; 64.85%, P=0.0360, Figure 4.14 C). The proportion of lung $CD56^{dim}$CD16- NK cells was equivalent between mild and moderate COPD lung donors (mild; 5.3% vs moderate; 8.75%, P=0.3177, Figure 4.14 D). Interestingly, CD49a expression on $CD56^{bright}$ NK cells was increased from 20.6% in mild disease to 43.4% in moderate COPD (P=0.0042, Figure 4.14 E). In addition, CD49a+ $CD56^{dim}$CD16- NK cells were also increased to 25% of NK cells in moderate COPD from 8.3% in mild disease (P=0.0318 respectively, Figure 4.14 F).

The results in Figure 4.13 and 4.14 indicate that both CD49a expression and the proportion of NK cell subsets are altered in worsening COPD. However, other factors could be responsible for these changes, such as the use of inhaled corticosteroids and donor smoking status as both parameters were statistically different between the two cohorts (P=0.0337 and P=0.0069 respectively, Table 4.2). Stratification of the COPD cohort based either on ICS use or smoking status did not generate any statistically significant differences in the proportion of NK cells, NK cell subsets or CD49a expression (Figures 4.15 and 4.16). Therefore, neither of these variables explained the increase in $CD56^{bright}$ NK cells or CD49a+ expression observed in Figures 4.13 and 4.14.

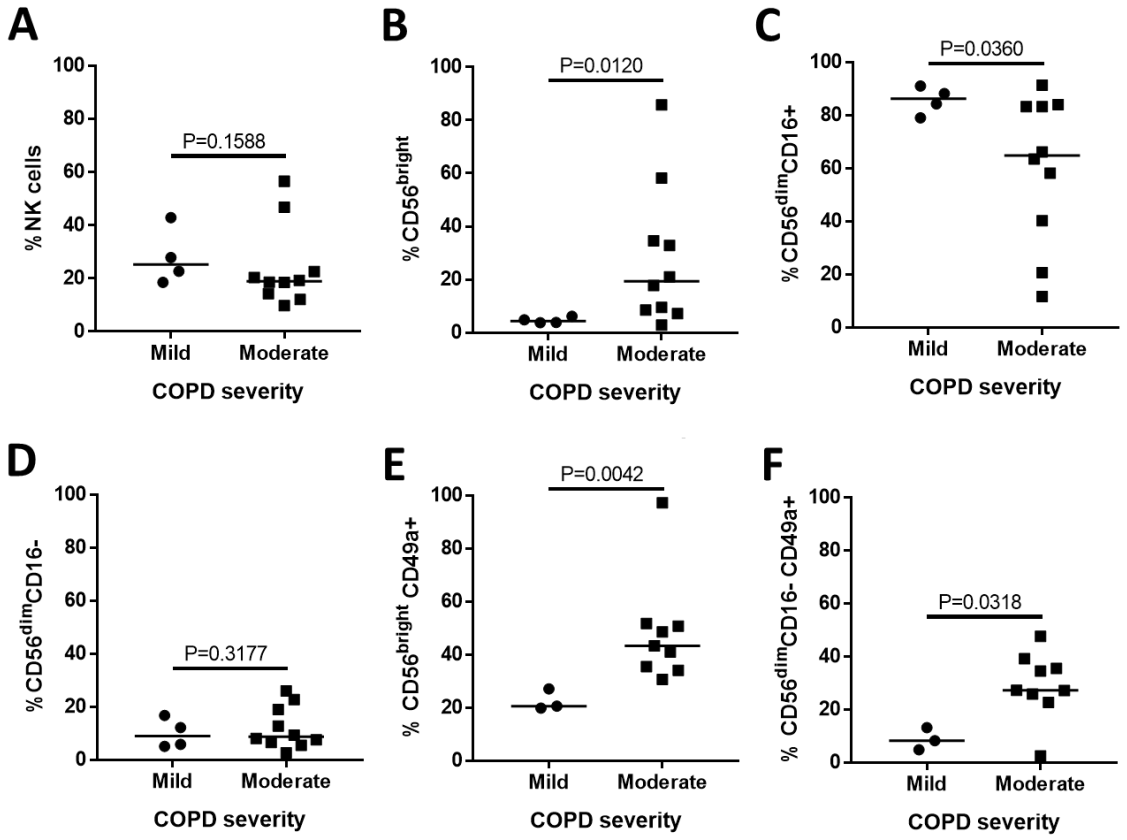

Figure 4.14: The proportion of total lung NK cells and NK cell subsets stratified by COPD severity. (**A**) The proportion of NK cells as a percentage of CD45+ lymphocytes in donors stratified by COPD severity (Mild COPD N=4, Moderate COPD N=10). Mild COPD was classified where FEV1% > 80%, and moderate COPD with FEV1% between 50 and 80 (**B, C, D**) Proportions of $CD56^{bright}$ and $CD56^{dim}CD16$- NK cell subsets in mild and moderate COPD. (**E, F**) Proportions of $CD56^{bright}CD49a$+ (**E**) and $CD56^{dim}CD16$- CD49a+ cells (**F**) in COPD disease (Mild COPD N=3, Moderate COPD N=9). Statistical analysis by two-tailed Mann-Whitney U test. Lines describe medians.

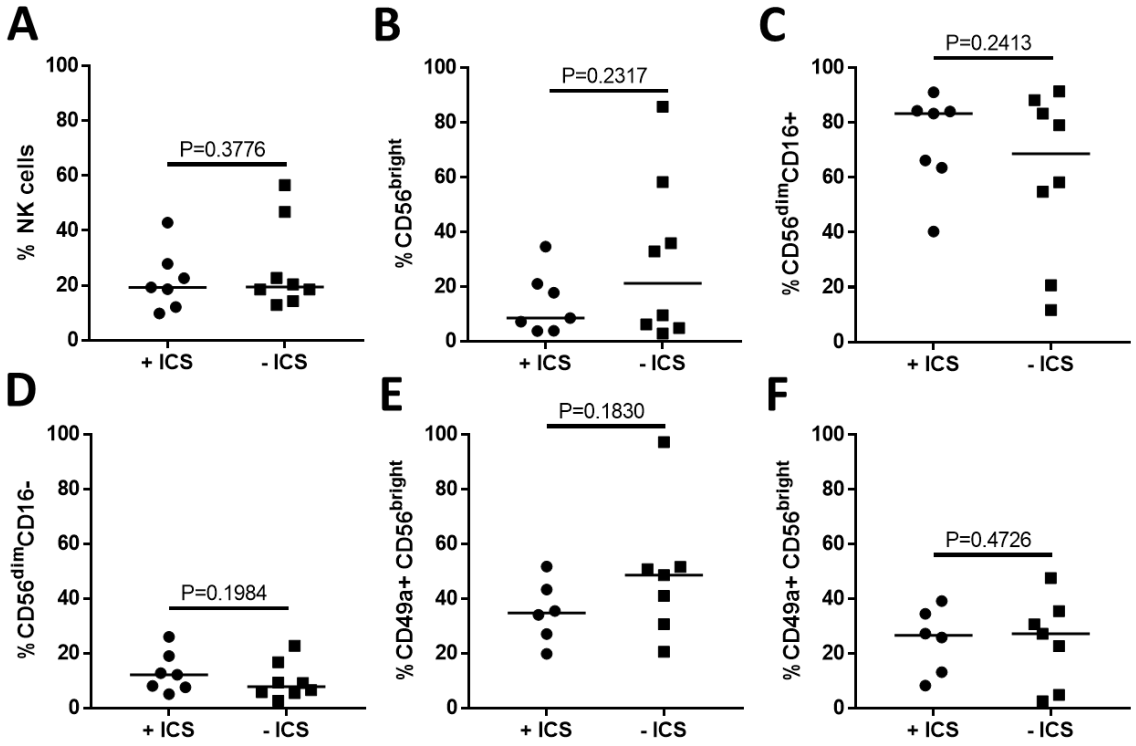

Figure 4.15: Proportions of total lung NK cells and NK cell subsets based on donor corticosteroid (ICS) use. (**A**) The proportion of NK cells as a percentage of CD45+ lymphocytes in COPD donors that were using ICS (N=7) versus those that weren't (N=8). (**B, C, D**) Proportions of $CD56^{bright}$ and $CD56^{dim}CD16$- NK cell subsets in ICS using and non-using COPD lung. (**E, F**) Proportions of CD49a expression on $CD56^{bright}$ (**E**) and $CD56^{dim}CD16$- (**F**) lung NK cells (donors not using ICS N=7). Statistical analysis by two-tailed Mann-Whitney U test. Lines describe medians.

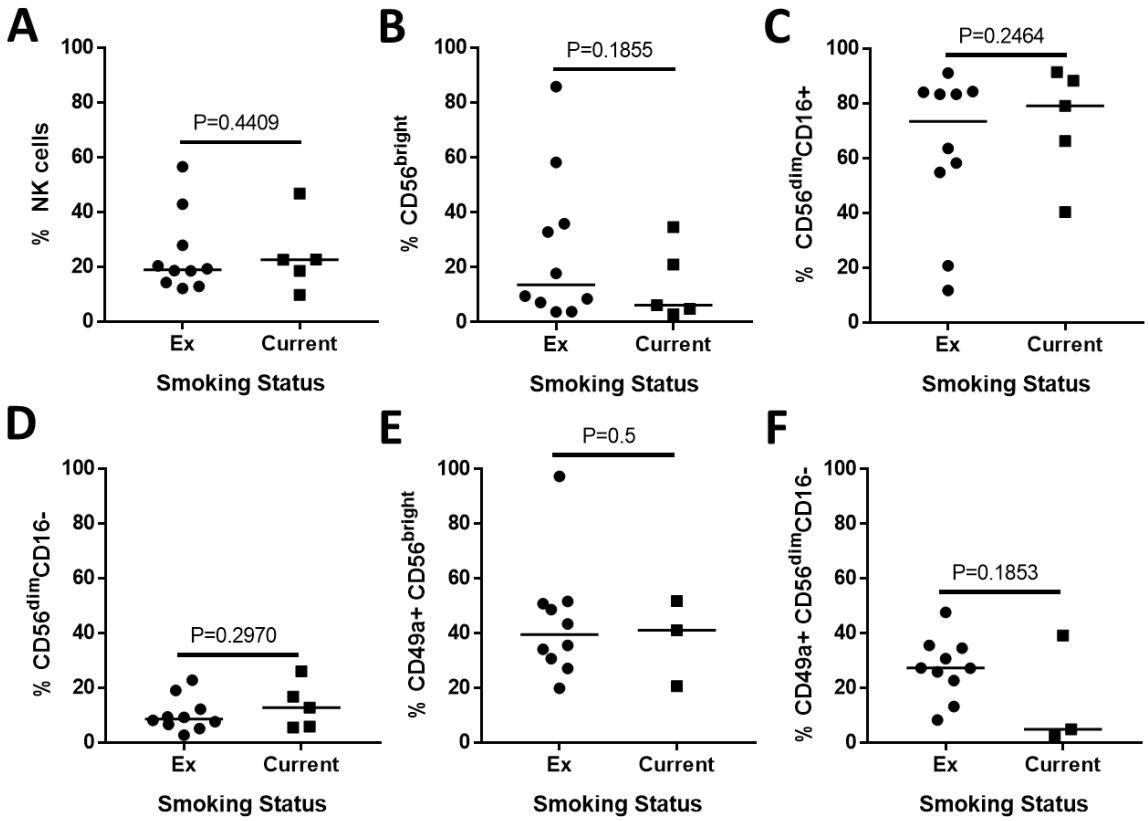

Figure 4.16: Total NK cell and NK cell subsets proportions are not affected by smoking status. (**A**) The proportion of NK cells as a percentage of CD45+ lymphocytes in COPD donors that were current (N=4) or ex-smokers (N=10). (**B, C, D**) Proportions of $CD56^{bright}$ and $CD56^{dim}CD16-$ NK cell subsets in current and ex-smokers with COPD. (**E, F**) Proportions of CD49a expression on $CD56^{bright}$ (**E**) and $CD56^{dim}CD16-$ (**F**) NK cells (Current smokers N=3, ex-smokers N=10). All statistical analysis by Mann-Whitney U test. Lines describe medians.

4.3 Discussion

4.3.1 Isolating NK cells from the Lung Parenchyma

In this chapter NK cells were successfully isolated from human lung parenchyma by a process of washing, resting and collagenase digestion [428, 429, 460]. NK cells were defined as CD45+CD3-CD56+ cells, a gating strategy designed to exclude lung ILC populations which do not express CD56 (Figure 2.3) [463]. Although 50% of the NCR+ ILC3s are CD56 positive the total human lung ILC3 population comprise less than 0.025% of CD45+ cells and would therefore CD56+NCR+ILC3s would make a minimal contribution to this analysis [463, 464].

Collagenase digestion of the lung parenchyma was favoured to allow analysis of the NK cells most adherent within the lung tissue. Even so, as the lungs are a highly vascularised organ we expect to find some circulating NK cells within the collagenase-digested lung tissue. Indeed, the lung NK cell phenotype closely mirrored that of the peripheral blood (Figures 4.4 and 4.5) [465]. $CD56^{bright}$ and $CD56^{dim}$ NK cell subsets were largely preserved by collagenase digestion with a slight increase in $CD56^{dim}$CD16- NK cells and decrease in $CD56^{dim}$CD16+ NK cells indicating a small amount of NK cell activation (Figure 4.3). Enzymatic digestion is harsher and more damaging to tissue, potentially providing stressed and activated cells as targets for NK cell activation. $CD56^{dim}$CD16+ NK cells are expected to be the most susceptible to activation during tissue processing, as these are the most terminally differentiated, cytotoxic NK cells and may take on a $CD56^{dim}$CD16- phenotype following activation and prior to cell death [314, 316, 317, 320, 449]. Despite this, digestion of lung tissue is essential to isolating NK cells that may be resident in this tissue, as has been observed in the human liver [301]. Preserving cellular phenotypes during the process of isolating primary cells is an issue when working with human tissues and is explored in Chapter 3. There is a balance to be struck between harvesting cells efficiently and maintaining their phenotype, a particular problem with innate immune cells given their plasticity [466, 467]. However, the focus of this thesis was to investigate how NK cells are shaped by the pulmonary environment and to do this a source of human lung NK cells was required. To obtain this we accept that some change in phenotype is possible following extraction from the body and have made efforts to understand how culture conditions and isolation procedures affect the phenotypes of interest. In general, the methods used in this thesis were found to largely preserve NK cell phenotype and function (as discussed in Chapter 3).

4.3.2 Lung NK cells are phenotypically similar to the Peripheral Blood

NK cells were found to make up a substantial proportion (10.9% ±13.25, N=22) of lung-associated lymphocytes and were found at a similar proportion in matched peripheral blood (11.1% ± 4.65, Figure 4.4). This differs from the findings in Marquardt *et al* 2016 which reported increased proportions of NK cells in human lung tissue (15% of lung CD45+ cells vs 10% in the blood) [362]. This might reflect differences in sample size between studies, as Marquardt *et al*. measured the NK cell phenotype in 84 lung donors [362]. Given the positive skew in the percentage of lung NK cells presented in this thesis, it may be that a greater sample size would be required to replicate this finding by Marquardt *et al* [362].

In terms of CD56 and CD16 expression, NK cells isolated from the lung were phenotypically similar to blood from the same donor. 69.3% ± 27.15 of lung-associated NK cells were the most mature $CD56^{dim}CD16+$ (stage 5) NK cell, the largest subset found in the blood (88.8% ± 15.45, P=0.8311 Figure 4.4 E). $CD56^{dim}CD16-$ NK cells were also found in similar proportions between the blood and lung (14.6% vs 9.55%, P=0.5029 Figure 4.4 F). These data confirm the results of Marquardt *et al*. which described a predominantly $CD56^{dim}CD16+$ human lung NK cell phenotype, much like the blood [362]. Given the high degree of vascularisation in this tissue these findings may reflect a high degree of circulating NK cells within the lung parenchyma.

The proportion of lung $CD56^{bright}$ NK cells was increased from 3.3% in the blood to 10.86% in the lung (P<0.0001, Figure 4.4 C) with a trend towards decreased $CD56^{dim}CD16+$ cells (P=0.0522, Figure 4.4 E) corroborating previous findings [362]. Although $CD56^{bright}$ NK cells are enriched in the lung relative to the blood, they are still at a relatively small proportion compared to other organs such as the liver where 50% of the NK cells are $CD56^{bright}$ [301]. Therefore, the $CD56^{bright}$:$CD56^{dim}$ ratio in the lungs is much closer to that found in the peripheral blood. Furthermore, lung and blood NK cells were equivalent in terms of their overall maturity and receptor expression. As discussed in section 1.4.2 and described in Figure 1.3 NK cell maturation is accompanied by the gradual acquisition of inhibitory and activating receptors. The distribution of CD57, CD158b, NKp46 and NKG2D on $CD56^{bright}$ and $CD56^{dim}$ subsets of the peripheral blood in this thesis is consistent with reports from the literature [266]. The expression of CD57, CD158b, NKp46 and NKG2C were all found to be equivalent between the lung and blood (Figures 4.5 and 4.6). The dominant NK cell phenotype in both the lungs and blood is $CD56^{dim}CD16+CD57+$, a phenotype that is potently cytotoxic and strongly IFN-γ producing (Figure 4.5 and Figure 4.4) [275]. Taken together these results

demonstrate that the majority of lung NK cells are terminally differentiated, mature and potentially highly cytotoxic [266, 275]. Only NKG2D was differentially expressed between the blood and lung (P=0.0488) due to an increased expression of NKG2D on $CD56^{dim}$CD16- lung NK cells (Figure 4.6 C and D). Otherwise lung NK cells are phenotypically similar to the peripheral blood. Thus, it appears that the bulk of NK cells found in lung tissue are likely to be circulating NK cells.

In apparent contrast with the lung NK cell phenotype reported here and by Marquardt *et* al, lung NK cells are commonly reported as hypofunctional [362, 364-366]. Both the BAL and alveolar macrophages have been shown to reversibly repress NK cell function and therefore may be responsible for inhibiting NK cell functionality in the lung [265, 364, 365]. Interestingly, an altered expression of inhibitory and activating KIR was found on NK cells isolated from the lung by Marquardt *et al*, which may be responsible for the limited function of lung NK cells [362]. In the work presented in this thesis there was a small non-significant trend for increased CD158b expression on lung NK cells compared to the blood (P=0.0742, Figure 4.5C), suggesting that some KIR receptors may be differentially expressed between blood and lung. However, an increased sample size in this data would further corroborate this assessment. Furthermore, the CD158b antibody is not specific for one KIR allele but binds KIR2DL2, KIR2DL3 and KIR2DS2, therefore future analyses of KIR expression could use antibodies designed to distinguish between these alleles. The expression of individual KIR alleles was beyond the scope of this study but would be an interesting avenue of further investigation. How NK cell receptor expression may be modulated in the lungs is unknown but is likely to be induced by soluble mediators in the pulmonary environment [265, 364, 365]. Cytokines can alter the NK cell receptor expression, fine-tuning the integration of inhibitory and activating signalling pathways [468].

Strict regulation of NK cell activation in the pulmonary environment may act to preserve the unique structural architecture of the lung, on which much of gas exchange depends. If dysregulated the presence of potent cytotoxic NK cells could compromise tissue integrity and therefore gas exchange across the alveolar spaces. In support of this theory, lung NK cell cytotoxicity has been associated with COPD and emphysema in the mouse [86, 361, 469, 470]. Therefore, the extent of lung NK cell reactivity will be explored in Chapter 5.

4.3.3 A Resident Population of CD49a+CD103+CD69+ NK cells exist in the Human Lung

Lung NK cells were investigated for CD49a and CD103 expression, integrins associated with NK cell residency in the liver and uterus (Figure 4.7) [299-301, 340]. A minority of $CD56^{bright}$ and $CD56^{dim}$CD16- lung NK cells were found to express both CD49a and CD103 (Figure 4.7). However, these proteins are not found in the peripheral blood, suggesting that NK cells positive for these proteins are resident within the lung parenchyma. Interestingly CD49a expression in the lung was much greater than the reported expression in the liver [301]. CD49a+ liver-resident NK cells were identified in only 12/29 liver perfusates and made up 2.3% of total liver NK cells [301]. In contrast all lung samples in this study possessed CD49a+ NK cells, with a median proportion of 13.3 ± 11% CD49a+ cells (Figure 4.7 A). CD69, another putative marker of residency was also enriched on lung $CD56^{bright}$ NK cells [299-301, 340]. CD49a, CD103 and CD69 were strongly co-expressed on lung NK cell and CD49a+CD103+CD69+ made up one of the largest proportions of $CD56^{bright}$ NK cells (Figure 4.8). However, there was a range of residency marker expression on lung NK cells as this thesis identified many cell populations that were single or double positive for residency markers. In contrast, the majority of peripheral NK cells were triple negative for residency markers, however some blood NK cells expressed CD69 (Figure 4.8 and 4.9). Triple negative and CD69 single positive cells were also identified in the lungs, further indicating that non-resident $CD56^{bright}$ NK cells may also be circulating through the lungs.

Unexpectedly, $CD56^{dim}$CD16- NK cells were also found to express CD49a and CD103 in the lungs (Figure 4.9) and $CD56^{dim}$CD16- NK cells triple positive for CD49a, CD103 and CD69 were identified. $CD56^{dim}$CD16- NK cells possessed the same triple positive, double positive and single positive populations as $CD56^{bright}$ NK cells (Figure 4.9 C and Figure 4.8 F) but CD49a+CD103+CD69+ cells made up a smaller proportion of total $CD56^{dim}$CD16- lung NK cells (P=0.0234). Lung $CD56^{dim}$CD16- NK cells were dominated by cells that were negative for all the assessed residency markers (34.2%) with strong expression of CD69 but not CD49a or CD103 (36%), much closer to the phenotype of the peripheral blood. Thus far the majority of identified rNK cells are $CD56^{bright}$, $CD56^{dim}CD16^{dim}$ resident NK cells have recently been identified in nasal lavage [322, 340]. $CD56^{dim}$CD16- NK cells are increased in situations where NK cell viability is lowered or following activation [314, 316, 317, 320]. Therefore, based on reports in the literature and the results presented in section 3.2.1, CD49a+ and CD103+ $CD56^{dim}$CD16- NK cells may be a result of activated or dying resident $CD56^{bright}$ NK cells undergoing CD56 and CD16 shedding [314, 316, 317, 320].

CD49a and CD103 may have important functional roles in retaining NK cells within the lung environment [328, 329, 471]. CD49a, also known as integrin alpha 1, binds collagen IV and laminin, important components in the lung extracellular matrix [328, 329]. Whereas CD103 contributes to the integrin E protein and binds E-cadherin [471]. The localization of CD49a+ and CD103+ NK cells within the lung parenchyma remains to be explored but may be governed by this integrin expression. For instance CD49a+ CD8+ T cells have been shown to localize to basal membranes of the airway epithelium and vasculature, whereas the largely CD49a- CD4+ T cells are found within the interstitial spaces [331]. It is possible that the CD49a+ rNK cells identified in this thesis may also localize to basement membranes of the airway epithelium. In which case rNK cells would be well placed to respond to respiratory insult. The location of rNK cells within the lung parenchyma is therefore an important area for future research.

The function of resident NK cell populations in human organs remains much of a mystery but are potentially shaped by the local microenvironment [293, 340]. Recent studies have suggested that salivary gland rNKs may prevent autoimmunity by eliminating activation T cells, whereas in the adipose tissue rNK cells may promote inflammation [342, 343]. Furthermore, hepatic CD49a+ NK cells produce TNF-α, GM-CSF and IL-2 more efficiently than circulating NK cells [301, 338, 341]. Therefore, rNK cells may contribute to organ homeostasis and moderate immune responses in the lungs. The presumably constant presence of resident NK cells in human organs may allow them to function in the initial innate barrier to infection [344]. Interestingly, liver resident NK cells have also been associated with NK cell memory responses including more potent secondary responses to hapten challenge [336, 345]. In addition human $CD56^{bright}$CD49a+ NK cells possess an oligoclonal KIR repertoire and increased NKG2C expression in the liver, leading the authors to suggest that these CD49a+ NK cells may have undergone the selective expansion indicative of memory formation [301]. However, the connection between NK cell residency and memory is not well understood.

In this chapter lung $CD56^{bright}$ CD49a+ NK cells were found to differentially express NKp46, NKG2D and NKG2C (Figure 4.10). NKp46 expression was reduced on CD49a+ NK cells (P=0.0254) whilst NKG2D and NKG2C were increased (P=0.0078 and P=0.0049 respectively). NKG2D expression was also increased on CD49a+ $CD56^{dim}$CD16- NK cells with a similar trend for reduced NKp46 on CD49a+$CD56^{dim}$CD16- NK cell which did not reach statistical significance (P=0.0420 and P=0.0640 respectively). This altered expression of activating receptors by CD49a+ lung NK cells hints at an enhanced functional responsiveness to pathogens and is further explored in chapter 5.

4.3.4 CCR5 may play a role in NK Cell Trafficking to the Lungs

The generation and homing of resident NK cell populations remains much of a mystery. Organ chemotactic signaling has been implicated in enforcing resident NK cell populations in the human liver and uterus [300, 332]. Unique chemokine receptor profiles have been identified on resident NK cells in these organs including CCR5, CXCR3 and CXCR6 [300, 332]. The nature of resident NK cell recruitment or generation within the lung environment is unknown and to investigate this the expression of CCR5 was measured in the lung and peripheral blood.

As shown in Figure 4.11 CCR5 was expressed by a small proportion of peripheral blood NK cells, corroborating previous reports [472]. In the lung CCR5 expression was enriched on lung NK cells by 13.2% when compared to the blood (P=0.002). The highest expression of CCR5 was on lung $CD56^{dim}$CD16- NK cells (P=0.0046) with a trend for increased expression on $CD56^{bright}$ and $CD56^{dim}$CD16+ NK cells which did not reach significance (P=0.1675 and P=0.7685 respectively). CCR5 is involved in NK cell recruitment to inflammation, including infection in the liver, skin and CNS [473]. This may explain why the highest expression of CCR5 was found on NK cells exhibiting an activated ($CD56^{dim}$CD16-) phenotype (see section 3.2 and Figure 4.9B). Interestingly, CCR5 expression was found to be increased on CD49a+ NK cells compared to the CD49a- lung cells indicating that this chemokine receptor may also play a role in resident NK cell retention in the lungs (Figure 4.11 C and D $CD56^{bright}$ P=0.0039 and $CD56^{dim}$CD16- P=0.0078). However, CCR5 expression was also found to be increased on CD49a- lung NK cells compared to the blood ($CD56^{bright}$ P=0.0078 and $CD56^{dim}$CD16- P=0.0039) suggesting that non-resident lung NK cells were also enriched for this chemokine receptor and sensitive to CCR5 ligand (CCL3 and CCL5) signaling.

CCR5 ligands are associated with lymphocyte recruitment to the lungs during a number of inflammatory contexts [474]. For instance CCL3 is produced by the lung following respiratory syncytial virus (RSV), *K. pneumonia, C. neoformans* and respiratory herpes infection [475-478]. In addition CCL5 is upregulated following RSV infection and pneumococcal carriage [479, 480]. CCR5 was strongly expressed by lung NK cells and therefore may be important in canonical NK cell homing to the lung during these infections. Interestingly this chemokine receptor has also been found to govern NK cell recruitment to the lungs during IAV infection in mice [168].

Lastly, it is not known whether lung CD49a+CD103+ NK cells are self-perpetuating or replenished from the circulation. Either way the micro-environment within the lungs must play a role in maintaining this population. The results presented here implicate CCL3 and CCL5 chemotactic signaling in this process. To investigate this further the basal expression of CCR5 ligands could be analyzed in resting lung tissue to determine whether the human lung might provide a unique niche for resident NK cells.

Moreover, these findings should be interpreted cautiously as a CCL3-CCR5 axis has been implicated in the recruitment of leukocytes to murine lung tumors and CCL5 promotes lung cancer growth and metastasis [481, 482]. As all lung tissue was supplied from cancer resection surgeries we cannot exclude cancer as a cause for increased CCR5 expression on lung NK cells. Therefore, these results could be strengthened by analysis of an alternative source of lung tissue such as bullectomy surgery.

4.3.5 Distorted NK Cell Phenotypes Correlate with COPD Severity

NK cell function is dysregulated in human COPD, with increased NK cell cytotoxicity induced by priming from antigen-presenting cells [361, 461, 483, 484]. To understand how COPD status may affect the NK cell phenotypes reported in sections 4.4.2 and 4.2.5 the data was interrogated based on donor diagnosis of COPD and severity. The proportion of NK cells in the lungs was not found to be affected by COPD status or disease severity (Figure 4.13 and 4.14), in agreement with Hodge *et al*. and Freeman *et al.* [361, 483]. Hodge *et al.* (2013) previously found that a current smoking status was associated with increased proportion of NK cells regardless of COPD [483]. However, this was not reported in Freeman *et al.* (2014) and no difference in the proportion of lung NK cells in current and ex-smokers were found in our analysis of COPD donors (Figure 4.16) [361]. In addition, no differences were found in the proportion of NK cells or NK cell subsets when blood NK cells were stratified by smoking status (Figure 3.10).

Although NK cells appeared unchanged between COPD and non-COPD lung tissue donors (Figure 4.12) a distorted $CD56^{bright}$ and $CD56^{dim}$ ratio was observed these measures were correlated with FEV1% (Figure 4.13). COPD donors with moderate disease were found to have more $CD56^{bright}$ NK cells (P=0.012, Figure 4.14 B) and fewer $CD56^{dim}$CD16+ NK cells (P=0.036, Figure 4.14 C). This change in $CD56^{bright}$/ $CD56^{dim}$ ratio in moderate COPD could not be explained by ICS use or smoking status within the COPD cohort, indicating that it may well be a disease-related change (Figures 4.15 and

4.16). $CD56^{bright}$ NK cells have been shown to be more potent produces of IFN-γ and TNF-α than $CD56^{dim}$ NK cells, therefore donors with moderate COPD may also have a shift in the lung NK cell phenotype to one that is more cytokine producing [259, 295, 302-304, 308, 309]. The altered ratio of $CD56^{bright}$ and $CD56^{dim}$ NK cells could also result from proliferation of $CD56^{bright}$ NK cells or a loss of $CD56^{dim}$CD16+ NK cells. As greater NK cell cytotoxicity is found in the lungs of COPD patients, this could result in increased apoptosis of activated $CD56^{dim}$ NK cells and may explain the skewed subset proportions presented in Figure 4.14 [361, 461, 483, 484].

The results in Figure 4.14 contradict Freeman *et al.* 2014 which found equivalent CD56+CD16- and CD56+CD16+ NK cells in severe COPD lung tissue compared to mild COPD donors [361]. Although there are significant differences to the gating strategy between this thesis and Freeman *et al.* 2014, including identification of a $CD56^{dim}$CD16- population. The small sample size of mild COPD donors in our cohort limits the strength of our conclusions, therefore increasing this number would increase the validity of these findings.

In terms of CD49a expression, no differences were found between the lung NK cells of COPD and non-COPD donors (Figure 4.12 E and F). However, CD49a expression was increased in moderate COPD donors in both $CD56^{bright}$ and $CD56^{dim}$CD16- NK cell subsets (Figure 4.14 E and F). Increased CD49a expression on $CD56^{bright}$ NK cells also correlated with reduced FEV1% and worsening lung function (Figure 4.14). The increased proportion of CD49a+ NK cells in moderate COPD could indicate an expansion of the resident NK cell population. Alternatively, this may reflect a loss of non-resident NK cells through activation and apoptosis, although this would require differential activation of CD49a+ and CD49a- NK cells in COPD. Based on the parameters analyzed here it appeared that increased CD49a expression was solely correlated with worsening lung function. CD49a expression was unchanged between lung donors when stratified by ICS use or smoking status (Figure 4.15 and Figure 4.16). It is therefore interesting that CD49a expression was not initially found to be different between COPD and non-COPD lung tissue, a finding which suggests there could be non-COPD related expansions of this population.

As discussed in section 1.4.6.3, some memory-like features have been described for CD49a+ NK cells and this protein is associated with lymphocyte residency [299-301, 344]. It is therefore possible that the inflammatory environment within the COPD lung might affect resident/memory NK cell formation. There is some evidence to support this as smoke exposure has been shown to prime

the NK cell response to viruses through the upregulation of the stress molecules recognized by NK cell NKG2D [470]. Thus sustained inflammation might result in the acquisition of NK cell memory to inappropriate stimuli.

In conclusion a distorted NK cell phenotype was observed in lung donors with moderate COPD, with more extreme changes correlating with worsening lung function. This likely reflects the dysregulation of NK cell cytotoxic function reported in the literature and may have implications for NK cell cytokine production in COPD. Furthermore, CD49a, a marker of NK cell residency was increased in donors with more severe disease. Therefore, these data suggest there may be dysregulation within the resident lung NK cell population which could have significant consequences for disease pathology.

4.3.6 Summary

The results presented in this chapter show that NK cells can be successfully identified within the human lung parenchyma and constitute a large proportion of lung lymphocytes. NK cells isolated from the lungs mirrored the CD56/CD16 phenotype of the circulation as well as activating receptor expression and differentiation state. An expanded population of $CD56^{bright}$ NK cells was identified in the lungs and this was found to contain NK cells expressing CD49a, CD103 and CD69. These unique lung-resident NK cells may have significant implications for local innate immune function. Increased CD49a expression correlated with worsening lung function in lung donors with COPD and severity of disease was associated with distorted proportions of $CD56^{bright}$ and $CD56^{dim}$ NK cells. The function of NK cells, circulating and resident, remain poorly understood in the human lung, but may have important implications for antiviral immunity. Therefore, a functional analysis of lung NK cells is required to determine their roles in human respiratory infection.

Chapter 5 Human Lung NK Cells in Viral Infection

5.1 Introduction

IAV is a major cause of annual mortality, as well as a significant exacerbator of COPD [1, 485]. Innate immune responses have an important role in the control of this virus but the functional contribution of NK cells remains to be fully understood [64]. Peripheral NK cell activation been reported following human IAV vaccination and the activating receptors NKp46 and NKG2D have been implicated in binding IAV-infected human cells [254, 319, 376, 378, 379]. In Chapter 4 of this thesis NK cells were found to make up a substantial proportion of the human lung CD45+ leukocytes (10.9% ±13.25, section 4.2.2) and therefore may be well placed to contribute to anti-IAV immunity in this organ [200]. However, the function of NK cells in *in vivo* IAV is inconsistent, as animal models have implicated NK cells in both protective and detrimental roles [107-113, 227]. A greater understanding of the NK cell contribution to human IAV infection may benefit immunization strategies through increased knowledge of innate immune function during this infection.

This chapter will investigate the immune responses of NK cells in *ex vivo* IAV-infected human lung parenchyma and explore the functional relevance of the NK cell phenotypes characterized in Chapter 4 [428]. We and others have shown that the human lung NK cell is highly differentiated, with a potently cytotoxic phenotype [362]. Despite this, or perhaps because of it, NK cells are inhibited by the resting lung environment [364-366]. This regulation of NK cell function may have important implications for pulmonary disease. Furthermore, in section 4.2.4 lung resident NK cell populations were identified for the first time. Resident NK cells strongly expressed CD49a, a protein associated with NK cell memory, as well as a distorted expression of IAV-recognition receptors [426]. CD49a+ liver NK cells were found to be protective in a murine model of IAV infection and we will investigate the function of human CD49a+ NK cells in the lung. We speculate that CD49a+ NK cells are shaped by lung insult and homeostasis and thus may represent a population of trained innate immune cells with recall to influenza infection [344, 486]. To investigate these aspects of IAV infection, macroscopically normal tissue, distal to lung tumors, was taken from lung resection surgeries at Southampton General Hospital. Lung tissue was infected with IAV virus as described in section 2.13 and infection characterized by flow cytometry and ELISA. Flow cytometric analyses of NK cell function were developed in this model and used to assess NK cell subsets and CD49a+ cell function.

5.2 Results

5.2.1 Infecting Human Lung Tissue with Influenza A Virus

Human lung parenchyma was cut into 4-6mm^2 fragments and washed as described in section 2.12.1. Lung explants were then infected with 200,000 PFU/mL of live or UV-irradiated H3N2 X31 influenza. Extracellular influenza virus was removed 2 hpi and lung tissue incubated for a further 22h to allow viral replication. Infected lung parenchyma was digested by collagenase treatment and interrogated by flow cytometry as shown in Figure 5.1 A and described in section 2.12.2. Lung cells were distinguished based on expression of CD45, HLA-DR and EpCAM [54, 428, 429, 487]. Macrophages were defined as CD45+HLA-DR+ cells, epithelia as CD45-EpCAM+ cells (Figure 5.1 A) and lymphocytes based on size and CD45 expression (Figure 2.1).

X31 infection was quantified through the detection of intracellular IAV nucleoprotein-1 (NP-1) (Figure 5.1 B and C). 22.3% of airway macrophages and 7.1% of the epithelia were infected with IAV (P=0.0078 and P=0.0078 respectively, Figure 5.2 A and B). Increased NP-1 was also detected in CD45-EpCAM- cells and CD45+HLA-DR- cells (P=0.0156 and P=0.0391), however the relative amount of NP-1 expression, as shown by MFI, was minimal in these cell types (Figure 5.2 C). Thus airway macrophages and epithelia are the major sites of X31 replication in this model, with an infection level consistent with McKendry *et al* and Nicholas *et al* [428, 429]. Likewise, UV-irradiated X31 (UV-X31) was also not found to replicate in macrophages (P=0.3891, Figure 2.5 A), with a negligible decrease in NP-1+ epithelia compared to uninfected (NT) controls (UV-X31; 1.25% vs NT; 1.7%, P=0.0391, Figure 5.2 B) [428, 429]. In addition, macrophage, epithelial cell and lymphocyte viability was assessed in infected tissue explants (Figure 5.2 D, E and F). In this case cell types were defined prior to the live/dead gating shown in Figure 5.1 A. Cellular viability was largely preserved in the explant model, as epithelial and lymphocyte viability was unaffected by live X31-infection (P=0.3438 and P=0.0781, Figure 5.2 E and F). However, macrophage viability was reduced from 43% to 29% by live X31-infection (P=0.0071, Figure 5.2 D) and might reflect the high burden of virus in these cells (Figure 5.2 A and C).

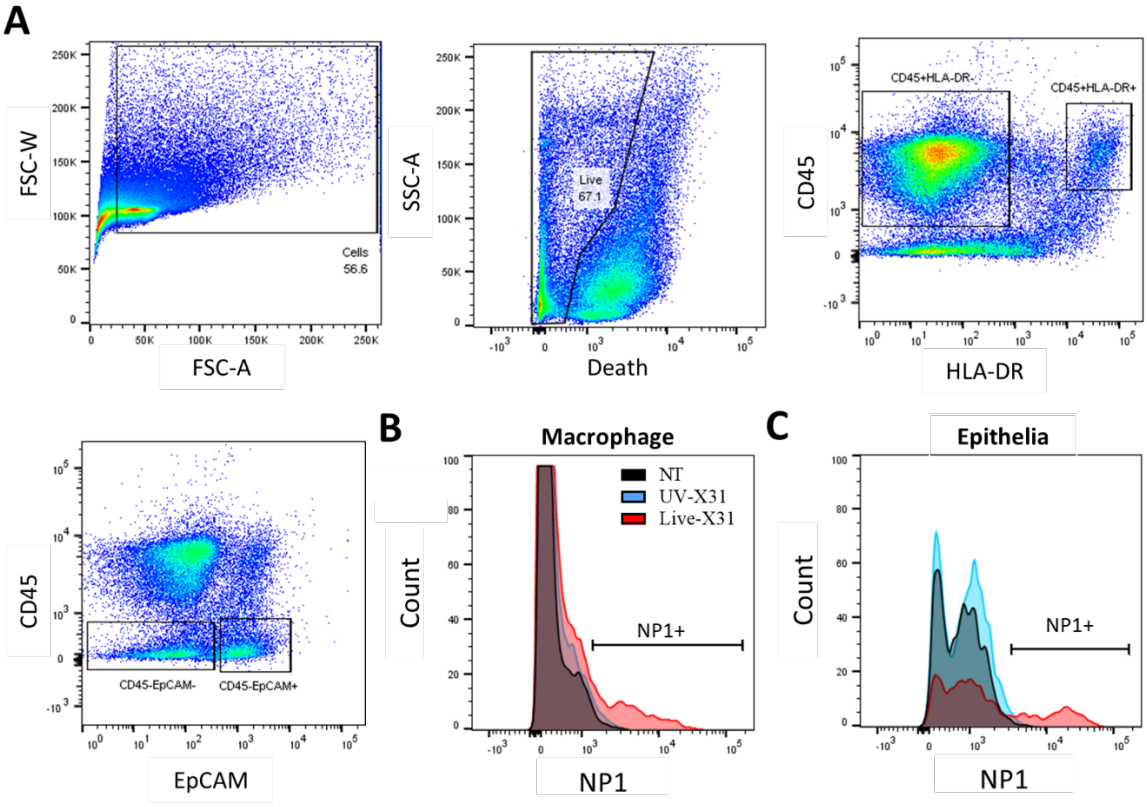

Figure 5.1: X31 IAV infection of human lung explants. (**A**) Representative gating strategy to define lung explant cells. Macrophages were defined as CD45+HLA-DR+ cells and epithelial cells as CD45-EpCAM+ cells. (**B, C**) Representative flow cytometry plots of IAV NP-1 expression in macrophages (**B**) and epithelial cells (**C**) either infected with UV-irradiated X31 (blue line), live X31 (red line) or not treated (NT, black line).

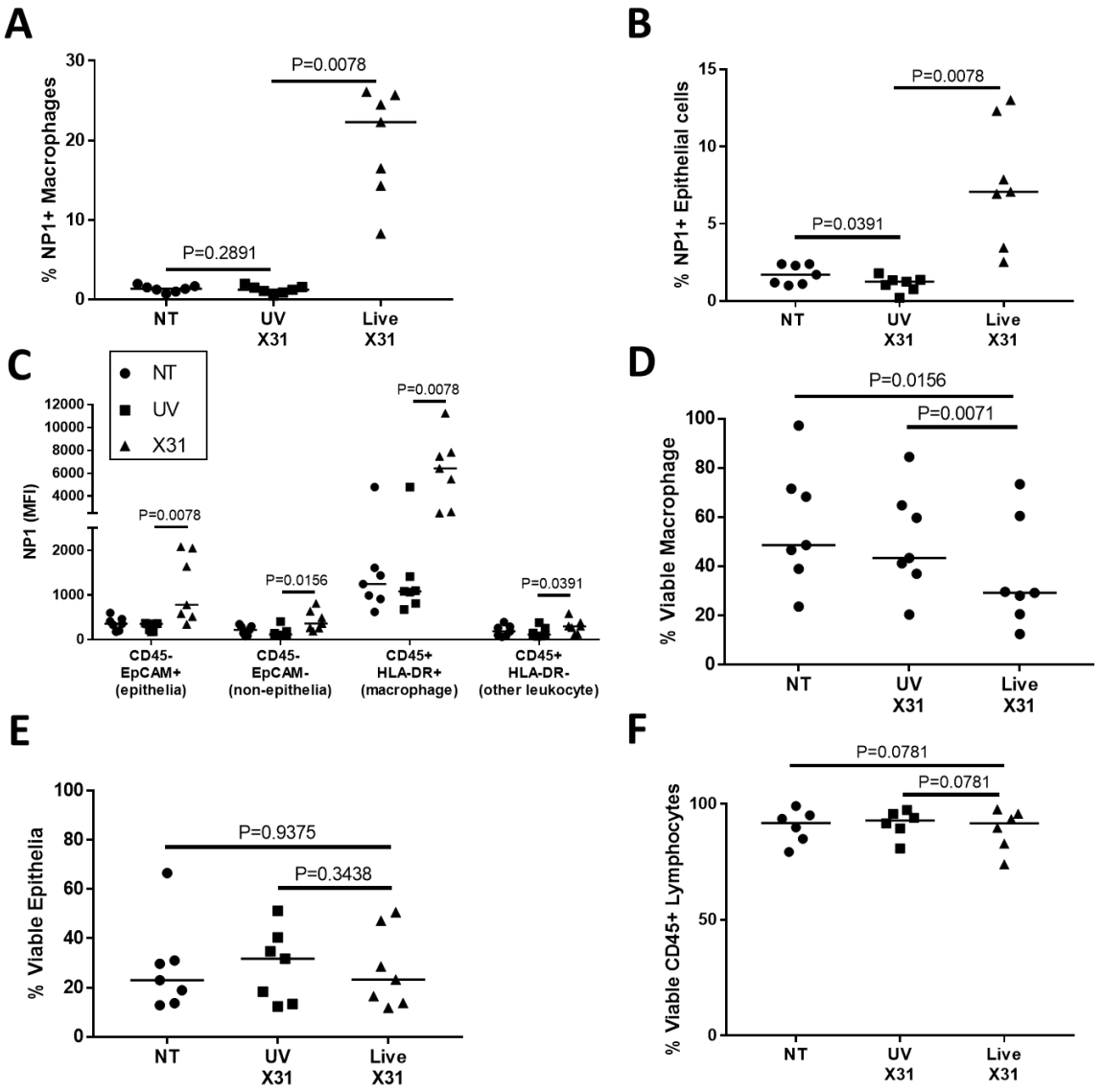

Figure 5.2: Influenza infects the airway epithelia and macrophages. Lung explants were infected with live or UV-irradiated X31 IAV for 2h before extracellular virus was removed and explants incubated for a further 22h. Lung explants were then digested and interrogated by flow cytometry (**A, B**) Percentage of NP-1+ macrophages (**A**) and epithelial cells (**B**) following IAV infection. (**C**) X31 infection measured by NP-1 MFI in CD45+HL-DR+ (Macrophages), CD45+HLA-DR- cells, CD45-EpCAM+ (Epithelial cells) and CD45-EpCAM- cells. (**D, E, F**) Cellular viability following X31 infection of macrophages (**D**), epithelia (**E**) and lymphocytes (**F**). Lymphocytes were defined based on size and CD45 expression as described in Figure 2.3. Cell types were defined prior to gating on cellular viability. Statistical analysis by Wilcoxon signed-rank test. Lines describe medians, N=7.

Airway epithelia and macrophages both showed signs of cellular activation following IAV infection, as antigen presenting pathways were upregulated by both cells (Figure 4.3). HLA class I expression was strongly increased on macrophages 24h post IAV infection (P=0.0156, Figure 4.3 A) with greater expression of HLA-A/B/C on macrophages infected with the virus compared to those that were not infected (P=0.0078, Figure 5.3 B). Likewise, increased HLA-A/B/C was detected on epithelial cells positive for IAV NP-1 protein (P=0.0078 Figure 5.3 F), although this did not reach significance on the whole epithelial cell population (P=0.1481, Figure 5.3 E). A smaller proportion of the epithelial cells are infected compared to macrophages (7.1% vs 22.3% respectively, Figure 5.2 A and B) and thus IAV-induced change may not be detected when observing the whole epithelial population.

5.2.2 Anti-Viral Molecules are produced by IAV Infected Lung Explants

Gzm-B and IFN-γ are key anti-viral molecules associated with NK cell activation and were used to assess the kinetics of lymphocyte activation during IAV infection of lung explants. The production of extracellular IFN-γ and Gzm-B was investigated by ELISA over a 30 h time course (N=3, Figure 5.4) [200]. Extracellular IFN-γ was not detected in untreated (NT) or UV-irradiated X31 treated tissue (Figure 5.4 A). However, around 250 pg/mL of basal Gzm-B was detected in NT explants and did not differ between NT and UV-irradiated X31 treated lung tissue (24h; P=0.5, Figure 5.4 B and D). During live IAV infection both IFN-γ and Gzm-B were increased in culture supernatants between 16 and 24 h of infection, with IFN-γ plateauing at 30 hpi (Figure 5.4 B). At 24 hpi both IFN-γ and Gzm-B were significantly increased in live X31-infected explants compared to UV-irradiated controls (P=0.0039 and P=0.0078 respectively, Figure 5.4 C and D). Taken together these results demonstrate a successful model of IAV infection in the human lung, through which infected cells are activated and anti-viral molecules produced within 24 h of infection.

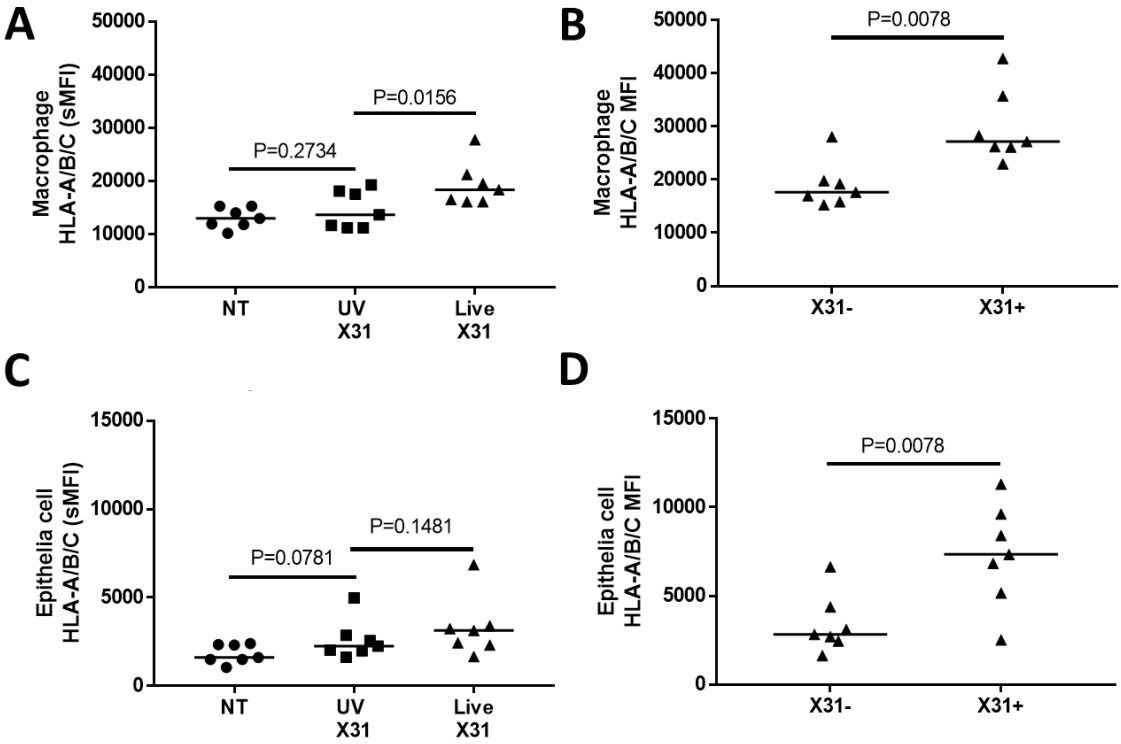

Figure 5.3: X31-infected cells upregulate antigen presenting molecules. HLA-ABC expression on macrophages (**A**) and epithelial cells (**C**) from tissue explants infected with UV-irradiated X31, live X31 or not-treated (NT), N=7. (**B, D**) Macrophages (**B**) or epithelial cells (**D**) from live-X31 treated tissue were stratified based on infection with virus, as determined by intracellular NP-1 expression. HLA-A/B/C expression in X31+ and X31- cells are shown. Statistical analysis by one-tailed Wilcoxon signed-rank test. Lines describe medians.

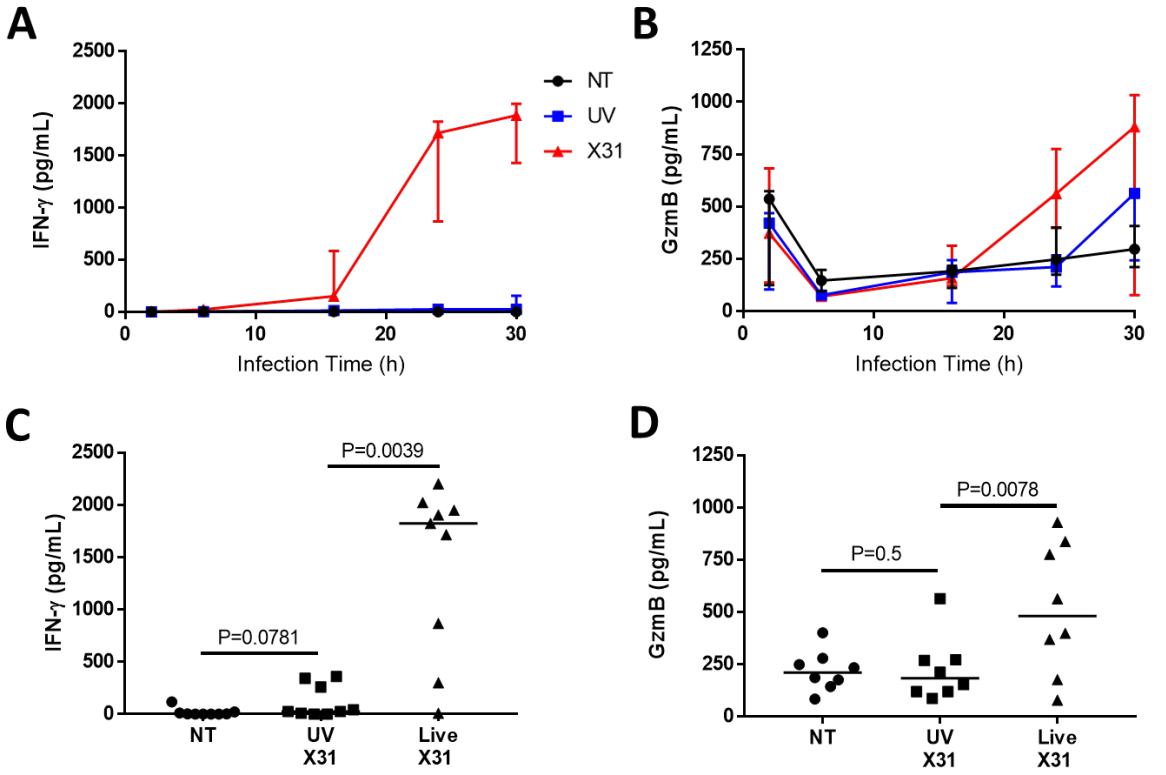

Figure 5.4: Anti-viral molecules are produced by X31-infected human lung explants. (**A, B**) Time course of extracellular IFN-γ (**A**) and Gzm-B (**B**) detection in explant supernatants following UV-irradiated or live X31 infection compared to non-treated (NT) explants (N=3, except 6h N=2). Medians are plotted alongside the interquartile range. (**C, D**) Extracellular IFN-γ (**C**) and Gzm-B (**D**) 24h post-infection (N=9).

5.2.3 IAV Infection of Human Lung Explants does not affect the NK cell Phenotype

As lung NK cell activation will be assessed in this model, the effect of IAV infection on the proportion of NK cells, CD56/CD16 phenotype and CD49a expression were analysed as shown in Figure 5.5. NK cells were defined as shown in Figure 2.1 and discussed in Chapters 3 and 4. The proportions of NK cells and NK cell subsets was stable over time in the resting explant and during live influenza infection (Figure 5.5 A, B and C). Interestingly, PMA/I stimulation dramatically altered the proportion of $CD56^{bright}$ and $CD56^{dim}$ NK cell with a marked increase in $CD56^{dim}$CD16- NK cells and reduction in other subsets. This phenotypic change most likely reflects the strong NK cell activation induced by these molecules [314, 316, 317, 320]. Finally, CD49a expression on the lung NK cells was unaffected by IAV infection or time (Figure 5.5 D).

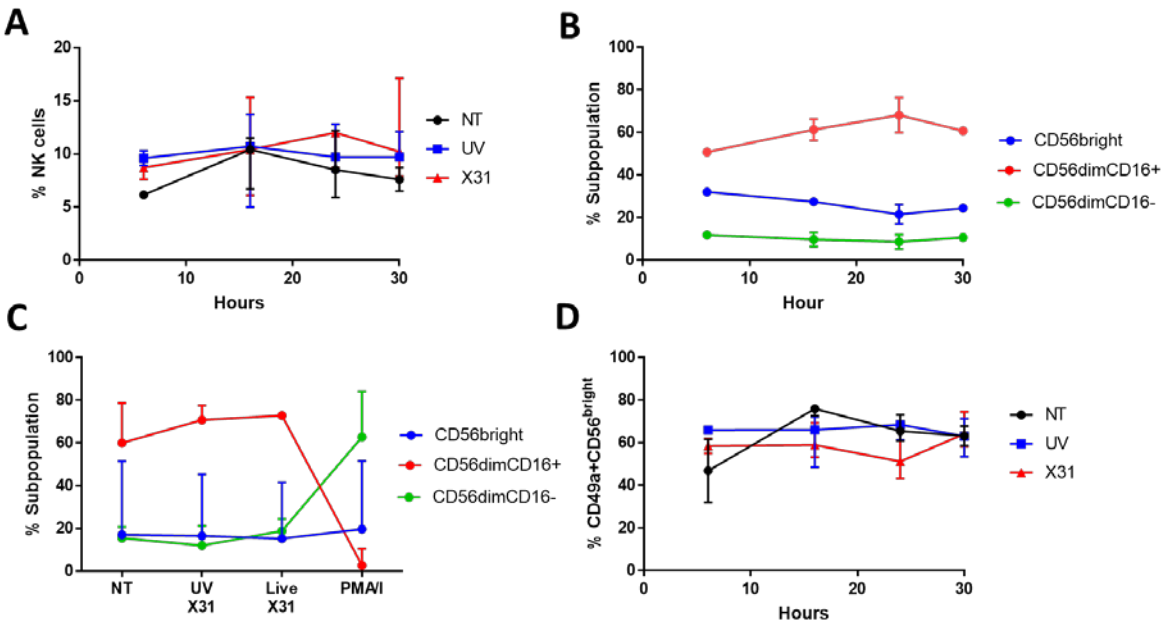

Figure 5.5: The NK cell phenotype is stable during explant infection. (**A**) The proportion of NK cells within CD45+ lung lymphocytes in uninfected (NT) lung and explants infected with UV-irradiated X31 and live X31 (N=3, except 6h N=2). (**B**) The proportion of $CD56^{bright}$ and $CD56^{dim}$ NK cells in lung tissue during 30h of culture. (**C**) $CD56^{bright}$ and $CD56^{dim}$ NK cell subpopulations in lung explants infected with X31 and PMA/I for 24h. (**D**) The proportion of $CD56^{bright}$ CD49a+ NK cells in NT, UV-irradiated X31 and live X31 treated lung tissue over time (N=3, except 6h N=2). Medians are plotted alongside the interquartile range. Error bars are not shown where they are smaller than the height of the symbol.

5.2.4 Measuring Lymphocyte Activation in Lung Explants by Flow Cytometry

To assess the response of NK cells to IAV infection, flow cytometry measures of NK cell activation were developed in the explant tissue. NK cell activation was measured by IFN-γ production and NK cell surface expression of CD107a was used as an indirect measure of killing (Figure 5.6) [185]. Following 24 h stimulation by PMA/I, the lung tissue was digested by collagenase, filtered and stained for lymphocyte markers, CD107a and IFN-γ. Lung T cells were defined as CD45+CD3+ cells as shown in Figure 2.1

CD107a was found to be increased three-fold on both NK cell and T cell surfaces (P=0.0313 and P=0.0313 respectively, Figure 5.6 A and B). This fits with previous reports, as T cell CD107a has been detected previously in lung explants [429]. To capture intracellular IFN-γ, 2μM monensin was added to lung explants 1h after PMA/I stimulation and incubated for a total of 24 h (Figure 5.6 D and F). The speed of lymphocyte IFN-γ production was also investigated with a 6 h stimulation with PMA/I (Figure 5.6 C and E). Interestingly, IFN-γ was not detected in NK cells after 6 h of PMA/I stimulation but was at 24 h post-stimulation, with a two-fold increase in MFI (NT; 48 MFI vs PMA/I; 90 MFI, N=3, Figure 5.6 C and D). These results indicate that a long exposure to PMA/I and monensin are required to detect intracellular IFN-γ in NK cells. However, intracellular IFN-γ could be detected in T cells much sooner after PMA stimulation, with a two-fold increase in MFI 6 h post-stimulation (Figure 5.6 E). T cell IFN-γ production was further increased following a 24 h incubation with PMA/I and monensin (Figure 5.6 F) to double that seen for NK cells (NK cell; 90 MFI, vs T cell; 206 MFI). Therefore, PMA/I appeared to be a much stronger stimulator of lung T cells than NK cells. Together, these results demonstrate a successful method for measuring lymphocyte activation and cytokine production in human lung tissue which can be applied during IAV infection.

5.2.5 Human Lung NK cell Activation in response to IAV Infection

As described in section 5.2.1, lung explants were infected with either live X31 IAV, UV-irradiated X31 or left untreated. Lymphocytes were isolated by collagenase digestion and activation measured by flow cytometry. The ELISA data shown in Figure 5.4 indicates that lymphocyte activation most likely occurs between 16 and 24 hpi. To investigate the activation kinetics specifically in NK cells, NK cell surface CD107a was measured over a 30 h time course of X31 infection. Live IAV infection of human lung parenchyma resulted in increased surface expression of CD107a by NK cells, as shown in Figure 5.7 A. Average CD107a levels rose on NK cell surfaces early in infection with a small rise 6 hpi, which continued over 24 h before plateauing 30 hpi (Figure 5.7 B N=3, except 6h N=2). NK cell CD107a expression was most variable at the 16h time point and most consistent 24 hpi, thus the 24 h time point was taken forward to analyze NK cell degranulation (Figure 5.7 C). At 24 hpi NK cell surface CD107a expression was significantly increased in live-X31 infection relative to UV-irradiated controls (P=0.0469, N=6, Figure 5.7 D) and unchanged in untreated and UV-irradiated controls (P=0.0938, Figure 5.7 D).

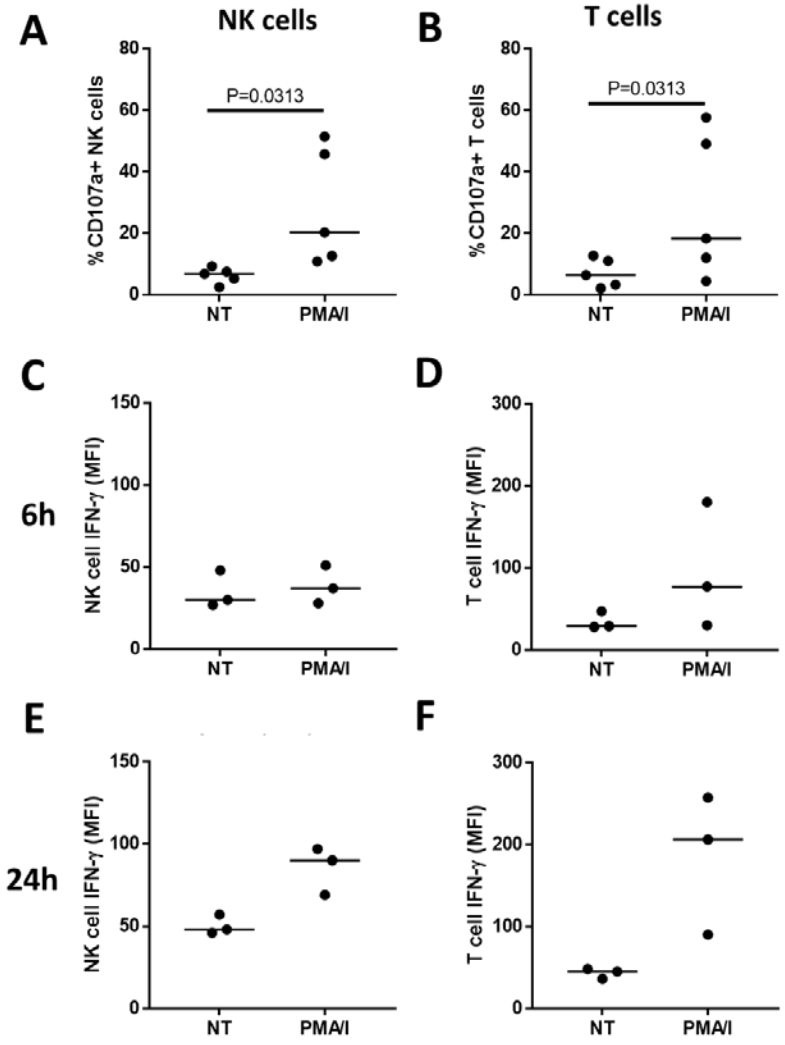

Figure 5.6: PMA/I stimulation of human lung explants activates lymphocytes. (**A, B**) Lung explants were stimulated with PMA/I for 24h and surface CD107a measured on NK cells (**A**) and T cells (**B**). Statistical analysis by one-tailed Wilcoxon signed rank test. (**C, D, E** and **F**) Intracellular IFN-γ production was measured following 6h (**C, D**) and 24h (**E, F**) stimulation of tissue explants with PMA/I. Monensin was added to lung explants 1 h after the addition of PMA/I to capture intracellular IFN-γ. Lung NK cell (**C, E**) and T cell (**D, F**) IFN-γ production is shown. Lines describe medians.

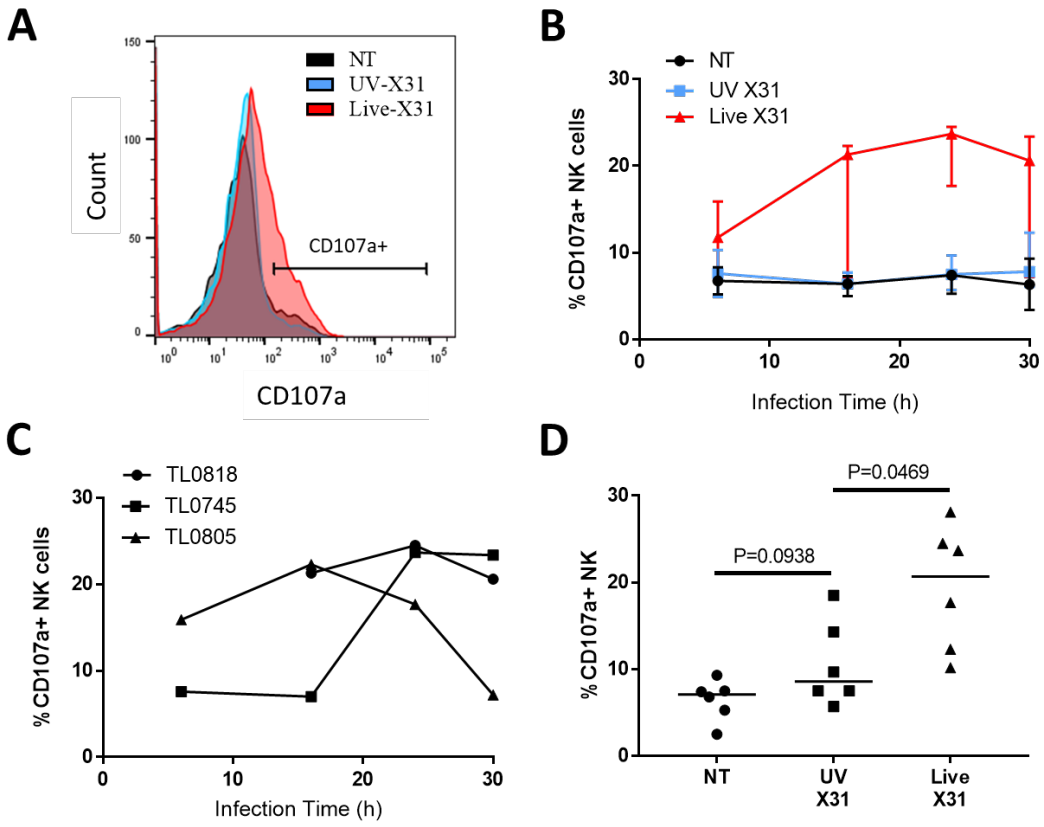

Figure 5.7: NK cell activation following X31-infection of human lung explants. (**A**) Representative flow cytometry plot of NK cell CD107a expression in IAV infected explants. (**B**) Median NK cell CD107a expression over time. Bars show interquartile range (N=3, except 6h N=2). Error bars are not shown when smaller than the height of the symbol. (**C**) NK cell CD107a expression over time in three individual X31-infected explants. Lines denote individual donors. (**D**) NK cell CD107a expression following 24 h infection of human lung explants with UV-irradiated or live X31 or no-treatment (NT). Lines describe medians, statistical analysis by one-tailed Wilcoxon signed-rank test.

A major function of NK cells is to provide early IFN-γ during infection [200]. To detect the intracellular accumulation of this cytokine monensin was added to cell cultures, but this was shown to inhibit X31 replication (Figure 5.8). The percentage of infected macrophages dropped from 26% to 5.3% with monensin treatment and from 7.1% to 3.4% of infected epithelial cells (N=3, Figure 5.8 A and B). monensin blocks traffic from the golgi apparatus and most likely inhibited IAV protein movement prior to virion assembly [488]. It was therefore necessary to allow IAV infection to occur before capturing lymphocyte IFN-γ production. The greatest rise in IAV-induced extracellular IFN-γ occurred between 16 and 24 hpi, as shown by ELISA in Figure 5.4. Therefore, lung explants were infected with IAV for 2 h, extracellular virus washed off, and lung tissue incubated for a further 14 h, for a total infection time of 16 h. X31 replication was still detectable at this time point, but with

fewer cells infected relative to 24 hpi (7.5% of macrophages and 5% of epithelia, N=3, Figure 5.8 and Figure 5.2). Monensin was added to lung explants 16 hpi and incubated for another 24 h before tissue digestion and intracellular staining, thus resulting in a total infection time of 40 h. These timings were chosen as a 24 h exposure to stimulation and monensin was required to detect NK cell IFN-γ (as shown in Figure 5.6). The extent of IAV infection was not measured in the tissue 40 hpi but as monensin efficiently inhibited the capacity for IAV to replicate (Figure 5.8 A and B) it is unlikely that it would be greater than that seen for the 24h time point (Figure 5.2). Monensin may affect cellular function within the tissue explant, but blocking golgi transport is required to detect the accumulation of intracellular cytokine by flow cytometry. Using this method, increased intracellular IFN-γ was detected in the NK cells of IAV infected tissue relative to UV controls (P=0.0156, Figure 5.8 E and F). As with CD107a expression, NK cell IFN-γ production was also found to be equivalent between UV-irradiated X31 treatment and untreated explants (P=0.1563, Figure 5.8 F) thus indicating that UV-irradiated X31 is not stimulating NK cell activation. For all experiments measuring lymphocyte IFN-γ $3.15x10^7$ IU/mL of a 2017 stock of X31 was used. This viral dose was titrated to give the same infection of macrophages and epithelia as seen for the 2012 X31 stock of virus used to measure lung NK cell CD107a (see Figure 2.5).

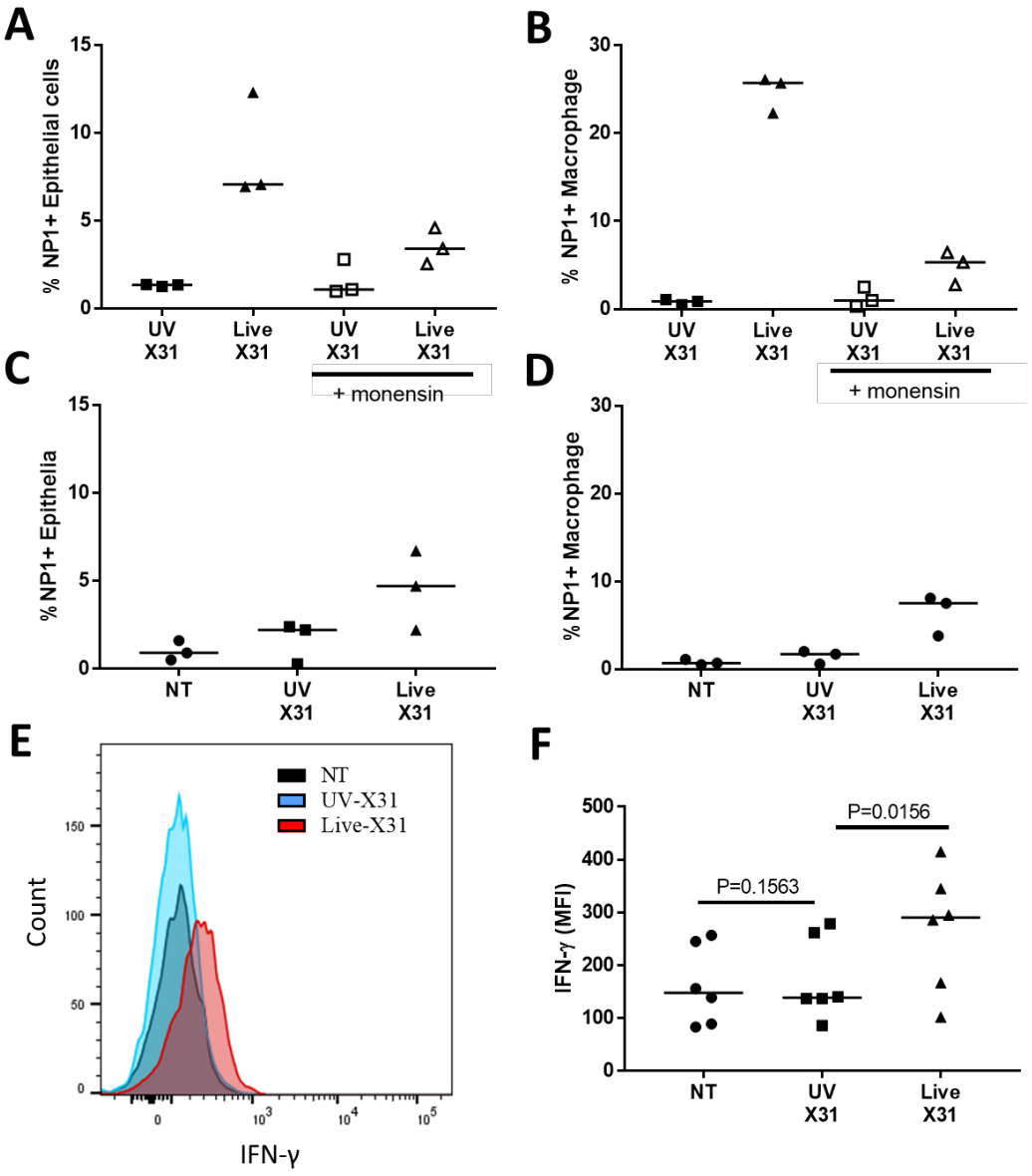

Figure 5.8: Detecting intracellular IFN-γ in X31-infected lung explants. (**A, B**) The addition of monensin to explants to detect intracellular molecules prevents influenza replication. IAV replication was determine by intracellular NP-1 expression in both airway epithelial cells (**A**) and macrophages (**B**) 24 hpi, N=3. (**C**, **D**) IAV replication is detectable in both the epithelial cells (**C**) and macrophages (**D)** of infected lung explants 16 hpi, N=3 (**E, F**) NK cell intracellular IFN-γ measured by flow cytometry following 16h infection with X31 IAV and 24h incubation with monensin. (**E**) Representative image of NK cell intracellular IFN-γ in IAV infected lung explants.

5.2.6 CD56^{bright} and CD56^{dim} NK cell Activation in IAV Infected Lung Tissue

CD56^{bright} and CD56^{dim} NK cells have been suggested to play different roles within the body, with CD56^{dim} NK cells thought to possess a greater cytotoxic potential and CD56^{bright} NK cells producing more cytokines [189, 259, 295, 302-304, 308-312]. However, these results mainly come from artificial stimulation with cytokine and cancer cell lines and can depend on the stimulation [189, 259, 295, 302-304, 308-312]. To assess whether CD56^{bright} and CD56^{dim} NK cells respond differently during a viral infection, NK cell CD107a and IFN-γ production was measured on CD56^{bright}, and CD56^{dim} NK cell subsets.

In terms of degranulation both CD56^{bright} and CD56^{dim} NK cells increased surface CD107a in response to IAV infection (P=0.0156 for all, Figure 5.9 A). Interestingly, CD56^{dim}CD16- NK cells expressed more CD107a in untreated lung explants (Figure 5.9 B) than basal CD56^{bright} and CD56^{dim}CD16+ NK cells which fits with the description of CD56^{dim}CD16- as more activated NK cells [189, 259, 295, 302-304, 308-312]. However, when the basal level of CD107a expression was factored in, NK cell degranulation during IAV infection was not dominated by either CD56^{dim}CD16+ or CD56^{dim}CD16- NK cells. All NK cell subsets had an equivalent (approximately five-fold) upregulation of surface CD107a (Figure 5.9 A). Furthermore, analyses of CD56^{bright} and CD56^{dim} intracellular IFN-γ showed that all subsets produced IFN-γ in response to IAV infection (CD56^{bright}; P=0.0156, CD56^{dim}CD16+; P=0.0469, CD56^{dim}CD16-; P=0.0156, Figure 5.9 C). Furthermore, the IFN-γ MFI was comparable between CD56^{bright} and CD56^{dim} NK cell subsets. Taken together, these results show an equivalent response from lung CD56^{bright} and CD56^{dim} NK cells to IAV infection.

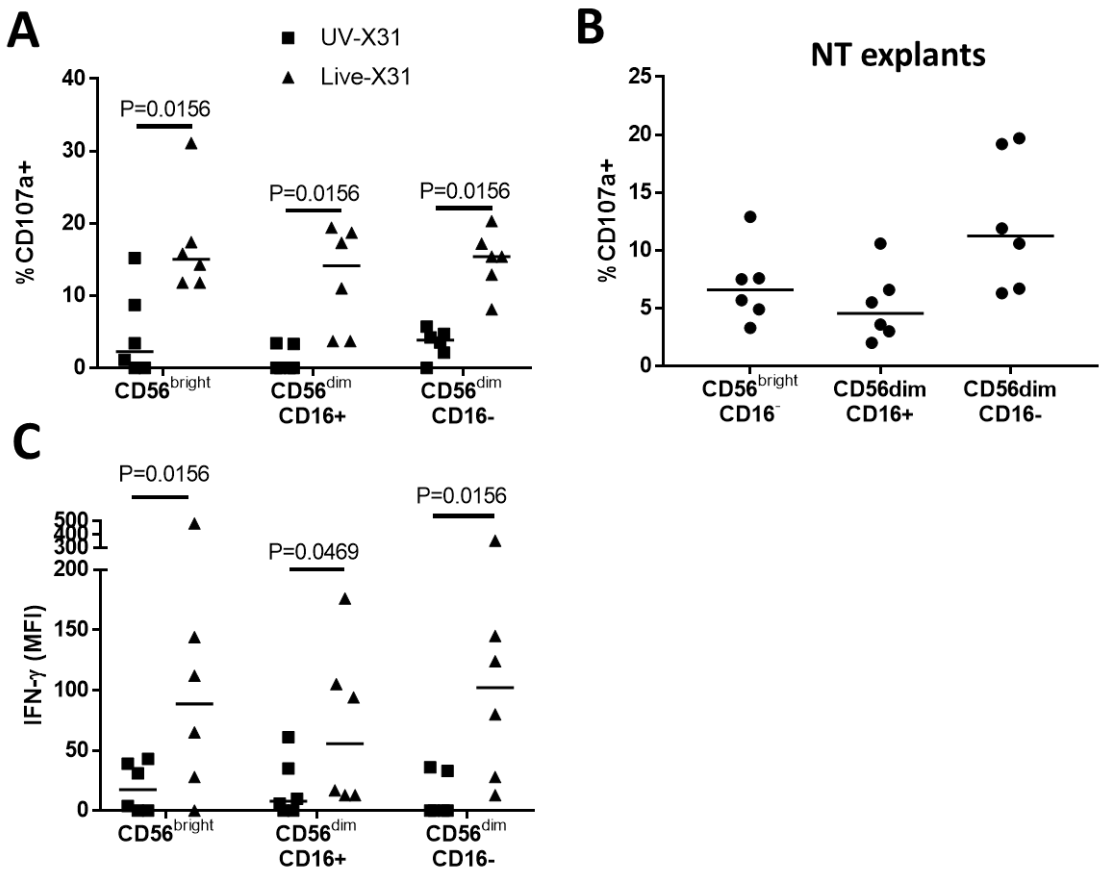

Figure 5.9: CD56 ^{bright} and CD56^{dim} NK cell activation to IAV infection. Lung explants were infected with X31 for 24 h prior to measurement of NK cell surface CD107a. (**A**) CD107a expression on CD56^{bright} and CD56^{dim} NK cell subsets following live and UV-irradiated X31 infection. Uninfected (NT) background CD107a expression was subtracted from all values. (**B**) NK cell subset expression of CD107a in non-treated explants. (**C**) Intracellular IFN-γ in CD56^{bright} and CD56^{dim} NK cell subsets. Uninfected (NT) background IFN-γ expression was subtracted from all values. Lung tissue was infected for 16 h before incubating with monensin. Lines describe medians, statistical analysis performed by one-tailed Wilcoxon-signed rank test, N=6.

5.2.7 CD49a+ NK cell Function in IAV Infected Human Lungs

CD49a+ NK cells expression has been linked to memory response in hapten challenge and viral infections [346-350, 426]. Multiple influenza infections are experienced throughout life and we hypothesised that human lung CD49a+ NK cells may possess an enhanced responsiveness to IAV infection. Thus degranulation and IFN-γ production of CD49a+ and CD49a- NK cells were analysed in IAV infected lung tissue. When measuring surface CD107a expression, $CD56^{bright}$CD49a+ NK cell degranulation was found to be slightly increased during live X31 infection when compared with $CD56^{bright}$ CD49a- NK cells (P=0.0313, Figure 5.9 A). Interestingly, this trend was not found when lung explants were stimulated with PMA/I, during which $CD56^{bright}$ CD49a+ and CD49a- cells degranulate equivalently (P=0.5). CD107a was also assessed on $CD56^{dim}$CD16- NK cells, which were also found to express CD49a (Figure 4.7). However, there was no difference in CD107a expression between $CD56^{dim}$CD16- CD49a+ and CD49a- cells in IAV infected tissue (P=0.1563, Figure 5.9 B).

When comparing CD49a+ and CD49a- IFN-γ production, there no difference between $CD56^{bright}$CD49a+ and $CD56^{bright}$CD49a- IFN-γ in live IAV infection (P=0.1563, Figure 5.9 C). Whereas $CD56^{dim}$CD16- CD49a+ NK cells produced more intracellular IFN-γ compared to CD49a- cells (CD49a+; 352 MFI vs CD49a-; 163.5 MFI, N=6, P=0.0469, Figure 5.10 E H). This trend was not found in PMA/I stimulated lung explants where $CD56^{dim}$CD16- CD49a+ and CD49a- cells responded equivalently (P=0.3135, Figure 5.10 E). Taken with the measures of NK cell degranulation this data indicates a slightly enhanced function of CD49a+ lung NK cells to IAV infection but with differences in the response of $CD56^{bright}$ and $CD56^{dim}$ NK cells. However, the physiological relevance of these changes remains to be seen.

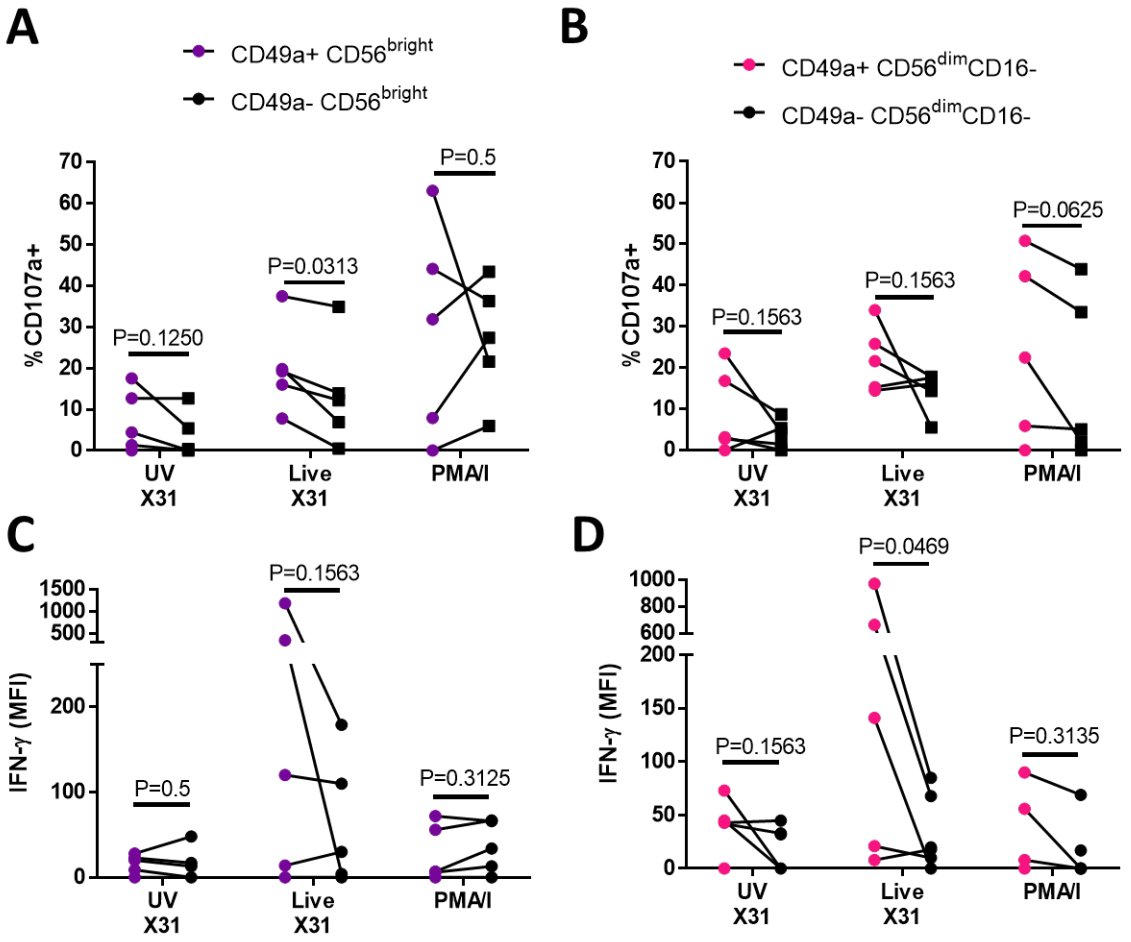

Figure 5.10: Activation of CD49a+ and CD49a- NK cells in IAV infected lung tissue. Lung explants were infected with X31 or treated with PMA/I for 24h before measurement of NK cell degranulation (**A, B**) CD49a+ and CD49a- NK cell surface CD107a in $CD56^{bright}$ (**A**) and $CD56^{dim}CD16$- (**B**) NK cells, N=5. (**C, D**) Intracellular IFN-γ was measured in both CD49a+ and CD49a- cells in $CD56^{bright}$ (**C**) and $CD56^{dim}CD16$- (**D**) NK cell subsets (N=6, except PMA N=5). For IFN-γ detection the lung tissue was infected for 16 h before incubation with monensin for a further 24h. Lung explants were stimulated with PMA/I for the same total time as IAV infection. Lines describe medians. Statistical analysis by one-tailed Wilcoxon signed-rank test.

5.2.8 NK cells and T cells share Effector Function in IAV Infected Lung Tissue

T cells have also been shown to secrete IFN-γ during infection and some subsets demonstrate significant cytotoxicity against infected cells [489]. To investigate the likelihood that T cells contributed to the rise of extracellular IFN-γ and Gzm-B in IAV infected tissue (Figure 5.4) T cell degranulation and IFN-γ production was measured by flow cytometry (Figure 5.11). This found that T cell expression of CD107a and IFN-γ were both significantly increased in IAV infected lungs and indicates that these cells may also contributed to the release of Gzm-B and IFN-γ in human IAV infection (P=0.0156 and P=0.0156 respectively, Figure 5.11 A and C). In addition, as CD49a is expressed on lung T cells, the function of CD49a+ T cells was assessed in this study [331]. CD49a has been associated with differential localisation of T cells within the lungs and thus may be important in T cell residency [331]. 53.8 ± 12.8% of lung explant T cells expressed CD49a in this study and the functional response of these cells was explored relative to CD49a- lung T cells. CD49a+ T cell CD107a expression was equivalent to CD49a- cells in live-IAV infected lung tissue and PMA/I stimulation (P=0.0781 and P=0.3125 respectively, Figure 5.11 B). However, IFN-γ production in CD49a+ T cells was enhanced relative to CD49a- T cells during live IAV infection (P=0.0156, Figure 5.11 D) but not in PMA/I stimulated tissue or UV-X31 treated controls (P=0.0625 and P=0.1250 respectively, Figure 5.11 D). This might indicate that CD49a expression on T cells may be associated with greater cytokine production, as seen for $CD56^{dim}$CD16- NK cells.

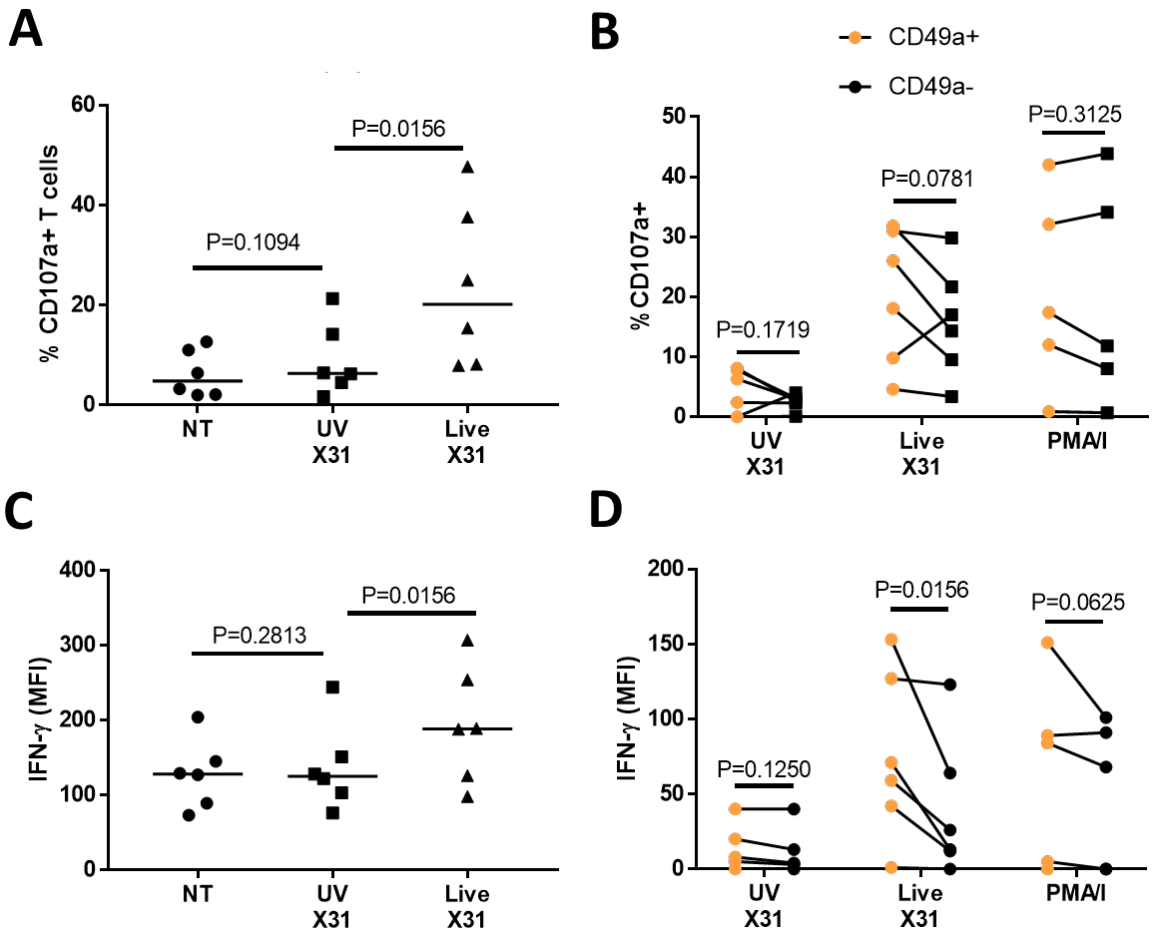

Figure 5.11: Human lung T cell activation to IAV infection. (A, B) Lung explants were infected with UV-irradiated or live IAV for 24 h. Explants were then digested and CD107a measured on T cell surfaces by flow cytometry. (**C, D**) To detect IFN-γ, lung explants were infected with IAV for 16h before the addition of monensin and further incubation for 24 h. (**B, D**) CD49a+ and CD49a- T cell CD107a expression (**B**) and IFN-γ production (**D**) following live influenza infection and PMA/I treatment. Lines describe medians. Statistical analysis by one-tailed Wilcoxon signed-rank test, N=6.

5.3 Discussion

5.3.1 *Ex Vivo* Influenza Infection of Lung Explants are consistent with previous reports

This chapter reports the successful infection of human lung explants with IAV virus (Figures 5.1 and 5.2) with an equivalent infection to that reported previously [428, 429]. Live X31 infection was compared against UV-irradiated X31, which is inert and does not replicate within human lung tissue (P=0.2891, Figure 5.2 A and B). UV-irradiated X31 was used to control for the effects of PRR stimulation by initial exposure to viral particles. This allowed us to discern the effects of viral invasion and replication on lung immune function. UV-irradiated X31 did not stimulate activation of any of the cell types investigated in this study, including lung epithelia, macrophages, T cells or NK cells.

IAV infection was measured by intracellular expression of NP-1, which is only produced during viral replication (Figure 5.2) [488]. Airway macrophages and epithelia were the dominant cell types infected with influenza (22.3% and 7.2% respectively, Figure 5.2). Substantial increases in IAV, determined by NP-1 MFI, were found in both these cell types with a small amount of NP-1 expression in CD45-EpCAM- cells and CD45+HLA-DR- cells (Figure 5.2 C). These results suggest that a small amount of X31 is able to infect non-epithelial structural cells and leukocytes, a feature that may be due to the high levels of extracellular virus required to infect airway tissue (500,000 PFU/mL 2012 X31 stock). However, significant viral tropism for the airway epithelia and macrophages is observed in this model, as previously reported in the literature [45, 490].

A greater proportion of airway macrophages were infected compared to airway epithelia (22.3% vs 7.1%). This may reflect greater accessibility of macrophages to IAV virus in the culture media than the epithelia. Alternatively, it may reflect greater IAV uptake by airway macrophages, possibly though macrophage phagocytosis [140, 491]. The enhanced expression of IAV NP-1 could also be explained if macrophages provided a better resource for viral replication, although this is unlikely given the macrophage's role as an early sentinel and antigen presenting cell [45]. Rodgers *et al*. also reported a 20% infection of human alveolar macrophages by H3N2 IAV but without viral exit to the culture media. Abortive replication of H1 and H3 IAV in alveolar macrophages has since been corroborated by a number of studies, suggesting that IAV accumulates, but is not able to disseminate from these cells [45]. Interestingly in this model, macrophage viability was reduced in IAV infected lung explants (P=0.0071, Figure 5.2), possibly reflecting the higher burden of IAV

infection as IAV has also been shown to increase macrophages phagocytosis and apoptosis [140, 491, 492]. Increased macrophage death in IAV-infected tissue might also reflect lymphocyte-mediated destruction as both NK cells and T cells were activated by IAV infection (Figures 5.7, 5.8 and 5.11).

The effect of IAV on infected cells was further characterized in terms of antigen presenting molecules. These results demonstrate the activation of IAV-infected cells, with increased expression of class I HLA molecules on infected airway epithelial cells and macrophages (Figure 5.3). These results suggest that antigen presentation may be increased in IAV-infected explants. Furthermore, strong anti-viral responses were detected in IAV infected lung tissue with significantly increased extracellular IFN-γ and Gzm-B 24 hpi (P=0.0039 and P=0.0078 respectively, Figure 5.4 C and D). Both IFN-γ and Gzm-B rose in explant supernatants between 16 and 24h of infection (Figure 5.4 A and N). The timing of this response indicates that the secretion of these molecules is a secondary response to initial inflammatory signalling by cytokines such as IFN-α and IFN-β [493, 494]. Interestingly extracellular Gzm-B appeared to be reduced in control conditions at the 6 h time point compared to 2 h (Figure 5.4 B). At 2 hpi culture supernatant was collected and explants washed to remove extracellular virus. Thus the increased basal expression of Gzm-B in untreated and UV-irradiated X31 controls at the initial two-hour time point may indicate a small amount of Gzm-B release following explant removal from the body. This is probably reduced at the six-hour time point due to tissue washing. Taken together these results demonstrate that *ex vivo* lung infection provides reliable infection of airway macrophages and epithelia as well as immune cell activation. Thus this model was used to explore the lung NK cell response to IAV infection.

5.3.2 NK Cells are Activated during Influenza Infection of Human Lung

Infection of human lung explants was carried out in 0.5% FCS RPMI as described in section 2.13 as FCS protein may inhibit viral infection and replication [495, 496]. However, FCS was found to be important for NK cell survival and maintenance, as shown in Figure 3.3 and discussed in section 3.3.1. Removal of FCS from culture media increased the proportion of peripheral blood $CD56^{dim}$CD16- NK cells (Figure 3.3). Thus the NK cell phenotype may have been affected by the lack of FCS in the culture medium. Indeed, the proportion of $CD56^{dim}$CD16- NK cells in untreated lung explants was slightly higher in untreated explants in 0.5% FCS-RPMI compared to 10% FCS RPMI (13.8% vs 8.7%, Figure 5.5B and Figure 4.4 F). Although lung explants were cultured in 0.5% FCS-RPMI for 24 h longer, which could contribute to this difference in CD56dimCD16- NK cells.

Functional responses of human lung NK cells to IAV infection were characterized by flow cytometry and the kinetics of NK cell activation explored. This included the development of a novel method to detect intracellular cytokine within the human lung tissue. NK cells were strongly activated during IAV infection of lung tissue with a rapid CD107a response beginning 6 hpi and peaking at 24 hpi (Figure 5.7 B). In an *in vivo* setting of influenza infection, peak NK cell response occurs 3 days after infection [112, 364, 372, 382, 393, 394]. However, the speed of response seen in this thesis most likely reflects the fact infection was *ex vivo* and with a high titre of virus. Nevertheless, these data support the concept of NK cells as early responders to viral infection. Interestingly, lung T cells were found to respond at a similar rate despite a reported week long delay in the T cell response in the mouse lung (Figure 5.11) [497]. T cells isolated from human lung parenchyma have been shown to be predominantly memory T cells with little to no presence of naïve T cells, which might explain an equivalent response time with NK cells [460]. As H3N2 is a current circulating strain of IAV we would expect T cells possessing memory to IAV antigens to be present in the lung parenchyma [486].

The timing of NK cell degranulation during IAV infection appeared highly variable between individual donors (Figure 5.7 C). For instance, NK cell CD107a expression was increased in two of three lung tissue donors at the 16 h time point, whilst no CD107a expression was seen in the other donor. This variation may arise from the quality of tissue received or differences in disease state, co-morbidities, medication, age or commensal microbiota of donors. It might also reflect heterogeneity in immune responses and viral replication within individual humans, which are rooted in both genetic and environmental variability [498]. However, this experiment is at a small sample size due to a limited availability of the tissue size required to repeat this work. Increasing the sample size would give more information on the degree of variability between NK cell responses in individuals.

In the three individuals analyzed the 24 h time point was the most consistent for measuring NK cell CD107a expression, thus this time point was subsequently used. Lung NK cells demonstrated increased evidence of degranulation 24 h post live IAV infection ($P=0.04969$, Figure 5.8 A), indicating the release of NK cell cytotoxic granules towards target cells and suggesting possible clearance of infected cells [185, 499]. IAV infection also stimulated significant upregulation of NK cell IFN-γ production ($P=0.0156$, Figure 5.9 E). IFN-γ is an important anti-viral cytokine, upregulating anti-viral machinery in neighbouring cells and strongly stimulating many arms of the immune response [500]. Thus, lung NK cells may promote anti-viral immunity within the lung tissue through this inflammatory signalling pathway. These findings fit with reports of NK cell activation following

IAV vaccination in the blood and against IAV-infected monocyte-derived dendritic cells and suggest that human NK cells may contribute to anti-IAV responses in the human lung [254, 319].

Importantly, this data demonstrates that NK cells are not hyporesponsive during IAV infection but rather are strongly activated and may play an important role in viral control. The mechanisms by which NK cells are released from their inhibited state during IAV infection are largely unknown. However, NK cell activation may be stimulated by inflammatory cytokine signalling, or by change to the balance of activating and inhibitory ligand expression on infected cells [199, 468]. For instance NKG2D, NKp46 and a number of KIR have been implicated in NK cell recognition of infected cells [254, 376, 378, 379, 384, 385]. Understanding NK cell regulation during respiratory infections may have important implications for human lung diseases where inflammation is chronic and could result in dysregulated NK cell function [86].

5.3.3 CD56^{bright} and CD56^{dim} NK Cells respond equivalently to IAV Infection

Many studies have described CD56^{bright} NK cells as cytokine producing and CD56^{dim} NK cells as cytotoxic [259, 295, 302-304, 308, 309]. However, "cytotoxic" CD56^{dim} NK cells can also release large-amounts of cytokines upon receptor ligation and CD56^{bright} NK cells become cytotoxic following cytokine stimulation [189, 310-312]. To assess the function of CD56^{bright} and CD56^{dim} NK cells in the *ex vivo* lung model the degranulation and IFN-γ production of NK cell subsets were also analysed (Figure 5.9). CD56^{bright} and CD56^{dim} NK cells were both found to degranulate and upregulate IFN-γ production equivalently in live IAV infected lung tissue (Figure 5.9). Thus it appears that the mechanism determining NK cell activation to IAV infection may be shared by CD56^{bright} and CD56^{dim} NK cells, despite differences in receptor expression on the subsets [296]. NK cell activation to IAV-infected cells may involve increased activating receptor ligation or KIR engagement from infected cells, as has been suggested by the literature [254, 376, 378, 379, 384, 385]. However, IAV-induced pro-inflammatory cytokine signalling may also play a role in stimulating NK cell activity [114, 378]. In fact, the pro-inflammatory environment of IAV-infected lungs may enable the activation of both CD56^{bright} and CD56^{dim} NK cells as cytokine treatment can modulate NK cell subset function *in vitro* [189, 310-312].

Unfortunately, from this data it is not possible to conclude that NK cell subsets kill equivalently during IAV infection as CD107a is an indirect measure of NK cell killing. CD56^{bright} cells have been shown to express more Gzm-K and less Gzm-B than CD56^{dim} NK cells which might result in a different

capacity for cellular killing [501, 502]. In future, measuring intracellular accumulation of granzyme molecules within lung lymphocytes may shed more light on the differences between the cytotoxic potential of $CD56^{bright}$ and $CD56^{dim}$ NK cells in the lungs. This question could also be investigated more directly by cytotoxicity assays against IAV-infected target cells following sorting of $CD56^{bright}$ and $CD56^{dim}$ NK cells.

5.3.4 Lung CD49a+ NK Cells may be more Functionally Responsive to Respiratory Virus

CD49a, an integrin associated with both NK cell residency and memory was identified on lung NK cells in section 4.2.5 [340, 344, 348-350, 426]. Both $CD56^{bright}$ and $CD56^{dim}$CD16- lung NK cells strongly expressed CD49a, as shown in Figure 4.8 and 4.9. As IAV is a common respiratory pathogen which humans experience multiple times throughout their lifetime, this virus may stimulate the generation of innate immune memory as well as adaptive memory [486, 503]. Thus, the hypothesis is that CD49a+ lung NK cells may possess enhanced recall responses to IAV. To investigate this, the surface CD107a and intracellular IFN-γ expression of CD49a+ and CD49a- NK cells were analysed (Figure 5.10).

A greater proportion of $CD56^{bright}$ CD49a+ NK cells were found to degranulate in response to IAV infection compared to $CD56^{bright}$ CD49a- NK cells (P=0.0313, Figure 5.10 A), an effect not seen with PMA/Ionomycin stimulation (P=0.5, Figure 10 A). This suggests that $CD56^{bright}$ CD49a+ NK cells might have an enhanced degranulation response that is specific to viral infection, as the total potential of the lung NK cells to express CD107a was unchanged. However, this difference did not extend to cytokine production as $CD56^{bright}$ CD49a+ IFN-γ production was equivalent to $CD56^{bright}$ CD49a- cells (P=0.1563, Figure 5.9 G). In section 4.2.5 the activating receptor profile of CD49a+ NK cells was different to CD49a- NK cells, including enhanced NKG2D expression on $CD56^{bright}$CD49a+ NK cells (Figure 4.10 B). NKG2D has been implicated in releasing NK cell cytotoxicity towards IAV infected cells which may explain the increased degranulation of these cells in IAV infected lung [254]. Increased NKG2D expression was also found on $CD56^{dim}$CD16-CD49a+ lung NK cells (P=0.0420, Figure 4.10 E). Likewise, there was a trend towards increased CD107a expression on $CD56^{dim}$CD16-CD49a+ cells in IAV infected lungs, although this did not reach significance (P=0.1563, Figure 5.10 B). Interestingly IFN-γ upregulation was found to be greater in $CD56^{dim}$CD16- CD49a+ cells relative to CD49a- cells (P=0.0469, Figure 5.10 D), contrasting with $CD56^{bright}$CD49a+ cells (P=0.1563, Figure 5.10 C). It is unclear why there would be differences between the response of $CD56^{bright}$ CD49a+ and $CD56^{dim}$CD16- CD49a+ cells but could reflect the more activated state of $CD56^{dim}$CD16- cells

[189, 259, 295, 302-304, 308-312]. However, the small sample size in these experiments may inhibit the detection of statistical significance, particularly given the heterogeneity within human immunological data. For instance, in some individuals there were large differences in the IFN-γ expression of $CD56^{bright}$CD49a+ and $CD56^{bright}$cCD49a- cells, but not in others. Sample quantity and availability are limiting factors in our capacity to carry out these experiments however repetition of this work would better confirm any functional differences in CD49a+ and CD49a- lung NK cells and would be an important aspect of further work.

Taken together, these results suggest an enhanced function of CD49a+ lung NK cells to IAV and indicate that NK cell memory of influenza infection might exist within the adult human lung. However, corroboration of CD49a+ cell transcription factor expression and epigenetic state is required to fully conclude this. In murine studies, liver CD49a+ NK cells from mice infected with IAV were protective following adoptive transfer and subsequent influenza challenge [426]. However, rather confusingly, murine lung CD49a+ NK cells were not protective in this model [426]. The authors suggest that lung CD49a+ NK cells may be inhibited by the high degree of lung inflammation caused by mouse-adapted IAV [426]. The work of Li *et al* demonstrates that the training of CD49a+ NK cells may make significant contributions to clearance of infection *in vivo* [426]. However, the physiological relevance of CD49a+ cells to human infections remains to be seen. The resident NK cell localisation within the lung structure remains a mystery but may be similar to that observed for T cells [331]. CD49a+ T cells are found to localise to the collagen-IV rich basement membranes in human lung and skin [331].

The generation of resident local mucosal immunity in humans could have important implications for interventions in lung disease and IAV vaccine design, offering a possibility for increasing strain cross-reactivity and effectiveness [344]. Furthermore, immune signalling from resident NK cell populations has not been investigated in human infection and may be an important mechanism of coordination between different arms of the immune system. Interestingly CD49a expression was found to be increased on $CD56^{bright}$ lung NK cells during worsening COPD (Figure 4.13), which may indicate dysregulation of this cell population during chronic lung disease. However, the full functional role of human CD49a+ lung NK cells and their contributions to lung disease remain be elucidated.

5.3.5 T cell CD49a Expression is also associated with Enhanced Function

As described by previous reports, T cell degranulation could also be measured in lung explants following IAV infection, indicating that these cells may also contribute to Gzm-B release and infected cell clearance (P=0.0156, Figure 5.11 A) [429]. In addition, for the first time this study reports the detection of increased IFN-γ production by T cells in IAV infected explants (P=0.0156, Figure 5.11 C). Thus, lung T cell and NK cells share this effector function. The T cells analysed in this study are predominantly memory T cells, which might explain why the speed of IFN-γ production was equivalent to that of the NK cells [429, 460].

CD49a expression is also associated with T cell residency and memory and therefore CD49a+ T cell responses were analysed as a control for our observations in the NK cell population [504]. In this study CD49a was found on approximately half (53.8 ± 12.8%) of the CD3+ T cell population. Unfortunately, an analysis of CD49a expression on CD4 and CD8 T cells was beyond the scope of this study due to restraints on the number of flow cytometry channels available. In the murine lung, Richter *et al* found that CD49a was expressed on 70% of CD8 lung cells and 28% of CD4 T cells [331]. Interestingly CD49a defines a population of Trm cells and is associated with a more activated T cell phenotype in the skin, gut, cervix and lung with increased production of IFN-γ and TNF-α [331, 505]. CD3 engagement of by CD8+CD103+CD49a+ Trm in the skin was shown to increase IFN-γ production relative to CD49a- T cells [505]. Indeed, IAV stimulates IFN-γ production primarily from CD4+ CD49a+ and CD8+CD49a+ T cells [506, 507]. This fits with our findings demonstrating increased IFN-γ production in CD49a+ T cells in IAV infected lung (P=0.0156, Figure 5.11 D). However, surface CD107a was not found to be different between CD49a+ and CD49a- T cells (P=0.0781, Figure 5.11 B) thus CD49a expression may not be related to changes in T cell degranulation and thus cytotoxic potential, although this would require further analysis.

Blocking CD49a function was shown to reduce virus-specific CTLS in the lung, indicating that CD49a plays a role in the retention of Trm cells [506]. As discussed in section 1.4.6 CD49a binds collagen IV, a component of the lung epithelia basement membranes [331]. This explains the localisation of the predominantly CD49a+ CD8 T cells around basement membranes of airways or blood vessel, with most CD4+ T cells found in the interstitial space [331]. It has also been suggested that CD49a contact with the extracellular matrix causes anti-apoptotic signalling within T cells, thus maintaining Trm populations in the organs [506, 508]. A mechanism that may be important in preserving Trm cells following T cell population collapse during infection resolution [506, 509]. The anchorage of Trm cells to organ extracellular matrices may retain a population of T cells tailored to control recurrent infection [505, 506, 508, 509]. It is possible that a similar mechanism maintains resident NK cell populations in the lung, allowing NK cell surveillance of this mucosal surface.

5.3.6 Benefits and Limitations of the *Ex Vivo* Infection Model

The model of *ex vivo* influenza infection presented in this chapter presents a number of advantages compared to murine models including the ability to assess human immune responses in a physiologically relevant model of IAV infection. It also allows investigation into the function of cell populations unique to human lungs, whose responses may be shaped by individual immune history. Thus investigating the function of organ-resident NK cells in infection in animal models is challenging, particularly if their function revolves around differential expression of germ-line encoded receptors as these are not well shared between species [510]. However, analysis of human lung tissue is limited by a restricted availability of this resource as well as a high heterogeneity in cohort genetics and environmental exposure. Furthermore, as all lung cell types are included in this model it can be challenging to dissect out specific NK cell stimulating signals and to distinguish between the effects of other immune cells. To further investigate mechanisms of NK cell activation and functional responses, a more reductionist model is required and this is explored in Chapter 6.

5.3.7 Summary

In this chapter flow cytometric methods analyzing NK cell activation were developed in human lung tissue. An *ex vivo* model of IAV infection was used to explore the kinetics of NK cells responses, including lymphocyte CD107a expression and Gzm-B and IFN-γ production. Lung NK cells were shown to be highly responsive to IAV infection, with significant upregulation of CD107a and IFN-γ production. Thus human lung NK cells do not appear to hyporesponsive during viral infection. Furthermore, NK cell subsets were shown to respond equivalently to IAV infection, demonstrating that $CD56^{bright}$ and $CD56^{dim}$ NK cells share effector functions in human lung tissue. Finally, this chapter assessed the functional response of resident NK cells identified in chapter 4. Lung CD49a+ NK cells showed enhanced degranulation potential and IFN-γ production compared to CD49a- NK cells, although differences in the function of $CD56^{bright}$CD49a+ and $CD56^{dim}$CD16-CD49a+ cells were observed. Further investigation of the mechanisms of NK cell activation are required to better understand how these cells are regulated in the lungs and will be explored in chapter 6.

Chapter 6 Modelling NK Cell Activation to IAV-Infected Cells

6.1 Introduction

In this thesis lung NK cells were shown to both degranulate and produce IFN-γ upon IAV infection, indicating that NK cells may have important anti-viral functions within human lungs (section 5.2.5). Unfortunately, the complexity of the *ex vivo* infection model limits exploration of mechanisms of lung NK cell activation and regulation. Therefore, the mechanisms driving NK cell activation were also explored in co-culture models of blood-derived NK cells with either IAV-infected PBECs or MDMs.

Airway epithelia and macrophages are infected by IAV, as shown in Chapter 5. Both of these cell types provide early innate inflammatory signaling during IAV infection which may activate NK cell function [105, 511]. Airway macrophages have also been shown to inhibit NK cell function during steady-state lung conditions [366]. Given, the strategic location and production of pro-inflammatory cytokines by macrophages, and their repressive effect on NK cell function, there may be an important interplay between airway macrophages and NK cells in the lungs [105, 364-366, 512]. Investigating this intercellular interaction is therefore an important aspect in understanding pulmonary NK cell regulation [366]. On a more mechanistic level, NK cell activation is controlled by the integration of inhibitory and activating signalling from germ-line encoded NK cell receptors [199, 200]. Two activating receptors, NKp46 and NKG2D and have been implicated in NK cell recognition of IAV infected cells [254, 376, 378, 379]. In addition, some KIR alleles have been associated with IAV severity, however there is a great deal of conflict in the literature and receptor binding has not been modelled with physiologically relevant cell types, as discussed in section 1.5.2 [384, 385]. Pro-inflammatory cytokine signalling has also been shown to stimulate NK cell activation and therefore both these facets of NK cell biology are explored in this chapter [513, 514].

To do this, submerged lung epithelial cultures were grown out of bronchial brushings and MDMs were differentiated by 12 day GM-CSF culture of peripheral blood monocytes. MDMs cultured this way provide a well-established model of the *in vivo* human alveolar macrophage [85, 423, 431, 432]. PBECs and MDMs were then infected with X31 influenza prior to culture with autologous peripheral

NK cells (as shown in Figure 6.1). These models allowed the flow cytometric analysis of NK cell activation, however receptor expression and cytotoxic function was primarily investigated in the MDM-NK co-culture model. Furthermore, the effect of direct cell contacts with NK cells with target cells were investigated in a transwell system and by blocking specific receptor ligation. Cytokine signalling was also analysed from both MDMs and NK cells analysed by Luminex assay.

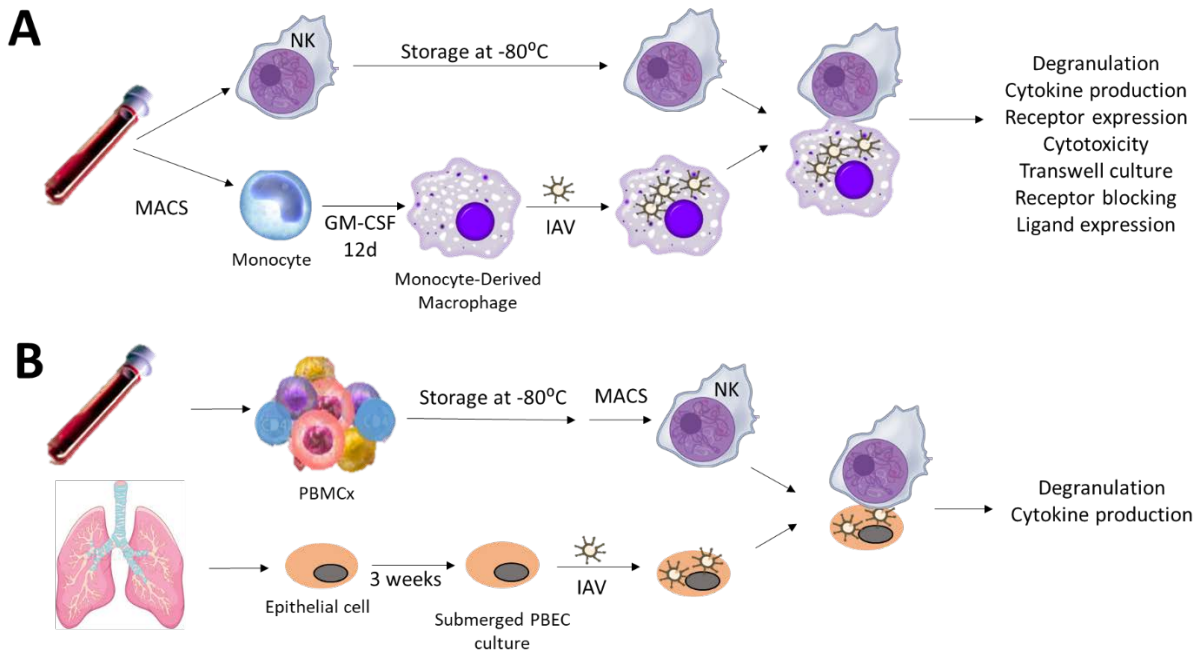

Figure 6.1: Diagrammatic representation of NK cell culture with autologous infected cells. (**A**) NK cell and monocyte-derived (MDM) co-cultures. Monocytes and NK cells were extracted from blood of healthy volunteers using density gradient centrifugation and MACS. Monocytes were identified through positive selection for CD14 and NK cells by negative selection. Purified NK cells were stored at -80°C until use. Meanwhile monocytes were cultured over 12 d in GM-CSF to promote differentiation to MDMs. (**B**) NK cell and PBEC co-culture. Epithelial cells were isolated from bronchial brushings of healthy donors and grown out into submerged PBEC cultures. Previously frozen PBMCs were defrosted and NK cells isolated by MACS negative selection. (**A, B**) Both MDMs and epithelial cells were infected with X31 H3N2 IAV virus for 24h prior to 6h culture with NK cells.

Results

6.2.1 Optimizing Co-Culture Conditions

The protocol for autologous MDM-NK cell co-culture is summarised in Figure 6.1 A, with further detail in section 2.2. In brief, autologous monocytes and NK cells were isolated from the blood of healthy donors (REC 13/SC/0416) by density gradient centrifugation followed by MACS. Monocytes were isolated based on a CD14+ sort and NK cells by negative selection. Monocytes were then cultured in 2 ng/mL GM-CSF for 12 days, allowing differentiation into MDMs. Meanwhile, freshly isolated NK cells were frozen in 10% DMSO/FCS and stored at -80°C until use. Neither MACS purification or cryopreservation were found to affect the proportions of $CD56^{bright}$ or $CD56^{dim}$ NK cells (Figure 3.3).

Prior to culture with NK cells, MDMs were infected with 500 PFU/mL of H3N2 X31 IAV for 24 h to allow sufficient IAV infection of the monolayer [433]. As reported previously, at 24 hpi a median 29% of the MDM monolayer was NP-1 positive with a lack of viral replication in UV-X31 treated controls (Figure 6.2A) [433]. In addition, this timing fits with findings from the *ex vivo* lung explant model of infection where optimal NK cell activation was observed 24 hours post influenza infection (Figure 5.7). MDMs were found to upregulate the expression of NK cell ligands including class I HLA (P=0.0313, Figure 6.2 B) and ligands for NKG2D and NKp46 24 hpi with H3N2 IAV (P=0.1563 and P=0.0313 respectively, Figure 6.2 C and D). UV-irradiated X31 did not induce any change in either MDM class I HLA, NKG2D ligands or NKp46 ligands (P=0.1875, P=0.1563 and P=0.3125 respectively Figure 6.2 B, C and D). NKG2D has been shown to bind both MIC-A/B and ULBP proteins in humans [251-254]. MIC-A/B expression on X31-infected MDMs was also analyzed by flow cytometry but was not detected on MDM surfaces (0.26% on IAV-infected MDMs N=5). This suggests that some, or all of the ULBP proteins may be responsible for increased NKG2D-Fc construct binding [251-254].

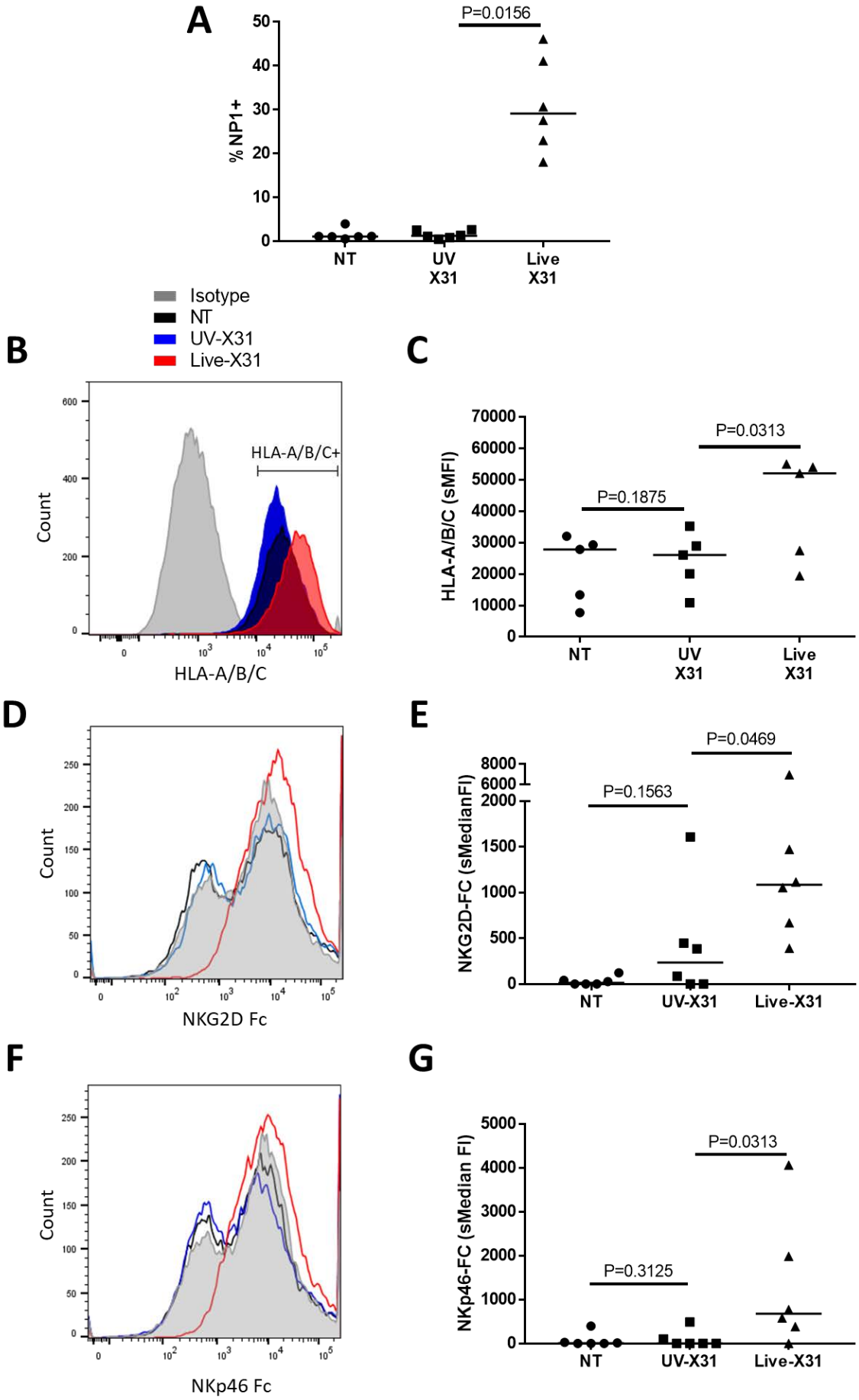
A
P=0.0156
% NP1+
NT
UV X31
Live X31
Isotype
NT
UV-X31
Live-X31
B
HLA-A/B/C+
Count
HLA-A/B/C
C
P=0.0313
P=0.1875
HLA-A/B/C (sMFI)
NT
UV X31
Live X31
D
Count
NKG2D Fc
E
P=0.0469
P=0.1563
NKG2D-FC (sMedianFI)
NT
UV-X31
Live-X31
F
Count
NKp46 Fc
G
P=0.0313
P=0.3125
NKp46-FC (sMedian FI)
NT
UV-X31
Live-X31

Figure 6.2: MDM surface proteins change with IAV infection. MDMs were infected with UV-irradiated or live X31 IAV or untreated (NT) for 24 h. (**A**) IAV replication was measured by intracellular NP-1 expression. (**B, C**) HLA-A/B/C expression on infected MDMs. (**D, E, F, G**) Ligands for the NK cell activating receptors NKG2D (**D, E**) and NKp46 (**F, G**) were detecting through binding of Fc-receptor chimera constructs and measured by flow cytometry. Lines show medians. Statistical analysis by two-tailed Wilcoxon signed-rank test.

Following 24 h infection with live-X31, MDMs were cultured with autologous NK cells and NK cell activation measured by flow cytometry. NK cells were cultured with MDMs at a number of E:T ratios to determine the optimal conditions to measure NK cell function, as shown in Figure 6.3 A. NK cell activation was detected by expression of intracellular IFN-γ following 6 h of co-culture. Target cells were X31-infected MDMs, however a PMA/I stimulation of a 1:1 co-culture was used as a control for NK cell activation. The greatest NK cell IFN-γ production was found at an E:T of 1:5 with minimal NK cell activation detected at a 1:1 and a 1:10 ratios (Figure 6.3 A). Therefore, an E:T of 1:5 was taken forward and used in all subsequent MDM-NK co-culture experiments.

The kinetics of NK cell activation in this model were assessed with time points of 2 and 6h co-culture with MDMs. Increased IFN-γ was detected in both 2 and 6h co-cultures relative to UV-X31 controls (P=0.0313 and P=0.0156 respectively, Figure 6.3 B and C) as was NK cell surface CD107a (P=0.0156 and P=0.0313 respectively, Figure 6.3 C and D). However, a 6 h co-culture time was preferred as this gave a greater increased in median IFN-γ expression to the 2 h time point (6h live-X31; 214 vs 2h; 171.5, Figure 6.3 D) and thus better detection of NK cell activation. NK cell culture with NT MDMs was found to maintain NK cell viability (Figure 6.4 G) and did not affect the proportion of either $CD56^{bright}$, $CD56^{dim}$CD16+ or $CD56^{dim}$CD16- NK cells (P=0.625, P=0.0625, P=0.0625, Figure 6.4 A, B and C). NK cell subsets were also stable in IAV-infected co-cultures ($CD56^{bright}$; P=0.4378, $CD56^{dim}$CD16+; P=0.4375 and $CD56^{dim}$CD16-; P=0.8125, Figure 6.4 D, E and F). A statistically significant small (median 0.4%) reduction in NK cell viability was observed in IAV-infected co-cultures (P=0.0156, Figure 6.4 H) however NK cell viability was largely maintained during contact with infected cells.

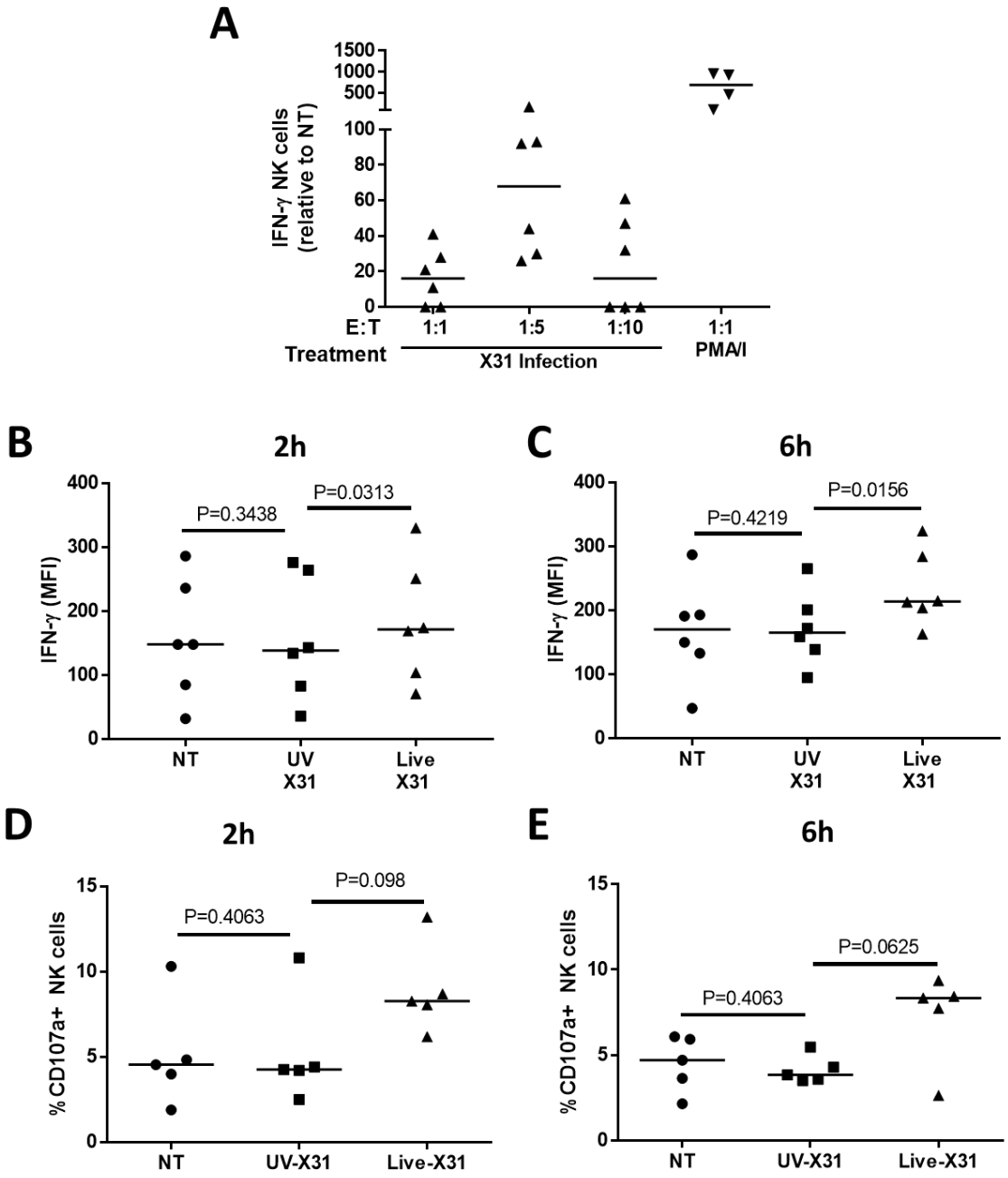

Figure 6.3: Determining the Effector : Target cell (E:T) ratio in NK-MDM co-cultures. (**A**) NK cells were cultured with IAV-infected MDMs for 6 h at a range of E:T ratios. 125, 000 MDMs were seeded per well in a 96-well plate. Co-cultures were also treated with PMA for 6h as a control. Monensin was added one hour after the addition of NK cells and NK cell activation was measured through the accumulation of intracellular IFN-γ. Background IFN-γ MFI was subtracted from all values. (**B, C, D, E**) Co-cultures were performed as described in **A** with 500 000 MDMs seeded per well in a 48-well plate. Untreated (N)T and UV-irradiated X31 treated MDM controls are shown. (**B, C**) NK cell intracellular IFN-γ following 2h and 6h co-culture at an E:T of 1:5, N=6. (**D, E**) NK cell surface CD107a during 2h and 6h co-culture at an E:T of 1:5, N=5. Statistical analysis by one-tailed Wilcoxon-signed tank test, lines show medians.

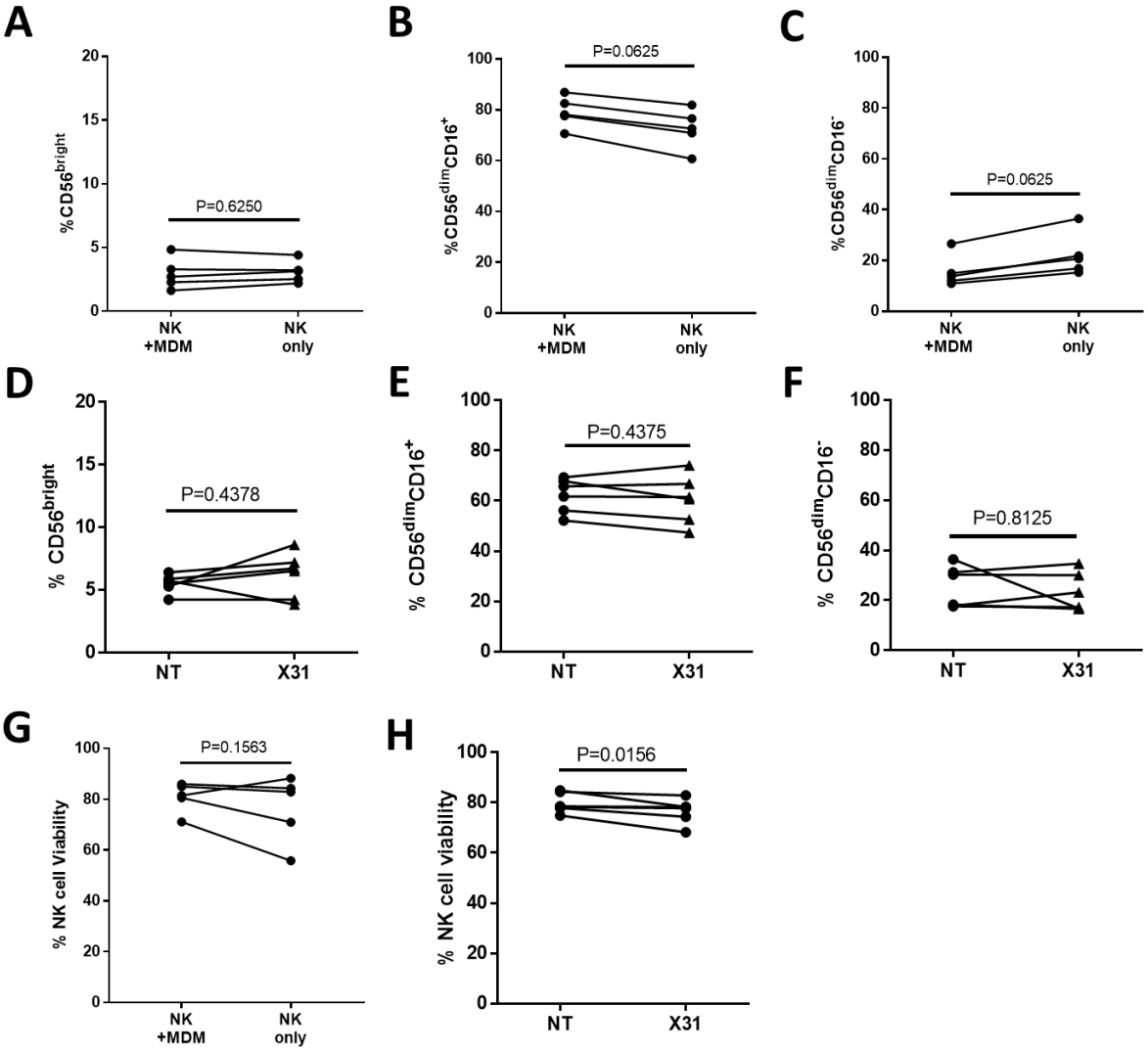

Figure 6.4: Culturing NK cells with autologous MDMs does not affect the NK cell phenotype. NK cells were cultured with mature MDMs for 6h at an E:T 1:5 and the expression of CD56 and CD16 measured by flow cytometry. Monensin was added to co-cultures for 5h prior to staining. (**A, B, C**) The proportions of $CD56^{bright}$ (**A**), $CD56^{dim}CD16+$ (**B**) and $CD56^{dim}CD16-$ (**C**) NK cells were unchanged when cultured with MDMs or on their own. (**D, E, F**) $CD56^{bright}$ (**D**) $CD56^{dim}CD16+$ (**E**) and $CD56^{dim}CD16-$ (**F**) NK cell proportions in uninfected and IAV-infected co-cultures. (**G, H**) NK cell viability was measured by flow cytometry in culture alone or with MDMs (**G**) and in IAV-infected co-cultures (**H**). Connecting lines show individuals. Statistical analysis by two-tailed Wilcoxon signed-rank test.

6.2.2 NK Cell Activation during Culture with IAV Infected MDMs is Contact Dependent

Peripheral blood NK cells were found to increase expression of both CD107a and IFN-γ upon culture with IAV-infected MDMs (P=0.0313 and P=0.0156 6.5 A and D), corroborating findings from *ex vivo* IAV infection of human lung tissue. IFN-γ production in the co-cultures was further analyzed by ELISA (Figure 6.5 F). Extracellular IFN-γ was detectable only when IAV-infected MDMs were cultured with NK cells (P=0.0078, Figure 6.5 D) indicating that NK cells are the most likely source of this cytokine. In addition, NK cell intracellular Gzm-B was also raised during culture with IAV-infected cells and there was a non-significant trend towards increased extracellular Gzm-B (P=0.0156 and P=0.0547 respectively Figure 6.5 C and E). However, there was high individual variability in this measure with a large range in Gzm-B expression even in NT co-cultures.

To determine the significance of cellular contact in stimulating NK cell activation, MDM-NK cell co-cultures were also performed in a trans-well system. This allowed the physical separation of NK cells from infected MDMs whilst still allowing cytokine signaling between the cells. Transwell separation of the co-cultures abrogated NK cell CD107a, IFN-γ and Gzm-B upregulation in IAV-infected co-cultures (P=0.2188, P=0.3438 and P=0.3438, Figure 6.5 A, C and D). This was confirmed by ELISA as extracellular IFN-γ could not be detected when NK cells were physically separated from IAV-infected MDMs (Figure 6.5 F). These results indicate that direct contact between NK cells and infected cells are essential to NK cell activation. However, NK cell viability was reduced by 15% in the transwell system along with a three-fold reduction in background extracellular Gzm-B and a five-fold increase in CD107a expression, which confounds the interpretation of some of these results. The lack of CD107a upregulation in IAV infected transwell co-cultures may not be due to the physical separation of NK cells from a stimulus but due to increased NK cell activation and fratricide using this transwell system [494, 515]. However, basal production of IFN-γ was unaffected by NK cell culture in transwells and more confidence can be given to these results. Taken together these results indicate that cell contact with infected cells are important in NK cell activation to IAV infection but further analysis is required to confirm this.

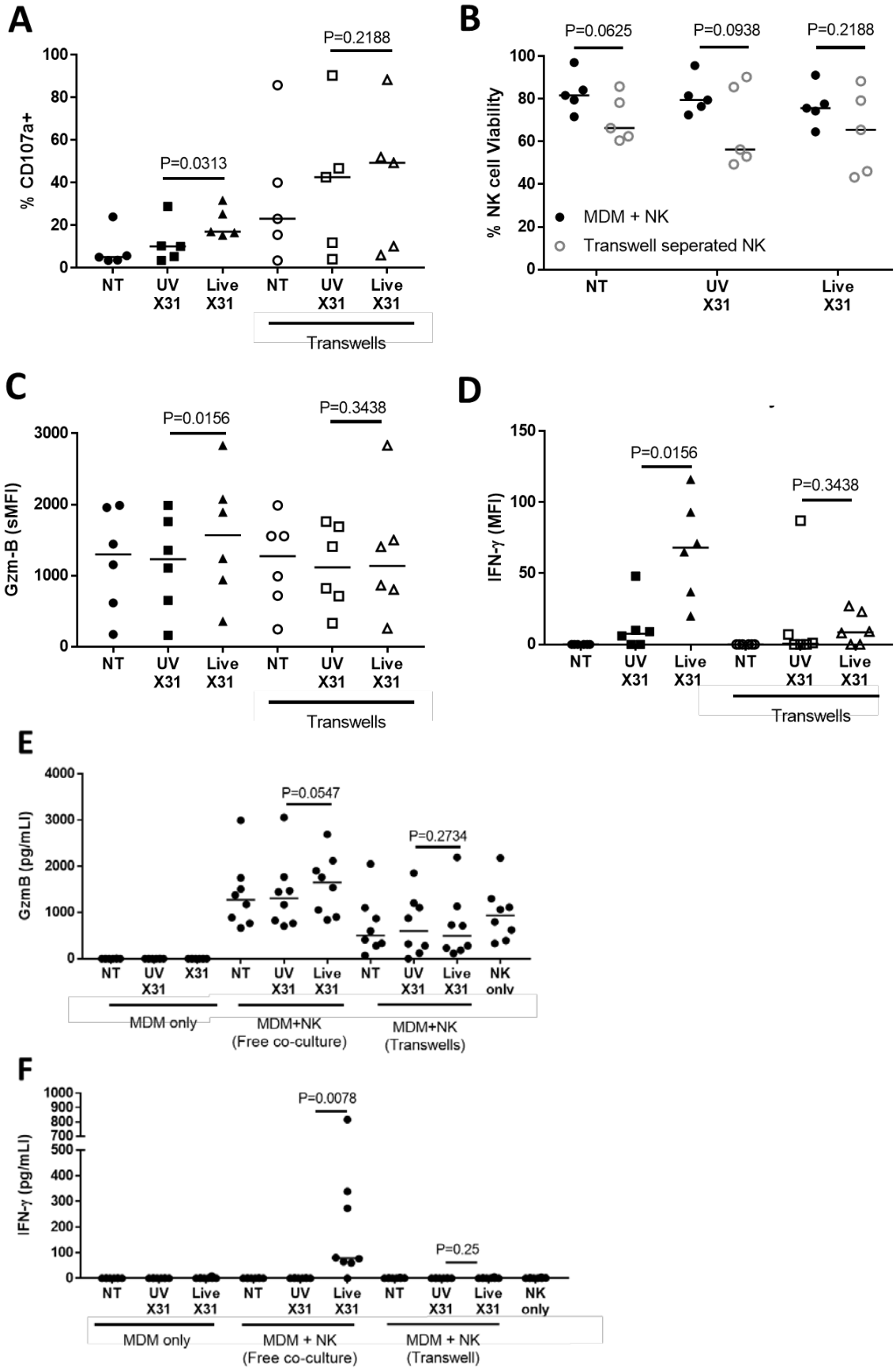
A
% CD107a+
P=0.2188
P=0.0313
NT
UV X31
Live X31
Transwells
B
% NK cell Viability
P=0.0625
P=0.0938
P=0.2188
MDM + NK
Transwell seperated NK
C
Gzm-B (sMFI)
P=0.0156
P=0.3438
D
IFN-γ (MFI)
E
GzmB (pg/mL)
P=0.0547
P=0.2734
NK only
MDM only
MDM+NK (Free co-culture)
MDM+NK (Transwells)
F
IFN-γ (pg/mL)
P=0.0078
P=0.25
MDM + NK (Free co-culture)
MDM + NK (Transwell)

Figure 6.5: NK cells activate and produce anti-viral molecules following contact with IAV-infected macrophages. Prior to culture with NK cells MDMs were infected with either UV-irradiated or live-X31 for 24 h. NT=non-treated. MDMs were then cultured directly with autologous NK cells or physically separated by transwells for 6 h. NK cell co-cultures were treated with monensin for 5h. (**A**) Surface CD107a expression on NK cells (N=5). (**B**) NK cell viability when cultured free with MDMs and when separated in a transwell system (N=5). (**C, D**) Accumulation of intracellular IFN-γ (**D**) and Gzm-B (**C**) detected by flow cytometry (N=6). (**E, F**) Extracellular IFN-γ (**F**) and Gzm-B (**E**) detected by ELISA in co-culture supernatants (N=8). Lines describe medians. Statistical analysis by one-tailed Wilcoxon signed-rank test.

6.2.3 CD56^{bright} and CD56^{dim} NK Cell Activation to IAV-Infected MDMs

CD56^{bright} and CD56^{dim} NK cells have been assigned different roles by some studies but were found to respond similarly during the *ex vivo* lung model of IAV infection presented in section 5.2.5 [259, 295, 302-304, 308, 309]. To corroborate these findings CD56^{bright} and CD56^{dim} degranulation, IFN-γ and Gzm-B production were analyzed following culture with IAV-infected macrophages (Figure 6.6). CD56^{bright} and CD56^{dim} NK cells were defined as shown in Figure 2.1. NK cell CD107a, IFN-γ and Gzm-B expression were all increased on CD56^{bright}, CD56^{dim}CD16+ and CD56^{dim}CD16- cells in IAV-infected co-cultures (Figure 6.6). However, the degree of upregulation in all three measures of NK cell activation appeared to be equivalent between the three NK cell subsets in IAV-infected co-cultures. Thus these results appear consistent with those reported in section 5.2.5 and suggest that CD56^{bright} and CD56^{dim} NK cells upregulate surface CD107a and produce IFN-γ and Gzm-B equivalently during IAV infection. All measures of activation are shown relative to the NT and thus take into account differences in expression between the NK cell subsets in unstimulated conditions. For instance Gzm-B is differentially expressed by CD56^{bright} and CD56^{dim} NK cells (Figure 6.6 D) [189, 304, 516].

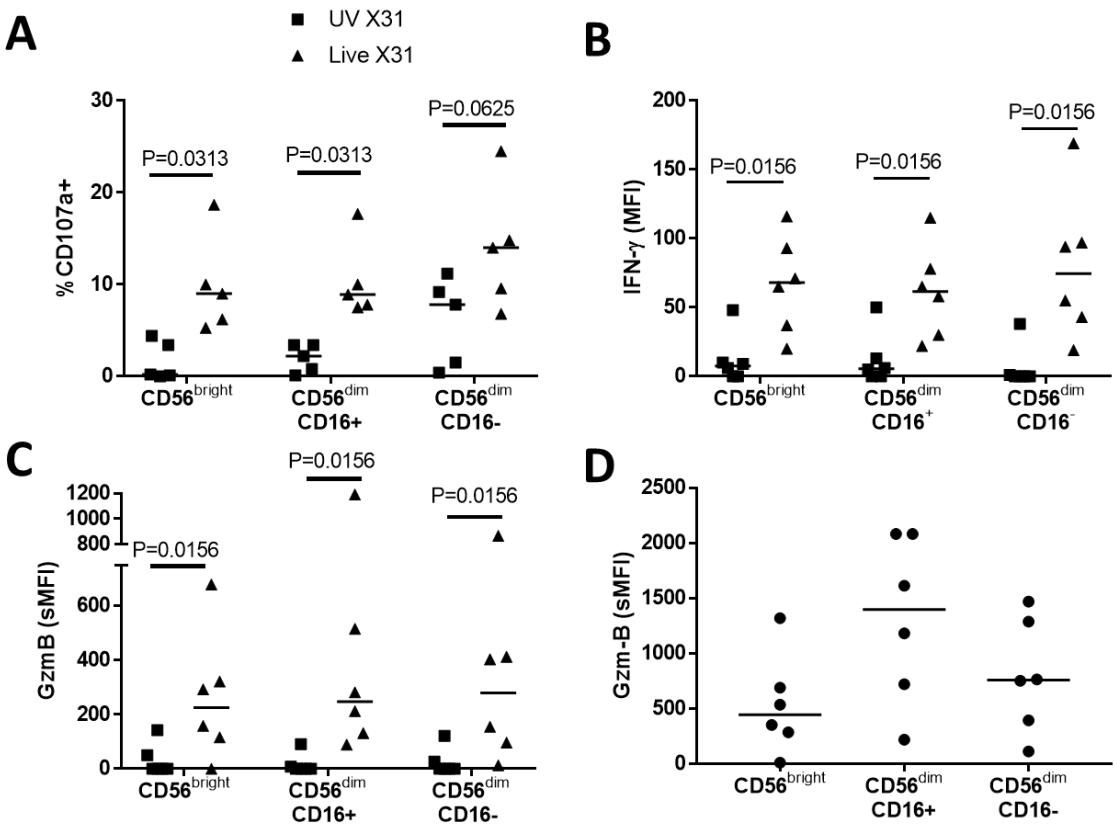

Figure 6.6: CD56^{bright} and CD56^{dim} NK cell activation to IAV infected MDMs. (**A, B**, **C**) Surface CD107a expression (**A**), IFN-γ (**B**) and Gzm-B production in NK cell subsets following 6h culture with IAV infected macrophages. Baseline non-treated values were subtracted from all data sets. Statistical analysis was performed by one-tailed Wilcoxon signed-rank test. (**D**) Baseline Gzm-B expression in NK cells cultured macrophages. Lines describe medians.

6.2.4 NK Cells are Cytotoxic towards IAV-Infected MDMs

Thus far, CD107a has been consistently upregulated by NK cells in response to IAV infection of lung tissue and macrophages (Figure 5.7 and 6.5 A). CD107a is trafficked to the cell surface during NK cell activation and is commonly used as an indirect measure of cytotoxicity [185]. Increase in both expression and release of the cytotoxic molecule, Gzm-B has also been observed in IAV-stimulated NK cells, further indicating an enhanced cytotoxic function of these cells (Figure 6.5 C and 6.6 C). However, to directly corroborate whether these changes result in increased target cell killing, macrophage viability was measured during culture with and without NK cells (Figure 6.7). MDM viability was measured by flow cytometry with an amine binding dye, with viability gates set from heat killed and unstained controls (Figure 6.7 A). This method found that MDM viability was slightly reduced (by 9%) in IAV infection (P=0.0098) but was further reduced by 14% when NK cells were present (P=0.042, Figure 6.7 B). However, NK cell culture was not found to affect MDM viability in

UV-X31 treated controls (P=0.2158 and P=0.3438 respectively, Figure 6.7 B). Therefore, these results suggest an NK cell-mediated cytotoxic effect on MDMs when they are infected with IAV.

To assess the importance of physical contact with MDMs on NK-cell mediated killing, MDM viability was also measured in the transwell system, as shown in Figure 6.7 C. For clarity, only IAV-infected MDM viability is shown. Unfortunately, the high variability in this measure make it difficult to interpret the effect of transwell co-culture on MDM viability. For instance, IAV-infected MDM viability was slightly reduced in transwell cultured compared to MDMs alone (59% viability vs 65.9% respectively, P=0.2129, Figure 6.7 C). However, it is possible that NK cell culture in transwells slightly improves the survival of infected MDMs as the median MDM viability in transwell cultures was slightly higher than in co-culture that allowed free movement of NK cells, although this was not found to be a statistically significant difference (59% vs 52.3%, P=0.2158). Thus transwell MDM viability was statistically similar to both MDMs culture alone and with NK cells, despite reduced MDM viability in the NK cell culture (P=0.042, Figure 6.7C). Thus it is not possible to conclude how the physical separation of NK cell in the transwell affected MDM viability during infection using this method.

Cellular viability was also measured by LDH activity in culture supernatants. Cytosolic LDH is released upon degradation of the plasma membrane during cell death, and as this is proportional to the number of lysed cells, thus extracellular LDH can be considered a relative measure of cell viability [517]. LDH activity was measured through the reduction of NAD+ to NADH and colorimetric change as described in section 2.10 [517]. Total cell numbers were different in cultures of MDMs alone or with NK cells (500 000 vs 600 000 respectively), therefore to control for cell number effect, LDH release was measured in NK cells cultured alone. However extracellular LDH was below detectable limits in NK cell only culture medium and therefore would make a minimal contribution to the analysis. Using this method, IAV infection was found to reduce total cell viability with increased LDH activity in IAV-infected MDM culture medium (P=0.0313, Figure 6.7 D) and the presence of NK cells did not affect culture viability in UV-X31 treated controls (P=0.4219, Figure 6.7 D). However, there was no difference in extracellular LDH when NK cells were cultured with IAV-infected MDMs relative to MDMs alone (P=0.4219, Figure 6.7 D). In addition, NK cell transwell co-culture was not found to alter MDM viability by LDH assay (P=0.2813, Figure 6.7 E). Thus different methods of measuring cell viability report different effects of NK cell on IAV-infected macrophages, making it difficult to draw conclusions from these results and requiring further investigation.

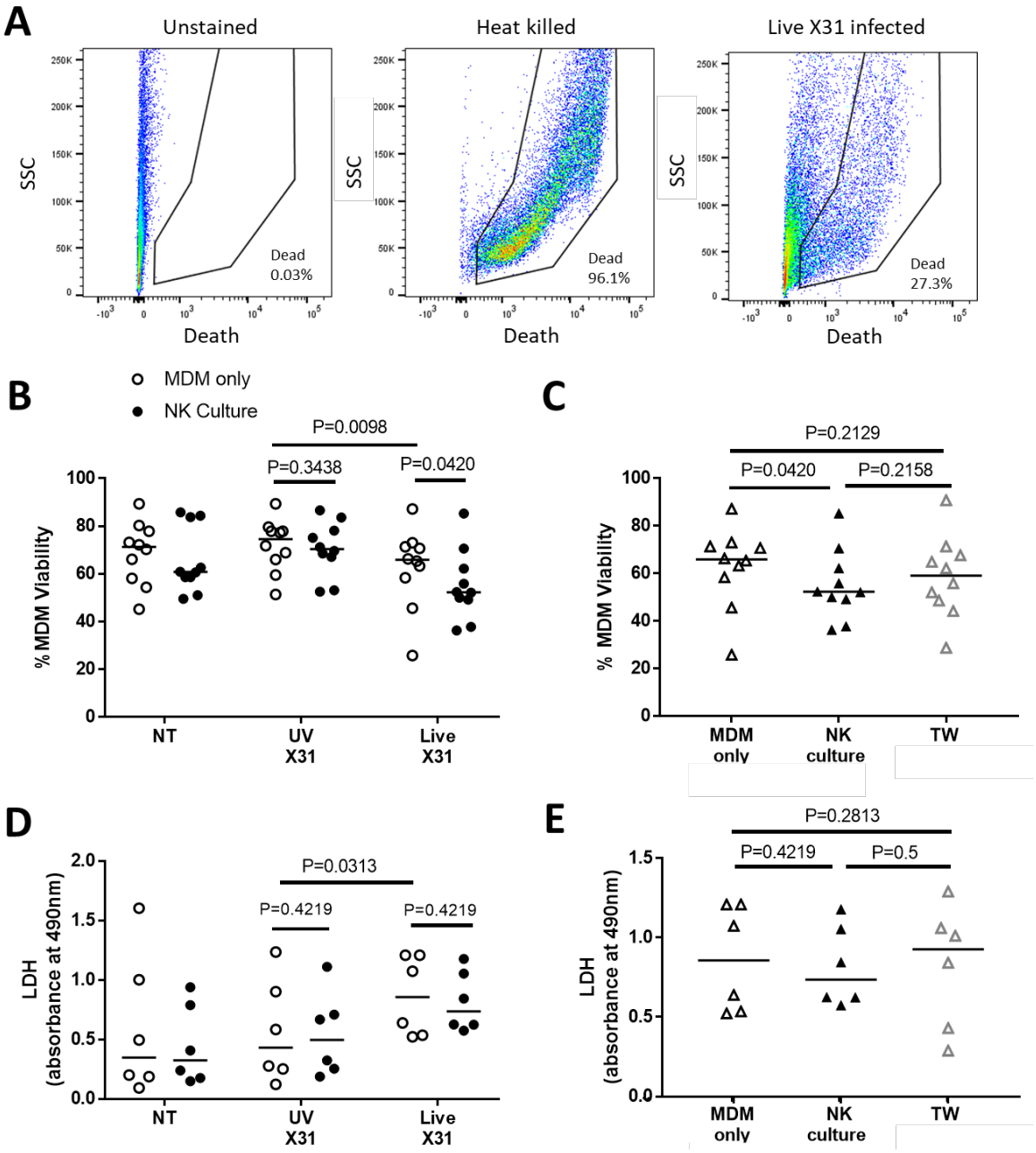

Figure 6.7: NK cell cytotoxicity towards IAV-infected macrophages. (**A, B, C**) MDM viability was measured by amine-binding dye and detected by flow cytometry. (**A**) Representative gating to determine MDM viability. Viability gates were set using heat killed and unstained controls. (**B**) MDM viability when cultured alone and with NK cells. (**C**) IAV-infected MDM viability when cultured alone, with NK cells and when physically separated from NK cells by a transwell system (TW) (N=10). (**C, D**) Cellular viability within cultures measured by extracellular LDH levels. (**D**) MDM viability when cultured alone and with NK cells. (**E**) IAV-infected MDM viability when cultured alone, with NK cells and in TW (N=6). Lines describe medians, statistical analysis by one-tailed Wilcoxon signed-rank test.

6.2.5 NK cell Activating Receptor Expression is altered by Culture with IAV-Infected Cells

Two NK cell activating receptors, NKG2D and NKp46 are thought to facilitate NK cell binding to IAV-infected cells [254, 376, 378, 379]. NKG2D binds molecules upregulated during cellular stress and NKp46 ligands has been found to bind viral HA but also binds unknown ligands on tumor cells [240, 241, 251-254, 381]. Ligands for both these receptors were found to be expressed on IAV-infected MDMs (Figure 6.2 C and D). Therefore, the expression of both these receptors was analyzed on NK cells during culture with IAV-infected MDMs (Figure 6.8). Receptor expression is presented as sMFI as NKp46 and NKG2D are constitutively expressed by NK cells [241, 249, 381].

$CD56^{bright}$ NK cells were found to express more NKG2D (P=0.0156) and NKp46 (P=0.0313) receptors than $CD56^{dim}$ NK cells (Figure 6.8 A and B), a finding consistent with the literature [267, 518]. Thus activating receptor expression was analyzed on each NK cell subset. Interestingly, NKp46 expression was increased on $CD56^{bright}$ NK cells (P=0.0156, Figure 6.8 C) during culture with IAV infected cells but unchanged on $CD56^{dim}$ subsets ($CD56^{dim}$CD16+ P=0.1484 and $CD56^{dim}$CD16- P=0.0781, Figure 6.8 D and E). In contrast NKG2D expression was reduced on $CD56^{bright}$ NK cells after IAV-infected co-cultures with a slight increase in NKG2D expression on $CD56^{dim}$CD16+ NK cells (P=0.0313 for both, Figure 6.8 F and G). No difference in NKG2D expression was found on $CD56^{dim}$CD16- NK cells (P=0.1094, Figure 6.8 H). Taken together these results show small changes to IAV-binding activating receptor expression when exposed to IAV infection, indicating that receptors may be involved in the NK cell response to IAV infected cells. However, the mechanism governing these changes and their physiological relevance remain to be understood.

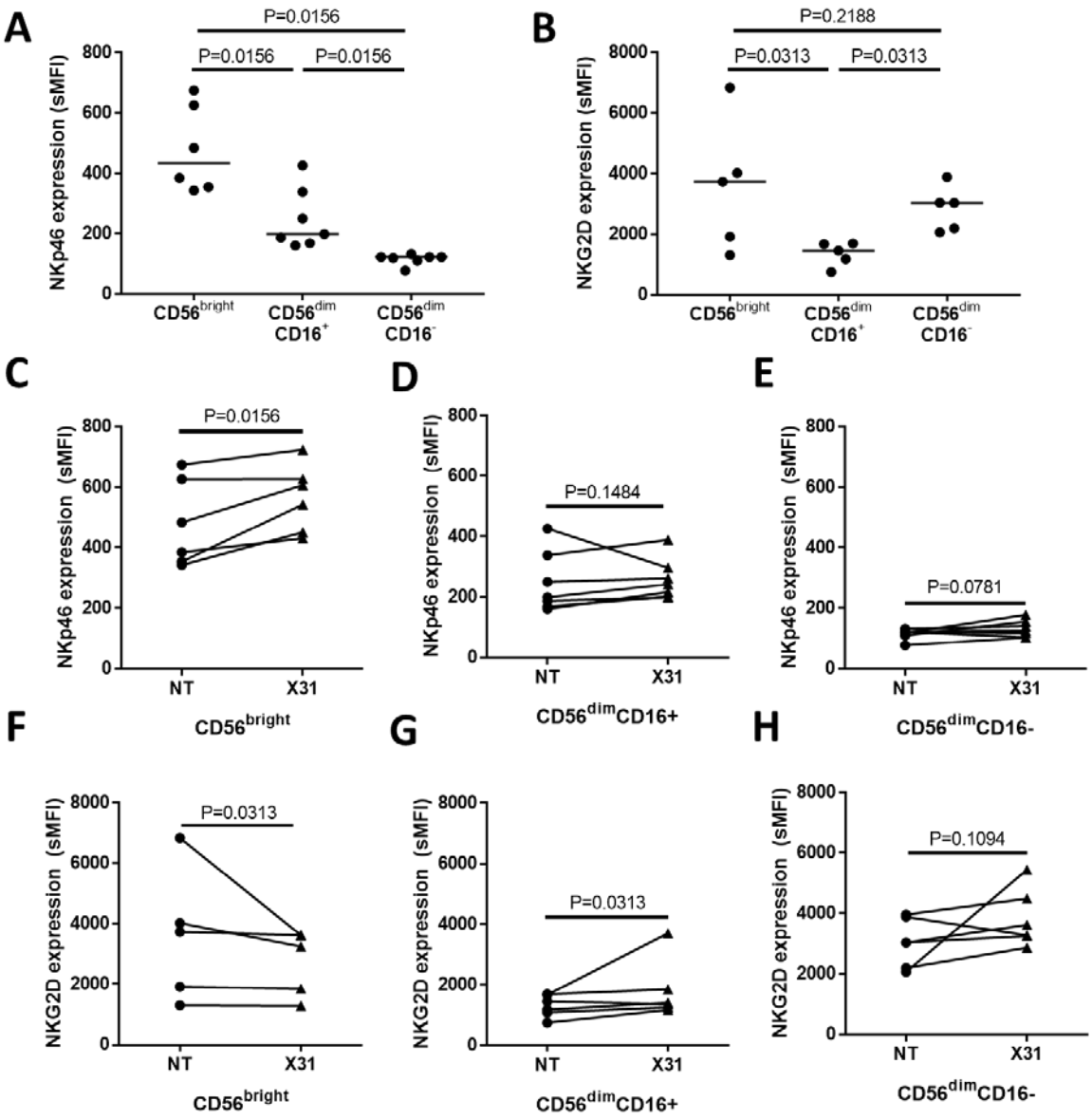

Figure 6.8: **Activating receptor expression on NK cell surfaces following culture with IAV-infected MDMs.** (**A, B**) Baseline NK cell subset expression of NKp46 (N=6) (**A**) and NKG2D (N=5) (**B**). Lines show medians. (**C, D, E**) NKp46 expression on CD56^{bright} (**C**), CD56^{dim}CD16+ (**D**) and CD56^{dim}CD16- (**E**) NK cells following culture with uninfected (NT) or X31-infected MDMs (X31). (**F, G, H**) NKG2D expression on CD56^{bright} (**F**), CD56^{dim}CD16+ (**G**) and CD56^{dim}CD16- (**H**) NK cells following culture with NT or X31-infected MDMs. Lines denote individuals, statistical analysis by two-tailed Wilcoxon signed-rank test.

6.2.6 NKG2D and NKp46 Signaling does not affect NK cell Activation to IAV-Infected MDMs

To further investigate the role of NKp46 and NKG2D in controlling NK cell activation to IAV infected cells the ligation of these receptors were blocked in IAV-infected co-cultures. Both NKG2D and NKp46 provide activating signals to NK cells, breaking NK cell inhibition, therefore blocking ligation of these receptors is expected to reduce NK cell activation to IAV-infected cells [199, 200]. As both of these receptors can recognize a number of different ligands, some of which are unknown, chimeric receptor constructs were used to block all receptor binding molecules [240, 241, 251-254, 381]. These protein chimeras consisted of the ligand binding region of either NKG2D or NKp46 bound to the constant region of human antibodies. To determine the concentration of receptor constructs required to saturate MDM ligands, the receptor constructs were first titrated against X31-infected MDMs, with construct binding detected by flow cytometry (Figure 6.9 A and B). NKG2D and NKp46 fusion constructs were found to saturate X31-infected cells even at low concentrations. However, to be certain of ligand blocking the highest concentration 10 µg/mL of NKG2D and 5µg/mL of NKp46 was used to block MDM surfaces.

To block receptor ligands, MDMs were incubated with the fusion constructs at 37°C, 5% CO_2, for 20 min prior to culture with NK cells. NK cell activation was measured by flow cytometry and off-target effects of the fusion constructs (Fc) were excluded by the use of a non-binding Fc construct control. The non-binding Fc was not found to differentially affect NK cell expression of CD107a or IFN-γ production (P=0.4063, Figure 6.9 G and H). In addition, the addition of receptor constructs was not found to affect NK cell activation in unstimulated co-cultures (Figure 6.9 I and J). MDMs were blocked with either NKp46 or NKG2D or both receptor Fc as shown in Figure 6.9. For clarity, blocking is only shown in IAV-infected co-cultures for Figures 6.9 C - H. NK cell surface CD107a was not altered by blockade of NKG2D of NKp46 ligands on IAV-infected MDM surfaces (P=0.3711 and P=0.4688 respectively, Figure 6.9 C and E). NK cell IFN-γ production was also found to be consistent between cultures blocked with NKG2D and NKp46 receptor constructs and controls (P=0.3438 and P=0.5, Figure 6.9 D and F). Furthermore, combination of NKG2D and NKp46 ligand blockade did not affect NK cell activation to IAV-infected macrophages (CD107a; P=0.1563, IFN-γ P=0.4063, Figure 6.9 G and H). Thus it appears that neither NKG2D nor NKp46 were essential to NK cell activation to IAV infected MDMs.

As described in Figure 6.8, $CD56^{bright}$ and $CD56^{dim}$ NK cells express different levels of NKG2D and NKp46 receptors [267, 518]. Therefore, the effect of blocking was analyzed individually on

$CD56^{bright}$, $CD56^{dim}$CD16+ and $CD56^{dim}$CD16- NK cells with surface CD107a reported in Figure 6.10 and intracellular IFN-γ production present in Figure 6.11. However, this analysis did not show any differences in either CD107a or IFN-γ upregulation in any of the NK cell subsets as a result of NKG2D and NKp46 ligand blocking.

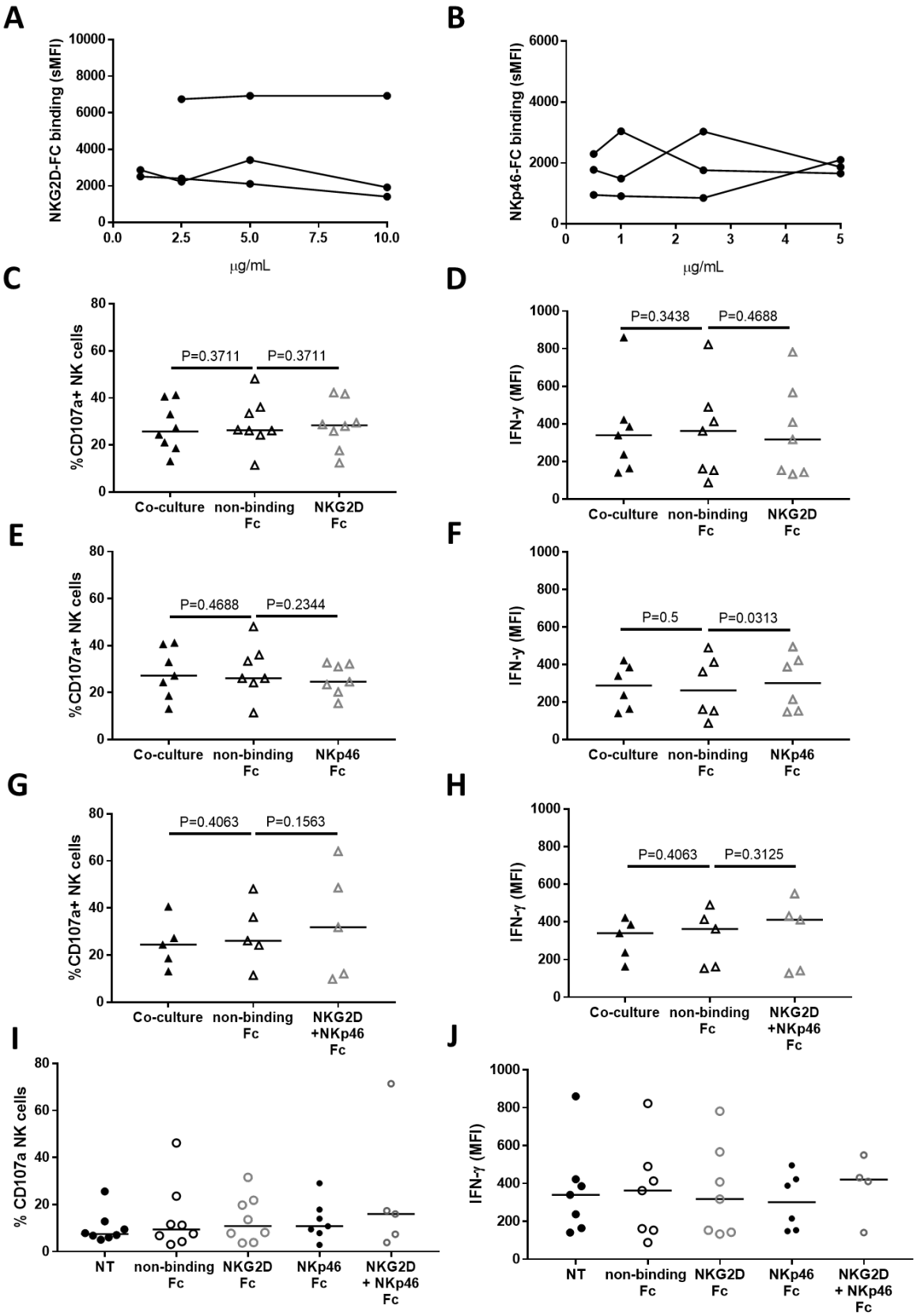
A
NKG2D-FC binding (sMFI)
μg/mL
B
NKp46-FC binding (sMFI)
μg/mL
C
%CD107a+ NK cells
P=0.3711
P=0.3711
Co-culture
non-binding Fc
NKG2D Fc
D
IFN-γ (MFI)
P=0.3438
P=0.4688
Co-culture
non-binding Fc
NKG2D Fc
E
%CD107a+ NK cells
P=0.4688
P=0.2344
Co-culture
non-binding Fc
NKp46 Fc
F
IFN-γ (MFI)
P=0.5
P=0.0313
Co-culture
non-binding Fc
NKp46 Fc
G
%CD107a+ NK cells
P=0.4063
P=0.1563
Co-culture
non-binding Fc
NKG2D +NKp46 Fc
H
IFN-γ (MFI)
P=0.4063
P=0.3125
Co-culture
non-binding Fc
NKG2D +NKp46 Fc
I
% CD107a NK cells
NT
non-binding Fc
NKG2D Fc
NKp46 Fc
NKG2D + NKp46 Fc
J
IFN-γ (MFI)
NT
non-binding Fc
NKG2D Fc
NKp46 Fc
NKG2D + NKp46 Fc

Figure 6.9: Blocking macrophage ligands for NK cell activating receptors NKG2D and NKp46 with receptor-Ig fusion constructs (Fc) during IAV-infected co-cultures. (**A, B**) Titration of NKG2D and NKp46 Fc constructs on X31-infected MDMs as detected by flow cytometry. (**C, D, E, F, G, H, I, J**) NK cell surface CD107a (**C, E, G, I**) expression and intracellular IFN-γ (**D, F, H, J**) production in X31-infected cultures. (**C, D**) MDMs were blocked with NKG2D Fc or non-binding Fc constructs 20min prior to NK cell culture and NK cell activation measured by flow cytometry. (**E, F**) MDMs were blocked with NKp46 Fc or non-binding Fc. (**G, H**) MDMs were blocked with both NKp46 and NKG2D Fc or non-binding Fc (**I, J**) Baseline NK cell surface CD107a and IFN-γ when in culture with resting (non-infected) MDMs treated with Fc constructs. Lines describe medians. Statistical analysis by one-tailed Wilcoxon signed-rank test.

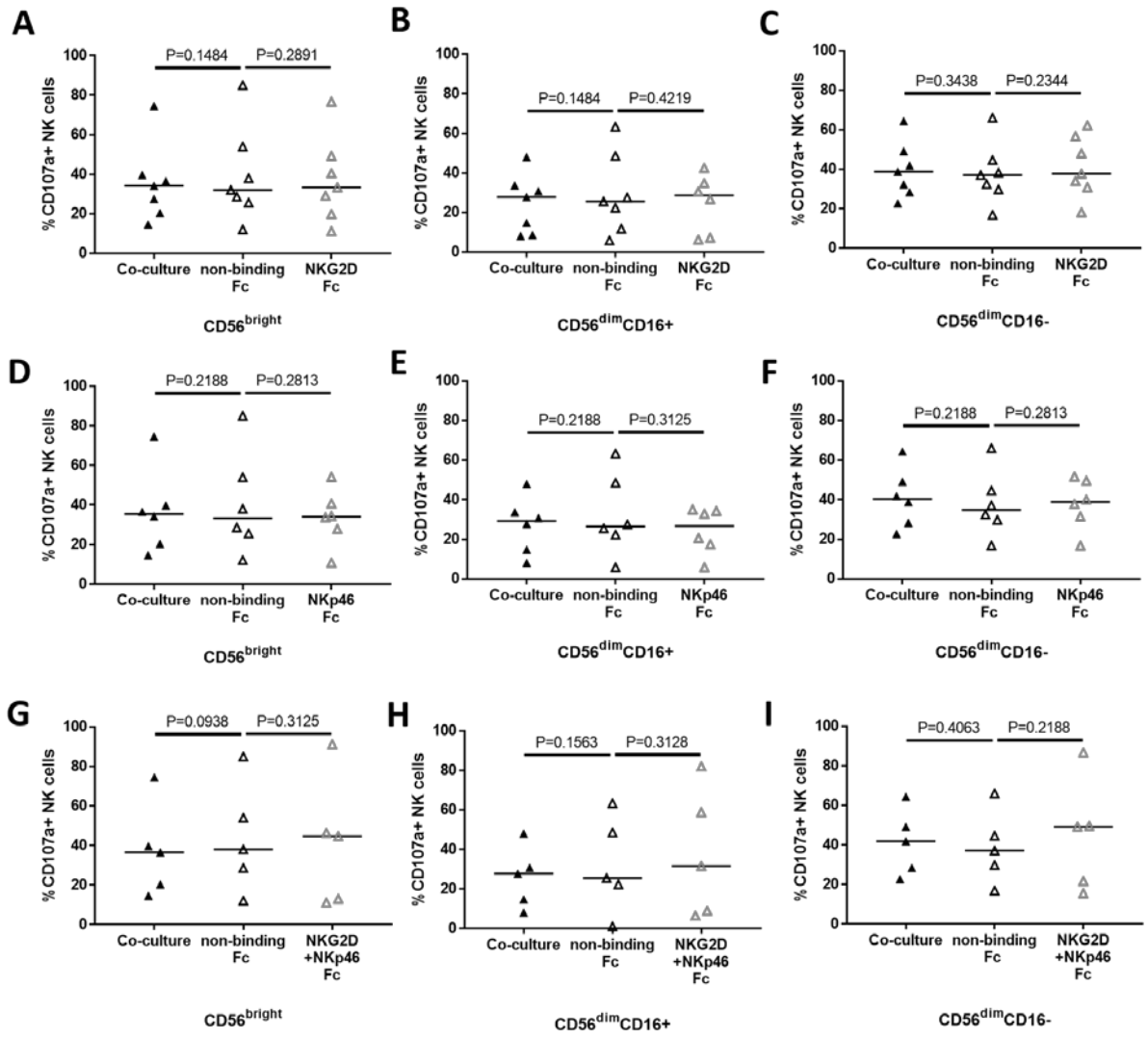

Figure 6.10: NK cell subset CD107a expression following blocking of NKG2D and NKp46 ligands on IAV-infected MDMs. MDMs were blocked with Fc constructs for 20 min prior to NK cell culture. NK cell activation was measured by change in surface CD107a. For clarity only IAV infected co-cultures are shown. **(A, B, C**) CD56^{bright} (**A**), CD56^{dim}CD16+ (**B**) and CD56^{dim}CD16- (**C**) activation following blocking of NKG2D ligands. **(D, E, F**) CD56^{bright} (**D**), CD56^{dim}CD16+ (**E**) and CD56^{dim}CD16- (**F**) activation following blocking of NKp46 ligands. **(G, H, I**) CD56^{bright} (**G**), CD56^{dim}CD16+ (**H**) and CD56^{dim}CD16- (**I**) activation following blocking of both NKG2D and NKp46 ligands. Lines describe medians. Statistical analysis by one-tailed Wilcoxon signed-rank test.

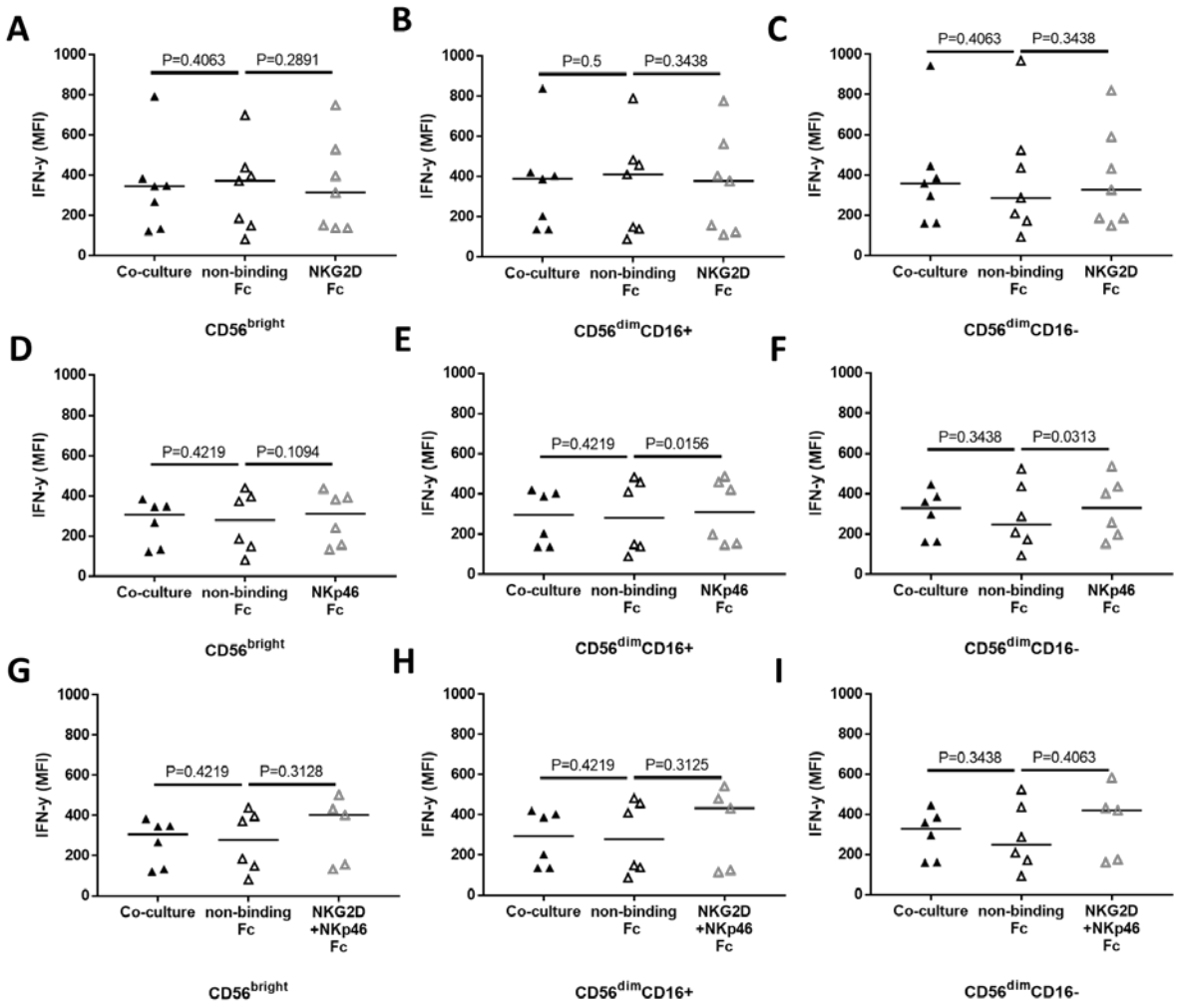

Figure 6.11: NK cell subset IFN-γ production following blocking of NKG2D and NKp46 ligands of IAV-infected MDMs. MDMs were blocked with Fc constructs 20 min prior to NK cell culture. NK cell activation was measured by change in intracellular IFN-γ. IAV infected co-cultures are shown. **(A, B, C)** $CD56^{bright}$ (**A**), $CD56^{dim}CD16+$ (**B**) and $CD56^{dim}CD16-$ (**C**) activation following blocking of NKG2D ligands. **(D, E, F)** $CD56^{bright}$ (**D**), $CD56^{dim}CD16+$ (**E**) and $CD56^{dim}CD16-$ (**F**) activation following blocking of NKp46 ligands. **(G, H, I)** $CD56^{bright}$ (**G**), $CD56^{dim}CD16+$ (**H**) and $CD56^{dim}CD16-$ (**I**) activation following blocking of both NKG2D and NKp46 ligands. Lines describe medians. Statistical analysis by Wilcoxon signed-rank test.

6.2.7 Inhibiting NK Cell Contact with HLA class I during IAV Infection Increases NK cell Activation

NK cell recognition of class I HLA molecules, and in particular HLA-C have important roles in controlling NK cell activation [199, 200]. NK cells are strongly inhibited by contacts with HLA on neighboring cell surfaces and release of this inhibition is required for NK cell activation, as described in section 1.2.1 [199, 200]. Interestingly, IAV-mediated HLA class I upregulation has been shown to inhibit NK cells in a mouse model of infection [227]. In this work, upregulated HLA class I molecules were confirmed on human airway macrophages, epithelia and MDMs following IAV infection (Figures 5.3 A and 6.2 B). To investigate whether IAV-mediated HLA upregulation is inhibiting NK cell function, class I HLA on MDM surfaces were blocked with a pan HLA-A/B/C antibody for 20 min prior to culture with NK cells. NK cell activation was then measured through the expression of surface CD107a and intracellular IFN-γ as shown in Figure 6.12.

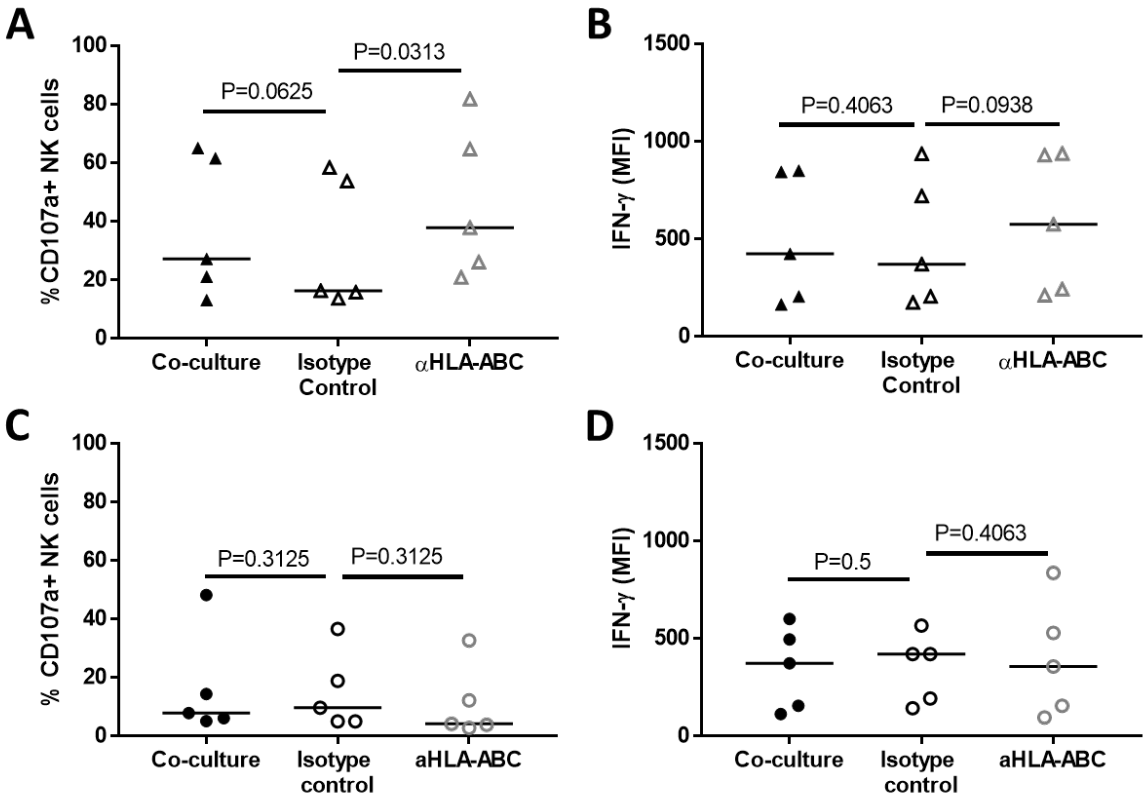

Figure 6.12: Blocking macrophage HLA class I during IAV infected co-cultures. (**A, B**) NK cell surface CD107a expression (**A**) and intracellular IFN-γ (**B**) production in X31-infected cultures. MDMs were blocked with αHLA-ABC or an isotype control antibody 20 min prior to culture with autologous NK cells. For clarity only live-X31 infected MDM-NK cell co-cultures are shown. (**C, D**) Baseline expression of NK cell surface CD107a and intracellular IFN-γ expression when cultured with non-infected MDMs treated with αHLA-ABC or isotype control. Statistical analysis by one-tailed Wilcoxon signed-rank test, lines describe medians.

NK cell activation in αHLA-ABC blocked co-cultures was compared to an isotype control antibody to control for non-specific effects of adding antibody to the co-cultures. Incubation of IAV-infected macrophages with the isotype control antibody was not found to affect NK cell activation relative to untreated co-cultures (CD107a; P=0.0625, IFN-γ; P=0.4063, Figure 6.12 A and B). In contrast prior incubation of macrophages with αHLA-A/B/C was found to stimulate a further two-fold increase in NK cell surface CD107a during culture with IAV-infected macrophages (P=0.0313, Figure 6.12 A). Inhibiting NK cell ligation with class I HLA increased surface CD107a in both $CD56^{bright}$ and $CD56^{dim}$CD16+ subsets (P=0.0313 for both, Figure 6.13 A and B). However, $CD56^{dim}$CD16- NK cells were unaffected by this treatment (P=0.1563, Figure 6.13 C). Interestingly a HLA class I effect was not found on NK cell IFN-γ production following contact with IAV-infected MDMs (Isotype control; 370 MFI vs αHLA-A/B/C 575 P=0.0938, Figure 6.12 B). This finding was consistent across $CD56^{bright}$ and $CD56^{dim}$ subsets ($CD56^{bright}$; P=0.0938, $CD56^{dim}$CD16+ P=0.1563 and $CD56^{dim}$CD16-; P=0.4378, Figure 6.13 D, E and F).

One mechanism by which NK cells become cytotoxic towards target cells is by ADCC [519]. Whereby antibody binding to target cells stimulates NK cell cytotoxicity through Fc binding receptors such as CD16 [519]. However, we can exclude ADCC from these experiments as incubation of αHLA-A/B/C with uninfected MDMs did not stimulate NK cell activation, thus binding of this antibody to MDM surfaces has not increased the antigenicity of these cells for NK cells (CD107a; P=0.3125 and IFN-γ; P=0.4063, Figure 6.12 C and D). 98.7% of uninfected (NT) MDMs express class I HLA molecules NT macrophages and would therefore still have been labelled by αHLA-A/B/C. Taken together these results demonstrate that during IAV infection the gross effect of MDM HLA class I is inhibitory to NK cell function, affecting both $CD56^{bright}$ and $CD56^{dim}$ NK cell CD107a expression. Interestingly IFN-γ production may be regulated by different mechanisms as NK cell intracellular IFN-γ was unaffected by a disrupted HLA class I signaling to the NK cell.

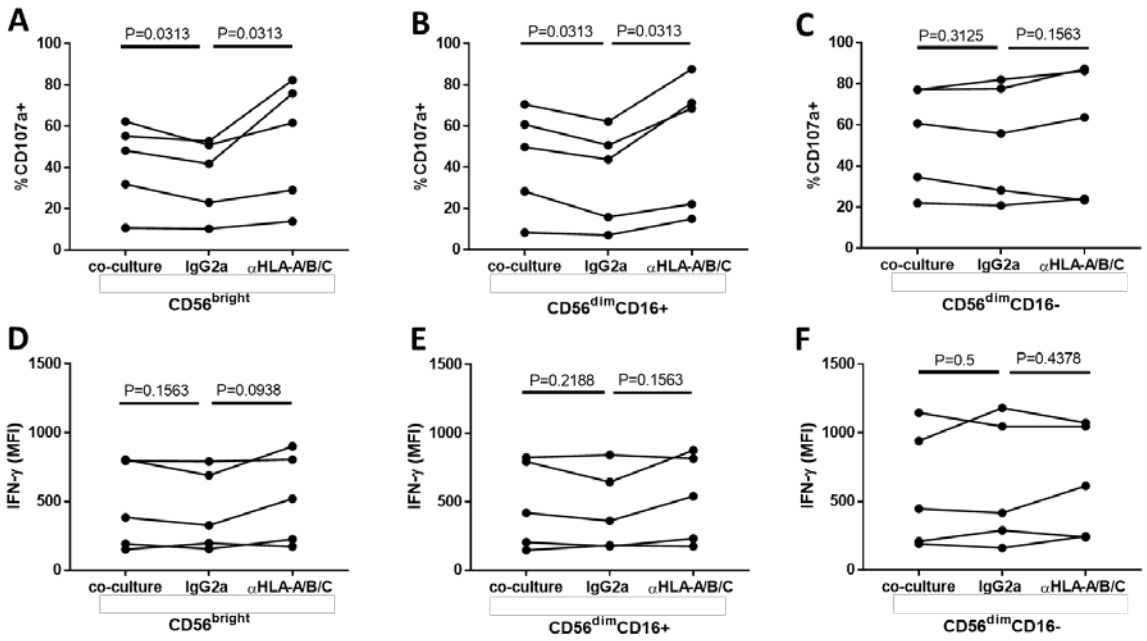

Figure 6.13: NK cell subset activation when HLA class I was blocked on IAV-infected MDM surfaces. MDMs were blocked with αHLA-ABC or an isotype control antibody 20min prior to culture with autologous NK cells. For clarity only X31-infected MDMs are shown. (**A, B, C**) NK cell surface CD107a expression on $CD56^{bright}$ (**A**), $CD56^{dim}CD16+$ (**B**) and $CD56^{dim}CD16-$ (**C**) NK cells. (**C, D, E**) NK cell IFN-γ production by $CD56^{bright}$, $CD56^{dim}CD16+$ and $CD56^{dim}CD16-$ NK cells. Statistical analysis by Wilcoxon-signed rank test. Lines denote individuals.

6.2.8 MDM – NK Cell Crosstalk is Altered by IAV Infection

IFN-γ is the archetypal cytokine secreted by NK cells during infection and disease but NK cells also secrete a wide range of cytokines depending on inflammatory context [197, 520, 521]. With the exception of IFN-γ, the cytokine profile of NK cells responding to IAV infection is unknown. To investigate this, the production of 28 cytokines, chemokines and other NK effector molecules were measured in culture mediums of IAV-infected MDMs alone and with NK cells. Uninfected controls including unstimulated MDMs and UV-X31 treated MDMs were also included. Molecules from the interleukin family and TNF-α are presented in Figure 6.14, chemokines in Figure 6.15 and Matrix Metalloproteinase-1 (MMP-1) and differentiation factors in Figure 6.16. This data is summarized in Table 6.1. MDMs were infected with X31 for 24 h, prior to replacement of culture media and NK cell co-culture for a further 6h. Culture supernatants were stored at -80°C until analysis by 23-plex ELISA, as described in section 2.11.

Molecule	Concentration in resting MDM culture (pg/mL)	Fold change in MDM release during IAV infection	Fold change in uninfected MDMs vs uninfected NK cell co-culture	Fold change in IAV-infected MDMs vs NK cell co-culture
IFN-β	1.1	1.6X Increase *(P=0.1922)*	N	N *(P>0.9999)*
IL-1α	3.28	7.9X Increase *(P=0.0061)*	N	N *(P>0.9999)*
IL-1β	1.48	4X Increase *(P=0.0079)*	N	N *(P>0.9999)*
IL-6	0.87	12.4X Increase *(P=0.0164)*	N	2.8X Increase *(P=0.6511)*
IL-8	479.6	N *(P=0.3846)*	N	N *(P>0.9999)*
IL-10	0.73	6X Increase *(P=0.0012)*	N	N *(P>0.9999)*
IL12p70	22.55	2.2X Increase *(P=0.0164)*	N	N *(P>0.9999)*
IL-15	0.64	7X Increase *(P=0.0101)*	N	N *(P>0.9999)*
IL-16	12.59	2.5X Increase *(P=0.1922)*	3.6X Increase	1.6X Increase *(P=0.1346)*
IL-17 A	1.27	N *(P=0.0758)*	N	N *(P>0.9999)*
IL-17 E	66.11	2.2X Increase *(P=0.0923)*	N	N *(P>0.9999)*
IL-18	5.52	2X Increase *(P=0.0061)*	N	N *(P>0.9999)*
IL-22	42.38	1.9X Increase *(P=0.0030)*	N	N *(P>0.9999)*
TNF-α	2.59	9.7X Increase *(P=0.0021)*	N	1.6X Increase *(P>0.9999)*
CXCL1	68.9	2.5X Increase *(P=0.0122)*	N	N *(P>0.9999)*
CCL2	510.8	5.2X Increase *(P=0.0923)*	N	1.8X Increase *(P=0.6511)*
CCL5	19.44	27X Increase *(P=0.0021)*	N	N *(P>0.9999)*
CCL7	901.2	11.2X Increase *(P=0.0156)*	N	Unknown
CCL22	1747	3.9X Decrease *(P=0.0164)*	N	N *(P=0.6511)*
XCL1	24.9	N *(P=0.4280)*	N	N *(P=0.4947)*
MMP1	112.1	2.5X Increase *(P=0.0261)*	N	N *(P>0.9999)*
GM-CSF	13.32	8.5X Increase *(P=0.0012)*	2.2X Increase	N *(P>0.9999)*
LIF	155	N *(P=0.9476)*	N	N *(P=0.7415)*

Table 6.1: Summary of extracellular molecule release from MDMs alone and in co-culture with NK cells. Statistical analysis by Friedman's test with Dunn's multiple comparison, P-values are shown italicized and in brackets. N = none, or a fold change less than 1.

At rest MDMs were found to express many different cytokines, some of which were detected at high concentrations, including IL-8, IL-17E and IL-22 (479.2pg/mL, 66.11 pg/mL and 42.38 pg/mL respectively, Figure 6.14 E, K and M). Low levels of IL-12 and IL-16 were also released from uninfected MDMs (23 pg/mL and 12.59 pg/mL, Figure G and I respectively) as were numerous chemokines, including CXCL1, CCL22, XCL1 (68.9 pg/mL, 1747 pg/mL and 24.9 pg/mL Figure 6.15 A, E, F). In addition, both Leukaemia Inhibitory factor (LIF) and MMP1 were found to be secreted by resting MDMs (155 and 112.1 pg/mL respectively, Figure 6.16 A and C). A small basal expression below 10 pg/mL was detected for many of the other molecules analyzed, as summarized in Table 6.1.

Substantial pro-inflammatory cytokine release was detected from MDM following infection with live X31 virus (Table 6.1). Notable increases included IL-1α (P=0.061, Figure 6.14 B), IL-17E (P=0.0923, Figure 6.14 K), IL-22 (P=0.0030, Figure 6.14 M) and TNF-α (P=0.0021, Figure 6.14 N). However, IL-6, IL-10, IL-16, IL-17 A and TNF-α were also all found to be secreted by IAV-infected MDMs (summarised in Table 6.1 and Figure 6.14). Furthermore, key NK cell stimulating cytokines IL-12, IL-15 and IL-18 were upregulated by IAV-infected MDMs (P=0.0164, P=0.0101 and P=0.0061 respectively, Figure 6.14 G, H and L). In contrast neither IFN-β, IL-8, IL-16, IL-17A or IL-17E secretion were significantly altered by IAV infection at this time point (Table 6.1).

IAV-infected macrophages also possessed a significantly different chemokine expression profile, with increases in CXCL1, CCL5 and CCL7 release (P=0.0122, P=0.0021 and P=0.0156, Figure 6.15 A, C and D). Interestingly, macrophage production of CCL22 was reduced in IAV-infected culture supernatants (P=0.0164, Figure 6.15 E). However, CCL2 and XCL1 production were unaffected by infection (P=0.0923 and P=0.4280 respectively, Figure 6.15 B and F). Unfortunately, CCL7 was outside the maximum range of detection in IAV-infected co-cultures in three individuals and thus it was not possible to draw conclusions about how NK cell culture affected the production of this chemokine (Figure 6.15 D). In addition, high concentrations of both MMP1 and the growth factor LIF were found in resting MDM cultures, but only MMP1 was found to be increased following IAV infection (P=0.0261 and P=0.9476 respectively, Figure 6.16 A and C). Finally, a significant rise in GM-CSF was also found post-IAV infection (P=0.0012, Figure 6.16 B).

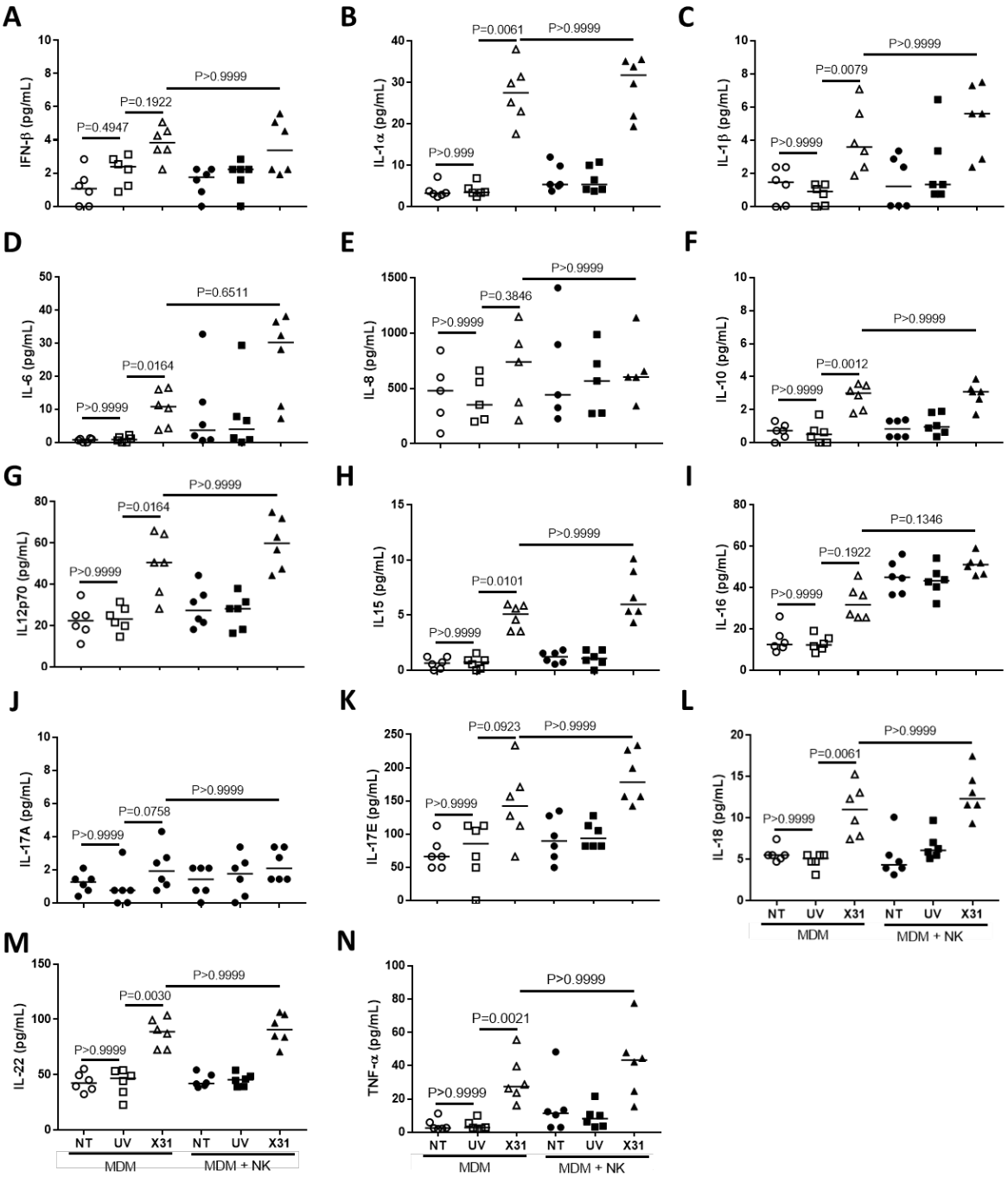

Figure 6.14: Cytokine expression in NK-MDM co-culture supernatants. MDMs infected with X31 IAV for 24h were cultured with or without NK cells for a further 6 h. Culture supernatants were harvested and analyzed by Luminex, N=6. Statistical analysis by Friedman's test with Dunn's multiple comparison correction, lines describe medians.

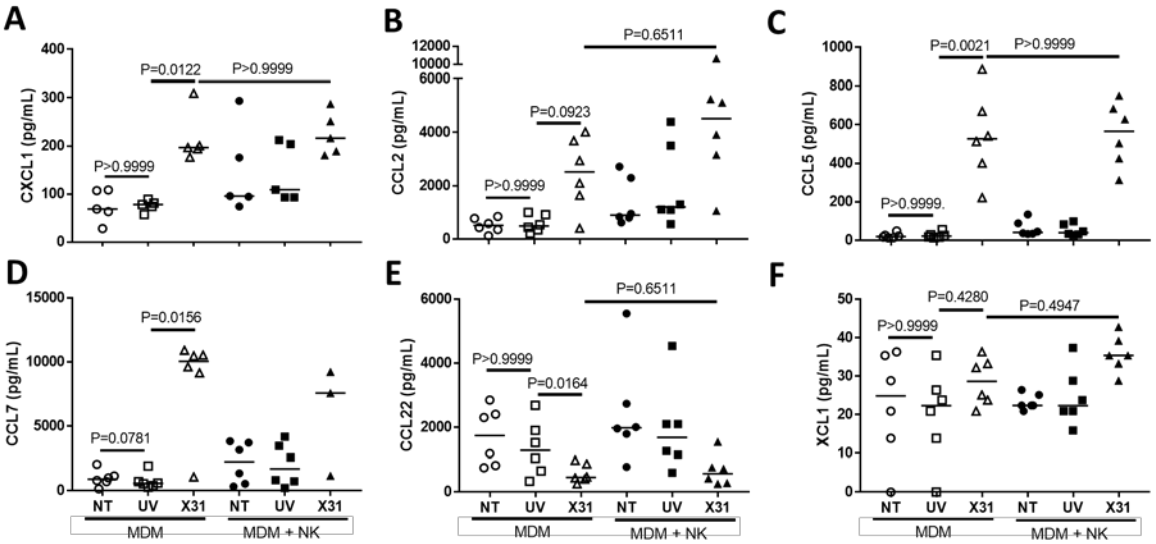

Figure 6.15: Chemokines in co-culture supernatants. MDMs infected with X31 IAV for 24h were cultured with or without NK cells for a further 6 h. Culture supernatants were harvested and analyzed by Luminex. Statistical analysis by Friedman's test with Dunn's multiple comparison correction except CCL7 expression which was analyzed by Wilcoxon signed-rank test. N=6, except CCL22 (**E**) N=5. Lines describe medians.

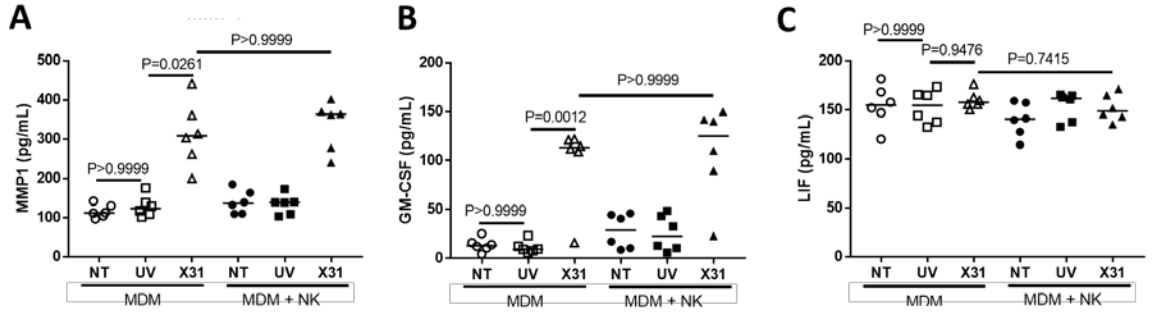

Figure 6.16: **Extracellular signaling molecules in co-culture supernatants.** MDMs infected with X31 IAV for 24h were cultured with or without NK cells for a further 6 h. Culture supernatants were harvested and analyzed by Luminex, N=6. Lines describe medians. Statistical analysis by Friedman's test with Dunn's multiple comparison correction.

To assess NK cell cytokine production during IAV infection, NK-MDM co-cultures were compared to MDM cultures alone. Unfortunately, due to high inter-donor variability and small sample size there were no statistically significant differences in cytokine secretion when NK cells were present. However, there was a three-fold increase in the median amount of extracellular IL-6 (P=0.6511, Figure 6.14 D) and a two-fold increase in CCL2 (P=0.6511, Figure 6.15 B). Furthermore, a smaller 1.5-fold increase was identified in both TNF-α and IL-16 secretion following NK cell culture (P>0.9999 and P=0.134 respectively, Figure 6.14 N and I). IL-16 was also found to be increased in uninfected co-cultures, indicating that basal expression of this cytokine may be altered simply by the presence of NK cells (NT MDM alone; 12.59 pg/mL vs NT MDM+NK; 45 pg/mL, Figure 6.14 I). There was also a slight (two-fold) rise in basal GM-CSF during NK cell culture but this was not found to be differentially expressed during IAV infected co-cultures compared to MDMs alone (P>0.9999, Figure 6.16 B).

To corroborate the findings in Figure 6.5 E and to act as an external control for the Luminex experiments, Gzm-B expression was also analysed. Gzm-B is primarily expressed by $CD56^{dim}$ NK cells (Figure 6.6 D) whereas $CD56^{bright}$ NK cells express more Gzm-A [189, 304, 516]. Therefore, the secretion of both these granzyme molecules was assessed. As MDMs do not express granzyme molecules (Figure 6.17) the effect of live-IAV infection on NK cell co-cultures was compared to uninfected UV-X31 treated co-cultures and is summarized in Table 6.2. Like the ELISA data presented in Figure 6.6 D luminex analysis reported a trend towards increased Gzm-B secretion by NK cells but did not reach statistical significance (P=0.0625, Figure 6.17B, N=5). One individual was excluded from the Gzm-B analysis due to anomalous values. Interestingly extracellular Gzm-A, was found to be slightly reduced (1.3 fold) in IAV-infected co-cultures, although this did not reach significance (UV-X31; 1174 pg/mL, live-X31; 902 pg/mL P=0.1094 Figure 6.17 B).

Molecule	Concentration in resting MDM culture (pg/mL)	Fold change in MDM release during IAV infection	Concentration during uninfected co-culture with NK cells (pg/mL)	Fold change in uninfected vs IAV-infected co-culture
Gzm-A	16.17	N *(0.9476)*	1422 (88X increase relative to MDMs alone)	1.3X Decrease *(P>0.9999)*
Gzm-B	9.63	3.4X Increase *(0.5289)*	195.8 (20X increase relative to MDMs alone)	9.4X Increase *(P=0.9315)*

Table 6.2: Summary of Gzm-A and Gzm-B release in MDM-NK cell co-cultures. Statistical analysis by Friedman's test with Dunn's multiple comparison, P-values are shown in italicized and in brackets. N = none, or a fold change less than 1

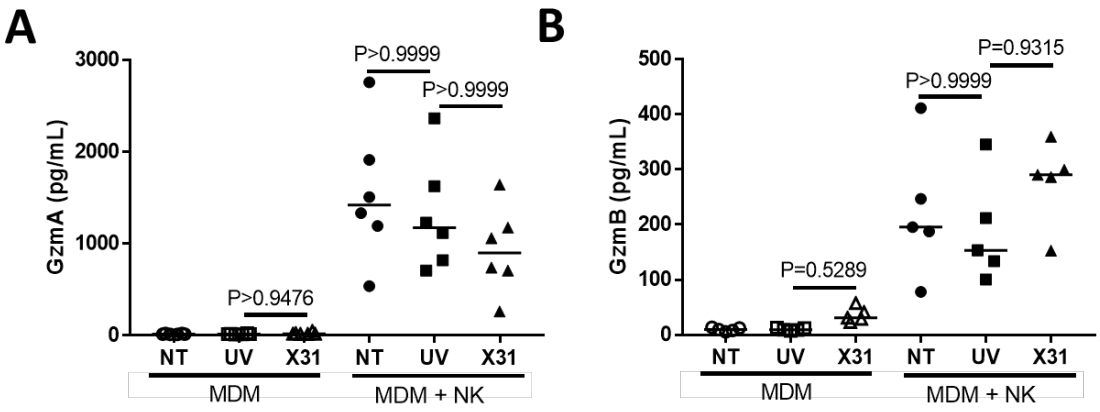

Figure 6.17: NK cell effector molecules in co-culture supernatants. MDMs infected with X31 IAV for 24h were cultured with or without NK cells for a further 6 h. Culture supernatants were harvested and analyzed by Luminex. Statistical analysis by Friedman's test with Dunn's multiple comparison. (**A**) Gzm-A N=6 (**B**) Gzm-B N=5. Lines describe medians.

6.2.9 IAV Infected Lung Epithelia activate Autologous NK Cells

The majority of this chapter has explored the relationship between macrophages and NK cells during an IAV infection, as macrophages play an important role in regulating NK cells and in the initial anti-IAV pro-inflammatory signaling [105, 364-366, 512]. However, *in vivo* the majority of IAV-infected cells are epithelia [118, 490]. In IAV-infected lung explants NK cells were found to strongly respond to IAV infection but it was not possible to directly identify the cells they were responding to (as discussed in section 5.2.4). To confirm epithelial-mediated activation of NK cells in IAV infection, lung epithelial cells were grown out of bronchial brushings taken from healthy controls (MICA II REC 15/SC/0528) and cultured with autologous blood NK cells, as shown in Figure 6.1 B. Submerged cultures of primary bronchial epithelial cells (PBEC) were infected with X31 H3N2 IAV as described in section 2.5.

X31 virus was initially titrated in PBEC cultures to reproduce a level of infection similar to the MDM model (Figure 6.18 A). Following 24 h infection with 57, 000 IU of the 2017 stock of X31, 35% of the PBEC monolayer were infected with IAV, as detected by intracellular NP-1 (N=4, Figure 6.18 B). PBEC viability was slightly reduced by viral infection, falling from 92.4% viable cells in UV-X31 treated monolayers to 86.8% in live-IAV infection (N=4, Figure 6.18 B). However, PBEC viability was still high enough for use in a co-culture model. Following expansion and infection of PBEC cultures, PBMCs previously isolated from the same donors were thawed and NK cells isolated by negative selection MACS, as described in section 2.6. Autologous NK cells were then cultured with PBECS infected with live-X31, or uninfected UV-X31 treated or non-treated controls. Two E:T ratios were tested in this co-culture system, however NK cell IFN-γ production was only detected at an E:T of 1:10, lower than that seen for culture with macrophages (N=3, Figure 6.18 D). Interestingly background NK cell CD107a was much higher in non-treated PBEC co-cultures compared to MDMs (PBEC; 28.6% vs MDM; 5.1%) indicating that resting autologous PBECs were stimulating some NK cell activation. At an E:T of 1:10 NK cell CD107a and IFN-γ expression were both increased when PBECs were infected with IAV (N=3, Figure 6.18 E and F). Surface CD107a was increased on 24.6% of NK cells in IAV-infected co-cultures relative to UV-X31 treated co-culture and IFN-γ MFI increased three-fold. Intracellular Gzm-B was also measured in NK cells but no difference in expression was detected during IAV-infected cultures (Figure 6.18 G). Thus these results demonstrate potent NK cell activity towards both IAV-infected macrophages and epithelial cells. Further analysis of the mechanisms governing activation towards IAV infected epithelia is required to illuminate the similarities and differences in the NK cell response to these two cell types.

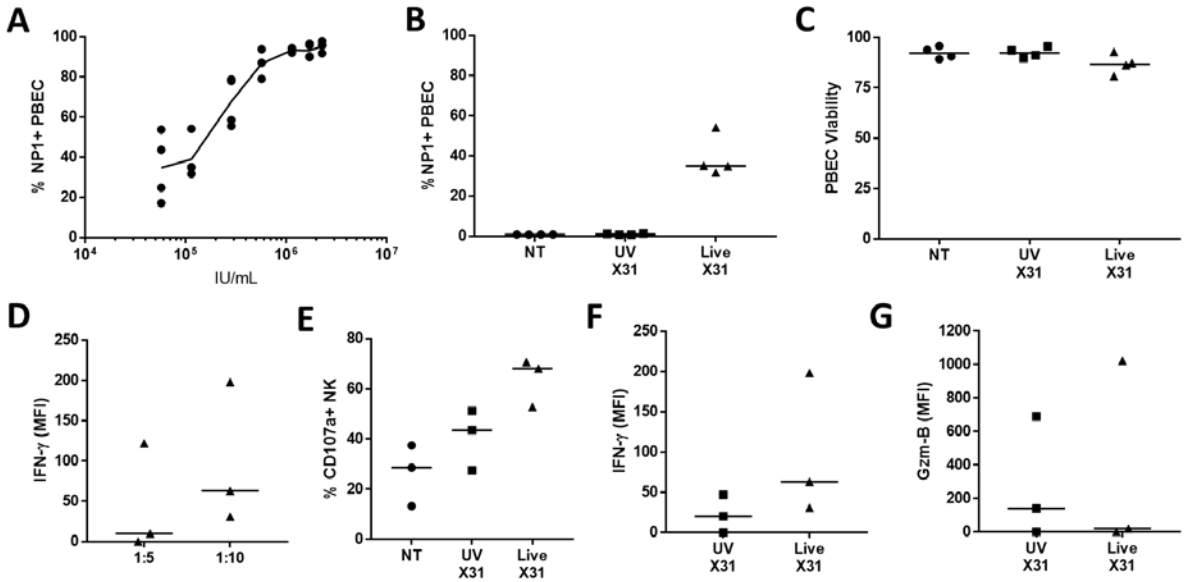

Figure 6.18: Autologous NK cells respond to IAV infected lung epithelia. Primary bronchial epithelial cultures were grown from basal cells collected from bronchial brushings of healthy donors. PBECs were infected with UV-irradiated X31, live X31 or not-treated (NT) for 24 h prior to culture with autologous peripheral blood NK cells. (**A**) X31 titration in PBECs, intracellular staining of IAV NP-1 was used to determine degree of IAV infection. (**B**) NP-1 expression in PBECs infected with 57, 000 IU of X31. (**C**) PBEC viability 24 hpi with X31 IAV, determined by flow cytometry. (**D**) Intracellular IFN-γ production in NK cells cultured with X31-infected PBECs at different effector : target ratios. (**E**) NK cell surface CD107a following culture with IAV-infected epithelial cells. (**F, G**) NK cell intracellular production of IFN-γ and Gzm-B following culture with X31-infected PBECs. Values are normalized to NT cultures. Lines describe medians.

6.3 Discussion

6.3.1 Culturing Autologous NK Cells with IAV-Infected Macrophages and Epithelial Cells

Airway macrophages (AM) were one of the major sites of IAV replication in human lung tissue (Figure 5.2) and are essential to generating anti-IAV immune responses [53, 126-134]. To further explore NK cell interactions with infected macrophages, a model of autologous MDM-NK cell co-culture was developed using peripheral blood from healthy donors (Figure 6.1 A). The use of autologous cells in these experiments was essential to generate physiologically relevant data as specific KIR-HLA interactions within an individual are important for NK cell education and function [522]. The class I HLA and KIR genes are some of the most polyallelic sequences in the human genome and thus there is a great deal of heterogeneity between HLA-KIR interactions in individuals [522]. Therefore NK cells taken from one individual may respond differently when exposed to the HLA class I of another individual and this has been a major caveat in measuring human NK cell responses in the literature [522].

Peripheral blood monocytes were isolated and differentiated into macrophages through extended culture with GM-CSF [85, 423, 431, 432]. In recent years the stimulus used to differentiate monocytes has been shown to generate a wide range of macrophage phenotypes and transcriptional profiles [523-525]. In this study GM-CSF differentiation was chosen because this growth factor has been shown to generate MDMs most phenotypically similar to alveolar macrophages [85, 431, 523, 524, 526]. GM-CSF has an essential role in governing human alveolar macrophage physiology *in vivo,* as GM-CSF deficiency results in impaired macrophage maturation and severe lung disease [527]. Therefore GM-CSF derived MDMs have a similar scavenger receptor profile to alveolar macrophages, including the expression of CD204, CD206, CD163, CD169, CD200R1 and CD80 [432, 526]. AM and GM-CSF derived MDMs also share a similar phagocytic capacity and cytokine production [85, 431]. Furthermore, GM-CSF derived MDMs can be infected with IAV *in vitro* ($P=0.0156$, Figure 6.2) and undergo similar changes to the expression of antigen presenting molecules ($P=0.0313$, Figure 6.2 B) [433].

It should be noted that there are some differences between GM-CSF derived MDMs and AM infection, for instance most studies report that H3N2 IAV replication is abortive in AMs but productive in MDMs [45]. This suggests that IAV might have a different capacity to co-opt cellular machinery in AMs and MDMs [45]. In addition, there are some phenotypic differences as GM-CSF-

derived MDMs have been found to express higher levels of CD64 and CD36 receptors relative to AMs [526]. However, given the strong resemblance to airway macrophages and susceptibility to IAV infection, the blood-derived macrophages used in this study provided a relevant physiological model of the IAV-infected airway macrophage and the best *in vitro* method to study the interactions with NK cells [85, 431, 523, 524, 526].

IAV-infected MDMs were cultured with NK cells at E:T ratios ranging from 1:1 and 1:10 (Figure 6.3). This range was chosen based on a similar published co-culture between monocyte-derived DCs and NK cells [254]. A ratio of 1:5 was selected as it was found to produce the greatest NK cell activation following contact with X31 infected cells (Figure 6.3). Minimal IFN-γ production was detected at a 1:1 and 1:10 E:T ratios. The reasons for this lack of detection at higher and lower E:T is unclear, however there may be too few NK cells in the 1:10 ratio for accurate measurement and IFN-γ may peak at a different time in the 1:1 ratio than assessed here. The timing of NK cell IFN-γ production and CD107a expression were explored in the co-culture model and both CD107a and intracellular IFN-γ were upregulated 2h and 6h after culture with infected MDMs, indicating a rapid NK cell response to infected cells (Figure 6.3). However, a much greater difference in IFN-γ could be detected after 6h of co-culture and a longer co-culture time was considered better to detect any effects on MDM viability (6.3 B and C). The speed of NK cell activation to IAV-infected MDMs suggests that NK cells may be stimulated by early "alarm" molecules following PRR detection of X31 in the MDM [64, 134]. This may be in the form of early pro-inflammatory and anti-viral cytokines such at IFN-α/β/λ, which primes NK cell activation in other models of infection [402, 512, 528, 529]. As discussed previously in section 5.3.1 blood-derived macrophages were also treated with UV-irradiated X31 (UV-X31). UV-X31 did not replicate in MDMs, nor stimulate changes to MDM surface proteins (Figure 6.2). Likewise, no NK cell response was detected in response to these cells. These results demonstrate that resting MDMs do not provide activating signals to NK cells as NK cells do not release IFN-γ and have minimal CD107a expression when cultured with resting MDMs (Figure 6.5).

Interestingly the E:T required to detect optimal NK cell activation in MDM-NK co-cultures (1:5) was lower than that described for autologous DC-NK cell interactions, which required an E:T of 1:1 [254]. This could indicate that NK cells are more sensitive to IAV-infected macrophages, although it might also reflect differences in IAV infection between the cells, including strain and co-culture time used in these two studies [254]. The E:T required to measure NK cell activation to IAV-infected human cells is lower than that for cancer cell lines such as K562, which typically range from 5:1 to 50:1

[530-533]. This difference in E:T ratios may be because NK cells are more sensitive to the autologous target cells used in this work and by Draghi *et al* [254]. However the lower ratio might also reflect the nature of macrophage interactions with NK cells, as these cells are found spaced throughout the airway epithelium and elicit strong immune responses following detection of pathogen [54].

To complement the analysis of NK cell function described in whole lung tissue and directly for IAV-infected macrophages, a co-culture model was also developed between autologous peripheral NK cells and lung epithelia. Submerged PBEC cultures were grown out of bronchial brushings from healthy donors, infected with X31 IAV and cultured with autologous peripheral blood NK cells, as shown in Figure 6.1B. These experiments demonstrate that lung epithelia are also capable of stimulating NK cell CD107a and IFN-γ expression (Figure 6.18 E and F). Interestingly a smaller E:T was required to detect NK cell activation, which could indicate that IAV infected epithelia are more capable of stimulating NK cell activation (Figure 6.18 D). The mechanisms of NK cell activation to IAV-infected epithelia are largely unknown, although NKG2D signaling has been implicated in mouse models [470]. In recent years structural cells have been proposed to have significant roles for controlling innate immune activation [534, 535]. This may be particularly relevant in IAV infection where the majority of infected lung cells are the airway epithelium [118, 490]. Thus this remains an important subject for further work.

6.3.2 NK cells respond to IAV Infected MDMs in a Contact-Dependent Manner

Given the importance of airway macrophages in the regulation of NK cell function and control of IAV, the cellular crosstalk between these cells and mechanisms of NK cell activation were further explored. Having optimised the MDM-NK cell co-culture conditions in section 6.2.1, IAV-infected macrophages were shown to increase surface CD107a on NK cells (P=0.0313, Figure 6.5 A) and increase NK cell expression of the antiviral molecules Granzyme-B and IFN-γ, as detected by flow cytometry (P=0.0156 for both, Figure 6.5 C and D). IFN-γ release during IAV infected co-culture was further confirmed by ELISA (P=0.0078, Figure 6.5 F). IFN-γ was below detectable limits in uninfected co-cultures and when MDMs were cultured alone, indicating the NK cells released this cytokine only following interaction with infected MDM (Figure 6.5 F). In addition, there was a non-significant trend towards increased extracellular Granzyme-B in X31-infected co-cultures (P=0.055, Figure 6.5 E). These results suggest both cytokines and cytotoxic molecules are released by NK cells following contact with influenza infected macrophages. These findings corroborate those of Siren *et al* and Kronstad *et al* who observed IFN-γ production from the NK-92 cell line in response to IAV infected

MDMs or autologous monocytes and NK cells respectively [375, 378]. Draghi *et al* also demonstrated NK cell activation to IAV-infected monocyte-derived dendritic cells [254]. Taken together these results demonstrate a potentially important anti-role for NK cells during IAV infections and confirm findings from the *ex vivo* explant model of infection discussed in Chapter 5.

To explore the contribution of NK cell contact with infected cells, co-cultures were also performed using a transwell system. Both Gzm-B and IFN-γ production were abrogated when NK cells were physically separated from infected MDMs (P=0.3438 for both, Figure 6.5 C, D). IFN-release was also inhibited by transwell culture with IAV-infected MDMs with no detectable IFN-γ in culture media (P=0.25, Figure 6.5 F). Likewise, no rise in extracellular Gzm-B was detected in transwell culture (P=0.2734, Figure 6.5 E). These results corroborate that of Draghi *et al* and Kronstad *et al* and indicate that both cytotoxic effector and cytokine release from NK cell depend on direct physical contacts with MDMs [254, 375]. Interestingly these molecules are not trafficked by the same endosomal pathways [536]. NK cell lytic granules undergo targeted polarised release whereas cytokine vesicles do not [536]. Therefore, these data demonstrate that cellular contacts with IAV-infected cells converge to stimulate the release of both types of compartments, whether this occurs by the same cellular contact is unknown. Unfortunately, it was not possible to conclude whether NK cell CD107a expression was also dependent on contact with IAV-infected macrophages as increased background expression was observed in transwell culture, possibly reflecting the reduced NK cell viability in this culture setting (Figure 6.5 B). However, targeted NK cell cytotoxicity has been extensively shown to require cellular contacts [200, 254].

$CD56^{bright}$ and $CD56^{dim}$ NK cells have been suggested to play different functional roles within the body but both subsets were found to respond equivalently in the *ex vivo* model of IAV infection presented in Chapter 5 (Figure 5.9) [271, 304-306, 308, 309]. To confirm these findings, the CD107a, IFN-γ and Gzm-B expression of $CD56^{bright}$, $CD56^{dim}$CD16+ and $CD56^{dim}$CD16- NK cells were measured in the MDM-NK cell model of IAV infection and are presented in Figure 6.6. As before, NK cell surface CD107a and intracellular IFN-γ and Gzm-B were distributed equally throughout the $CD56^{bright}$ and $CD56^{dim}$ NK cells (Figure 6.6). This is interesting considering IFN-γ and Gzm-B upregulation was totally dependent on cell contacts and suggests that there is a mechanism of contact-dependent stimulation that is shared between both $CD56^{bright}$ and $CD56^{dim}$ NK cells. CD107a expression was comparable between NK cell subsets but $CD56^{bright}$ and $CD56^{dim}$ NK cells express different Gzm molecules and therefore may have different mechanisms of triggering target cell apoptosis [189, 304, 516]. Direct contributions of $CD56^{bright}$ and $CD56^{dim}$ NK cells to target cell killing

would require further corroboration through flow cytometry sorting prior to culture with target cells.

Jost *et al* reported that IAV infection reduced numbers of peripheral blood $CD56^{bright}$ NK cells in infected PBMCS [374]. However, no phenotypic changes were observed on NK cells either following culture with uninfected macrophages or following IAV infection (Figure 6.4). This finding fits with the work of Long *et al.* who described stable $CD56^{bright}$ and $CD56^{dim}$ populations in PBMCs of IAV vaccinated individuals [537]. The discrepancy with Jost *et al* may be due to differences in infection protocol as cells infected by influenza *in vivo* are not found in the peripheral blood, therefore NK cells may have been activated by different mechanisms in whole PBMCs compared to MDMs [374]. From the results presented here NK cell subsets were stable during contact with IAV-infected cells with no difference in the types of responses exhibited.

6.3.3 NK cells may exert a cytopathic effect on infected macrophages

Robust NK cell responses during IAV infection of human lungs and MDMs have been described in this work (section 5.2.4 and Figure 6.5). Here, we have measured NK cell degranulation through surface expression of CD107a, a protein trafficked to the cell surface following granule exocytosis [499]. This is an established method of measuring NK cell degranulation and an indirect measure of NK cell cytotoxicity [185]. To further investigate NK cell cytotoxicity in IAV infections MDM viability was measure alone and in culture with NK cells. When MDM viability was assessed by flow cytometry NK cell culture was found to increase MDM cell death when MDMs were infected by IAV ($P=0.042$, Figure 6.7 B) but not during UV-X31 treated co-cultures ($P=0.3438$). However, no difference was found in extracellular LDH between IAV-infected MDMs cultured alone or with NK cells ($P=0.4129$, Figure 6.7 D). This may be due to higher detection of extracellular LDH in IAV-infected MDMs alone ($P=0.0313$, Figure 6.7 D). Measuring LDH is considered to be a weaker measure of cellular viability as this is a relative measure and a less sensitive test [538]. Extracellular LDH may also be affected by changes to cellular metabolism, which may be occurring in MDMs during IAV [539]. However, as results from flow cytometry and LDH analysis do not agree, further analysis of MDM viability is required, potentially through the more sensitive Terminal deoxynucleotidyl transferase (TdT) dUTP Nick-End Labelling (TUNEL) assay, which detects DNA damage [540, 541].

6.3.4 Signalling through NKG2D and NKp46 Receptors is Redundant to the NK cell response to IAV-Infected Macrophages

NKp46 and NKG2D activating receptors have both been implicated in NK cell recognition of influenza-infected dendritic cells and therefore may provide the contact-dependent signals to IAV infection identified in Figure 6.5 [254]. Ligands for both these receptors were identified on IAV-infected MDMs by chimeric receptor constructs (NKG2D; P=0.0469 and NKp46; P=0.0313, Figure 6.2). NKG2D binds cellular "stress" ligands including MIC-A/B and ULBP1-6 [542]. Siren *et al.*2004 reported increased MIC-B mRNA in influenza-infected MDMs, however neither MIC-A nor MIC-B proteins were expressed on X31-infected MDMs in the results presented here [378]. Therefore the NKG2D ligands detected in Figure 6.2 C are most likely from the ULBP family of proteins, which have been shown to be expressed on influenza-infected DCs [254]. Therefore, further investigation into MDM expression of ULBP proteins is required. NKp46 ligands detected on IAV-infected MDM surfaces in Figure 6.2 D could be viral HA, as has been suggested by Mandelboim *et al.,* however NKp46 also has unknown ligands which cannot be excluded without further investigation [241, 376, 379, 381].

NKp46 expression was increased on $CD56^{bright}$ NK cells and NKG2D increased on $CD56^{dim}$CD16+ NK cells following culture with X31-MDMs (Figure 6.8 C and G). It is unclear what significance upregulation of NKp46 and NKG2D on the NK cell subset would have on the NK cell response to influenza *in vivo*. Increased expression of these activating receptors would presumably make $CD56^{bright}$ NK cells more sensitive to NKp46 ligands and $CD56^{dim}$ NK cells to NKG2D ligands. These results again contrast with the work of Jost *et al* 2011, which described reduced NKp46 expression on NK cells in influenza infected PBMCs [543]. However, the NKp46 downregulation observed by Jost *et al* may be a result of the cross talk with other leukocytes present in the PBMC fraction which are not included in the model of IAV infection presented here. NKG2D and NKp46 receptor upregulation may be due to increased signalling through these receptors within the NK cell and together with the observed expression of receptor ligands infected cell surfaces (both here and by Draghi *et al*) these data support a role for these receptors in triggering NK cell activation [254]. However, fusion construct binding of NKG2D and NKp46 ligands did not affect either NK cell degranulation or IFN-γ either in total NK cells, or NK cell subsets (Figures 6.9, 6.10 and 6.11). Furthermore, the differential expression of NKp46 and NKG2D receptors on $CD56^{bright}$ and $CD56^{dim}$ NK cells did not lend any greater sensitivity to IAV infection (Figure 6.6). This contrasts with the work of Draghi *et al*, which successfully blocked IAV-induced NK cell IFN-γ production with NKG2D receptor constructs, despite a comparable methodology and high concentration of fusion

constructs [254]. Interestingly Kronstad *et al*. did not identify NKG2D ligands in H3N2 infected MDMs and blocking NKG2D did not diminish the NK cell response to H1N1 IAV-infected monocytes [375]. Therefore, NKG2D ligands may not be important in macrophage stimulation of NK cells in IAV infection. This suggests macrophages and dendritic cells use different mechanisms to stimulate NK cell function during IAV infection. Interestingly, virally infected epithelial cells strongly upregulate stress ligands capable of binding NKG2D, however it remains to be seen how important this interaction is in NK cell targeting of structural cells [544]. Macrophage surface protein is extensively modulated during IAV infection, it may be that there is greater redundancy in signalling to NK cell than has been observed for dendritic cells [54].

The data presented in Figure 6.9, 6.10 and 6.11 suggests that the increase in macrophage ligands for NKp46 and NKG2D are redundant in stimulating NK cell activation. Thus, other ligand-NK cell receptor pairs are implicated in controlling NK cell responses to IAV infection in macrophages. A recent mass cytometry study on IAV infected monocytes by Kronstad *et al* showed that CD95:Fas-L and CD111:CD96 monocyte:NK cell interactions were predictive of an NK cell response to H3N2 infection [375]. CD48:2B4 was also identified by Kronstad *et al*. as 2B4 acts as a co-receptor for NKp46, this might explain why NKp46 has been associated with NK cell responses to IAV in humans and mice[373, 375, 377, 382]. However, in this study NKp46 signalling from macrophages was found to be redundant to NK cell activation (Figure 6.9).

NK cells respond to a number of soluble mediators including IFN-α/β, IL-12, IL-15 and IL-18 [468, 494, 514]. Kronstad *et al*. demonstrated an important role for IFN-α signalling in generating an NK cell IFN-γ response to IAV infection as blocking IFN-α in monocyte-NK cell culture supernatants reduced NK cell production of IFN-γ [375]. Interestingly cell contacts were also found to be essential to NK cell activation as transwell culture also abrogated IFN-γ production and CD107a expression [375]. This suggests that dual stimuli are required to activate NK cells in IAV infection, including both early type I IFN from infected cells as well as contact with cell surfaces. Thus it appears that NK cell function during IAV infection may rely on initial cytokine priming, altering the sensitivity of NK cells to the activating signals that trigger NK cell cytotoxicity and cytokine production [375, 468]. Therefore, combinatorial blockade of all activating ligands as well as IFN-α may be required to abolish NK cell activation to IAV-infected macrophages.

6.3.5 IAV Manipulation of HLA Class I may represent a Mechanism of Viral Escape from NK Cell-Mediated Killing

Direct contact between NK cells and MDMs was essential for NK cell activation as separation of the two cells in a transwell system abrogated both Granzyme-B production and IFN-γ release (Figure 6.5). This suggests that changes to the MDM surface as a result of IAV infection may determine NK cell activation but neither NKG2D nor NKp46 signalling was not found to stimulate NK cell activation (Figure 6.9). However, another set of molecules important in regulating NK cell activation, the class I HLA, were upregulated on IAV-infected cells (Figure 5.2 and 6.2). To investigate the effect of this change in surface HLA, HLA class I ligands on human MDMs were blocked with anti-HLA-A/B/C prior to culture with NK cells. Blocking with αHLA-ABC or isotype control did not affect NK cell activation in response to uninfected MDMs, demonstrating that ADCC was not stimulated by the addition of antibody to co-cultures (Figure 6.12 C and D). However, blocking class I HLA increased NK cell CD107a expression during culture with X31-infected MDMs (P=0.0313, Figure 6.12 A). This result indicates that gross HLA class I signalling has an inhibitory effect on NK cell degranulation during influenza infection, consistent with the "missing self" mechanism of NK cell activation discussed in section 1.4.2. This effect was found on all $CD56^{bright}$ and $CD56^{dim}$ NK cell subsets (Figure 6.13). Interestingly IFN-γ production was not affected by antibody blocking of HLA-A/B/C molecules on macrophage surfaces (Figure 6.12 B and 6.13). Thus NK cell degranulation and cytokine production appear differentially regulated by contacts with the HLA class I.

The class I HLA, and in particular HLA-C provide many inhibitory signals to NK cells, preventing NK cell activation to normal somatic cells [222]. In other infections CMV, HSV and HIV class I HLA is reduced on infected cell surfaces, thus releasing NK cells from their inhibitory contacts and stimulating NK cell cytotoxicity towards infected cells [545-549]. However, HLA I molecules were found to be upregulated on both IAV infected macrophages and epithelial cells (Figure 5.2). Furthermore, the gross effect of the class I HLA on IAV infected cells was inhibitory to NK cells, suggesting that HLA upregulation might represent mechanism of immunomodulation by IAV (Figure 6.12) [227, 550]. This type of immunomodulation has been observed for Zika virus which also induces HLA I upregulation [551]. Interestingly, despite the inhibitory effect of HLA I on NK cells (Figure 6.2), NK cells were still activated in response to influenza infected cells, indicating that infected cells do not totally evade the NK cell response. The upregulation of activating ligands from target cells could explain this phenomenon but two key IAV-binding receptors were shown to be redundant to NK cell activation to IAV infection (Figure 6.9). Another explanation for this NK cell activation is that IAV-infection causes such a strong release of pro-inflammatory cytokines (Figures

6.14, 6.15 and 6.16) which may stimulate NK cell function [375]. In fact this cytokine signalling may be important in amplifying intracellular activating receptor signals within the NK cell [375, 468].

6.3.6 IAV Infection alters the Crosstalk between MDMs and NK Cells

To investigate MDM-NK cell communication via soluble mediators a panel of pro-inflammatory cytokines, chemokines and growth factors were measured in co-culture supernatants by Luminex assay. IAV infection was found to strongly upregulate pro-inflammatory cytokine signaling from MDMs including IL-1α, IL-6, IL-16, IL-17A, IL-17E, IL-22 and TNF-α (Figure 6.14). This fits with the described role for macrophages in early innate signaling during infection and is consistent with previous reports [52, 54, 100, 134, 136, 142, 143, 552-554]. Macrophage inflammatory signaling may enhance NK cell signaling from NK cell activating receptors as has been suggested for IFN-α [375]. Unfortunately, it was not possible to include IFN-α in this Luminex format. However IFN-β, another type I IFN important in stimulating NK cell activation, was found to be upregulated by IAV-infected macrophages 24 hpi [433, 494, 555]. In the Luminex data presented here there was a trend for increased extracellular IFN-β post-IAV infection but this did not reach significance (P=0.1922, Figure 6.14 A). These results represent culture supernatants 24 – 30 hpi and may therefore indicate a waning of the IFN-β response within this time. IL-10 and IL-22 were also found to be increased by IAV-infection of MDMs, as these cytokines are largely considered to be anti-inflammatory this could indicate a shift toward inflammation resolution in macrophage signaling at this later time-point [556, 557].

Furthermore, IL-12, 15 and 18 were all found to be upregulated by IAV infection of MDMs, implicating macrophages in activating NK cell function during IAV infection [86, 468, 514]. Interestingly IL-15 has been implicated in priming NK cell cytotoxicity towards lung epithelial cells in COPD [86]. Influenza is a major exacerbator of COPD symptoms and enhanced pro-inflammatory signaling during IAV infection may further dysregulate NK cell function in the COPD lung [86, 558]. Interestingly a small amount of basal IL-12 secretion (22.6 pg/mL) was detected from MDMs suggesting that resting macrophages may provide small amount of NK cell survival signals in the lung [468, 514]. In contrast negligible amounts of IL-15 or IL-18 were secreted by resting macrophages.

IAV infection also strongly altered the MDM chemokine profile, with increased CXCL1 (GROα), CCL5 (RANTES), CCL7 (MCP-3) and XCL1 (lymphotactin). These chemokines are important in recruiting a number of leukocytes including neutrophils, monocytes, eosinophils, dendritic cells and T cells to sites of inflammation [553, 559-562]. CCL5 has also been shown to recruit NK cells during IAV infection [168]. In addition receptors for CCL7 are expressed by NK cells and CCL7 transcripts are strongly upregulated by IAV-infected lungs [101, 563]. Therefore macrophages may also play an important role in recruiting NK cells to sites of influenza infection through the release of CCL5 and CCL7 [101, 563]. Interestingly CCR5, a receptor for CCL5, was strongly expressed on lung NK cells when compared to the blood and further enriched on resident NK cell populations (Figure 4.11), implicating that this molecule may have an important role in regulating NK cell trafficking to the lung.

Interestingly MDM production of CCL22 (MCP-1) was reduced during IAV infection (P=0.0164, Figure 6.15 E). Macrophage CCL22 expression was previously shown to be upregulated by Th2 cytokines and causes migration of dendritic cells and Th2 cells, thus regulating the Th2- related immune response [564]. Generation of a Th2 response enhances humoral and antibody mediated immunity against extracellular pathogens and is therefore inappropriate for an intracellular virus [565]. Thus the observed downregulation of macrophage CCL22 may indicate a shift towards the promotion of the anti-viral Th1 response from IAV-infected macrophages [564].

Direct analysis of NK cell function was assessed in these experiments through granzyme expression in the co-cultures. Measurement of NK cell Gzm-B release by Luminex assay confirmed findings from ELISA experiments (Figure 6.17 and 6.5 E), as a non-significant trend for increased extracellular Gzm-B was found in IAV-infected co-cultures by both methods, although Luminex reported an overall lower level of extracellular Gzm-B compared to ELISA. Furthermore, a small amount of Gzm-B was detected in IAV-infected MDM culture media that was not found to be significantly increased relative to UV-X31 controls (P=0.5289). However, Gzm-B upregulation has been detected in monocytes following TLR8 stimulation, a similar mechanism may be occurring at low-level in X31-infected MDMs [566]. In addition, high inter-individual heterogeneity was observed in extracellular Gzm-B by both techniques indicating that genetic or environmental variability in the cohort may affect this aspect of NK cell biology. Interestingly there was also a non-significant trend for reduced extracellular Gzm-A in IAV-infected co-cultures. Gzm-A is predominantly expressed by $CD56^{bright}$ NK cells, a subset which was also found to increase intracellular Gzm-B during contact with IAV infected MDMs, indicating that there may a shift in the type of Gzm molecules produced by NK cells during

infection (Figure 6.6 C) [189, 304, 516]. However, this may require further confirmation, possibly through flow cytometry.

This study also investigated NK cell production of inflammatory molecules by comparing cytokine and chemokine concentrations in cultures of macrophages alone and with NK cells. This preliminary data suggests that IL-6, IL-16, TNF-α and CCL2 release could be increased when NK cells are present during IAV infection (Figure 6.14 D, H, N and Figure 6.15 B). Unfortunately, none of these trends reached statistical significance, which may be due to low sample size as multiple corrections increase the stringency of statistical testing. Therefore, these results require confirmation at a greater sample size, potentially through an alternative method such as ELISA. In addition, a longer NK cell incubation time may improve detection of these molecules. Increased detection of IL-1, IL-16, TNF-α and CCL2 in IAV infected NK-MDM co-cultures could be explained by NK cell secretion of these molecules during IAV infection but could also result from a positive feedback on MDM cytokine production. For instance NK cell-produced IFN-γ may upregulate macrophage cytokine and chemokine production [197]. Therefore, confirmation of the cellular origins of these molecules is required. This might include RT-PCR confirmation of gene expression in adherent (MDM) and non-adherent (NK) cells in the co-culture. Alternatively, the production of intracellular cytokine could be assessed by intracellular flow cytometry in both the NK cells and MDMs.

The results presented here demonstrate a significant pro-inflammatory role for macrophages during IAV infection, a finding that is consistent with the literature [54, 567]. Macrophages also upregulate a number of chemokines important in immune cell recruitment, including CCL5 and CCL7 which may drive NK cell recruitment to the lungs during IAV infection [101, 563]. From this preliminary data IL-6, IL-16, TNF-α and CCL2 may be produced by NK cells during contact with IAV infected cells but this does not exclude the possibility that macrophage production of these molecules is enhanced by interaction with NK cells. Confirmation of this data is required, but the findings may have important implications for our understanding of macrophage-NK cell interactions in the lungs and how this may impact the functioning of other immune compartments.

6.3.7 Summary

In this chapter NK cell activation was measured in response to both autologous IAV-infected MDMs and lung epithelia. Increased NK cell CD107a and IFN-γ expression were stimulated by both sets of target cells, demonstrating that NK cells are capable of responding to all *in vivo* IAV infected cells. The production of Gzm-B and IFN-γ by NK cells was found to be dependent on contact with IAV-infected cells. However, NKG2D and NKp46 signalling was redundant in contact-stimulated NK cell activation. Interestingly, IAV-infected MDM class I HLA was found to be inhibitory to NK cell degranulation. Given the increased expression of HLA-A/B/C on IAV-infected lung epithelia and macrophages, this inhibition of NK cell degranulation may represent an NK cell evasion strategy evolved by IAV. However, NK cell activation to IAV was still detected despite inhibitory HLA signalling indicating that infected macrophages provide as yet unidentified activating signals or loss of inhibitory receptor ligation. Infected MDMs upregulate a number of pro-inflammatory cytokine and this cytokine signalling may influence NK cell sensitivity to activating ligand expression on NK cell surfaces, releasing their inhibited state and allowing cytotoxicity and IFN-γ production. Furthermore, preliminary Luminex data implicates NK cells in the production of IL-6, IL-16 and TNF-α in IAV infection, advancing our understanding of NK cell cytokine production in infection. Understanding how NK cells become activated in viral disease, their functions and regulation may allow the improvement of vaccination and intervention in exacerbations of chronic lung disease. For instance, modulating pro-inflammatory cytokine signalling might allow fine-tuning of NK cell responsiveness during inflammation.

Chapter 7 Discussion and Further Work

7.1 Introduction

Complicated NK cell biology is currently being elucidated in the liver and uterus, identifying tissue residency, memory responses and functional contributions to viral infections and chronic disease [293, 340, 344]. However, the role of NK cells in the lung is less well understood and resident NK cell populations have not been investigated in this organ [293, 362, 568]. Therefore, the aim of this thesis was to investigate the phenotype and function of lung NK cells during respiratory infection and disease, primarily focusing on IAV infection.

Influenza is a major contributor to annual mortality, a pandemic risk and exacerbator of chronic lung disease [1, 17, 18]. Thus far, blood NK cells have been found to bind IAV-infected human cells *in vitro,* but the functional contribution of these cells to viral clearance and disease pathology in humans is unknown [241, 254, 373-377]. Many *in vitro* human studies use mixed PBMC infection models but influenza infection is rarely systemic and infects airway epithelium and macrophages *in vivo* [23, 54]. Therefore, this thesis extends knowledge of lung NK cell function by using *ex vivo* models of IAV infected human lung and PBECs. Furthermore, mechanisms of NK cell activation and cross-talk with airway macrophages were investigated in a blood-derived MDM-NK cell co-culture model. These data support the hypothesis that NK cells play a functional role in anti-influenza immunity and may have important implications for moderating immune function in vaccination and disease. In addition, human lung resident NK cells were characterized by multi-parameter flow cytometry, with evidence of unique receptor expression profiles and enhanced responsiveness to lung infection. This chapter will discuss the clinical implications of these findings, including wider implications for lung immunity to infection and disease. Outstanding questions will be outlined throughout, identifying key areas of interest for further research.

7.2 Lung NK Cell biology is different to other Human Organs

In organs such as the liver and uterus, human NK cells possess a phenotype that is dramatically different from the circulation [293]. For instance, liver and uterine NK cells have a predominantly $CD56^{bright}$ phenotype with differential expression of surface proteins, including chemokine receptors and KIR [293]. Based on the findings in this thesis and data from Marquardt *et al* this situation is very different in the lungs [362]. In this thesis NK cells isolated from the human lungs and blood were analyzed by multi-parameter flow cytometry, enabling a comparison of cellular phenotypes. NK cells were defined as CD45+CD3-CD56+ cells, a commonly used gating strategy designed to exclude ILC populations [463]. Consistent with previous reports, CD56+CD3- NK cells made up a significant proportion (18.55%) of CD45+ lymphocytes in the human lung and were found to be predominantly mature, canonical NK cells, corroborating the work of Marquardt *et al* 2017 [362, 364, 365]. Similar to the blood, lung NK cells were predominantly $CD56^{dim}$CD16+ with strong expression of CD57 and activating receptors including NKG2D, NKG2C and NKp46. $CD56^{dim}$CD16+ NK cells represent the most mature, cytotoxic-ready NK cell phenotype and cells expressing CD57 show a further enhanced functional potential, including greater IFN-γ production [267, 270, 272, 273, 569]. Thus it appears that the human lungs have a ready population of innate killer cells to draw upon during infection [293]. This predominance of mature NK cells in the lungs may have important functional implications for combating infections in this organ [362].

The majority of lung NK cells described here and by Marquardt *et al*. are phenotypically similar to those of the peripheral blood. Although a small population of phenotypically distinct resident cells were identified in this thesis, this finding suggests that the bulk of lung NK cells may be travelling through the lung vasculature [362]. Unfortunately, due to various practical issues, investigating NK cell localization within the lung tissue was not possible in the timeframe of this thesis. Thus the extent to which NK cell extravasation and migration occurs in health and the nature of NK cell trafficking in the lungs remains unknown. However, respiratory infections such as IAV cause lung NK cell numbers to rise in animal models, during which time NK cells can be found between the structural cells of the lung [112, 364, 372, 382, 393, 394]. This suggests that circulating NK cells can be recruited into the lung interstitium when required, however the replication and trafficking of resident NK cell populations have not yet been explored and may also contribute to the observed rise in pulmonary NK cells [112, 364, 372, 382, 393, 394].

7.3 Characterization of Lung Resident CD49a+ NK Cells

A key hypothesis of this thesis was that resident NK cells exist in the human lung. This hypothesis was confirmed through analysis of residency marker expression (CD49a, CD69 and CD103) on lung NK cells. A substantial proportion of $CD56^{bright}$ NK cells were identified as CD49a+CD69+CD103+ cells, consistent with findings in the liver and uterus [299-301]. CD49a and CD103 make up integrin complexes, anchoring lymphocytes to collagen IV and E-cadherin respectively, whilst CD69 blocks the action of S1P1 and tissue egress [323-327]. The lack of CD49a+CD69+CD103+ NK cells in the peripheral blood further suggested that these cells are resident within the lung tissue. Furthermore, lung $CD56^{bright}$ rNK cells were shown to possess distinct phenotypes, including enhanced expression of activating receptors NKG2D and NKG2C, increased CCR5 expression and reduced expression of NKp46 which may influence rNK function. Unexpectedly, $CD56^{dim}$CD16- NK cells were also found to express markers of residency. As a $CD56^{dim}$CD16- phenotype is induced upon NK cell activation and cell death, $CD65^{dim}$CD16- CD49a+CD103+CD69+ cells may represent $CD56^{bright}$ NK cells post-activation [314, 316, 317, 320]. Interestingly, residency markers have also recently been reported on $CD56^{dim}CD16^{dim}$ NK cells in nasal lavage, confirming the findings in this thesis [322]. Therefore, the presence of "resident" $CD56^{dim}$CD16- NK cells may be a lung-unique finding. It is possible that lung resident NK cells are more consistently activated as a result of the constant exposure to microbes, pollution, chemical irritants, dust and debris at this mucosal surface resulting in a $CD56^{dim}$CD16- phenotype.

CD49a expression can also be used as a distinguishing feature of ILC1 [301, 570]. However, as discussed in section 7.2 NK cells were classified through the expression of CD56 which is not expressed by non-cytotoxic ILC1 [463]. Although 50% of NCR+ ILC3 cells also express CD56, thus far these cells have not been reported to express CD49a [463]. Therefore, novel CD49a+ NK (CD3-CD56+) cells were identified in this thesis. These classifications of ILC and NK cells were based on the most up to date information given by Spitz *et al* however there is a great deal of confusion and controversy in the literature in identifying ILC1s and NK cells [463]. This originates from the use of only a few surface proteins to delineate groups of cells which share similar functions and mechanisms of action [463]. For instance CD49a is an ECM anchoring protein found on memory T cells, resident NK cells and ILC1s [301, 505, 570].

Both resident NK cells and circulating NK cells share many phenotypic similarities with ILCs, including NKp46, T-bet, the IL-12R and IFN-γ production, making it difficult to distinguish between them [570]. Although extremely similar in phenotype, NK cells and ILC1 are considered separate cell types due to differences in transcription factor expression, function and surface protein [262, 463, 571]. One method of distinguishing ILCs and NK cells is based on the expression of transcription factors, EOMES and T-bet, as ILC1s do not express EOMES [262, 336, 570]. However, resident CD49a+ NK cells are also EOMES negative [338, 340]. The main difference between NK cells and ILC1s is that ILC1s lack cytotoxicity [262, 336, 570]. In the model of IAV infection presented here rNK were shown to upregulate surface CD107a in response to IAV infection, indicating a putative cytotoxic function of this population [185]. Given the expression of CD56 and CD107a upregulation, these cells are therefore most likely to be rNK cells, consistent with the populations described for the liver and uterus [299-301].

In recent years, a new appreciation for immune cell plasticity within the ILC subsets has emerged as only cytokine stimulation is required to change ILC phenotypes [571, 572]. Given the similarity of rNK cells to ILC1, a shared transcription factor profile and some evidence that rNK may develop from an ILC precursor, it may be more appropriate to consider resident NK cells as part of this ILC continuum [338, 340]. Although there are significant phenotypic and functional similarities between the ILC1 and circulating NK cells, cNKs seem to be more static in phenotype and function [571]. Therefore, circulating NK cells may represent a differentiated effector cell with pre-determined function, whilst resident NK cells and the ILC families provide coordination of immune responses, adapting to environmental change through plasticity in functional phenotype [571, 572]. However, recent reports in mice have implicated TGF-β in switching cNK cells into an rNK / ILC1-like phenotype, challenging this view [573, 574]. Indeed, there are many outstanding questions regarding resident NK cell biology. At what point do resident NK cells seed organs? When do they take on a unique functional phenotype? How plastic are rNK cells and how do they influence human immunity?

7.4 NK Cells Contribute to Anti-Influenza Immunity in the Human Lung

One of the key hypotheses of this thesis was that NK cells contribute to anti-influenza immunity in the human lung. This was confirmed through the development of flow cytometric measures of NK cell activation in an *ex vivo* model of IAV-infected human lung. During IAV infection NK cells produced anti-viral molecules, with evidence of cytotoxicity provided by measures of

degranulation. Of note is that active IAV replication was essential to stimulating NK cell function as UV-irradiated X31 did not promote NK cell function. NK cells isolated from the lungs are often reported as hypofunctional, however this thesis reveals that IAV infected human lungs are capable of stimulating NK cell activity, indicating that lung NK cells are not inert but are tightly regulated by the pulmonary environment [362, 364-366]. This may be important given their cytotoxic nature and capacity to destroy somatic cells [86, 361]. Dysregulated NK cell cytotoxicity could result in the destruction of airway tissue, as has been suggested in COPD [86, 361].

NK cells were found to be significant early producers of IFN-γ during influenza infection, with substantial extracellular levels of this cytokine detected within 6h of meeting influenza-infected macrophages. IFN-γ is a pleiotropic cytokine, with multiple effects on both leukocytes and structural cells and is particularly important in generating Th1 responses [197]. Therefore, NK cell activation during IAV infection may stimulate immune cell function and play an important role in generating effective adaptive immunity [197]. Interestingly, rapid IFN-γ was also produced by lung T cells (within 24 hpi of *ex vivo* lung infection). All the lung T cells identified in this model have a memory phenotype (CD45RO+), with no reported naïve (CD45RO-) T cells [460]. Therefore, as H3N2 is a circulating strain of IAV, it is possible that X31 infection stimulated lung memory T cells capable of recognizing IAV infection. This would explain the rapidity of the T cell response, as in naive animals, T cell immunity is not produced until 5 -7 dpi [43, 101-104]. T cells, NK cells and NKT cells are predominant sources of IFN-γ in the body, however other immune cells may also contribute to this function [197]. For instance APCs have been found to produce IFN-γ following extensive IL-12 stimulation [575]. However, the results of this thesis do not support macrophage production of IFN-γ as MDMs were not found to secrete this cytokine, despite significant upregulation of IL-12. In addition, innate B cells have been found to produce IFN-γ in bacterial infections, however IFN-γ production in these cells has yet to be investigated in IAV infected lungs [576]. Thus, this thesis provides strong evidence that NK cells may be a major source of the early IFN-γ in immunologically naive lung, providing the initial priming of immune responses directed towards intracellular pathogens [197]. The extent to which this may be supported by DCs and innate B cells remains unknown.

Interestingly, preliminary findings from a Luminex assay of infected MDM-NK cell co-cultures suggest that NK cells may also produce IL-6, IL-16, TNF-α and CCL2 during IAV infection. Both IL-6 and TNF-α are pro-inflammatory, stimulating many different aspects of the immune system [577, 578]. For instance IL-16 is involved in T cell recruitment and modulation whilst CCL2 recruits

monocytes and macrophages, suggesting that NK cells may also be involved in cellular recruitment during IAV infection [520, 562, 579]. This Luminex data requires further investigation, but if corroborated may indicate greater NK cell contribution to pro-inflammatory signaling and immune cell recruitment than is currently understood.

As well as pro-inflammatory cytokine production, measures of NK cell degranulation were found during IAV infection of lung tissue, epithelial cells and MDMs, indicating NK cell killing of infected cells [185]. Furthermore, flow cytometry detection of upregulated NK cell Gzm-B and a corresponding reduction in MDM viability detected by flow cytometry indicated substantial NK cell-mediated cytotoxicity towards IAV infected macrophages. Further confirmation of MDM viability should be performed by more specific methods of apoptosis detection, but these results suggest that NK cells may also control IAV infection through destruction of infected cells. This follows given the described phenotype for lung NK cells, where the cytotoxic potential may be quite high [267, 270, 272, 273, 569].

So far mouse models have provided inconsistent and contradictory reports for the effect of NK cells in IAV infection, with both detrimental and protective roles outlined [107-113, 227]. The data presented in this thesis suggests that human NK cell contact with IAV infected cells would promote NK cell cytotoxicity and IFN-γ release, potentially aiding immune control of this virus. However, it is not possible to conclude whether NK cell activation may help or hinder *in vivo* human IAV infection from this data. Nevertheless, co-evolution of both IAV proteins and NK cell receptors in humans suggest that NK cells have provided a selection pressure on IAV evolution and *vice versa*, indicating NK cell control of this virus [375, 580]. For instance cells infected with older strains of IAV H3N2 are lysed less effectively than cells infected with more recently emerged strains, suggesting that IAV may evolve to downregulate NK cell responses over time [580].

7.5 NK Cell Activation to IAV requires physical contact and therefore recruitment to sites of Infection

Cellular contacts with target cells is crucial to determining NK cell activation and cytotoxicity [199]. The importance of direct cellular signalling on NK cell activation was explored in this thesis with an MDM-NK cell co-culture model. Physical contact with infected macrophages was essential to NK

cell production of cytotoxic molecules and release of IFN-γ, even in the strongly pro-inflammatory environment of infected MDMs. These findings demonstrate the specificity of NK cell activation; NK cells must physically encounter virally-infected cells to activate [199]. This implies that NK cell activation in human IAV infection must come from NK cells within sites of infection i.e. the epithelial barrier. Thus circulating NK cells would have to be recruited into the lung interstitium to respond to IAV infection. However, it is not known whether the same dependency on physical contacts is required for rNK cell activation to influenza infection, as it was not possible to model this with peripheral NK cells. If physical contact is required for rNK cell activation these cells may be more strategically located to respond to influenza infection than their circulating counterparts [293, 340].

In mice circulating NK cells have been shown to be recruited to IAV infection through CCR5 and CXCR3 mediated chemotaxis [168]. This may be prompted by epithelial and macrophage chemotactic signalling as these cells have been shown to produce ligands for CCR5 and CXCR3 during IAV infection [145-148]. In agreement with this finding, this thesis reports greater CCR5 expression on human lung NK cells compared to matched peripheral blood. Interestingly, there was an even greater expression of CCR5 on lung rNK cells, suggesting that lung rNK cells may have increased sensitivity to chemotactic signalling through this receptor and could be recruited to sites of influenza infection through this mechanism. Airway macrophages may be a key contributor to NK cell recruitment through CCR5 as these cells have been previously shown to express CCR5 ligands; CCL3 and CCL4 [145, 147, 148]. This thesis also provides evidence that airway macrophages may secrete another CCR5 ligand, CCL5, during IAV infection (Figure 6.15 C). In addition to NK cell recruitment airway macrophages may also enhance NK cell activation and survival during IAV infection through IL-12, 15 and 18 signalling, as the secretion of these cytokines was upregulated by IAV-infected MDMs.

7.6 Mechanisms of NK cell Activation to Influenza-Infected Cells

NKp46 and NKG2D receptor ligation on NK cell surfaces have been linked to recognition of IAV-infected DCs and PBMCs *in vitro* and have been associated with IAV immunity in mouse models [254, 373, 379, 382]. However, *in vivo* IAV infects human airway epithelium and macrophages and is rarely systemic [23]. Therefore, the contribution of NKp46 and NKG2D ligation by IAV-infected macrophages was explored in this thesis. The interplay between NK cell and macrophages is an important mechanism of innate immunity in a number of inflammatory contexts, particularly at mucosal surfaces [409, 410]. Ligand-receptor interactions were blocked between MDM and NK cell

contacts by incubation with chimeric receptor constructs. However, NK cells were still found to produce IFN-γ and upregulate surface CD107a. Thus the findings in this thesis suggest that macrophages and dendritic cells do not share a common mechanism of NK cell activation to H3N2 IAV [254]. This was an unexpected result as NKp46 and NKG2D ligands were both detected on the surface of IAV-infected MDMs. In addition, altered receptor expression was measured on $CD56^{bright}$ and $CD56^{dim}$ NK cells during contact with infected cells; indicating modulation of receptor signalling in the NK cell subsets. These findings suggest that there is substantial redundancy in the capacity of macrophages to stimulate NK cell activation. This redundancy may enable macrophages to stimulate NK cell activation in a number of contexts, limiting viral evasion of the immune response [409, 410]. Unfortunately, the nature of NK cell activating stimuli presented by IAV-infected macrophages remain unknown. However, CD95:Fas-L, CD111:CD96 and CD48:2B4 interactions were recently identified in a mass-cytometry study of IAV-infected monocyte interactions with NK cells [375]. These ligand-receptor interactions could therefore be responsible for stimulating NK cell cytotoxicity towards IAV infected MDMs [375].

So far, detection of viral HA and non-specific cellular stress have been implicated in NK cell recognition of IAV infection [254, 376, 378, 379]. However, numerous HLA I binding molecules on the NK cell surface play an integral role in controlling NK cell activation, the most well-known of which are the KIR family of receptors [199]. The gross-effect of these interactions were analyzed in this thesis by blocking all interaction with the class I HLA. These results demonstrate a significant inhibitory role for the combined signaling from HLA I in IAV infection. Given the upregulation of HLA I on the surface of IAV infected cells, this might represent evasion of the NK cell response by the IAV virus [203, 227]. Evasion of NK cell killing has been described for a number of viruses, which typically try to enhance the inhibitory signals NK cells receive through HLA I engagement [546, 551, 581]. Given the long co-evolution time of humans and IAV, this type of viral immunomodulation is certainly possible [582]. A number of inhibitory KIR have been associated with IAV severity in humans, but with inconsistent results between studies [384, 385]. Unfortunately, surveying and analyzing the contribution of the many different HLA-binding receptors to NK cell activation was beyond the scope of this study but this remains an important area for further investigation.

In addition to physical contacts, IAV-related pro-inflammatory signaling is likely to be important in stimulating NK cell function as this promotes NK cell survival and cytokine production, in some cases by reducing the threshold for intracellular activating signaling [375, 404, 514]. IAV-infected MDMs produce a number of NK cell activating cytokines including IFN-β IL-12, IL-15 and IL-18, as shown by

this thesis and previous work [433]. In addition, IL-1β, IL-6, IL-10 have also been found to affect NK cell cytokine production and cytotoxicity and were all produced by IAV infected MDMs [433, 583-586]. A summary of the main cytokine and receptor interactions investigated in this study are presented in Figure 7.1. It remains to be seen whether blocking pro-inflammatory cytokines could reduce the NK cell response to influenza. Interestingly, the most pathogenic strains of IAV such as the avian H5 strains induce massive cytokine release from airway macrophages [587]. It is thought that hypercytokinemia in IAV overstimulates immune cells, increasing destruction of the epithelial barrier which leads to bacterial invasion, pneumonia and death [587]. Whether this cytokine storm affects NK cell function remains to be explored, however increased NK cell activation has been found for the most pathogenic strains of IAV [588]. Finally, the mechanisms by which NK cells respond to IAV infected epithelial cells are currently unknown but represent an important area for research. Elucidating the mechanisms by which NK cells respond to infected airway epithelium is essential to understanding NK cell contribution to cellular clearance in infection and may have implications for understanding chronic disease [86].

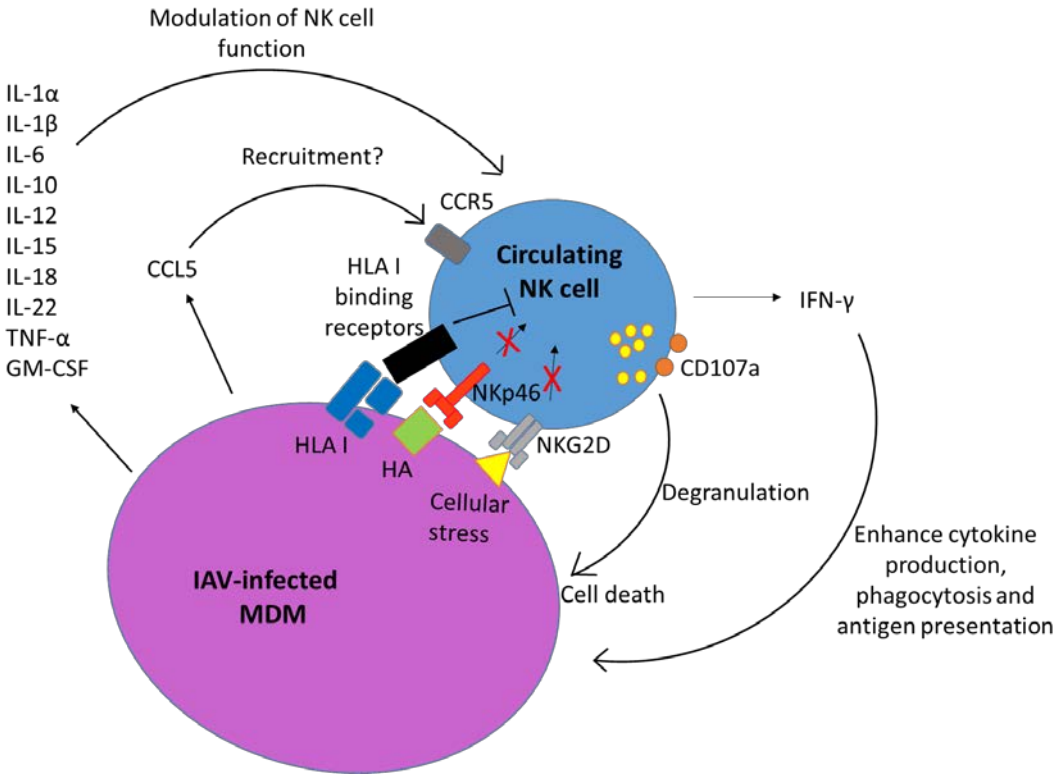

Figure 7.1: Summary diagram of the proposed relationship between MDMs and NK cells during IAV infection.

7.7 CD56^{bright} and CD56^{dim} NK cell Contributions to Anti-Influenza Immunity

Interestingly CD56^{bright} and CD56^{dim} NK cells were found to respond equivalently to IAV infection in all three of the human models explored in this thesis. All NK cell subsets produced IFN-γ upon contact with infected cells and showed similar upregulation of cytotoxic markers including surface CD107a and Gzm-B production. Thus these results suggest that the whole NK cell population, including more immature NK cells are recruited to anti-viral responses and do not agree with a number of studies which have found distinct roles for CD56^{bright} and CD56^{dim} NK cells [259, 295, 302-304, 308, 309]. However, the reported distinction in NK cell subset function is usually based on one type of *in vitro* stimulation, which is either through culture with cytokines, PMA/I or cancer cell lines [259, 295, 302-304, 308, 309]. In contrast some *in vitro* stimuli has been shown cause CD56^{dim} NK cells to produce cytokines (such as NKG2D and 2B4 engagement) and CD56^{bright} NK cells to kill (IL-2, 12 and 15 treatment) [189, 310-312]. As IAV has been shown to initiate both these types of stimuli, it is therefore possible that the combined signaling NK cells receive from IAV infected cells triggers both CD56^{bright} and CD56^{dim} effector responses [377, 406, 407, 589]. This aspect of NK cell function could be investigated further by direct investigation into CD56^{bright} and CD56^{dim} cytotoxicity and the production of cytokines not assessed in this work such as TNF-α.

7.8 Functional Relevance of Resident NK cells to IAV Infection

The concept of organ-resident NK cell populations is a relatively recent one and the functions of these cells in health and disease are only just being discovered. So far, a range of functions have been suggested including limiting autoimmunity in the salivary gland, promoting inflammation in adipose tissue and injury in the kidneys [340]. One of the aims of this thesis was to investigate lung rNK cell function in the context of respiratory virus. Resident NK cells were found to activate in response to IAV infection with increased markers of degranulation and IFN-γ production. The full functional contribution of resident NK cells to IAV infection remains to be seen, however the strategic location of rNK may enable a more rapid IFN-γ release and cytotoxic response than their circulating counterparts. As rNK are already present within the lung tissue rNK may be able to act as first responders to infection [168]. The precise localization of rNK within the lung remains to be explored however there is some evidence that CD49a expression anchors CD8+ T cells to the basal membrane of the lung epithelium and a similar mechanism may well be used by rNK cells [331].

One of the earliest functions suggested for rNK cells was of memory to infection and inflammatory stimuli [301, 345]. Therefore, one of the hypotheses of this thesis was that lung rNK cells would have an enhanced response to IAV infection. This was investigated by *ex vivo* infection with X31, a H3N2 virus, comparable to IAV strains currently circulating in the population [1]. Confirming this hypothesis, lung $CD56^{bright}$CD49a+ NK cells had a greater upregulation of CD107a and $CD56^{dim}$CD16-CD49a+ NK cell produced more IFN-γ during *ex vivo* IAV infection. Furthermore, an enhanced functional response was not found for rNK cell populations when lung tissue was stimulated with PMA/I, indicating that there may be a virus-specific effect on the activation of rNK populations. This may be mediated by the enhanced expression of activating NKG2D receptors on rNK cells, as NKG2D has been shown to recognize IAV-infected dendritic cells. However, this thesis has shown that NKG2D interactions are redundant for NK cell recognition of MDMs. It therefore remains to be seen if NKG2D ligands facilitate NK cell recognition of IAV-infected epithelial cells. The nature of direct NK cell memory to antigens is controversial and is most likely a feature of innate cell training through either altered surface protein, signaling pathways or epigenetic state [344]. For instance "memory" NK cells have been found to have a more open IFN-γ locus which may enable the more potent cytokine response seen in the liver [338, 341, 590, 591]. Therefore, further confirmation of a memory-like phenotype in lung rNK cells could be provided by analysis of the epigenetic profile relative to circulating NK cell.

7.9 NK Cell Function in COPD

In the COPD lung NK cell function has been shown to be dysregulated, with enhanced cytotoxicity of lung epithelial cells, a phenomenon that has been linked to the onset of emphysema [86, 361, 470]. It is thought that NK cells may initiate epithelial cell killing through the recognition of stress ligands by the NKG2D receptor, as MIC-A is upregulated on the COPD epithelium [469, 470]. In this thesis, significant changes to the NK cell phenotype were observed during worsening COPD. For instance, more severe disease was found to correlate with a significant enhancement in the proportion of $CD56^{bright}$ cells, with a corresponding reduction in $CD56^{dim}$CD16+ NK cells. $CD56^{dim}$CD16+ NK cells demonstrate significant cytotoxicity in other areas of the body and therefore may be strongly activated during COPD [200, 295, 302, 304, 308, 309]. Sustained NK cell activation ultimately results in NK cell apoptosis which might explain the distorted $CD56^{bright}$:$CD56^{dim}$ ratio seen in COPD lung tissue [86, 314, 316, 317, 320, 361].

The increase in NK cell cytotoxicity in COPD has been suggested to be caused by dendritic cell priming of NK cells through trans-presentation of IL-15 on the dendritic cell surface [86]. However, it remains unclear why dendritic cells are providing such stimulation to NK cells. Finch *et al* suggest that this distorted DC activity may originate from inflammatory epithelial signaling following damage and stress, but this has not yet been shown [86]. Interestingly macrophage function is also dysregulated in COPD, with reduced phagocytosis and altered inflammatory cytokine production [85, 592]. It is therefore possible that macrophage-mediated inhibition and regulation of respiratory NK cells may also be affected in COPD and represents an important area of research into COPD pathology.

IAV is a major exacerbator of COPD, and as discussed in section 7.3 this thesis has demonstrated substantial anti-viral effector functions of NK cells in human IAV infection. However, the NK cell contribution to viral exacerbation in COPD is unknown and should be investigated further. Based on the results of this thesis, IAV infection in a COPD patient may further increase NK cell cytotoxicity by increasing the number of target cells for NK cell destruction. In addition, the extensive pro-inflammatory signaling initiated upon IAV infection may increase NK cell sensitivity towards cellular stress [470]. Thus IAV infection may increase NK-cell mediated destruction of non-infected lung epithelium and worsen disease. Although IAV is not the only viral pathogen that can exacerbate COPD there is little research on NK cell activation in other human respiratory infections [568]. Thus it is difficult to speculate on the potential role for NK cells in non-IAV COPD exacerbations.

The organ microenvironment is expected to play an important role in generating resident NK cell phenotype and function. Given the pro-inflammatory state of the COPD lung it is possible that rNK training by the respiratory environment may be altered relative to health, although this remains an open question [86, 470]. In support of this, enhanced CD49a expression was found on both $CD56^{bright}$ and $CD56^{dim}$CD16- lung NK cells in the lung tissue obtained from more severe COPD patients. However, the functional outcome of an altered rNK cell population is uncertain, particularly given that this thesis has outlined an enhanced functional role of rNK cells in IAV infection but COPD patients are more susceptible to viral infection [593]. This may suggest that the capacity of rNK (and indeed cNK) to effectively respond to viral infection and promote clearance is impaired in COPD.

7.10 Importance of Appropriate Modelling to Investigate IAV Infection

Murine studies of lung NK cell function have provided important insights into the functional role of NK cells in the pulmonary environment [107-113, 227]. However, resident NK cell function is likely to be strongly shaped by the organ environment and a lifetime of environmental stimuli [340]. For the lungs this includes allergens, pollution, smoke, changes in microbiota and pathogen exposure, which cannot easily be replicated in a rodent. Therefore, the characterization of human resident NK cells requires physiologically relevant models of human infection and disease. Furthermore, the strong evolutionary divergence between mouse and human NK cell receptors limits the translation of findings from murine studies to humans, particularly when there is a lack of a shared history of pathogen exposure. This may be a reason why mouse models of influenza infection provide inconsistent and often contradictory findings on NK cell function (reviewed in section 1.5.2) and highlights the importance of using other models to corroborate and extend findings from the mouse. [107-113, 227]. The use of different murine genetic backgrounds, viral strains and dose may also be confounding factors in the interpretation of these studies.

As there is no known natural murine influenza virus, murine IAV infection has been engineered *in vitro* [594]. However, repeated passage to adapt influenza for the murine airways may have altered the functioning of this virus from a human-infecting strain [594]. In addition, murine IAV infection also relies on a genetic susceptibility to IAV in inbred laboratory strains, as outbred mice are resistant to IAV infection [595]. Thus, the immune responses measured in such studies may not be physiologically relevant to humans, particularly as all murine IAV infection models are effectively observing the introduction of a new viral species. Humans have been co-evolving with IAV for approximately 20,000 years and this shared evolutionary history has shaped NK cell receptor structure and viral immunomodulation of these cells [375, 580]. Unfortunately, the impact of this co-evolution on immune cell responses may not be effectively represented by murine IAV infection. Therefore, studies using human samples are also required to pick apart host-pathogen interactions in a way that benefits translational research.

7.11 Limitations of the Study

Investigating the phenotype and function of human lung NK cells required human lung tissue, of which cancer resection surgery is one of the few available sources. Macroscopically normal lung tissue was taken distal to tumour sites and individuals had not undergone radiation or

chemotherapy. Furthermore the human lung NK cell phenotype reported here is consistent with NK cells from healthy mouse lungs in terms of maturity and differentiation [364, 365]. Even so, disease state, smoking history and medication remain confounding factors in the use of this material [362]. In addition, effects from neighbouring tumour and tumour-associated stroma cannot be excluded and this remains a caveat in the interpretation of this work. A further drawback of experimenting on human lung tissue is the extensive genetic and environmental heterogeneity between individuals. This can be seen in the range of NK cell functional responses and phenotype data in this thesis. In addition, low cell yields from lung tissue limited functional data sets to a small number of repeats. Where possible functional readouts were supported by co-culture models using healthy peripheral blood. However, it was not possible to explore resident NK cell function in the co-culture models due to a lack of this cell population in the peripheral blood.

An additional limitation of this study was the reliance on GM-CSF to stimulate a lung-like phenotype from blood monocytes [85, 423, 431, 432]. Although there are many phenotypic similarities between GM-CSF derived MDMs and airway macrophages, this model cannot completely recapitulate the *in vivo* phenotype [526]. For instance GM-CSF differentiation will push monocytes towards one consistent phenotype, but *in vivo* macrophages demonstrate substantial phenotypic malleability and plasticity, including surface protein expression and cytokine secretion [144, 596]. Thus it was not possible to explore how different macrophage phenotypes might affect NK cells function in this model. Furthermore, MDMs are not as restrictive to IAV replication as airway macrophages and this could also affect the type of interactions MDMs have with NK cells [45].

7.12 Further Work

Since their discovery in the 1970s, NK cells have been found to contribute to numerous human infections, cancer and chronic inflammatory disease [200]. However, there is a lack of knowledge about how NK cells contribute infection and disease in the lungs. This thesis has explored some phenotypic and functional questions in relation to IAV infection, but there are a number of outstanding questions and areas for further work. For instance, novel populations of resident NK cells were identified within the lung parenchyma but the biology of these cells is largely unknown. Thus, further phenotypic analysis by FACS sorting and single cell transcriptomic analysis would benefit our understanding of the ways lung rNK cell function differ from conventional NK cells. In addition, both resident and non-resident lung NK cell trafficking could be assessed through immunofluorescent staining of healthy and IAV infected lung parenchyma. Furthermore,

preliminary data from this thesis showing enhanced function of lung resident NK cells should be extended. This could be done by developing co-culture models with lung NK cells against suitable infected targets. In addition, the systems driving this enhanced recall could be further explored through comparison of the cNK and rNK epigenetic state and by mechanistic analysis of rNK cell receptor ligation.

NK cells are well known for their production of IFN-γ but the production of other cytokines by both resident and circulating NK cells is poorly understood and rarely investigated. This thesis has provided pilot data indicating that circulating NK cells may have important pro-inflammatory effects through the production of IL-6, IL-16, TNF-α and CCL2 but further corroboration of this data is needed. Thus, lung resident and non-resident NK cell cytokine production could be analysed in IAV-infected lungs by flow cytometry or by transcriptomic analysis following sorting. This could also be investigated in MDM-NK or PBEC-NK cell co-cultures by ELISA, intracellular flow cytometry or RT-PCR following NK cell isolation.

In addition, analysis of how pro-inflammatory signaling controls NK cell activation to IAV-infected cells may fill in an important gap in the current understanding of anti-IAV immune responses. This could be done by sequential cytokine blocking in autologous co-cultures of either macrophages or epithelial cells. Further elucidation of the mechanism of NK cell activation to IAV-infected macrophages is also required, as NKp46 and NKG2D were found to be redundant [375]. In addition, the physical contacts driving NK cell activation to infected epithelial cells are currently unknown but could be further explored in the PBEC-NK cell model developed in this thesis. This is an important area for further work as it could reveal mechanisms by which NK cell function could be modulated. This thesis' findings in the MDM-NK cell co-culture could also be further confirmed by using lung macrophages in autologous co-culture. To do this, lung macrophages could be washed out of lung tissue and infected whilst NK cells are sorted from digested lung tissue by FACS or MACS.

In addition, NK cells may play important roles in combating other respiratory virus infection, such as RSV and rhinovirus (RV). For instance, NK cells have been shown to be recruited and activated during murine rhinovirus infection and are detrimental in a mouse model of RSV infection [597, 598]. Human NK cell responses to these viruses are less well understood but are important avenues for further work. For instance IFN-γ is a major stimulator of Th1 responses, and as RSV strongly stimulates a Th2 response it would be interesting to examine if this NK cell effector function is

perturbed during RSV infection [599]. No vaccines currently exist for either RSV or RV despite high mortality in children and exacerbation of chronic lung diseases such as COPD and asthma [600-603]. A better knowledge of the immune response to these infections is therefore required to reduce virus-related mortality [600-603].

Lastly, the role of human NK cells in bacterial and fungal lung infections is largely unexplored [568]. In mouse models NK cells promote clearance of respiratory infection by fungi *Cryptococcus neoformans* and *Aspergillus fumigatus* as well as bacterial species including *Bordetella pertussis, Francisella tularentis, Legionella pneumophila, Haemophilus influenzae, Pseudomonas aeruginosa* and *Staphylococcus aureus* [568]. NK cells have also been identified as detrimental to outcomes of *Streptococcus pneumoniae* infection [568]. Understanding the NK cell responses to lung infection is an important area of research as it could lead to new methods of manipulating pulmonary immunity during vaccination and disease [86, 604]. Furthermore, NK cell control of respiratory bacteria may be important in IAV pathogenesis as IAV-related lethality is associated with bacterial co-infection and secondary pneumonias [2, 6-13].

7.13 Summary

This thesis has shown that NK cells have potent cytotoxic and cytokine responses to IAV infection in lung tissue, responding to both infected epithelial cells and macrophages. Thus, NK cells have been shown to be capable of responding to human respiratory viral infection with potentially important contributions to anti-viral immunity in this organ. A newly identified resident NK cell population was also described in the lung parenchyma. This resident NK cell population responded to IAV infection, with enhanced degranulation and IFN-γ production relative to circulating NK cells. Increased residency marker expression was also found to correlate with COPD severity indicating dysregulation of these cells in chronic disease. Finally, NKG2D and NKp46 activating receptor signaling has been implicated in IAV-infected cell recognition but receptor ligation was found to be redundant during the NK cells response to IAV infected MDMs. Thus, there may be numerous mechanisms by which macrophages regulate NK cell function during respiratory infection, confirming the important interplay between these two innate immune cells. Further investigation into the mechanisms and regulation of respiratory NK cell activation may enable future modulation of NK cell function in the treatment of chronic disease and respiratory vaccination.

List of References

1. World Health Organisation. Influenza (Seasonal) Fact Sheet No 211. 2014 Nov 2016]; Available from: http://www.who.int/mediacentre/factsheets/fs211/en/.

2. Sheng, Z.M., D. Chertow, X. Ambroggio, S. McCalf, R.M. Przygodzki, R.E. Cunningham, O.A. Maximova, J.C. Kash, D.M. Morens and J.K. Taubenberger, 2011 Autopsy Series of 68 Cases Dying before and During the 1918 Influenza Pandemic Peak. *PNAS*. 108(39).

3. Joseph, C., Y. Togawa and N. Shindo, 2013 Bacterial and Viral Infections Associated with Influenza. *Influenza Other Respir Viruses*. 7 Suppl 2: p. 105.

4. Donaldson, G.C. and J.A. Wedzicha, 2006 Copd Exacerbations .1: Epidemiology. *Thorax*. 61(2): p. 164.

5. Mallia, P., M. Contoli, G. Caramori, A. Pandit, S.L. Johnston and A. Papi, 2007 Exacerbations of Asthma and Chronic Obstructive Pulmonary Disease (Copd): Focus on Virus Induced Exacerbations. *Curr Pharm Des*. 13(1): p. 73.

6. Li, W., B. Moltedo and T.M. Moran, 2012 Type I Interferon Induction During Influenza Virus Infection Increases Susceptibility to Secondary Streptococcus Pneumoniae Infection by Negative Regulation of Γδ T Cells. *Journal of Virology*. 86(22): p. 12304.

7. Shahangian, A., E.K. Chow, X. Tian, J.R. Kang, A. Ghaffari, S.Y. Liu, J.A. Belperio, G. Cheng and J.C. Deng, 2009 Type I Ifns Mediate Development of Postinfluenza Bacterial Pneumonia in Mice. *J Clin Invest*. 119(7): p. 1910.

8. Sun, K. and D.W. Metzger, 2008 Inhibition of Pulmonary Antibacterial Defense by Interferon-[Gamma] During Recovery from Influenza Infection. *Nat Med*. 14(5): p. 558.

9. McNamee, L.A. and A.G. Harmsen, 2006 Both Influenza-Induced Neutrophil Dysfunction and Neutrophil-Independent Mechanisms Contribute to Increased Susceptibility to a Secondary Streptococcus Pneumoniae Infection. *Infection and Immunity*. 74(12): p. 6707.

10. Simonsen, L., M.J. Clarke, G.D. Williamson, D.F. Stroup, N.H. Arden and L.B. Schonberger, 1997 The Impact of Influenza Epidemics on Mortality: Introducing a Severity Index. *Am J Public Health*. 87(12): p. 1944.

11. LeVine, A.M., V. Koeningsknecht and J.M. Stark, 2001 Decreased Pulmonary Clearance of S. Pneumoniae Following Influenza a Infection in Mice. *J Virol Methods*. 94(1-2): p. 173.

12. Jakab, G.J., G.A. Warr and M.E. Knight, 1979 Pulmonary and Systemic Defenses against Challenge with Staphylococcus Aureus in Mice with Pneumonia Due to Influenza a Virus. *J Infect Dis*. 140(1): p. 105.

13. Simonsen, L., K. Fukuda, L.B. Schonberger and N.J. Cox, 2000 The Impact of Influenza Epidemics on Hospitalizations. *J Infect Dis*. 181(3): p. 831.

14. Mossad, S.B., 2016 Influenza: Still More Important Than Zika Virus in 2016-2017. *Cleve Clin J Med*. 83(11): p. 836.

15. Loo, Y.-M. and M. Gale, 2007 Influenza: Fatal Immunity and the 1918 Virus. *Nature*. 445(7125): p. 267.

16. CDC Centres for Disease Control and Prevention, 2010 Estimates of Deaths Associated with Seasonal Influenza - Unites States, 1976-2007. *Accessed Jan 2015*. http://www.cdc.gov/mmwr/preview/mmwrhtml/mm5933a1.htm.

17. Horimoto, T. and Y. Kawaoka, 2001 Pandemic Threat Posed by Avian Influenza a Viruses. *Clin Microbiol Rev*. 14(1): p. 129.

18. Wedzicha, J.A., 2004 Role of Viruses in Exacerbations of Chronic Obstructive Pulmonary Disease. *Proc Am Thorac Soc*. 1(2): p. 115.

19. Seemungal, T.A., G.C. Donaldson, A. Bhowmik, D.J. Jeffries and J.A. Wedzicha, 2000 Time Course and Recovery of Exacerbations in Patients with Chronic Obstructive Pulmonary Disease. *Am J Respir Crit Care Med*. 161(5): p. 1608.

20. Seemungal, T., R. Harper-Owen, A. Bhowmik, I. Moric, G. Sanderson, S. Message, P. Maccallum, T.W. Meade, D.J. Jeffries, S.L. Johnston and J.A. Wedzicha, 2001 Respiratory Viruses, Symptoms, and Inflammatory Markers in Acute Exacerbations and Stable Chronic Obstructive Pulmonary Disease. *Am J Respir Crit Care Med*. 164(9): p. 1618.

21. Aaron, S.D., 2014 Management and Prevention of Exacerbations of Copd. *BMJ*. 349.

22. Neumann, G., T. Noda and Y. Kawaoka, 2009 Emergence and Pandemic Potential of Swine-Origin H1n1 Influenza Virus. *Nature*. 459(7249): p. 931.

23. Eisfeld, A.J., G. Neumann and Y. Kawaoka, 2015 At the Centre: Influenza a Virus Ribonucleoproteins. *Nat Rev Micro*. 13(1): p. 28.

24. Weis, W., J.H. Brown, S. Cusack, J.C. Paulson, J.J. Skehel and D.C. Wiley, 1988 Structure of the Influenza Virus Haemagglutinin Complexed with Its Receptor, Sialic Acid. *Nature*. 333(6172): p. 426.

25. Rogers, G.N., J.C. Paulson, R.S. Daniels, J.J. Skehel, I.A. Wilson and D.C. Wiley, 1983 Single Amino Acid Substitutions in Influenza Haemagglutinin Change Receptor Binding Specificity. *Nature*. 304(5921): p. 76.

26. Shtyrya, Y.A., L.V. Mochalova and N.V. Bovin, 2009 Influenza Virus Neuraminidase: Structure and Function. *Acta naturae*. 1(2): p. 26.

27. Neverov, A.D., S. Kryazhimskiy, J.B. Plotkin and G.A. Bazykin, 2015 Coordinated Evolution of Influenza a Surface Proteins. *PLOS Genetics*. 11(8): p. e1005404.

28. Gultyaev, A.P., M.I. Spronken, M. Richard, E.J.A. Schrauwen, R.C.L. Olsthoorn and R.A.M. Fouchier, 2016 Subtype-Specific Structural Constraints in the Evolution of Influenza a Virus Hemagglutinin Genes. *Scientific Reports*. 6: p. 38892.

29. Centers for Disease Control and Prevention. Summary of the 2015-2016 Influenza Season. 2016 22/11/2016]; Available from: http://www.cdc.gov/flu/about/season/flu-season-2015-2016.htm.

30. Centers for Disease Control and Prevention. 2013-2014 Influenza Season. 2014 22/11/2016]; Available from: http://www.cdc.gov/flu/pastseasons/1314season.htm.

31. Sieczkarski, S.B. and G.R. Whittaker, 2002 Influenza Virus Can Enter and Infect Cells in the Absence of Clathrin-Mediated Endocytosis. *Journal of Virology*. 76(20): p. 10455.

32. Rust, M.J., M. Lakadamyali, F. Zhang and X. Zhuang, 2004 Assembly of Endocytic Machinery around Individual Influenza Viruses During Viral Entry. *Nat Struct Mol Biol*. 11(6): p. 567.

33. Chen, C. and X. Zhuang, 2008 Epsin 1 Is a Cargo-Specific Adaptor for the Clathrin-Mediated Endocytosis of the Influenza Virus. *Proceedings of the National Academy of Sciences*. 105(33): p. 11790.

34. Yoshimura, A. and S. Ohnishi, 1984 Uncoating of Influenza Virus in Endosomes. *J Virol*. 51(2): p. 497.

35. Pinto, L.H. and R.A. Lamb, 2006 The M2 Proton Channels of Influenza a and B Viruses. *Journal of Biological Chemistry*. 281(14): p. 8997.

36. Wiley, D.C. and J.J. Skehel, 1987 The Structure and Function of the Hemagglutinin Membrane Glycoprotein of Influenza Virus. *Annu Rev Biochem*. 56: p. 365.

37. Carr, C.M., C. Chaudhry and P.S. Kim, 1997 Influenza Hemagglutinin Is Spring-Loaded by a Metastable Native Conformation. *Proceedings of the National Academy of Sciences*. 94(26): p. 14306.

38. Martin, K. and A. Helenius, 1991 Transport of Incoming Influenza Virus Nucleocapsids into the Nucleus. *J Virol*. 65(1): p. 232.

39. Jackson, D.A., A.J. Caton, S.J. McCready and P.R. Cook, 1982 Influenza Virus Rna Is Synthesized at Fixed Sites in the Nucleus. *Nature*. 296(5855): p. 366.

40. Kummer, S., M. Flöttmann, B. Schwanhäusser, C. Sieben, M. Veit, M. Selbach, E. Klipp and A. Herrmann, 2014 Alteration of Protein Levels During Influenza Virus H1n1 Infection in Host Cells: A Proteomic Survey of Host and Virus Reveals Differential Dynamics. *PLOS ONE*. 9(4): p. e94257.

41. Nayak, D.P., E.K.-W. Hui and S. Barman, 2004 Assembly and Budding of Influenza Virus. *Virus Research*. 106(2): p. 147.

42. Meier-Ewert, H. and R.W. Compans, 1974 Time Course of Synthesis and Assembly of Influenza Virus Proteins. *Journal of Virology*. 14(5): p. 1083.

43. Baccam, P., C. Beauchemin, C.A. Macken, F.G. Hayden and A.S. Perelson, 2006 Kinetics of Influenza a Virus Infection in Humans. *Journal of Virology*. 80(15): p. 7590.

44. Upham, J.P., D. Pickett, T. Irimura, E.M. Anders and P.C. Reading, 2010 Macrophage Receptors for Influenza a Virus: Role of the Macrophage Galactose-Type Lectin and Mannose Receptor in Viral Entry. *Journal of Virology*. 84(8): p. 3730.

45. Cline, T.D., D. Beck and E. Bianchini, 2017 Influenza Virus Replication in Macrophages: Balancing Protection and Pathogenesis. *The Journal of general virology*. 98(10): p. 2401.

46. Gill, J.R., Z.M. Sheng, S.F. Ely, D.G. Guinee, M.B. Beasley, J. Suh, C. Deshpande, D.J. Mollura, D.M. Morens, M. Bray, W.D. Travis and J.K. Taubenberger, 2010 Pulmonary Pathologic

Findings of Fatal 2009 Pandemic Influenza a/H1n1 Viral Infections. *Arch Pathol Lab Med*. 134(2): p. 235.

47. Chen, Y., W. Deng, C. Jia, X. Dai, H. Zhu, Q. Kong, L. Huang, Y. Liu, C. Ma, J. Li, C. Xiao, Y. Liu, Q. Wei and C. Qin, 2009 Pathological Lesions and Viral Localization of Influenza a (H5n1) Virus in Experimentally Infected Chinese Rhesus Macaques: Implications for Pathogenesis and Viral Transmission. *Arch Virol*. 154(2): p. 227.

48. Lohr, C.V., E.E. DeBess, R.J. Baker, S.L. Hiett, K.A. Hoffman, V.J. Murdoch, K.A. Fischer, D.M. Mulrooney, R.L. Selman and W.M. Hammill-Black, 2010 Pathology and Viral Antigen Distribution of Lethal Pneumonia in Domestic Cats Due to Pandemic (H1n1) 2009 Influenza a Virus. *Vet Pathol*. 47(3): p. 378.

49. Powe, J.R. and W.L. Castleman, 2009 Canine Influenza Virus Replicates in Alveolar Macrophages and Induces Tnf-Alpha. *Vet Pathol*. 46(6): p. 1187.

50. Yu, W.C., R.W. Chan, J. Wang, E.A. Travanty, J.M. Nicholls, J.S. Peiris, R.J. Mason and M.C. Chan, 2011 Viral Replication and Innate Host Responses in Primary Human Alveolar Epithelial Cells and Alveolar Macrophages Infected with Influenza H5n1 and H1n1 Viruses. *J Virol*. 85(14): p. 6844.

51. Rodgers, B. and C.A. Mims, 1981 Interaction of Influenza Virus with Mouse Macrophages. *Infection and Immunity*. 31(2): p. 751.

52. Lehmann, C., H. Sprenger, M. Nain, M. Bacher and D. Gemsa, 1996 Infection of Macrophages by Influenza a Virus: Characteristics of Tumour Necrosis Factor-A (Tnfα) Gene Expression. *Research in Virology*. 147(2): p. 123.

53. Tate, M.D., D.L. Pickett, N. van Rooijen, A.G. Brooks and P.C. Reading, 2010 Critical Role of Airway Macrophages in Modulating Disease Severity During Influenza Virus Infection of Mice. *J Virol*. 84(15): p. 7569.

54. Duan, M., M.L. Hibbs and W. Chen, 2017 The Contributions of Lung Macrophage and Monocyte Heterogeneity to Influenza Pathogenesis. *Immunol Cell Biol*. 95(3): p. 225.

55. Hurt, A.C., P. Selleck, N. Komadina, R. Shaw, L. Brown and I.G. Barr, 2007 Susceptibility of Highly Pathogenic a(H5n1) Avian Influenza Viruses to the Neuraminidase Inhibitors and Adamantanes. *Antiviral Research*. 73(3): p. 228.

56. Sheu, T.G., A.M. Fry, R.J. Garten, V.M. Deyde, T. Shwe, L. Bullion, P.J. Peebles, Y. Li, A.I. Klimov and L.V. Gubareva, 2011 Dual Resistance to Adamantanes and Oseltamivir among Seasonal Influenza a(H1n1) Viruses: 2008–2010. *Journal of Infectious Diseases*. 203(1): p. 13.

57. Deyde, V.M., X. Xu, R.A. Bright, M. Shaw, C.B. Smith, Y. Zhang, Y. Shu, L.V. Gubareva, N.J. Cox and A.I. Klimov, 2007 Surveillance of Resistance to Adamantanes among Influenza a(H3n2) and a(H1n1) Viruses Isolated Worldwide. *Journal of Infectious Diseases*. 196(2): p. 249.

58. Dharan, N.J., L.V. Gubareva, J.J. Meyer and et al., 2009 Infections with Oseltamivir-Resistant Influenza a(H1n1) Virus in the United States. *JAMA*. 301(10): p. 1034.

59. Krammer, F. and P. Palese, 2015 Advances in the Development of Influenza Virus Vaccines. *Nat Rev Drug Discov*. 14(3): p. 167.

60. Greenberg, H.B. and P.A. Piedra, 2004 Immunization against Viral Respiratory Disease: A Review. *Pediatr Infect Dis J*. 23(11 Suppl): p. S254.

61. Hoft, D.F.*, et al.*, 2011 Live and Inactivated Influenza Vaccines Induce Similar Humoral Responses, but Only Live Vaccines Induce Diverse T-Cell Responses in Young Children. *Journal of Infectious Diseases*. 204(6): p. 845.

62. Soema, P.C., R. Kompier, J.-P. Amorij and G.F.A. Kersten, 2015 Current and Next Generation Influenza Vaccines: Formulation and Production Strategies. *European Journal of Pharmaceutics and Biopharmaceutics*. 94: p. 251.

63. Coffman, R.L., A. Sher and R.A. Seder, 2010 Vaccine Adjuvants: Putting Innate Immunity to Work. *Immunity*. 33(4): p. 492.

64. Iwasaki, A. and P.S. Pillai, 2014 Innate Immunity to Influenza Virus Infection. *Nat Rev Immunol*. 14(5): p. 315.

65. Iwasaki, A. and R. Medzhitov, 2015 Control of Adaptive Immunity by the Innate Immune System. *Nat Immunol*. 16(4): p. 343.

66. Barnes, P.J., 2000 Chronic Obstructive Pulmonary Disease. *New England Journal of Medicine*. 343(4): p. 269.

67. World Health Organisation. The Top 10 Causes of Death. 2014 [Accessed 07/08/2015]; Available from: http://www.who.int/mediacentre/factsheets/fs310/en/.

68. US Department of Health and Human Service. The Health Consequences of Smoking-50 Years of Progress: A Report of the Surgeon General. 2014 [Accessed 07/08/2015]]; Available from: http://www.surgeongeneral.gov/library/reports/50-years-of-progress/.

69. Lindberg, A., B. Eriksson, L.G. Larsson, E. Ronmark, T. Sandstrom and B. Lundback, 2006 Seven-Year Cumulative Incidence of Copd in an Age-Stratified General Population Sample. *Chest*. 129(4): p. 879.

70. Sze, M.A., P.A. Dimitriu, S. Hayashi, W.M. Elliott, J.E. McDonough, J.V. Gosselink, J. Cooper, D.D. Sin, W.W. Mohn and J.C. Hogg, 2012 The Lung Tissue Microbiome in Chronic Obstructive Pulmonary Disease. *Am J Respir Crit Care Med*. 185(10): p. 1073.

71. Annoni, R., T. Lancas, R. Yukimatsu Tanigawa, M. de Medeiros Matsushita, S. de Morais Fernezlian, A. Bruno, L. Fernando Ferraz da Silva, P.J. Roughley, S. Battaglia, M. Dolhnikoff, P.S. Hiemstra, P.J. Sterk, K.F. Rabe and T. Mauad, 2012 Extracellular Matrix Composition in Copd. *Eur Respir J*. 40(6): p. 1362.

72. Gogebakan, B., R. Bayraktar, M. Ulasli, S. Oztuzcu, D. Tasdemir and H. Bayram, 2014 The Role of Bronchial Epithelial Cell Apoptosis in the Pathogenesis of Copd. *Mol Biol Rep*. 41(8): p. 5321.

73. Bhat, T.A., L. Panzica, S.G. Kalathil and Y. Thanavala, 2015 Immune Dysfunction in Patients with Chronic Obstructive Pulmonary Disease. *Annals of the American Thoracic Society*. 12 Suppl 2(Suppl 2): p. S169.

74. Sze, M.A., J.C. Hogg and D.D. Sin, 2014 Bacterial Microbiome of Lungs in Copd. *Int J Chron Obstruct Pulmon Dis*. 9: p. 229.

75. Wu, D., C. Hou, Y. Li, Z. Zhao, J. Liu, X. Lu, X. Shang and Y. Xin, 2014 Analysis of the Bacterial Community in Chronic Obstructive Pulmonary Disease Sputum Samples by Denaturing Gradient Gel Electrophoresis and Real-Time Pcr. *BMC Pulm Med*. 14: p. 179.

76. Huang, Y.J., E. Kim, M.J. Cox, E.L. Brodie, R. Brown, J.P. Wiener-Kronish and S.V. Lynch, 2010 A Persistent and Diverse Airway Microbiota Present During Chronic Obstructive Pulmonary Disease Exacerbations. *Omics*. 14(1): p. 9.

77. Hilty, M., C. Burke, H. Pedro, P. Cardenas, A. Bush, C. Bossley, J. Davies, A. Ervine, L. Poulter, L. Pachter, M.F. Moffatt and W.O. Cookson, 2010 Disordered Microbial Communities in Asthmatic Airways. *PLoS One*. 5(1): p. e8578.

78. Di Marco, F., P. Santus, N. Scichilone, P. Solidoro, M. Contoli, F. Braido and A.G. Corsico, 2017 Symptom Variability and Control in Copd: Advantages of Dual Bronchodilation Therapy. *Respir Med*. 125: p. 49.

79. Chalmers, J.D., A. Tebboth, A. Gayle, A. Ternouth and N. Ramscar, 2017 Determinants of Initial Inhaled Corticosteroid Use in Patients with Gold a/B Copd: A Retrospective Study of Uk General Practice. *NPJ Prim Care Respir Med*. 27(1): p. 43.

80. Andersson, F., S. Borg, S.-A. Jansson, A.-C. Jonsson, Å. Ericsson, C. PrÜTz, E.V.A. RÖNmark and B.O. LundbÄCk, 2002 The Costs of Exacerbations in Chronic Obstructive Pulmonary Disease (Copd). *Respiratory Medicine*. 96(9): p. 700.

81. Bhatt, S.*, et al.*, 2013 The Global Distribution and Burden of Dengue. *Nature*. 496(7446): p. 504.

82. Shaykhiev, R. and R.G. Crystal, 2013 Innate Immunity and Chronic Obstructive Pulmonary Disease: A Mini-Review. *Gerontology*. 59(6): p. 481.

83. Manzel, L.J., L. Shi, P.T. O'Shaughnessy, P.S. Thorne and D.C. Look, 2011 Inhibition by Cigarette Smoke of Nuclear Factor-Kappab-Dependent Response to Bacteria in the Airway. *Am J Respir Cell Mol Biol*. 44(2): p. 155.

84. Pilette, C., V. Godding, R. Kiss, M. Delos, E. Verbeken, C. Decaestecker, K. De Paepe, J.P. Vaerman, M. Decramer and Y. Sibille, 2001 Reduced Epithelial Expression of Secretory Component in Small Airways Correlates with Airflow Obstruction in Chronic Obstructive Pulmonary Disease. *Am J Respir Crit Care Med*. 163(1): p. 185.

85. Taylor, A.E., T.K. Finney-Hayward, J.K. Quint, C.M. Thomas, S.J. Tudhope, J.A. Wedzicha, P.J. Barnes and L.E. Donnelly, 2010 Defective Macrophage Phagocytosis of Bacteria in Copd. *Eur Respir J*. 35(5): p. 1039.

86. Finch, D.K., V.R. Stolberg, J. Ferguson, H. Alikaj, M.R. Kady, B.W. Richmond, V.V. Polosukhin, T.S. Blackwell, L. McCloskey, J.L. Curtis and C.M. Freeman, 2018 Lung Dendritic Cells Drive Nk Cytotoxicity in Chronic Obstructive Pulmonary Disease Via Il-15ralpha. *Am J Respir Crit Care Med*.

87. Van Pottelberge, G.R., K.R. Bracke, I.K. Demedts, K. De Rijck, S.M. Reinartz, C.M. van Drunen, G.M. Verleden, F.E. Vermassen, G.F. Joos and G.G. Brusselle, 2010 Selective Accumulation of Langerhans-Type Dendritic Cells in Small Airways of Patients with Copd. *Respir Res*. 11: p. 35.

88. Hoenderdos, K. and A. Condliffe, 2013 The Neutrophil in Chronic Obstructive Pulmonary Disease. *Am J Respir Cell Mol Biol*. 48(5): p. 531.

89. Fan, V.S., S.A. Gharib, T.R. Martin and M.M. Wurfel, 2016 Copd Disease Severity and Innate Immune Response to Pathogen-Associated Molecular Patterns. *International journal of chronic obstructive pulmonary disease*. 11: p. 467.

90. Wedzicha, J.A. and T.A.R. Seemungal, 2007 Copd Exacerbations: Defining Their Cause and Prevention. *The Lancet*. 370(9589): p. 786.

91. Seemungal, T.A., G.C. Donaldson, E.A. Paul, J.C. Bestall, D.J. Jeffries and J.A. Wedzicha, 1998 Effect of Exacerbation on Quality of Life in Patients with Chronic Obstructive Pulmonary Disease. *Am J Respir Crit Care Med*. 157(5 Pt 1): p. 1418.

92. Mallia, P*., et al.*, 2011 Experimental Rhinovirus Infection as a Human Model of Chronic Obstructive Pulmonary Disease Exacerbation. *Am J Respir Crit Care Med*. 183(6): p. 734.

93. Rohde, G., A. Wiethege, I. Borg, M. Kauth, T.T. Bauer, A. Gillissen, A. Bufe and G. Schultze-Werninghaus, 2003 Respiratory Viruses in Exacerbations of Chronic Obstructive Pulmonary Disease Requiring Hospitalisation: A Case-Control Study. *Thorax*. 58(1): p. 37.

94. Tan, W.C., X. Xiang, D. Qiu, T.P. Ng, S.F. Lam and R.G. Hegele, 2003 Epidemiology of Respiratory Viruses in Patients Hospitalized with near-Fatal Asthma, Acute Exacerbations of Asthma, or Chronic Obstructive Pulmonary Disease. *Am J Med*. 115(4): p. 272.

95. Neuzil, K.M., T.Z. O'Connor, G.J. Gorse and K.L. Nichol, 2003 Recognizing Influenza in Older Patients with Chronic Obstructive Pulmonary Disease Who Have Received Influenza Vaccine. *Clin Infect Dis*. 36(2): p. 169.

96. Beckham, J.D., A. Cadena, J. Lin, P.A. Piedra, W.P. Glezen, S.B. Greenberg and R.L. Atmar, 2005 Respiratory Viral Infections in Patients with Chronic, Obstructive Pulmonary Disease. *J Infect*. 50(4): p. 322.

97. Papi, A., C.M. Bellettato, F. Braccioni, M. Romagnoli, P. Casolari, G. Caramori, L.M. Fabbri and S.L. Johnston, 2006 Infections and Airway Inflammation in Chronic Obstructive Pulmonary Disease Severe Exacerbations. *Am J Respir Crit Care Med*. 173(10): p. 1114.

98. Bekkat-Berkani, R., T. Wilkinson, P. Buchy, G. Dos Santos, D. Stefanidis, J.-M. Devaster and N. Meyer, 2017 Seasonal Influenza Vaccination in Patients with Copd: A Systematic Literature Review. *BMC Pulmonary Medicine*. 17(1): p. 79.

99. Wang, J., M.P. Nikrad, T. Phang, B. Gao, T. Alford, Y. Ito, K. Edeen, E.A. Travanty, B. Kosmider, K. Hartshorn and R.J. Mason, 2011 Innate Immune Response to Influenza a Virus in Differentiated Human Alveolar Type Ii Cells. *Am J Respir Cell Mol Biol*. 45(3): p. 582.

100. Sareneva, T., S. Matikainen, M. Kurimoto and I. Julkunen, 1998 Influenza a Virus-Induced Ifn-A/B and Il-18 Synergistically Enhance Ifn-Γ Gene Expression in Human T Cells. *The Journal of Immunology*. 160(12): p. 6032.

101. Pommerenke, C., E. Wilk, B. Srivastava, A. Schulze, N. Novoselova, R. Geffers and K. Schughart, 2012 Global Transcriptome Analysis in Influenza-Infected Mouse Lungs Reveals the Kinetics of Innate and Adaptive Host Immune Responses. *PLOS ONE*. 7(7): p. e41169.

102. Wilkinson, T.M.*, et al.*, 2012 Preexisting Influenza-Specific Cd4+ T Cells Correlate with Disease Protection against Influenza Challenge in Humans. *Nat Med*. 18(2): p. 274.

103. Eichelberger, M., W. Allan, M. Zijlstra, R. Jaenisch and P.C. Doherty, 1991 Clearance of Influenza Virus Respiratory Infection in Mice Lacking Class I Major Histocompatibility Complex-Restricted Cd8+ T Cells. *The Journal of Experimental Medicine*. 174(4): p. 875.

104. Bender, B.S., T. Croghan, L. Zhang and P.A. Small, 1992 Transgenic Mice Lacking Class I Major Histocompatibility Complex-Restricted T Cells Have Delayed Viral Clearance and Increased Mortality after Influenza Virus Challenge. *The Journal of Experimental Medicine*. 175(4): p. 1143.

105. Taubenberger, J.K. and D.M. Morens, 2008 The Pathology of Influenza Virus Infections. *Annu Rev Pathol*. 3: p. 499.

106. Nakaya, H.I.*, et al.*, 2015 Systems Analysis of Immunity to Influenza Vaccination across Multiple Years and in Diverse Populations Reveals Shared Molecular Signatures. *Immunity*. 43(6): p. 1186.

107. Stein-Streilein, J. and J. Guffee, 1986 In Vivo Treatment of Mice and Hamsters with Antibodies to Asialo Gm1 Increases Morbidity and Mortality to Pulmonary Influenza Infection. *J Immunol*. 136(4): p. 1435.

108. Gazit, R., R. Gruda, M. Elboim, T.I. Arnon, G. Katz, H. Achdout, J. Hanna, U. Qimron, G. Landau, E. Greenbaum, Z. Zakay-Rones, A. Porgador and O. Mandelboim, 2006 Lethal Influenza Infection in the Absence of the Natural Killer Cell Receptor Gene Ncr1. *Nat Immunol*. 7(5): p. 517.

109. Nogusa, S., B.W. Ritz, S.H. Kassim, S.R. Jennings and E.M. Gardner, 2008 Characterization of Age-Related Changes in Natural Killer Cells During Primary Influenza Infection in Mice. *Mech Ageing Dev*. 129(4): p. 223.

110. Kumar, P., M.S. Thakar, W. Ouyang and S. Malarkannan, 2013 Il-22 from Conventional Nk Cells Is Epithelial Regenerative and Inflammation Protective During Influenza Infection. *Mucosal Immunol*. 6(1): p. 69.

111. Abdul-Careem, M.F., M.F. Mian, G. Yue, A. Gillgrass, M.J. Chenoweth, N.G. Barra, M.V. Chew, T. Chan, A.A. Al-Garawi, M. Jordana and A.A. Ashkar, 2012 Critical Role of Natural Killer Cells in Lung Immunopathology During Influenza Infection in Mice. *J Infect Dis*. 206(2): p. 167.

112. Zhou, G., S.W. Juang and K.P. Kane, 2013 Nk Cells Exacerbate the Pathology of Influenza Virus Infection in Mice. *Eur J Immunol*. 43(4): p. 929.

113. Zhou, K., J. Wang, A. Li, W. Zhao, D. Wang, W. Zhang, J. Yan, G.F. Gao, W. Liu and M. Fang, 2016 Swift and Strong Nk Cell Responses Protect 129 Mice against High-Dose Influenza Virus Infection. *J Immunol*. 196(4): p. 1842.

114. Chen, X., S. Liu, M.U. Goraya, M. Maarouf, S. Huang and J.-L. Chen, 2018 Host Immune Response to Influenza a Virus Infection. *Frontiers in immunology*. 9: p. 320.

115. Alexopoulou, L., A.C. Holt, R. Medzhitov and R.A. Flavell, 2001 Recognition of Double-Stranded Rna and Activation of Nf-Kappab by Toll-Like Receptor 3. *Nature*. 413(6857): p. 732.

116. Le Goffic, R., J. Pothlichet, D. Vitour, T. Fujita, E. Meurs, M. Chignard and M. Si-Tahar, 2007 Cutting Edge: Influenza a Virus Activates Tlr3-Dependent Inflammatory and Rig-I-Dependent Antiviral Responses in Human Lung Epithelial Cells. *J Immunol*. 178(6): p. 3368.

117. Kroeker, A.L., P. Ezzati, A.J. Halayko and K.M. Coombs, 2012 Response of Primary Human Airway Epithelial Cells to Influenza Infection: A Quantitative Proteomic Study. *Journal of proteome research*. 11(8): p. 4132.

118. Stegemann-Koniszewski, S., A. Jeron, M. Gereke, R. Geffers, A. Kröger, M. Gunzer and D. Bruder, 2016 Alveolar Type Ii Epithelial Cells Contribute to the Anti-Influenza a Virus Response in the Lung by Integrating Pathogen- and Microenvironment-Derived Signals. *mBio*. 7(3): p. e00276.

119. Haller, O., H. Arnheiter, I. Gresser and J. Lindenmann, 1979 Genetically Determined, Interferon-Dependent Resistance to Influenza Virus in Mice. *The Journal of Experimental Medicine*. 149(3): p. 601.

120. Schoggins, J.W., S.J. Wilson, M. Panis, M.Y. Murphy, C.T. Jones, P. Bieniasz and C.M. Rice, 2011 A Diverse Range of Gene Products Are Effectors of the Type I Interferon Antiviral Response. *Nature*. 472(7344): p. 481.

121. Helft, J*., et al.*, Cross-Presenting Cd103+ Dendritic Cells Are Protected from Influenza Virus Infection. *The Journal of Clinical Investigation*. 122(11): p. 4037.

122. Ank, N., M.B. Iversen, C. Bartholdy, P. Staeheli, R. Hartmann, U.B. Jensen, F. Dagnaes-Hansen, A.R. Thomsen, Z. Chen, H. Haugen, K. Klucher and S.R. Paludan, 2008 An Important Role for Type Iii Interferon (Ifn-Λ/Il-28) in Tlr-Induced Antiviral Activity. *The Journal of Immunology*. 180(4): p. 2474.

123. Ank, N., H. West, C. Bartholdy, K. Eriksson, A.R. Thomsen and S.R. Paludan, 2006 Lambda Interferon (Ifn-Lambda), a Type Iii Ifn, Is Induced by Viruses and Ifns and Displays Potent Antiviral Activity against Select Virus Infections in Vivo. *Journal of virology*. 80(9): p. 4501.

124. Crotta, S., S. Davidson, T. Mahlakoiv, C.J. Desmet, M.R. Buckwalter, M.L. Albert, P. Staeheli and A. Wack, 2013 Type I and Type Iii Interferons Drive Redundant Amplification Loops to Induce a Transcriptional Signature in Influenza-Infected Airway Epithelia. *PLOS Pathogens*. 9(11): p. e1003773.

125. Ioannidis, I., B. McNally, M. Willette, M.E. Peeples, D. Chaussabel, J.E. Durbin, O. Ramilo, A. Mejias and E. Flaño, 2012 Plasticity and Virus Specificity of the Airway Epithelial Cell Immune Response During Respiratory Virus Infection. *Journal of Virology*. 86(10): p. 5422.

126. Kim, H.M., Y.-W. Lee, K.-J. Lee, H.S. Kim, S.W. Cho, N. van Rooijen, Y. Guan and S.H. Seo, 2008 Alveolar Macrophages Are Indispensable for Controlling Influenza Viruses in Lungs of Pigs. *Journal of Virology*. 82(9): p. 4265.

127. Tumpey, T.M., A. Garcia-Sastre, J.K. Taubenberger, P. Palese, D.E. Swayne, M.J. Pantin-Jackwood, S. Schultz-Cherry, A. Solorzano, N. Van Rooijen, J.M. Katz and C.F. Basler, 2005 Pathogenicity of Influenza Viruses with Genes from the 1918 Pandemic Virus: Functional Roles of Alveolar Macrophages and Neutrophils in Limiting Virus Replication and Mortality in Mice. *J Virol*. 79(23): p. 14933.

128. Schneider, C., S.P. Nobs, A.K. Heer, M. Kurrer, G. Klinke, N. van Rooijen, J. Vogel and M. Kopf, 2014 Alveolar Macrophages Are Essential for Protection from Respiratory Failure and Associated Morbidity Following Influenza Virus Infection. *PLoS Pathog*. 10(4): p. e1004053.

129. Purnama, C., S.L. Ng, P. Tetlak, Y.A. Setiagani, M. Kandasamy, S. Baalasubramanian, K. Karjalainen and C. Ruedl, 2014 Transient Ablation of Alveolar Macrophages Leads to Massive Pathology of Influenza Infection without Affecting Cellular Adaptive Immunity. *Eur J Immunol*. 44(7): p. 2003.

130. Huang, F.F., P.F. Barnes, Y. Feng, R. Donis, Z.C. Chroneos, S. Idell, T. Allen, D.R. Perez, J.A. Whitsett, K. Dunussi-Joannopoulos and H. Shams, 2011 Gm-Csf in the Lung Protects against Lethal Influenza Infection. *Am J Respir Crit Care Med*. 184(2): p. 259.

131. Gordon, S.B. and R.C. Read, 2002 Macrophage Defences against Respiratory Tract Infections. *Br Med Bull*. 61: p. 45.

132. Murray, P.J. and T.A. Wynn, 2011 Protective and Pathogenic Functions of Macrophage Subsets. *Nat Rev Immunol*. 11(11): p. 723.

133. Scott, M.J., J.J. Hoth, M.K. Stagner, S.A. Gardner, J.C. Peyton and W.G. Cheadle, 2004 Cd40-Cd154 Interactions between Macrophages and Natural Killer Cells During Sepsis Are Critical for Macrophage Activation and Are Not Interferon Gamma Dependent. *Clin Exp Immunol*. 137(3): p. 469.

134. Wang, J., M.P. Nikrad, E.A. Travanty, B. Zhou, T. Phang, B. Gao, T. Alford, Y. Ito, P. Nahreini, K. Hartshorn, D. Wentworth, C.A. Dinarello and R.J. Mason, 2012 Innate Immune Response of Human Alveolar Macrophages During Influenza a Infection. *PLoS One*. 7(3): p. e29879.

135. Westphalen, K., G.A. Gusarova, M.N. Islam, M. Subramanian, T.S. Cohen, A.S. Prince and J. Bhattacharya, 2014 Sessile Alveolar Macrophages Communicate with Alveolar Epithelium to Modulate Immunity. *Nature*. 506(7489): p. 503.

136. Kumagai, Y., O. Takeuchi, H. Kato, H. Kumar, K. Matsui, E. Morii, K. Aozasa, T. Kawai and S. Akira, 2007 Alveolar Macrophages Are the Primary Interferon-Alpha Producer in Pulmonary Infection with Rna Viruses. *Immunity*. 27(2): p. 240.

137. Arndt, U., G. Wennemuth, P. Barth, M. Nain, Y. Al-Abed, A. Meinhardt, D. Gemsa and M. Bacher, 2002 Release of Macrophage Migration Inhibitory Factor and Cxcl8/Interleukin-8 from Lung Epithelial Cells Rendered Necrotic by Influenza a Virus Infection. *Journal of Virology*. 76(18): p. 9298.

138. Sakai, S., H. Kawamata, N. Mantani, T. Kogure, Y. Shimada, K. Terasawa, T. Sakai, N. Imanishi and H. Ochiai, 2000 Therapeutic Effect of Anti-Macrophage Inflammatory Protein 2 Antibody on Influenza Virus-Induced Pneumonia in Mice. *Journal of Virology*. 74(5): p. 2472.

139. Tate, M.D., L.J. Ioannidis, B. Croker, L.E. Brown, A.G. Brooks and P.C. Reading, 2011 The Role of Neutrophils During Mild and Severe Influenza Virus Infections of Mice. *PLOS ONE*. 6(3): p. e17618.

140. Hashimoto, Y., T. Moki, T. Takizawa, A. Shiratsuchi and Y. Nakanishi, 2007 Evidence for Phagocytosis of Influenza Virus-Infected, Apoptotic Cells by Neutrophils and Macrophages in Mice. *J Immunol*. 178(4): p. 2448.

141. Kaufmann, A., R. Salentin, R.G. Meyer, D. Bussfeld, C. Pauligk, H. Fesq, P. Hofmann, M. Nain, D. Gemsa and H. Sprenger, 2001 Defense against Influenza a Virus Infection: Essential Role of the Chemokine System. *Immunobiology*. 204(5): p. 603.

142. Peschke, T., A. Bender, M. Nain and D. Gemsa, 1993 Role of Macrophage Cytokines in Influenza a Virus Infections. *Immunobiology*. 189(3-4): p. 340.

143. Nain, M., F. Hinder, J.H. Gong, A. Schmidt, A. Bender, H. Sprenger and D. Gemsa, 1990 Tumor Necrosis Factor-Alpha Production of Influenza a Virus-Infected Macrophages and Potentiating Effect of Lipopolysaccharides. *The Journal of Immunology*. 145(6): p. 1921.

144. Hussell, T. and T.J. Bell, 2014 Alveolar Macrophages: Plasticity in a Tissue-Specific Context. *Nat Rev Immunol*. 14(2): p. 81.

145. Chan, M.C., C.Y. Cheung, W.H. Chui, S.W. Tsao, J.M. Nicholls, Y.O. Chan, R.W. Chan, H.T. Long, L.L. Poon, Y. Guan and J.S. Peiris, 2005 Proinflammatory Cytokine Responses Induced by Influenza a (H5n1) Viruses in Primary Human Alveolar and Bronchial Epithelial Cells. *Respir Res*. 6: p. 135.

146. Lam, W.Y., A.C. Yeung, I.M. Chu and P.K. Chan, 2010 Profiles of Cytokine and Chemokine Gene Expression in Human Pulmonary Epithelial Cells Induced by Human and Avian Influenza Viruses. *Virol J*. 7: p. 344.

147. Osterlund, P., J. Pirhonen, N. Ikonen, E. Ronkko, M. Strengell, S.M. Makela, M. Broman, O.J. Hamming, R. Hartmann, T. Ziegler and I. Julkunen, 2010 Pandemic H1n1 2009 Influenza a Virus Induces Weak Cytokine Responses in Human Macrophages and Dendritic Cells and Is Highly Sensitive to the Antiviral Actions of Interferons. *J Virol*. 84(3): p. 1414.

148. Woo, P.C., E.T. Tung, K.H. Chan, C.C. Lau, S.K. Lau and K.Y. Yuen, 2010 Cytokine Profiles Induced by the Novel Swine-Origin Influenza a/H1n1 Virus: Implications for Treatment Strategies. *J Infect Dis*. 201(3): p. 346.

149. Bedoret, D*., et al.*, Lung Interstitial Macrophages Alter Dendritic Cell Functions to Prevent Airway Allergy in Mice. *The Journal of Clinical Investigation*. 119(12): p. 3723.

150. Vignola, A.M., P. Chanez, G. Chiappara, A. Merendino, E. Zinnanti, J. Bousquet, V. Bellia and G. Bonsignore, 1996 Release of Transforming Growth Factor-Beta (Tgf-Beta) and Fibronectin by Alveolar Macrophages in Airway Diseases. *Clin Exp Immunol*. 106(1): p. 114.

151. Coker, R.K., G.J. Laurent, S. Shahzeidi, N.A. Hernandez-Rodriguez, P. Pantelidis, R.M. du Bois, P.K. Jeffery and R.J. McAnulty, 1996 Diverse Cellular Tgf-Beta 1 and Tgf-Beta 3 Gene Expression in Normal Human and Murine Lung. *Eur Respir J*. 9(12): p. 2501.

152. Watanabe, Y., Y. Hashimoto, A. Shiratsuchi, T. Takizawa and Y. Nakanishi, 2005 Augmentation of Fatality of Influenza in Mice by Inhibition of Phagocytosis. *Biochem Biophys Res Commun*. 337(3): p. 881.

153. Herold, S., M. Steinmueller, W. von Wulffen, L. Cakarova, R. Pinto, S. Pleschka, M. Mack, W.A. Kuziel, N. Corazza, T. Brunner, W. Seeger and J. Lohmeyer, 2008 Lung Epithelial Apoptosis in Influenza Virus Pneumonia: The Role of Macrophage-Expressed Tnf-Related Apoptosis-Inducing Ligand. *The Journal of Experimental Medicine*. 205(13): p. 3065.

154. Peppelenbosch, M.P., M. DeSmedt, G. Pynaert, S.J.H. van Deventer and J. Grooten, 2000 Macrophages Present Pinocytosed Exogenous Antigen Via Mhc Class I Whereas Antigen

Ingested by Receptor-Mediated Endocytosis Is Presented Via Mhc Class Ii. *The Journal of Immunology*. 165(4): p. 1984.

155. Hamilton-Easton, A. and M. Eichelberger, 1995 Virus-Specific Antigen Presentation by Different Subsets of Cells from Lung and Mediastinal Lymph Node Tissues of Influenza Virus-Infected Mice. *Journal of virology*. 69(10): p. 6359.

156. Vermaelen, K. and R. Pauwels, 2005 Pulmonary Dendritic Cells. *American Journal of Respiratory and Critical Care Medicine*. 172(5): p. 530.

157. Tai, Y., Q. Wang, H. Korner, L. Zhang and W. Wei, 2018 Molecular Mechanisms of T Cells Activation by Dendritic Cells in Autoimmune Diseases. *Frontiers in pharmacology*. 9: p. 642.

158. Pozzi, L.-A.M., J.W. Maciaszek and K.L. Rock, 2005 Both Dendritic Cells and Macrophages Can Stimulate Naive Cd8 T Cells in Vivo to Proliferate, Develop Effector Function, and Differentiate into Memory Cells. *The Journal of Immunology*. 175(4): p. 2071.

159. Högner, K., T. Wolff, S. Pleschka, S. Plog, A.D. Gruber, U. Kalinke, H.-D. Walmrath, J. Bodner, S. Gattenlöhner, P. Lewe-Schlosser, M. Matrosovich, W. Seeger, J. Lohmeyer and S. Herold, 2013 Macrophage-Expressed Ifn-B Contributes to Apoptotic Alveolar Epithelial Cell Injury in Severe Influenza Virus Pneumonia. *PLOS Pathogens*. 9(2): p. e1003188.

160. Jakab, G.J., 1982 Immune Impairment of Alveolar Macrophage Phagocytosis During Influenza Virus Pneumonia. *American Review of Respiratory Disease*. 126(5): p. 778.

161. Astry, C.L. and G.J. Jakab, 1984 Influenza Virus-Induced Immune Complexes Suppress Alveolar Macrophage Phagocytosis. *Journal of Virology*. 50(2): p. 287.

162. Vasin, A.V., O.A. Temkina, V.V. Egorov, S.A. Klotchenko, M.A. Plotnikova and O.I. Kiselev, 2014 Molecular Mechanisms Enhancing the Proteome of Influenza a Viruses: An Overview of Recently Discovered Proteins. *Virus Research*. 185: p. 53.

163. Klemm, C., Y. Boergeling, S. Ludwig and C. Ehrhardt, 2018 Immunomodulatory Nonstructural Proteins of Influenza a Viruses. *Trends in Microbiology*. 26(7): p. 624.

164. de Chassey, B., A. Aublin-Gex, A. Ruggieri, L. Meyniel-Schicklin, F. Pradezynski, N. Davoust, T. Chantier, L. Tafforeau, P.-E. Mangeot, C. Ciancia, L. Perrin-Cocon, R. Bartenschlager, P. André and V. Lotteau, 2013 The Interactomes of Influenza Virus Ns1 and Ns2 Proteins Identify New Host Factors and Provide Insights for Adar1 Playing a Supportive Role in Virus Replication. *PLOS Pathogens*. 9(7): p. e1003440.

165. Khaperskyy, D.A., S. Schmaling, J. Larkins-Ford, C. McCormick and M.M. Gaglia, 2016 Selective Degradation of Host Rna Polymerase Ii Transcripts by Influenza a Virus Pa-X Host Shutoff Protein. *PLOS Pathogens*. 12(2): p. e1005427.

166. Zamarin, D., A. García-Sastre, X. Xiao, R. Wang and P. Palese, 2005 Influenza Virus Pb1-F2 Protein Induces Cell Death through Mitochondrial Ant3 and Vdac1. *PLOS Pathogens*. 1(1): p. e4.

167. McAuley, J.L., F. Hornung, K.L. Boyd, A.M. Smith, R. McKeon, J. Bennink, J.W. Yewdell and J.A. McCullers, 2007 Expression of the 1918 Influenza a Virus Pb1-F2 Enhances the Pathogenesis of Viral and Secondary Bacterial Pneumonia. *Cell Host & Microbe*. 2(4): p. 240.

168. Carlin, L.E., E.A. Hemann, Z.R. Zacharias, J.W. Heusel and K.L. Legge, 2018 Natural Killer Cell Recruitment to the Lung During Influenza a Virus Infection Is Dependent on Cxcr3, Ccr5, and Virus Exposure Dose. *Front Immunol*. 9: p. 781.

169. Moraru, M., L.E. Black and A. Muntasell, 2015 Nk Cell and Ig Interplay in Defense against Herpes Simplex Virus Type 1: Epistatic Interaction of Cd16a and Igg1 Allotypes of Variable Affinities Modulates Antibody-Dependent Cellular Cytotoxicity and Susceptibility to Clinical Reactivation.

170. Ahlenstiel, G., 2013 The Natural Killer Cell Response to Hcv Infection. *Immune Netw*. 13(5): p. 168.

171. Naranbhai, V., M. Altfeld, S.S. Karim, T. Ndung'u, Q.A. Karim and W.H. Carr, 2013 Changes in Natural Killer Cell Activation and Function During Primary Hiv-1 Infection. *PLoS One*. 8(1): p. e53251.

172. Beziat, V*., et al.*, 2013 Nk Cell Responses to Cytomegalovirus Infection Lead to Stable Imprints in the Human Kir Repertoire and Involve Activating Kirs. *Blood*. 121(14): p. 2678.

173. Junqueira-Kipnis, A.P., A. Kipnis, A. Jamieson, M.G. Juarrero, A. Diefenbach, D.H. Raulet, J. Turner and I.M. Orme, 2003 Nk Cells Respond to Pulmonary Infection with Mycobacterium Tuberculosis, but Play a Minimal Role in Protection. *J Immunol*. 171(11): p. 6039.

174. Artavanis-Tsakonas, K. and E.M. Riley, 2002 Innate Immune Response to Malaria: Rapid Induction of Ifn-Gamma from Human Nk Cells by Live Plasmodium Falciparum-Infected Erythrocytes. *J Immunol*. 169(6): p. 2956.

175. Smyth, M.J., J.R. Ortaldo, Y. Shinkai, H. Yagita, M. Nakata, K. Okumura and H.A. Young, 1990 Interleukin 2 Induction of Pore-Forming Protein Gene Expression in Human Peripheral Blood Cd8+ T Cells. *The Journal of Experimental Medicine*. 171(4): p. 1269.

176. Grossman, W.J., J.W. Verbsky, B.L. Tollefsen, C. Kemper, J.P. Atkinson and T.J. Ley, 2004 Differential Expression of Granzymes a and B in Human Cytotoxic Lymphocyte Subsets and T Regulatory Cells. *Blood*. 104(9): p. 2840.

177. Orange, J.S., 2008 Formation and Function of the Lytic Nk-Cell Immunological Synapse. *Nat Rev Immunol*. 8(9): p. 713.

178. Zamai, L., M. Ahmad, I.M. Bennett, L. Azzoni, E.S. Alnemri and B. Perussia, 1998 Natural Killer (Nk) Cell–Mediated Cytotoxicity: Differential Use of Trail and Fas Ligand by Immature and Mature Primary Human Nk Cells. *The Journal of Experimental Medicine*. 188(12): p. 2375.

179. Burkhardt, J.K., S. Hester, C.K. Lapham and Y. Argon, 1990 The Lytic Granules of Natural Killer Cells Are Dual-Function Organelles Combining Secretory and Pre-Lysosomal Compartments. *J Cell Biol*. 111(6): p. 2327.

180. Lichtenheld, M.G., K.J. Olsen, P. Lu, D.M. Lowrey, A. Hameed, H. Hengartner and E.R. Podack, 1988 Structure and Function of Human Perforin. *Nature*. 335(6189): p. 448.

181. Shi, L., C.M. Kam, J.C. Powers, R. Aebersold and A.H. Greenberg, 1992 Purification of Three Cytotoxic Lymphocyte Granule Serine Proteases That Induce Apoptosis through Distinct Substrate and Target Cell Interactions. *The Journal of Experimental Medicine*. 176(6): p. 1521.

182. Heusel, J.W., R.L. Wesselschmidt, S. Shresta, J.H. Russell and T.J. Ley, Cytotoxic Lymphocytes Require Granzyme B for the Rapid Induction of DNA Fragmentation and Apoptosis in Allogeneic Target Cells. *Cell*. 76(6): p. 977.

183. Darmon, A.J., D.W. Nicholson and R.C. Bleackley, 1995 Activation of the Apoptotic Protease Cpp32 by Cytotoxic T-Cell-Derived Granzyme B. *Nature*. 377(6548): p. 446.

184. Fernandes-Alnemri, T., R.C. Armstrong, J. Krebs, S.M. Srinivasula, L. Wang, F. Bullrich, L.C. Fritz, J.A. Trapani, K.J. Tomaselli, G. Litwack and E.S. Alnemri, 1996 In Vitro Activation of Cpp32 and Mch3 by Mch4, a Novel Human Apoptotic Cysteine Protease Containing Two Fadd-Like Domains. *Proc Natl Acad Sci U S A*. 93(15): p. 7464.

185. Krzewski, K., A. Gil-Krzewska, V. Nguyen, G. Peruzzi and J.E. Coligan, 2013 Lamp1/Cd107a Is Required for Efficient Perforin Delivery to Lytic Granules and Nk-Cell Cytotoxicity. *Blood*. 121(23): p. 4672.

186. Hayakawa, Y., V. Screpanti, H. Yagita, A. Grandien, H.-G. Ljunggren, M.J. Smyth and B.J. Chambers, 2004 Nk Cell Trail Eliminates Immature Dendritic Cells in Vivo and Limits Dendritic Cell Vaccination Efficacy. *The Journal of Immunology*. 172(1): p. 123.

187. Iyori, M., T. Zhang, H. Pantel, B.A. Gagne and C.L. Sentman, 2011 Trail/Dr5 Plays a Critical Role in Nk Cell-Mediated Negative Regulation of Dendritic Cell Cross-Priming of T Cells(). *Journal of immunology (Baltimore, Md. : 1950)*. 187(6): p. 3087.

188. Sato, K., S. Hida, H. Takayanagi, T. Yokochi, N. Kayagaki, K. Takeda, H. Yagita, K. Okumura, N. Tanaka, T. Taniguchi and K. Ogasawara, 2001 Antiviral Response by Natural Killer Cells through Trail Gene Induction by Ifn–A/B *European Journal of Immunology*. 31(11): p. 3138.

189. Fauriat, C., E.O. Long, H.G. Ljunggren and Y.T. Bryceson, 2010 Regulation of Human Nk-Cell Cytokine and Chemokine Production by Target Cell Recognition. *Blood*. 115(11): p. 2167.

190. Cooper, M.A., T.A. Fehniger, S.C. Turner, K.S. Chen, B.A. Ghaheri, T. Ghayur, W.E. Carson and M.A. Caligiuri, 2001 Human Natural Killer Cells: A Unique Innate Immunoregulatory Role for the Cd56(Bright) Subset. *Blood*. 97(10): p. 3146.

191. Ferlazzo, G. and B. Morandi, 2014 Cross-Talks between Natural Killer Cells and Distinct Subsets of Dendritic Cells. *Front Immunol*. 5: p. 159.

192. Bradley, L.M., D.K. Dalton and M. Croft, 1996 A Direct Role for Ifn-Gamma in Regulation of Th1 Cell Development. *J Immunol*. 157(4): p. 1350.

193. Smeltz, R.B., J. Chen, R. Ehrhardt and E.M. Shevach, 2002 Role of Ifn-Gamma in Th1 Differentiation: Ifn-Gamma Regulates Il-18r Alpha Expression by Preventing the Negative Effects of Il-4 and by Inducing/Maintaining Il-12 Receptor Beta 2 Expression. *J Immunol*. 168(12): p. 6165.

194. Peters, P.M., J.R. Ortaldo, M.R. Shalaby, L.P. Svedersky, G.E. Nedwin, T.S. Bringman, P.E. Hass, B.B. Aggarwal, R.B. Herberman and D.V. Goeddel, 1986 Natural Killer-Sensitive Targets Stimulate Production of Tnf-Alpha but Not Tnf-Beta (Lymphotoxin) by Highly Purified Human Peripheral Blood Large Granular Lymphocytes. *The Journal of Immunology*. 137(8): p. 2592.

195. Klinman, D.M., A.K. Yi, S.L. Beaucage, J. Conover and A.M. Krieg, 1996 Cpg Motifs Present in Bacteria DNA Rapidly Induce Lymphocytes to Secrete Interleukin 6, Interleukin 12, and Interferon Gamma. *Proceedings of the National Academy of Sciences*. 93(7): p. 2879.

196. Iwasaki, A., E.F. Foxman and R.D. Molony, 2016 Early Local Immune Defences in the Respiratory Tract. *Nat Rev Immunol*. advance online publication.

197. Schroder, K., P.J. Hertzog, T. Ravasi and D.A. Hume, 2004 Interferon-Γ: An Overview of Signals, Mechanisms and Functions. *Journal of Leukocyte Biology*. 75(2): p. 163.

198. Szabo, S.J., B.M. Sullivan, S.L. Peng and L.H. Glimcher, 2003 Molecular Mechanisms Regulating Th1 Immune Responses. *Annu Rev Immunol*. 21: p. 713.

199. Vivier, E., J.A. Nunes and F. Vely, 2004 Natural Killer Cell Signaling Pathways. *Science*. 306(5701): p. 1517.

200. Vivier, E., E. Tomasello, M. Baratin, T. Walzer and S. Ugolini, 2008 Functions of Natural Killer Cells. *Nat Immunol*. 9(5): p. 503.

201. Kim, S., K. Iizuka, H.L. Aguila, I.L. Weissman and W.M. Yokoyama, 2000 In Vivo Natural Killer Cell Activities Revealed by Natural Killer Cell-Deficient Mice. *Proceedings of the National Academy of Sciences*. 97(6): p. 2731.

202. Mace, E.M., P. Dongre, H.T. Hsu, P. Sinha, A.M. James, S.S. Mann, L.R. Forbes, L.B. Watkin and J.S. Orange, 2014 Cell Biological Steps and Checkpoints in Accessing Nk Cell Cytotoxicity. *Immunol Cell Biol*. 92(3): p. 245.

203. Achdout, H., I. Manaster and O. Mandelboim, 2008 Influenza Virus Infection Augments Nk Cell Inhibition through Reorganization of Major Histocompatibility Complex Class I Proteins. *J Virol*. 82(16): p. 8030.

204. Augugliaro, R., S. Parolini, R. Castriconi, E. Marcenaro, C. Cantoni, M. Nanni, L. Moretta, A. Moretta and C. Bottino, 2003 Selective Cross-Talk among Natural Cytotoxicity Receptors in Human Natural Killer Cells. *Eur J Immunol*. 33(5): p. 1235.

205. Leung, W., 2011 Use of Nk Cell Activity in Cure by Transplant. *Br J Haematol*. 155(1): p. 14.

206. Ljunggren, H.-G. and K.-J. Malmberg, 2007 Prospects for the Use of Nk Cells in Immunotherapy of Human Cancer. *Nat Rev Immunol*. 7(5): p. 329.

207. Colonna, M., H. Nakajima and M. Cella, 1999 Inhibitory and Activating Receptors Involved in Immune Surveillance by Human Nk and Myeloid Cells. *J Leukoc Biol*. 66(5): p. 718.

208. Vales-Gomez, M., H.T. Reyburn, R.A. Erskine, M. Lopez-Botet and J.L. Strominger, 1999 Kinetics and Peptide Dependency of the Binding of the Inhibitory Nk Receptor Cd94/Nkg2-a and the Activating Receptor Cd94/Nkg2-C to Hla-E. *Embo j*. 18(15): p. 4250.

209. Lankry, D., H. Simic, Y. Klieger, F. Levi-Schaffer, S. Jonjic and O. Mandelboim, 2010 Expression and Function of Cd300 in Nk Cells. *J Immunol*. 185(5): p. 2877.

210. Cantoni, C., C. Bottino, R. Augugliaro, L. Morelli, E. Marcenaro, R. Castriconi, M. Vitale, D. Pende, S. Sivori, R. Millo, R. Biassoni, L. Moretta and A. Moretta, 1999 Molecular and Functional Characterization of Irp60, a Member of the Immunoglobulin Superfamily That Functions as an Inhibitory Receptor in Human Nk Cells. *Eur J Immunol*. 29(10): p. 3148.

211. Falco, M., R. Biassoni, C. Bottino, M. Vitale, S. Sivori, R. Augugliaro, L. Moretta and A. Moretta, 1999 Identification and Molecular Cloning of P75/Airm1, a Novel Member of the Sialoadhesin Family That Functions as an Inhibitory Receptor in Human Natural Killer Cells. *J Exp Med*. 190(6): p. 793.

212. Moretta, A., G. Tambussi, C. Bottino, G. Tripodi, A. Merli, E. Ciccone, G. Pantaleo and L. Moretta, 1990 A Novel Surface Antigen Expressed by a Subset of Human Cd3- Cd16+ Natural Killer Cells. Role in Cell Activation and Regulation of Cytolytic Function. *J Exp Med*. 171(3): p. 695.

213. Moretta, A., C. Bottino, D. Pende, G. Tripodi, G. Tambussi, O. Viale, A. Orengo, M. Barbaresi, A. Merli, E. Ciccone and et al., 1990 Identification of Four Subsets of Human Cd3-Cd16+ Natural Killer (Nk) Cells by the Expression of Clonally Distributed Functional Surface Molecules: Correlation between Subset Assignment of Nk Clones and Ability to Mediate Specific Alloantigen Recognition. *J Exp Med*. 172(6): p. 1589.

214. Middleton, D. and F. Gonzelez, 2010 The Extensive Polymorphism of Kir Genes. *Immunology*. 129(1): p. 8.

215. Brodin, P., T. Lakshmikanth, S. Johansson, K. Karre and P. Hoglund, 2009 The Strength of Inhibitory Input During Education Quantitatively Tunes the Functional Responsiveness of Individual Natural Killer Cells. *Blood*. 113(11): p. 2434.

216. Joncker, N.T., N.C. Fernandez, E. Treiner, E. Vivier and D.H. Raulet, 2009 Nk Cell Responsiveness Is Tuned Commensurate with the Number of Inhibitory Receptors for Self-Mhc Class I: The Rheostat Model. *J Immunol*. 182(8): p. 4572.

217. Yu, J., G. Heller, J. Chewning, S. Kim, W.M. Yokoyama and K.C. Hsu, 2007 Hierarchy of the Human Natural Killer Cell Response Is Determined by Class and Quantity of Inhibitory Receptors for Self-Hla-B and Hla-C Ligands. *J Immunol*. 179(9): p. 5977.

218. Ciccone, E., D. Pende, O. Viale, C. Di Donato, G. Tripodi, A.M. Orengo, J. Guardiola, A. Moretta and L. Moretta, 1992 Evidence of a Natural Killer (Nk) Cell Repertoire for (Allo) Antigen Recognition: Definition of Five Distinct Nk-Determined Allospecificities in Humans. *J Exp Med*. 175(3): p. 709.

219. Christiansen, F.T., C.S. Witt, E. Ciccone, D. Townend, D. Pende, D. Viale, L.J. Abraham, R.L. Dawkins and L. Moretta, 1993 Human Natural Killer (Nk) Alloreactivity and Its Association with the Major Histocompatibility Complex: Ancestral Haplotypes Encode Particular Nk-Defined Haplotypes. *J Exp Med*. 178(3): p. 1033.

220. Moretta, A., M. Vitale, C. Bottino, A.M. Orengo, L. Morelli, R. Augugliaro, M. Barbaresi, E. Ciccone and L. Moretta, 1993 P58 Molecules as Putative Receptors for Major Histocompatibility Complex (Mhc) Class I Molecules in Human Natural Killer (Nk) Cells. Anti-P58 Antibodies Reconstitute Lysis of Mhc Class I-Protected Cells in Nk Clones Displaying Different Specificities. *J Exp Med*. 178(2): p. 597.

221. Malnati, M.S., P. Lusso, E. Ciccone, A. Moretta, L. Moretta and E.O. Long, 1993 Recognition of Virus-Infected Cells by Natural Killer Cell Clones Is Controlled by Polymorphic Target Cell Elements. *J Exp Med*. 178(3): p. 961.

222. Parham, P., 2005 Mhc Class I Molecules and Kirs in Human History, Health and Survival. *Nat Rev Immunol*. 5(3): p. 201.

223. Karre, K., H.G. Ljunggren, G. Piontek and R. Kiessling, 1986 Selective Rejection of H-2-Deficient Lymphoma Variants Suggests Alternative Immune Defence Strategy. *Nature*. 319(6055): p. 675.

224. Johansson, S., M. Johansson, E. Rosmaraki, G. Vahlne, R. Mehr, M. Salmon-Divon, F. Lemonnier, K. Karre and P. Hoglund, 2005 Natural Killer Cell Education in Mice with Single or Multiple Major Histocompatibility Complex Class I Molecules. *J Exp Med*. 201(7): p. 1145.

225. Sim, M.J., J. Stowell, R. Sergeant, D.M. Altmann, E.O. Long and R.J. Boyton, 2016 Kir2dl3 and Kir2dl1 Show Similar Impact on Licensing of Human Nk Cells. *Eur J Immunol*. 46(1): p. 185.

226. Sun, J.C. and L.L. Lanier, 2008 Cutting Edge: Viral Infection Breaks Nk Cell Tolerance to "Missing Self". *J Immunol*. 181(11): p. 7453.

227. Mahmoud, A.B., M.M. Tu, A. Wight, H.S. Zein, M.M. Rahim, S.H. Lee, H.S. Sekhon, E.G. Brown and A.P. Makrigiannis, 2016 Influenza Virus Targets Class I Mhc-Educated Nk Cells for Immunoevasion. *PLoS Pathog*. 12(2): p. e1005446.

228. Tu, M.M., A.B. Mahmoud and A.P. Makrigiannis, 2016 Licensed and Unlicensed Nk Cells: Differential Roles in Cancer and Viral Control. *Frontiers in Immunology*. 7(166).

229. Pegram, H.J., D.M. Andrews, M.J. Smyth, P.K. Darcy and M.H. Kershaw, 2011 Activating and Inhibitory Receptors of Natural Killer Cells. *Immunol Cell Biol*. 89(2): p. 216.

230. Carr, W.H., D.B. Rosen, H. Arase, D.F. Nixon, J. Michaelsson and L.L. Lanier, 2007 Cutting Edge: Kir3ds1, a Gene Implicated in Resistance to Progression to Aids, Encodes a Dap12-Associated Receptor Expressed on Nk Cells That Triggers Nk Cell Activation. *The Journal of Immunology*. 178(2): p. 647.

231. Davis, Z.B., A. Cogswell, H. Scott, A. Mertsching, J. Boucau, D. Wambua, S. Le Gall, V. Planelles, K.S. Campbell and E. Barker, 2016 A Conserved Hiv-1-Derived Peptide Presented by Hla-E Renders Infected T-Cells Highly Susceptible to Attack by Nkg2a/Cd94-Bearing Natural Killer Cells. *PLOS Pathogens*. 12(2): p. e1005421.

232. O'Connor, G.M., J.P. Vivian, E. Gostick, P. Pymm, B.A.P. Lafont, D.A. Price, J. Rossjohn, A.G. Brooks and D.W. McVicar, 2015 Peptide-Dependent Recognition of Hla-B*57:01 by Kir3ds1. *Journal of Virology*. 89(10): p. 5213.

233. Naiyer, M.M*., et al.*, 2017 Kir2ds2 Recognizes Conserved Peptides Derived from Viral Helicases in the Context of Hla-C. *Sci Immunol*. 2(15).

234. Burian, A., K.L. Wang, K.A. Finton, N. Lee, A. Ishitani, R.K. Strong and D.E. Geraghty, 2016 Hla-F and Mhc-I Open Conformers Bind Natural Killer Cell Ig-Like Receptor Kir3ds1. *PLoS One*. 11(9): p. e0163297.

235. Jandus, C., K.F. Boligan, O. Chijioke, H. Liu, M. Dahlhaus, T. Démoulins, C. Schneider, M. Wehrli, R.E. Hunger, G.M. Baerlocher, H.-U. Simon, P. Romero, C. Münz and S. von Gunten,

2014 Interactions between Siglec-7/9 Receptors and Ligands Influence Nk Cell-Dependent Tumor Immunosurveillance. *The Journal of clinical investigation*. 124(4): p. 1810.

236. Borrego, F., 2013 The Cd300 Molecules: An Emerging Family of Regulators of the Immune System. *Blood*. 121(11): p. 1951.

237. Sivori, S., M. Vitale, L. Morelli, L. Sanseverino, R. Augugliaro, C. Bottino, L. Moretta and A. Moretta, 1997 P46, a Novel Natural Killer Cell-Specific Surface Molecule That Mediates Cell Activation. *J Exp Med*. 186(7): p. 1129.

238. Vitale, M., C. Bottino, S. Sivori, L. Sanseverino, R. Castriconi, E. Marcenaro, R. Augugliaro, L. Moretta and A. Moretta, 1998 Nkp44, a Novel Triggering Surface Molecule Specifically Expressed by Activated Natural Killer Cells, Is Involved in Non-Major Histocompatibility Complex-Restricted Tumor Cell Lysis. *J Exp Med*. 187(12): p. 2065.

239. Pende, D., S. Parolini, A. Pessino, S. Sivori, R. Augugliaro, L. Morelli, E. Marcenaro, L. Accame, A. Malaspina, R. Biassoni, C. Bottino, L. Moretta and A. Moretta, 1999 Identification and Molecular Characterization of Nkp30, a Novel Triggering Receptor Involved in Natural Cytotoxicity Mediated by Human Natural Killer Cells. *J Exp Med*. 190(10): p. 1505.

240. Achdout, H., T.I. Arnon, G. Markel, T. Gonen-Gross, G. Katz, N. Lieberman, R. Gazit, A. Joseph, E. Kedar and O. Mandelboim, 2003 Enhanced Recognition of Human Nk Receptors after Influenza Virus Infection. *J Immunol*. 171(2): p. 915.

241. Mandelboim, O., N. Lieberman, M. Lev, L. Paul, T.I. Arnon, Y. Bushkin, D.M. Davis, J.L. Strominger, J.W. Yewdell and A. Porgador, 2001 Recognition of Haemagglutinins on Virus-Infected Cells by Nkp46 Activates Lysis by Human Nk Cells. *Nature*. 409(6823): p. 1055.

242. Arnon, T.I., M. Lev, G. Katz, Y. Chernobrov, A. Porgador and O. Mandelboim, 2001 Recognition of Viral Hemagglutinins by Nkp44 but Not by Nkp30. *Eur J Immunol*. 31(9): p. 2680.

243. Pogge von Strandmann, E., V.R. Simhadri, B. von Tresckow, S. Sasse, Katrin S. Reiners, H.P. Hansen, A. Rothe, B. Böll, V.L. Simhadri, P. Borchmann, P.J. McKinnon, M. Hallek and A. Engert, Human Leukocyte Antigen-B-Associated Transcript 3 Is Released from Tumor Cells and Engages the Nkp30 Receptor on Natural Killer Cells. *Immunity*. 27(6): p. 965.

244. Bloushtain, N., U. Qimron, A. Bar-Ilan, O. Hershkovitz, R. Gazit, E. Fima, M. Korc, I. Vlodavsky, N.V. Bovin and A. Porgador, 2004 Membrane-Associated Heparan Sulfate

Proteoglycans Are Involved in the Recognition of Cellular Targets by Nkp30 and Nkp46. *J Immunol*. 173(4): p. 2392.

245. Brandt, C.S*., et al.*, 2009 The B7 Family Member B7-H6 Is a Tumor Cell Ligand for the Activating Natural Killer Cell Receptor Nkp30 in Humans. *The Journal of Experimental Medicine*. 206(7): p. 1495.

246. Pessino, A., S. Sivori, C. Bottino, A. Malaspina, L. Morelli, L. Moretta, R. Biassoni and A. Moretta, 1998 Molecular Cloning of Nkp46: A Novel Member of the Immunoglobulin Superfamily Involved in Triggering of Natural Cytotoxicity. *The Journal of Experimental Medicine*. 188(5): p. 953.

247. Welte, S., S. Kuttruff, I. Waldhauer and A. Steinle, 2006 Mutual Activation of Natural Killer Cells and Monocytes Mediated by Nkp80-Aicl Interaction. *Nat Immunol*. 7(12): p. 1334.

248. Zhang, Z., N. Wu, Y. Lu, D. Davidson, M. Colonna and A. Veillette, 2015 Dnam-1 Controls Nk Cell Activation Via an Itt-Like Motif. *J Exp Med*. 212(12): p. 2165.

249. Jamieson, A.M., A. Diefenbach, C.W. McMahon, N. Xiong, J.R. Carlyle and D.H. Raulet, 2002 The Role of the Nkg2d Immunoreceptor in Immune Cell Activation and Natural Killing. *Immunity*. 17(1): p. 19.

250. Spear, P., M.R. Wu, M.L. Sentman and C.L. Sentman, 2013 Nkg2d Ligands as Therapeutic Targets. *Cancer Immun*. 13: p. 8.

251. Bahram, S., M. Bresnahan, D.E. Geraghty and T. Spies, 1994 A Second Lineage of Mammalian Major Histocompatibility Complex Class I Genes. *Proc Natl Acad Sci U S A*. 91(14): p. 6259.

252. Ward, J., Z. Davis, J. DeHart, E. Zimmerman, A. Bosque, E. Brunetta, D. Mavilio, V. Planelles and E. Barker, 2009 Hiv-1 Vpr Triggers Natural Killer Cell-Mediated Lysis of Infected Cells through Activation of the Atr-Mediated DNA Damage Response. *PLoS Pathog*. 5(10): p. e1000613.

253. Nedvetzki, S., S. Sowinski, R.A. Eagle, J. Harris, F. Vely, D. Pende, J. Trowsdale, E. Vivier, S. Gordon and D.M. Davis, 2007 Reciprocal Regulation of Human Natural Killer Cells and Macrophages Associated with Distinct Immune Synapses. *Blood*. 109(9): p. 3776.

254. Draghi, M., A. Pashine, B. Sanjanwala, K. Gendzekhadze, C. Cantoni, D. Cosman, A. Moretta, N.M. Valiante and P. Parham, 2007 Nkp46 and Nkg2d Recognition of Infected Dendritic

Cells Is Necessary for Nk Cell Activation in the Human Response to Influenza Infection. *J Immunol*. 178(5): p. 2688.

255. Lanier, L.L., G. Yu and J.H. Phillips, 1991 Analysis of Fc Gamma Riii (Cd16) Membrane Expression and Association with Cd3 Zeta and Fc Epsilon Ri-Gamma by Site-Directed Mutation. *J Immunol*. 146(5): p. 1571.

256. Lanier, L.L., J.J. Ruitenberg and J.H. Phillips, 1988 Functional and Biochemical Analysis of Cd16 Antigen on Natural Killer Cells and Granulocytes. *J Immunol*. 141(10): p. 3478.

257. Kumar, V., J. Ben-Ezra, M. Bennett and G. Sonnenfeld, 1979 Natural Killer Cells in Mice Treated with 89strontium: Normal Target-Binding Cell Numbers but Inability to Kill Even after Interferon Administration. *The Journal of Immunology*. 123(4): p. 1832.

258. Seaman, W.E., M.A. Blackman, T.D. Gindhart, J.R. Roubinian, J.M. Loeb and N. Talal, 1978 Beta-Estradiol Reduces Natural Killer Cells in Mice. *J Immunol*. 121(6): p. 2193.

259. Freud, A.G., B. Becknell, S. Roychowdhury, H.C. Mao, A.K. Ferketich, G.J. Nuovo, T.L. Hughes, T.B. Marburger, J. Sung, R.A. Baiocchi, M. Guimond and M.A. Caligiuri, 2005 A Human Cd34(+) Subset Resides in Lymph Nodes and Differentiates into Cd56bright Natural Killer Cells. *Immunity*. 22(3): p. 295.

260. Kondo, M., I.L. Weissman and K. Akashi, 1997 Identification of Clonogenic Common Lymphoid Progenitors in Mouse Bone Marrow. *Cell*. 91(5): p. 661.

261. Sun, J.C. and L.L. Lanier, 2011 Nk Cell Development, Homeostasis and Function: Parallels with Cd8(+) T Cells. *Nat Rev Immunol*. 11(10): p. 645.

262. Spits, H., J.H. Bernink and L. Lanier, 2016 Nk Cells and Type 1 Innate Lymphoid Cells: Partners in Host Defense. *Nat Immunol*. 17(7): p. 758.

263. Kim, S., K. Iizuka, H.-S.P. Kang, A. Dokun, A.R. French, S. Greco and W.M. Yokoyama, 2002 In Vivo Developmental Stages in Murine Natural Killer Cell Maturation. *Nat Immunol*. 3(6): p. 523.

264. Chiossone, L., J. Chaix, N. Fuseri, C. Roth, E. Vivier and T. Walzer, 2009 Maturation of Mouse Nk Cells Is a 4-Stage Developmental Program. *Blood*. 113(22): p. 5488.

265. Hayakawa, Y. and M.J. Smyth, 2006 Cd27 Dissects Mature Nk Cells into Two Subsets with Distinct Responsiveness and Migratory Capacity. *The Journal of Immunology*. 176(3): p. 1517.

266. Freud, A.G., A. Yokohama, B. Becknell, M.T. Lee, H.C. Mao, A.K. Ferketich and M.A. Caligiuri, 2006 Evidence for Discrete Stages of Human Natural Killer Cell Differentiation in Vivo. *J Exp Med*. 203(4): p. 1033.

267. Luetke-Eversloh, M., M. Killig and C. Romagnani, 2013 Signatures of Human Nk Cell Development and Terminal Differentiation. *Frontiers in Immunology*. 4: p. 499.

268. Lanier, L.L., C. Chang, M. Azuma, J.J. Ruitenberg, J.J. Hemperly and J.H. Phillips, 1991 Molecular and Functional Analysis of Human Natural Killer Cell-Associated Neural Cell Adhesion Molecule (N-Cam/Cd56). *J Immunol*. 146(12): p. 4421.

269. Chan, A., D.L. Hong, A. Atzberger, S. Kollnberger, A.D. Filer, C.D. Buckley, A. McMichael, T. Enver and P. Bowness, 2007 Cd56bright Human Nk Cells Differentiate into Cd56dim Cells: Role of Contact with Peripheral Fibroblasts. *J Immunol*. 179(1): p. 89.

270. Chan, A., D.-L. Hong, A. Atzberger, S. Kollnberger, A.D. Filer, C.D. Buckley, A. McMichael, T. Enver and P. Bowness, 2007 Cd56bright Human Nk Cells Differentiate into Cd56dim Cells: Role of Contact with Peripheral Fibroblasts. *The Journal of Immunology*. 179(1): p. 89.

271. Fehniger, T.A., M.A. Cooper, G.J. Nuovo, M. Cella, F. Facchetti, M. Colonna and M.A. Caligiuri, 2003 Cd56bright Natural Killer Cells Are Present in Human Lymph Nodes and Are Activated by T Cell-Derived Il-2: A Potential New Link between Adaptive and Innate Immunity. *Blood*. 101(8): p. 3052.

272. Poli, A., T. Michel, M. Thérésine, E. Andrès, F. Hentges and J. Zimmer, 2009 Cd56(Bright) Natural Killer (Nk) Cells: An Important Nk Cell Subset. *Immunology*. 126(4): p. 458.

273. Freund, J., R.M. May, E. Yang, H. Li, M. McCullen, B. Zhang, T. Lenvik, F. Cichocki, S.K. Anderson and T. Kambayashi, 2016 Activating Receptor Signals Drive Receptor Diversity in Developing Natural Killer Cells. *PLoS Biol*. 14(8): p. e1002526.

274. Bjorkstrom, N.K., P. Riese, F. Heuts, S. Andersson, C. Fauriat, M.A. Ivarsson, A.T. Bjorklund, M. Flodstrom-Tullberg, J. Michaelsson, M.E. Rottenberg, C.A. Guzman, H.G. Ljunggren and K.J. Malmberg, 2010 Expression Patterns of Nkg2a, Kir, and Cd57 Define a Process of Cd56dim Nk-Cell Differentiation Uncoupled from Nk-Cell Education. *Blood*. 116(19): p. 3853.

275. Lopez-Verges, S., J.M. Milush, S. Pandey, V.A. York, J. Arakawa-Hoyt, H. Pircher, P.J. Norris, D.F. Nixon and L.L. Lanier, 2010 Cd57 Defines a Functionally Distinct Population of Mature Nk Cells in the Human Cd56dimcd16+ Nk-Cell Subset. *Blood*. 116(19): p. 3865.

276. Caligiuri, M.A., 2008 Human Natural Killer Cells. *Blood*. 112(3): p. 461.

277. Jamieson, A.M., P. Isnard, J.R. Dorfman, M.C. Coles and D.H. Raulet, 2004 Turnover and Proliferation of Nk Cells in Steady State and Lymphopenic Conditions. *J Immunol*. 172(2): p. 864.

278. Sun, J.C., J.N. Beilke, N.A. Bezman and L.L. Lanier, 2011 Homeostatic Proliferation Generates Long-Lived Natural Killer Cells That Respond against Viral Infection. *J Exp Med*. 208(2): p. 357.

279. Polansky, J.K., R. Bahri, M. Divivier, E.H. Duitman, C. Vock, D.A. Goyeneche-Patino, Z. Orinska and S. Bulfone-Paus, 2016 High Dose Cd11c-Driven Il15 Is Sufficient to Drive Nk Cell Maturation and Anti-Tumor Activity in a Trans-Presentation Independent Manner. *Sci Rep*. 6: p. 19699.

280. Cooper, M.A., J.E. Bush, T.A. Fehniger, J.B. VanDeusen, R.E. Waite, Y. Liu, H.L. Aguila and M.A. Caligiuri, 2002 In Vivo Evidence for a Dependence on Interleukin 15 for Survival of Natural Killer Cells. *Blood*. 100(10): p. 3633.

281. Ranson, T., C.A. Vosshenrich, E. Corcuff, O. Richard, W. Muller and J.P. Di Santo, 2003 Il-15 Is an Essential Mediator of Peripheral Nk-Cell Homeostasis. *Blood*. 101(12): p. 4887.

282. Huntington, N.D., N. Legrand, N.L. Alves, B. Jaron, K. Weijer, A. Plet, E. Corcuff, E. Mortier, Y. Jacques, H. Spits and J.P. Di Santo, 2009 Il-15 Trans-Presentation Promotes Human Nk Cell Development and Differentiation in Vivo. *J Exp Med*. 206(1): p. 25.

283. Gasteiger, G., S. Hemmers, M.A. Firth, A. Le Floc'h, M. Huse, J.C. Sun and A.Y. Rudensky, 2013 Il-2–Dependent Tuning of Nk Cell Sensitivity for Target Cells Is Controlled by Regulatory T Cells. *The Journal of Experimental Medicine*. 210(6): p. 1167.

284. Eidenschenk, C., E. Jouanguy, A. Alcaïs, J.-J. Mention, B. Pasquier, I.M. Fleckenstein, A. Puel, L. Gineau, J.-C. Carel, E. Vivier, F. Le Deist and J.-L. Casanova, 2006 Familial Nk Cell Deficiency Associated with Impaired Il-2- and Il-15-Dependent Survival of Lymphocytes. *The Journal of Immunology*. 177(12): p. 8835.

285. Taguchi, Y., T. Kondo, M. Watanabe, M. Miyaji, H. Umehara, Y. Kozutsumi and T. Okazaki, 2004 Interleukin-2-Induced Survival of Natural Killer (Nk) Cells Involving Phosphatidylinositol-3 Kinase-Dependent Reduction of Ceramide through Acid Sphingomyelinase, Sphingomyelin Synthase, and Glucosylceramide Synthase. *Blood*. 104(10): p. 3285.

286. Dunne, J., S. Lynch, C. O'Farrelly, S. Todryk, J.E. Hegarty, C. Feighery and D.G. Doherty, 2001 Selective Expansion and Partial Activation of Human Nk Cells and Nk Receptor-Positive T Cells by Il-2 and Il-15. *J Immunol*. 167(6): p. 3129.

287. Moroso, V., F. Famili, N. Papazian, T. Cupedo, L.J. van der Laan, G. Kazemier, H.J. Metselaar and J. Kwekkeboom, 2011 Nk Cells Can Generate from Precursors in the Adult Human Liver. *Eur J Immunol*. 41(11): p. 3340.

288. Vacca, P., C. Vitale, E. Montaldo, R. Conte, C. Cantoni, E. Fulcheri, V. Darretta, L. Moretta and M.C. Mingari, 2011 Cd34+ Hematopoietic Precursors Are Present in Human Decidua and Differentiate into Natural Killer Cells Upon Interaction with Stromal Cells. *Proc Natl Acad Sci U S A*. 108(6): p. 2402.

289. Chinen, H., K. Matsuoka, T. Sato, N. Kamada, S. Okamoto, T. Hisamatsu, T. Kobayashi, H. Hasegawa, A. Sugita, F. Kinjo, J. Fujita and T. Hibi, 2007 Lamina Propria C-Kit+ Immune Precursors Reside in Human Adult Intestine and Differentiate into Natural Killer Cells. *Gastroenterology*. 133(2): p. 559.

290. Andrews, D.M. and M.J. Smyth, 2010 A Potential Role for Rag-1 in Nk Cell Development Revealed by Analysis of Nk Cells During Ontogeny. *Immunol Cell Biol*. 88(2): p. 107.

291. Tian, Z., Y. Chen and B. Gao, 2013 Natural Killer Cells in Liver Disease. *Hepatology*. 57(4): p. 1654.

292. Carrega, P. and G. Ferlazzo, 2012 Natural Killer Cell Distribution and Trafficking in Human Tissues. *Front Immunol*. 3: p. 347.

293. Bjorkstrom, N.K., H.G. Ljunggren and J. Michaelsson, 2016 Emerging Insights into Natural Killer Cells in Human Peripheral Tissues. *Nat Rev Immunol*. 16(5): p. 310.

294. Romagnani, C*., et al.*, 2007 Cd56brightcd16- Killer Ig-Like Receptor- Nk Cells Display Longer Telomeres and Acquire Features of Cd56dim Nk Cells Upon Activation. *J Immunol*. 178(8): p. 4947.

295. Juelke, K., M. Killig, M. Luetke-Eversloh, E. Parente, J. Gruen, B. Morandi, G. Ferlazzo, A. Thiel, I. Schmitt-Knosalla and C. Romagnani, 2010 Cd62l Expression Identifies a Unique Subset of Polyfunctional Cd56dim Nk Cells. *Blood*. 116(8): p. 1299.

296. Montaldo, E., G. Del Zotto, M. Della Chiesa, M.C. Mingari, A. Moretta, A. De Maria and L. Moretta, 2013 Human Nk Cell Receptors/Markers: A Tool to Analyze Nk Cell Development, Subsets and Function. *Cytometry A*. 83(8): p. 702.

297. Ferlazzo, G., D. Thomas, S.-L. Lin, K. Goodman, B. Morandi, W.A. Muller, A. Moretta and C. Münz, 2004 The Abundant Nk Cells in Human Secondary Lymphoid Tissues Require Activation to Express Killer Cell Ig-Like Receptors and Become Cytolytic. *The Journal of Immunology*. 172(3): p. 1455.

298. Hydes, T., M. Abuhilal, T. Armstrong, J. Primrose, A. Takhar and S. Khakoo, 2015 Natural Killer Cell Maturation Markers in the Human Liver and Expansion of an Nkg2c+Kir+ Population. *Lancet*. 385 Suppl 1: p. S45.

299. Montaldo, E., P. Vacca, L. Chiossone, D. Croxatto, F. Loiacono, S. Martini, S. Ferrero, T. Walzer, L. Moretta and M.C. Mingari, 2016 Unique Eomes(+) Nk Cell Subsets Are Present in Uterus and Decidua During Early Pregnancy. *Front Immunol*. 6: p. 646.

300. Lugthart, G., J.E. Melsen, C. Vervat, M.M. van Ostaijen-ten Dam, W.E. Corver, D.L. Roelen, J. van Bergen, M.J.D. van Tol, A.C. Lankester and M.W. Schilham, 2016 Human Lymphoid Tissues Harbor a Distinct Cd69+Cxcr6+ Nk Cell Population. *The Journal of Immunology*. 197(1): p. 78.

301. Marquardt, N*., et al.*, 2015 Cutting Edge: Identification and Characterization of Human Intrahepatic Cd49a+ Nk Cells. *J Immunol*. 194(6): p. 2467.

302. Vossen, M.T., M. Matmati, K.M. Hertoghs, P.A. Baars, M.R. Gent, G. Leclercq, J. Hamann, T.W. Kuijpers and R.A. van Lier, 2008 Cd27 Defines Phenotypically and Functionally Different Human Nk Cell Subsets. *J Immunol*. 180(6): p. 3739.

303. Hamann, I., N. Unterwalder, A.E. Cardona, C. Meisel, F. Zipp, R.M. Ransohoff and C. Infante-Duarte, 2011 Analyses of Phenotypic and Functional Characteristics of Cx3cr1-Expressing Natural Killer Cells. *Immunology*. 133(1): p. 62.

304. Jacobs, R., G. Hintzen, A. Kemper, K. Beul, S. Kempf, G. Behrens, K.W. Sykora and R.E. Schmidt, 2001 Cd56bright Cells Differ in Their Kir Repertoire and Cytotoxic Features from Cd56dim Nk Cells. *Eur J Immunol*. 31(10): p. 3121.

305. Ferlazzo, G., D. Thomas, S.L. Lin, K. Goodman, B. Morandi, W.A. Muller, A. Moretta and C. Munz, 2004 The Abundant Nk Cells in Human Secondary Lymphoid Tissues Require Activation to Express Killer Cell Ig-Like Receptors and Become Cytolytic. *J Immunol*. 172(3): p. 1455.

306. Cooper, M.A., T.A. Fehniger, S.C. Turner, K.S. Chen, B.A. Ghaheri, T. Ghayur, W.E. Carson and M.A. Caligiuri, 2001 Human Natural Killer Cells: A Unique Innate Immunoregulatory Role for the Cd56bright Subset. *Blood*. 97(10): p. 3146.

307. Carrega, P., I. Bonaccorsi, E. Di Carlo, B. Morandi, P. Paul, V. Rizzello, G. Cipollone, G. Navarra, M.C. Mingari, L. Moretta and G. Ferlazzo, 2014 Cd56(Bright)Perforin(Low) Noncytotoxic Human Nk Cells Are Abundant in Both Healthy and Neoplastic Solid Tissues and Recirculate to Secondary Lymphoid Organs Via Afferent Lymph. *J Immunol*. 192(8): p. 3805.

308. Nagler, A., L.L. Lanier, S. Cwirla and J.H. Phillips, 1989 Comparative Studies of Human Fcriii-Positive and Negative Natural Killer Cells. *J Immunol*. 143(10): p. 3183.

309. Moretta, L., 2010 Dissecting Cd56dim Human Nk Cells. *Blood*. 116(19): p. 3689.

310. De Maria, A., F. Bozzano, C. Cantoni and L. Moretta, 2011 Revisiting Human Natural Killer Cell Subset Function Revealed Cytolytic Cd56(Dim)Cd16+ Nk Cells as Rapid Producers of Abundant Ifn-Gamma on Activation. *Proc Natl Acad Sci U S A*. 108(2): p. 728.

311. Beziat, V., D. Duffy, S.N. Quoc, M. Le Garff-Tavernier, J. Decocq, B. Combadiere, P. Debre and V. Vieillard, 2011 Cd56brightcd16+ Nk Cells: A Functional Intermediate Stage of Nk Cell Differentiation. *J Immunol*. 186(12): p. 6753.

312. Takahashi, E., N. Kuranaga, K. Satoh, Y. Habu, N. Shinomiya, T. Asano, S. Seki and M. Hayakawa, 2007 Induction of Cd16+ Cd56bright Nk Cells with Antitumour Cytotoxicity Not Only from Cd16- Cd56bright Nk Cells but Also from Cd16- Cd56dim Nk Cells. *Scand J Immunol*. 65(2): p. 126.

313. Amand, M., G. Iserentant, A. Poli, M. Sleiman, V. Fievez, I.P. Sanchez, N. Sauvageot, T. Michel, N. Aouali, B. Janji, C.M. Trujillo-Vargas, C. Seguin-Devaux and J. Zimmer, 2017 Human Cd56(Dim)Cd16(Dim) Cells as an Individualized Natural Killer Cell Subset. *Front Immunol*. 8: p. 699.

314. Romee, R., B. Foley, T. Lenvik, Y. Wang, B. Zhang, D. Ankarlo, X. Luo, S. Cooley, M. Verneris, B. Walcheck and J. Miller, 2013 Nk Cell Cd16 Surface Expression and Function Is Regulated by a Disintegrin and Metalloprotease-17 (Adam17). *Blood*. 121(18): p. 3599.

315. Lugthart, G., M.M. van Ostaijen-ten Dam, M.J. van Tol, A.C. Lankester and M.W. Schilham, 2015 Cd56(Dim)Cd16(-) Nk Cell Phenotype Can Be Induced by Cryopreservation. *Blood*. 125(11): p. 1842.

316. Grzywacz, B., N. Kataria and M.R. Verneris, 2007 Cd56dimcd16+ Nk Cells Downregulate Cd16 Following Target Cell Induced Activation of Matrix Metalloproteinases. *Leukemia*. 21(2): p. 356.

317. Lutz, C.T., A. Karapetyan, A. Al-Attar, B.J. Shelton, K.J. Holt, J.H. Tucker and S.R. Presnell, 2011 Human Nk Cells Proliferate and Die in Vivo More Rapidly Than T Cells in Healthy Young and Elderly Adults. *The Journal of Immunology*. 186(8): p. 4590.

318. Mamessier, E., L.C. Pradel, M.L. Thibult, C. Drevet, A. Zouine, J. Jacquemier, G. Houvenaeghel, F. Bertucci, D. Birnbaum and D. Olive, 2013 Peripheral Blood Nk Cells from Breast Cancer Patients Are Tumor-Induced Composite Subsets. *J Immunol*. 190(5): p. 2424.

319. Goodier, M.R., C. Lusa, S. Sherratt, A. Rodriguez-Galan, R. Behrens and E.M. Riley, 2016 Sustained Immune Complex-Mediated Reduction in Cd16 Expression after Vaccination Regulates Nk Cell Function. *Front Immunol*. 7: p. 384.

320. Penack, O., C. Gentilini, L. Fischer, A.M. Asemissen, C. Scheibenbogen, E. Thiel and L. Uharek, 2005 Cd56dimcd16neg Cells Are Responsible for Natural Cytotoxicity against Tumor Targets. *Leukemia*. 19(5): p. 835.

321. Koopman, L.A., H.D. Kopcow, B. Rybalov, J.E. Boyson, J.S. Orange, F. Schatz, R. Masch, C.J. Lockwood, A.D. Schachter, P.J. Park and J.L. Strominger, 2003 Human Decidual Natural Killer Cells Are a Unique Nk Cell Subset with Immunomodulatory Potential. *The Journal of Experimental Medicine*. 198(8): p. 1201.

322. Rebuli, M.E., E.A. Pawlak, D. Walsh, E.M. Martin and I. Jaspers, 2018 Distinguishing Human Peripheral Blood Nk Cells from Cd56dimcd16dimcd69+Cd103+ Resident Nasal Mucosal Lavage Fluid Cells. *Scientific Reports*. 8(1): p. 3394.

323. Matloubian, M., 2004 Lymphocyte Egress from Thymus and Peripheral Lymphoid Organs Is Dependent on S1p Receptor 1. *Nature*. 427: p. 355.

324. Allende, M.L., J.L. Dreier, S. Mandala and R.L. Proia, 2004 Expression of the Sphingosine-1-Phosphate Receptor, S1p1, on T-Cells Controls Thymic Emigration. *J. Biol. Chem.* 279: p. 15396.

325. Feng, C., 2002 A Potential Role for Cd69 in Thymocyte Emigration. *Int. Immunol.* 14: p. 535.

326. Nakayama, T., 2002 The Generation of Mature, Single-Positive Thymocytes in Vivo Is Dysregulated by Cd69 Blockade or Overexpression. *J. Immunol.* 168: p. 87.

327. Shiow, L.R., D.B. Rosen, N. Brdickova, Y. Xu, J. An, L.L. Lanier, J.G. Cyster and M. Matloubian, 2006 Cd69 Acts Downstream of Interferon-[Alpha]/[Beta] to Inhibit S1p1 and Lymphocyte Egress from Lymphoid Organs. *Nature*. 440(7083): p. 540.

328. Bank, I., M. Book and R. Ware, 1994 Functional Role of Vla-1 (Cd49a) in Adhesion, Cation-Dependent Spreading, and Activation of Cultured Human T Lymphocytes. *Cell Immunol*. 156(2): p. 424.

329. Patrick, C.W. and X. Wu, 2003 Integrin-Mediated Preadipocyte Adhesion and Migration on Laminin-1. *Annals of Biomedical Engineering*. 31(5): p. 505.

330. Cepek, K.L., S.K. Shaw, C.M. Parker, G.J. Russell, J.S. Morrow, D.L. Rimm and M.B. Brenner, 1994 Adhesion between Epithelial Cells and T Lymphocytes Mediated by E-Cadherin and the Aeβ7 Integrin. *Nature*. 372: p. 190.

331. Richter, M., S.J. Ray, T.J. Chapman, S.J. Austin, J. Rebhahn, T.R. Mosmann, H. Gardner, V. Kotelianski, A.R. deFougerolles and D.J. Topham, 2007 Collagen Distribution and Expression of Collagen-Binding A1β1 (Vla-1) and A2β1 (Vla-2) Integrins on Cd4 and Cd8 T Cells During Influenza Infection. *The Journal of Immunology*. 178(7): p. 4506.

332. Hudspeth, K., M. Donadon, M. Cimino, E. Pontarini, P. Tentorio, M. Preti, M. Hong, A. Bertoletti, S. Bicciato, P. Invernizzi, E. Lugli, G. Torzilli, M.E. Gershwin and D. Mavilio, 2016 Human Liver-Resident Cd56(Bright)/Cd16(Neg) Nk Cells Are Retained within Hepatic Sinusoids Via the Engagement of Ccr5 and Cxcr6 Pathways. *J Autoimmun*. 66: p. 40.

333. Stegmann, K.A., F. Robertson, N. Hansi, U. Gill, C. Pallant, T. Christophides, L.J. Pallett, D. Peppa, C. Dunn, G. Fusai, V. Male, B.R. Davidson, P. Kennedy and M.K. Maini, 2016 Cxcr6 Marks a Novel Subset of T-Betloeomeshi Natural Killer Cells Residing in Human Liver. *Scientific Reports*. 6: p. 26157.

334. Rasid, O., I.S. Ciulean, C. Fitting, N. Doyen and J.M. Cavaillon, 2016 Local Microenvironment Controls the Compartmentalization of Nk Cell Responses During Systemic Inflammation in Mice. *J Immunol*. 197(6): p. 2444.

335. Male, V., A. Sharkey, L. Masters, P.R. Kennedy, L.E. Farrell and A. Moffett, 2011 The Effect of Pregnancy on the Uterine Nk Cell Kir Repertoire. *Eur J Immunol*. 41(10): p. 3017.

336. Peng, H., X. Jiang, Y. Chen, D.K. Sojka, H. Wei, X. Gao, R. Sun, W.M. Yokoyama and Z. Tian, 2013 Liver-Resident Nk Cells Confer Adaptive Immunity in Skin-Contact Inflammation. *J Clin Invest*. 123(4): p. 1444.

337. Gordon, S.M., J. Chaix, L.J. Rupp, J. Wu, S. Madera, J.C. Sun, T. Lindsten and S.L. Reiner, 2012 The Transcription Factors T-Bet and Eomes Control Key Checkpoints of Natural Killer Cell Maturation. *Immunity*. 36(1): p. 55.

338. Daussy, C*., et al.*, 2014 T-Bet and Eomes Instruct the Development of Two Distinct Natural Killer Cell Lineages in the Liver and in the Bone Marrow. *J Exp Med*. 211(3): p. 563.

339. Constantinides, M.G., B.D. McDonald, P.A. Verhoef and A. Bendelac, 2014 A Committed Precursor to Innate Lymphoid Cells. *Nature*. 508: p. 397.

340. Peng, H. and Z. Tian, 2017 Diversity of Tissue-Resident Nk Cells. *Seminars in Immunology*. 31: p. 3.

341. Sojka, D.K., B. Plougastel-Douglas, L. Yang, M.A. Pak-Wittel, M.N. Artyomov, Y. Ivanova, C. Zhong, J.M. Chase, P.B. Rothman, J. Yu, J.K. Riley, J. Zhu, Z. Tian and W.M. Yokoyama, 2014 Tissue-Resident Natural Killer (Nk) Cells Are Cell Lineages Distinct from Thymic and Conventional Splenic Nk Cells. *Elife*. 3: p. e01659.

342. Schuster, I.S., M.E. Wikstrom, G. Brizard, J.D. Coudert, M.J. Estcourt, M. Manzur, L.A. O'Reilly, M.J. Smyth, J.A. Trapani, G.R. Hill, C.E. Andoniou and M.A. Degli-Esposti, 2014 Trail+ Nk Cells Control Cd4+ T Cell Responses During Chronic Viral Infection to Limit Autoimmunity. *Immunity*. 41(4): p. 646.

343. O'Sullivan, T.E., M. Rapp, X. Fan, O.E. Weizman, P. Bhardwaj, N.M. Adams, T. Walzer, A.J. Dannenberg and J.C. Sun, 2016 Adipose-Resident Group 1 Innate Lymphoid Cells Promote Obesity-Associated Insulin Resistance. *Immunity*. 45(2): p. 428.

344. Peng, H. and Z. Tian, 2017 Natural Killer Cell Memory: Progress and Implications. *Front Immunol*. 8: p. 1143.

345. Paust, S., H.S. Gill, B.Z. Wang, M.P. Flynn, E.A. Moseman, B. Senman, M. Szczepanik, A. Telenti, P.W. Askenase, R.W. Compans and U.H. von Andrian, 2010 Critical Role for the Chemokine Receptor Cxcr6 in Nk Cell-Mediated Antigen-Specific Memory of Haptens and Viruses. *Nat Immunol*. 11(12): p. 1127.

346. O'Leary, J.G., M. Goodarzi, D.L. Drayton and U.H. von Andrian, 2006 T Cell- and B Cell-Independent Adaptive Immunity Mediated by Natural Killer Cells. *Nat Immunol*. 7(5): p. 507.

347. Majewska-Szczepanik, M., S. Paust, U.H. von Andrian, P.W. Askenase and M. Szczepanik, 2013 Natural Killer Cell-Mediated Contact Sensitivity Develops Rapidly and Depends on Interferon-Alpha, Interferon-Gamma and Interleukin-12. *Immunology*. 140(1): p. 98.

348. Reeves, R.K., H. Li, S. Jost, E. Blass, H. Li, J.L. Schafer, V. Varner, C. Manickam, L. Eslamizar, M. Altfeld, U.H. von Andrian and D.H. Barouch, 2015 Antigen-Specific Nk Cell Memory in Rhesus Macaques. *Nat Immunol*. 16(9): p. 927.

349. Sun, J.C., J.N. Beilke and L.L. Lanier, 2009 Adaptive Immune Features of Natural Killer Cells. *Nature*. 457(7229): p. 557.

350. Min-Oo, G. and L.L. Lanier, 2014 Cytomegalovirus Generates Long-Lived Antigen-Specific Nk Cells with Diminished Bystander Activation to Heterologous Infection. *The Journal of Experimental Medicine*. 211(13): p. 2669.

351. Suliman, S*., et al.*, 2016 Bacillus Calmette-Guerin (Bcg) Revaccination of Adults with Latent Mycobacterium Tuberculosis Infection Induces Long-Lived Bcg-Reactive Nk Cell Responses. *J Immunol*. 197(4): p. 1100.

352. Goodier, M.R., A. Rodriguez-Galan, C. Lusa, C.M. Nielsen, A. Darboe, A.L. Moldoveanu, M.J. White, R. Behrens and E.M. Riley, 2016 Influenza Vaccination Generates Cytokine-Induced Memory-Like Nk Cells: Impact of Human Cytomegalovirus Infection. *J Immunol*. 197(1): p. 313.

353. Guma, M., M. Budt, A. Saez, T. Brckalo, H. Hengel, A. Angulo and M. Lopez-Botet, 2006 Expansion of Cd94/Nkg2c+ Nk Cells in Response to Human Cytomegalovirus-Infected Fibroblasts. *Blood*. 107(9): p. 3624.

354. Guma, M., A. Angulo, C. Vilches, N. Gomez-Lozano, N. Malats and M. Lopez-Botet, 2004 Imprint of Human Cytomegalovirus Infection on the Nk Cell Receptor Repertoire. *Blood*. 104(12): p. 3664.

355. Lopez-Vergès, S., J.M. Milush, B.S. Schwartz, M.J. Pando, J. Jarjoura, V.A. York, J.P. Houchins, S. Miller, S.-M. Kang, P.J. Norris, D.F. Nixon and L.L. Lanier, 2011 Expansion of a Unique Cd57+Nkg2chi Natural Killer Cell Subset During Acute Human Cytomegalovirus Infection. *Proceedings of the National Academy of Sciences*. 108(36): p. 14725.

356. Schlums, H.*, et al.*, 2015 Cytomegalovirus Infection Drives Adaptive Epigenetic Diversification of Nk Cells with Altered Signaling and Effector Function. *Immunity*. 42(3): p. 443.

357. Lee, J., T. Zhang, I. Hwang, A. Kim, L. Nitschke, M. Kim, J.M. Scott, Y. Kamimura, L.L. Lanier and S. Kim, 2015 Epigenetic Modification and Antibody-Dependent Expansion of Memory-Like Nk Cells in Human Cytomegalovirus-Infected Individuals. *Immunity*. 42(3): p. 431.

358. Sun, J.C., S. Madera, N.A. Bezman, J.N. Beilke, M.H. Kaplan and L.L. Lanier, 2012 Proinflammatory Cytokine Signaling Required for the Generation of Natural Killer Cell Memory. *The Journal of Experimental Medicine*. 209(5): p. 947.

359. Cooper, M.A., J.M. Elliott, P.A. Keyel, L. Yang, J.A. Carrero and W.M. Yokoyama, 2009 Cytokine-Induced Memory-Like Natural Killer Cells. *Proc Natl Acad Sci U S A*. 106(6): p. 1915.

360. Romee, R.*, et al.*, 2016 Cytokine-Induced Memory-Like Natural Killer Cells Exhibit Enhanced Responses against Myeloid Leukemia. *Science Translational Medicine*. 8(357): p. 357ra123.

361. Freeman, C.M., V.R. Stolberg, S. Crudgington, F.J. Martinez, M.K. Han, S.W. Chensue, D.A. Arenberg, C.A. Meldrum, L. McCloskey and J.L. Curtis, 2014 Human Cd56+ Cytotoxic Lung Lymphocytes Kill Autologous Lung Cells in Chronic Obstructive Pulmonary Disease. *PLoS One*. 9(7): p. e103840.

362. Marquardt, N.*, et al.*, 2017 Human Lung Natural Killer Cells Are Predominantly Comprised of Highly Differentiated Hypofunctional Cd69-Cd56dim Cells. *Journal of Allergy and Clinical Immunology*. 139(4): p. 1321.

363. Robertson, M.J., 2002 Role of Chemokines in the Biology of Natural Killer Cells. *J Leukoc Biol*. 71(2): p. 173.

364. Wang, J., F. Li, M. Zheng, R. Sun, H. Wei and Z. Tian, 2012 Lung Natural Killer Cells in Mice: Phenotype and Response to Respiratory Infection. *Immunology*. 137(1): p. 37.

365. Michel, T., A. Poli, O. Domingues, M. Mauffray, M. Theresine, N.H. Brons, F. Hentges and J. Zimmer, 2012 Mouse Lung and Spleen Natural Killer Cells Have Phenotypic and Functional Differences, in Part Influenced by Macrophages. *PLoS One*. 7(12): p. e51230.

366. Robinson, B.W., P. Pinkston and R.G. Crystal, 1984 Natural Killer Cells Are Present in the Normal Human Lung but Are Functionally Impotent. *J Clin Invest*. 74(3): p. 942.

367. Lauzon, W. and I. Lemaire, 1994 Alveolar Macrophage Inhibition of Lung-Associated Nk Activity: Involvement of Prostaglandins and Transforming Growth Factor-Beta 1. *Exp Lung Res*. 20(4): p. 331.

368. Kim, E.-H., Y.-K. Choi, C.-J. Kim, M.-H. Sung and H. Poo, 2015 Intranasal Administration of Poly-Gamma Glutamate Induced Antiviral Activity and Protective Immune Responses against H1n1 Influenza a Virus Infection. *Virology Journal*. 12: p. 160.

369. Ishikawa, H., S. Ino, H. Sasaki, T. Fukui, C. Kohda and K. Tanaka, 2016 The Protective Effects of Intranasal Administration of Il-12 Given before Influenza Virus Infection and the Negative Effects of Il-12 Treatment Given after Viral Infection. *Journal of Medical Virology*. 88(9): p. 1487.

370. Sellers, R.S., C.B. Clifford, P.M. Treuting and C. Brayton, 2012 Immunological Variation between Inbred Laboratory Mouse Strains:Points to Consider in Phenotyping Genetically Immunomodified Mice. *Veterinary Pathology*. 49(1): p. 32.

371. Tate, M.D., Y.M. Deng, J.E. Jones, G.P. Anderson, A.G. Brooks and P.C. Reading, 2009 Neutrophils Ameliorate Lung Injury and the Development of Severe Disease During Influenza Infection. *J Immunol*. 183(11): p. 7441.

372. Forberg, H., A.G. Hauge, M. Valheim, F. Garcon, A. Nunez, W. Gerner, K.H. Mair, S.P. Graham, S.M. Brookes and A.K. Storset, 2014 Early Responses of Natural Killer Cells in Pigs Experimentally Infected with 2009 Pandemic H1n1 Influenza a Virus. *PLoS One*. 9(6): p. e100619.

373. Jost, S., J. Reardon, E. Peterson, D. Poole, R. Bosch, G. Alter and M. Altfeld, 2011 Expansion of 2b4+ Natural Killer (Nk) Cells and Decrease in Nkp46+ Nk Cells in Response to Influenza. *Immunology*. 132(4): p. 516.

374. Jost, S., H. Quillay, J. Reardon, E. Peterson, R.P. Simmons, B.A. Parry, N.N. Bryant, W.D. Binder and M. Altfeld, 2011 Changes in Cytokine Levels and Nk Cell Activation Associated with Influenza. *PLoS One*. 6(9): p. e25060.

375. Kronstad, L.M., C. Seiler, R. Vergara, S.P. Holmes and C.A. Blish, 2017 Strain-Specific Human Natural Killer Cell Recognition of Influenza a Virus. *bioRxiv*.

376. Mendelson, M., Y. Tekoah, A. Zilka, O. Gershoni-Yahalom, R. Gazit, H. Achdout, N.V. Bovin, T. Meningher, M. Mandelboim, O. Mandelboim, A. David and A. Porgador, 2010 Nkp46 O-Glycan Sequences That Are Involved in the Interaction with Hemagglutinin Type 1 of Influenza Virus. *J Virol*. 84(8): p. 3789.

377. Duev-Cohen, A., Y. Bar-On, A. Glasner, O. Berhani, Y. Ophir, F. Levi-Schaffer, M. Mandelboim and O. Mandelboim, 2016 The Human 2b4 and Ntb-a Receptors Bind the Influenza Viral Hemagglutinin and Co-Stimulate Nk Cell Cytotoxicity. *Oncotarget*.

378. Siren, J., T. Sareneva, J. Pirhonen, M. Strengell, V. Veckman, I. Julkunen and S. Matikainen, 2004 Cytokine and Contact-Dependent Activation of Natural Killer Cells by Influenza a or Sendai Virus-Infected Macrophages. *J Gen Virol*. 85(Pt 8): p. 2357.

379. Glasner, A., A. Zurunic, T. Meningher, T. Lenac Rovis, P. Tsukerman, Y. Bar-On, R. Yamin, A.F. Meyers, M. Mandeboim, S. Jonjic and O. Mandelboim, 2012 Elucidating the Mechanisms of Influenza Virus Recognition by Ncr1. *PLoS One*. 7(5): p. e36837.

380. Mandelboim, O. and A. Porgador, 2001 Nkp46. *The International Journal of Biochemistry & Cell Biology*. 33(12): p. 1147.

381. Arnon, T.I., H. Achdout, N. Lieberman, R. Gazit, T. Gonen-Gross, G. Katz, A. Bar-Ilan, N. Bloushtain, M. Lev, A. Joseph, E. Kedar, A. Porgador and O. Mandelboim, 2004 The Mechanisms Controlling the Recognition of Tumor- and Virus-Infected Cells by Nkp46. *Blood*. 103(2): p. 664.

382. Gazit, R., R. Gruda, M. Elboim, T.I. Arnon, G. Katz, H. Achdout, J. Hanna, U. Qimron, G. Landau, E. Greenbaum, Z. Zakay-Rones, A. Porgador and O. Mandelboim, 2006 Lethal Influenza Infection in the Absence of the Natural Killer Cell Receptor Gene Ncr1. *Nat Immunol*. 7(5): p. 517.

383. Ahlenstiel, G., M.P. Martin, X. Gao, M. Carrington and B. Rehermann, 2008 Distinct Kir/Hla Compound Genotypes Affect the Kinetics of Human Antiviral Natural Killer Cell Responses. *J Clin Invest*. 118(3): p. 1017.

384. Aranda-Romo, S., C.A. Garcia-Sepulveda, A. Comas-Garcia, F. Lovato-Salas, M. Salgado-Bustamante, A. Gomez-Gomez and D.E. Noyola, 2012 Killer-Cell Immunoglobulin-Like Receptors (Kir) in Severe a (H1n1) 2009 Influenza Infections. *Immunogenetics*. 64(9): p. 653.

385. La, D., C. Czarnecki, H. El-Gabalawy, A. Kumar, A.F. Meyers, N. Bastien, J.N. Simonsen, F.A. Plummer and M. Luo, 2011 Enrichment of Variations in Kir3dl1/S1 and Kir2dl2/L3 among H1n1/09 Icu Patients: An Exploratory Study. *PLoS One*. 6(12): p. e29200.

386. Wines, B.D., H.A. Vanderven, S.E. Esparon, A.B. Kristensen, S.J. Kent and P.M. Hogarth, 2016 Dimeric Fcgammar Ectodomains as Probes of the Fc Receptor Function of Anti-Influenza Virus Igg. *J Immunol*. 197(4): p. 1507.

387. Jegaskanda, S., K.L. Laurie, T.H. Amarasena, W.R. Winnall, M. Kramski, R. De Rose, I.G. Barr, A.G. Brooks, P.C. Reading and S.J. Kent, 2013 Age-Associated Cross-Reactive Antibody-Dependent Cellular Cytotoxicity toward 2009 Pandemic Influenza a Virus Subtype H1n1. *Journal of Infectious Diseases*. 208(7): p. 1051.

388. Jegaskanda, S., H.A. Vanderven, H.X. Tan, S. Alcantara, K. Wragg, M.S. Parsons, A. Chung, J.A. Juno and S.J. Kent, 2018 Influenza Infection Enhances Antibody-Mediated Nk Cell Functions Via Type I Interferon Dependent Pathways. *J Virol*.

389. He, W., G.S. Tan, C.E. Mullarkey, A.J. Lee, M.M. Lam, F. Krammer, C. Henry, P.C. Wilson, A.A. Ashkar, P. Palese and M.S. Miller, 2016 Epitope Specificity Plays a Critical Role in Regulating Antibody-Dependent Cell-Mediated Cytotoxicity against Influenza a Virus. *Proc Natl Acad Sci U S A*. 113(42): p. 11931.

390. Liew, F.Y., S.M. Russell, G. Appleyard, C.M. Brand and J. Beale, 1984 Cross-Protection in Mice Infected with Influenza a Virus by the Respiratory Route Is Correlated with Local Iga Antibody Rather Than Serum Antibody or Cytotoxic T Cell Reactivity. *European Journal of Immunology*. 14(4): p. 350.

391. Clements, M.L., R.F. Betts, E.L. Tierney and B.R. Murphy, 1986 Serum and Nasal Wash Antibodies Associated with Resistance to Experimental Challenge with Influenza a Wild-Type Virus. *Journal of Clinical Microbiology*. 24(1): p. 157.

392. Belshe, R.B.*, et al.*, 2000 Correlates of Immune Protection Induced by Live, Attenuated, Cold-Adapted, Trivalent, Intranasal Influenza Virus Vaccine. *Journal of Infectious Diseases*. 181(3): p. 1133.

393. Stein-Streilein, J., M. Bennett, D. Mann and V. Kumar, 1983 Natural Killer Cells in Mouse Lung: Surface Phenotype, Target Preference, and Response to Local Influenza Virus Infection. *J Immunol*. 131(6): p. 2699.

394. Stein-Streilein, J., P.L. Witte, J.W. Streilein and J. Guffee, 1985 Local Cellular Defenses in Influenza-Infected Lungs. *Cell Immunol*. 95(2): p. 234.

395. Proudfoot, A.E.I., 2002 Chemokine Receptors: Multifaceted Therapeutic Targets. *Nature Reviews Immunology*. 2: p. 106.

396. Brady, J., S. Carotta, R.P. Thong, C.J. Chan, Y. Hayakawa, M.J. Smyth and S.L. Nutt, 2010 The Interactions of Multiple Cytokines Control Nk Cell Maturation. *J Immunol*. 185(11): p. 6679.

397. Trinchieri, G. and D. Santoli, 1978 Anti-Viral Activity Induced by Culturing Lymphocytes with Tumor-Derived or Virus-Transformed Cells. Enhancement of Human Natural Killer Cell Activity by Interferon and Antagonistic Inhibition of Susceptibility of Target Cells to Lysis. *J Exp Med*. 147(5): p. 1314.

398. Gidlund, M., A. Orn, H. Wigzell, A. Senik and I.O.N. Gresser, 1978 Enhanced Nk Cell Activity in Mice Injected with Interferon and Interferon Inducers. *Nature*. 273(5665): p. 759.

399. Herberman, R.B., J.Y. Djeu, J.R. Ortaldo, H.T. Holden, W.H. West and G.D. Bonnard, 1978 Role of Interferon in Augmentation of Natural and Antibody-Dependent Cell-Mediated Cytotoxicity. *Cancer Treat Rep*. 62(11): p. 1893.

400. Sato, K., S. Hida, H. Takayanagi, T. Yokochi, N. Kayagaki, K. Takeda, H. Yagita, K. Okumura, N. Tanaka, T. Taniguchi and K. Ogasawara, 2001 Antiviral Response by Natural Killer Cells through Trail Gene Induction by Ifn-Alpha/Beta. *Eur J Immunol*. 31(11): p. 3138.

401. Arimori, Y., R. Nakamura, H. Yamada, K. Shibata, N. Maeda, T. Kase and Y. Yoshikai, 2014 Type I Interferon Plays Opposing Roles in Cytotoxicity and Interferon-Gamma Production by Natural Killer and Cd8 T Cells after Influenza a Virus Infection in Mice. *J Innate Immun*. 6(4): p. 456.

402. Souza-Fonseca-Guimaraes, F., A. Young, D. Mittal, L. Martinet, C. Bruedigam, K. Takeda, C.E. Andoniou, M.A. Degli-Esposti, G.R. Hill and M.J. Smyth, 2015 Nk Cells Require Il-28r for Optimal in Vivo Activity. *Proceedings of the National Academy of Sciences*. 112(18): p. E2376.

403. Jewell, N.A., T. Cline, S.E. Mertz, S.V. Smirnov, E. Flaño, C. Schindler, J.L. Grieves, R.K. Durbin, S.V. Kotenko and J.E. Durbin, 2010 Lambda Interferon Is the Predominant Interferon Induced by Influenza a Virus Infection in Vivo. *J Virol*. 84(21): p. 11515.

404. Hwang, I., J.M. Scott, T. Kakarla, D.M. Duriancik, S. Choi, C. Cho, T. Lee, H. Park, A.R. French, E. Beli, E. Gardner and S. Kim, 2013 Activation Mechanisms of Natural Killer Cells During Influenza Virus Infection. *PLoS ONE*. 7(12): p. e51858.

405. Crouse, J., G. Bedenikovic, M. Wiesel, M. Ibberson, I. Xenarios, D. Von Laer, U. Kalinke, E. Vivier, S. Jonjic and A. Oxenius, 2014 Type I Interferons Protect T Cells against Nk Cell Attack Mediated by the Activating Receptor Ncr1. *Immunity*. 40(6): p. 961.

406. Hama, Y., M. Kurokawa, M. Imakita, Y. Yoshida, T. Shimizu, W. Watanabe and K. Shiraki, 2009 Interleukin 12 Is a Primary Cytokine Responding to Influenza Virus Infection in the Respiratory Tract of Mice. *Acta Virol*. 53(4): p. 233.

407. Nguyen, K.B., T.P. Salazar-Mather, M.Y. Dalod, J.B. Van Deusen, X.-q. Wei, F.Y. Liew, M.A. Caligiuri, J.E. Durbin and C.A. Biron, 2002 Coordinated and Distinct Roles for Ifn-Aβ, Il-12, and Il-15 Regulation of Nk Cell Responses to Viral Infection. *The Journal of Immunology*. 169(8): p. 4279.

408. Fernandez, N.C., A. Lozier, C. Flament, P. Ricciardi-Castagnoli, D. Bellet, M. Suter, M. Perricaudet, T. Tursz, E. Maraskovsky and L. Zitvogel, 1999 Dendritic Cells Directly Trigger Nk Cell Functions: Cross-Talk Relevant in Innate Anti-Tumor Immune Responses in Vivo. *Nat Med*. 5(4): p. 405.

409. Newman, K.C. and E.M. Riley, 2007 Whatever Turns You On: Accessory-Cell-Dependent Activation of Nk Cells by Pathogens. *Nat Rev Immunol*. 7(4): p. 279.

410. Michel, T., F. Hentges and J. Zimmer, 2012 Consequences of the Crosstalk between Monocytes/Macrophages and Natural Killer Cells. *Front Immunol*. 3: p. 403.

411. Brill, K.J., Q. Li, R. Larkin, D.H. Canaday, D.R. Kaplan, W.H. Boom and R.F. Silver, 2001 Human Natural Killer Cells Mediate Killing of Intracellular Mycobacterium Tuberculosis H37rv Via Granule-Independent Mechanisms. *Infect Immun*. 69(3): p. 1755.

412. Haller, D., P. Serrant, D. Granato, E.J. Schiffrin and S. Blum, 2002 Activation of Human Nk Cells by Staphylococci and Lactobacilli Requires Cell Contact-Dependent Costimulation by Autologous Monocytes. *Clin Diagn Lab Immunol*. 9(3): p. 649.

413. Schierloh, P., M. Aleman, N. Yokobori, L. Alves, N. Roldan, E. Abbate, C.S.M. del and S. de la Barrera, 2005 Nk Cell Activity in Tuberculosis Is Associated with Impaired Cd11a and Icam-1 Expression: A Regulatory Role of Monocytes in Nk Activation. *Immunology*. 116(4): p. 541.

414. Denis, M., D.L. Keen, N.A. Parlane, A.K. Storset and B.M. Buddle, 2007 Bovine Natural Killer Cells Restrict the Replication of Mycobacterium Bovis in Bovine Macrophages and Enhance Il-12 Release by Infected Macrophages. *Tuberculosis (Edinb)*. 87(1): p. 53.

415. Lapaque, N., T. Walzer, S. Meresse, E. Vivier and J. Trowsdale, 2009 Interactions between Human Nk Cells and Macrophages in Response to Salmonella Infection. *J Immunol*. 182(7): p. 4339.

416. Elhaik-Goldman, S*., et al.*, 2011 The Natural Cytotoxicity Receptor 1 Contribution to Early Clearance of Streptococcus Pneumoniae and to Natural Killer-Macrophage Cross Talk. *PLoS One*. 6(8): p. e23472.

417. Klezovich-Benard, M., J.P. Corre, H. Jusforgues-Saklani, D. Fiole, N. Burjek, J.N. Tournier and P.L. Goossens, 2012 Mechanisms of Nk Cell-Macrophage Bacillus Anthracis Crosstalk: A Balance between Stimulation by Spores and Differential Disruption by Toxins. *PLoS Pathog*. 8(1): p. e1002481.

418. Souza-Fonseca-Guimaraes, F., M. Parlato, F. Philippart, B. Misset, J.M. Cavaillon, M. Adib-Conquy and g. Captain study, 2012 Toll-Like Receptors Expression and Interferon-Gamma Production by Nk Cells in Human Sepsis. *Crit Care*. 16(5): p. R206.

419. Atochina, O. and D. Harn, 2005 Lnfpiii/Lex-Stimulated Macrophages Activate Natural Killer Cells Via Cd40-Cd40l Interaction. *Clin Diagn Lab Immunol*. 12(9): p. 1041.

420. Bellora, F., R. Castriconi, A. Dondero, G. Reggiardo, L. Moretta, A. Mantovani, A. Moretta and C. Bottino, 2010 The Interaction of Human Natural Killer Cells with Either Unpolarized or Polarized Macrophages Results in Different Functional Outcomes. *Proc Natl Acad Sci U S A*. 107(50): p. 21659.

421. Kloss, M., P. Decker, K.M. Baltz, T. Baessler, G. Jung, H.G. Rammensee, A. Steinle, M. Krusch and H.R. Salih, 2008 Interaction of Monocytes with Nk Cells Upon Toll-Like Receptor-Induced Expression of the Nkg2d Ligand Mica. *J Immunol*. 181(10): p. 6711.

422. Tripp, C.S., S.F. Wolf and E.R. Unanue, 1993 Interleukin 12 and Tumor Necrosis Factor Alpha Are Costimulators of Interferon Gamma Production by Natural Killer Cells in Severe Combined Immunodeficiency Mice with Listeriosis, and Interleukin 10 Is a Physiologic Antagonist. *Proc Natl Acad Sci U S A*. 90(8): p. 3725.

423. Staples, K.J., B. Nicholas, R.T. McKendry, C.M. Spalluto, J.C. Wallington, C.W. Bragg, E.C. Robinson, K. Martin, R. Djukanovic and T.M. Wilkinson, 2015 Viral Infection of Human Lung Macrophages Increases Pdl1 Expression Via Ifnbeta. *PLoS One*. 10(3): p. e0121527.

424. Monteerarat, Y.*, et al.*, 2010 Induction of Tnf-Alpha in Human Macrophages by Avian and Human Influenza Viruses. *Arch Virol*. 155(8): p. 1273.

425. Geiler, J., M. Michaelis, P. Sithisarn and J. Cinatl, Jr., 2011 Comparison of Pro-Inflammatory Cytokine Expression and Cellular Signal Transduction in Human Macrophages Infected with Different Influenza a Viruses. *Med Microbiol Immunol*. 200(1): p. 53.

426. Li, T., J. Wang, Y. Wang, Y. Chen, H. Wei, R. Sun and Z. Tian, 2017 Respiratory Influenza Virus Infection Induces Memory-Like Liver Nk Cells in Mice. *J Immunol*. 198(3): p. 1242.

427. Wortham, B.W., B.L. Eppert, J.L. Flury, S. Morgado Garcia and M.T. Borchers, 2013 Tlr and Nkg2d Signaling Pathways Mediate Cs-Induced Pulmonary Pathologies. *PLoS One*. 8(10): p. e78735.

428. Nicholas, B.*, et al.*, 2015 A Novel Lung Explant Model for the Ex Vivo Study of Efficacy and Mechanisms of Anti-Influenza Drugs. *Journal of immunology (Baltimore, Md. : 1950)*. 194(12): p. 6144.

429. McKendry, R.T., C.M. Spalluto, H. Burke, B. Nicholas, D. Cellura, A. Al-Shamkhani, K.J. Staples and T.M.A. Wilkinson, 2016 Dysregulation of Antiviral Function of Cd8(+) T Cells in the Chronic Obstructive Pulmonary Disease Lung. Role of the Pd-1–Pd-L1 Axis. *American Journal of Respiratory and Critical Care Medicine*. 193(6): p. 642.

430. Staples, K.J., T.S.C. Hinks, J.A. Ward, V. Gunn, C. Smith and R. Djukanović, 2012 Phenotypic Characterization of Lung Macrophages in Asthmatic Patients: Overexpression of Ccl17. *Journal of Allergy and Clinical Immunology*. 130(6): p. 1404.

431. Tudhope, S.J., T.K. Finney-Hayward, A.G. Nicholson, R.J. Mayer, M.S. Barnette, P.J. Barnes and L.E. Donnelly, 2008 Different Mitogen-Activated Protein Kinase-Dependent Cytokine Responses in Cells of the Monocyte Lineage. *J Pharmacol Exp Ther*. 324(1): p. 306.

432. Winkler, A.R., K.H. Nocka, T.H. Sulahian, L. Kobzik and C.M. Williams, 2008 In Vitro Modeling of Human Alveolar Macrophage Smoke Exposure: Enhanced Inflammation and Impaired Function. *Exp Lung Res*. 34(9): p. 599.

433. Cooper, G.E., Z.C. Pounce, J.C. Wallington, L.Y. Bastidas-Legarda, B. Nicholas, C. Chidomere, E.C. Robinson, K. Martin, A.S. Tocheva, M. Christodoulides, R. Djukanovic, T.M.A. Wilkinson and K.J. Staples, 2016 Viral Inhibition of Bacterial Phagocytosis by Human Macrophages: Redundant Role of Cd36. *PLOS ONE*. 11(10): p. e0163889.

434. Kirkwood, B.R. and J.A.C. Sterne, Essentials Medical Statistics. 2nd ed. 2008, Malden, Massacheusetts, USA: Blackwell Science Ltd.

435. Silver, J.S. and A.A. Humbles, 2017 Nk Cells Join the Plasticity Party. *Nature Immunology*. 18: p. 959.

436. Cichocki, F., E. Sitnicka and Y.T. Bryceson, 2014 Nk Cell Development and Function – Plasticity and Redundancy Unleashed. *Seminars in Immunology*. 26(2): p. 114.

437. Benali, R., F. Dupuit, M. Chevillard, J. Jacquot, B. Haye and E. Puchelle, 1991 Modulations of the Epithelial Phenotype and Functional Activity of Cultured Bovine Tracheal Gland Cells: Dependence on the Culture Medium and Passage Number. *Biol Cell*. 73(1): p. 49.

438. Ortaldo, J.R., R.T. Winkler-Pickett, S. Nagata and C.F. Ware, 1997 Fas Involvement in Human Nk Cell Apoptosis: Lack of a Requirement for Cd16-Mediated Events. *J Leukoc Biol*. 61(2): p. 209.

439. Poli, A., T. Michel, M. Theresine, E. Andres, F. Hentges and J. Zimmer, 2009 Cd56bright Natural Killer (Nk) Cells: An Important Nk Cell Subset. *Immunology*. 126(4): p. 458.

440. Uhrberg, M., P. Parham and P. Wernet, 2002 Definition of Gene Content for Nine Common Group B Haplotypes of the Caucasoid Population: Kir Haplotypes Contain between Seven and Eleven Kir Genes. *Immunogenetics*. 54(4): p. 221.

441. Lutz, C.T., M.B. Moore, S. Bradley, B.J. Shelton and S.K. Lutgendorf, 2005 Reciprocal Age Related Change in Natural Killer Cell Receptors for Mhc Class I. *Mech Ageing Dev*. 126(6-7): p. 722.

442. Le Garff-Tavernier, M., V. Béziat, J. Decocq, V. Siguret, F. Gandjbakhch, E. Pautas, P. Debré, H. Merle-Beral and V. Vieillard, 2010 Human Nk Cells Display Major Phenotypic and Functional Changes over the Life Span. *Aging Cell*. 9(4): p. 527.

443. Almeida-Oliveira, A., M. Smith-Carvalho, L.C. Porto, J. Cardoso-Oliveira, A.d.S. Ribeiro, R.R. Falcão, E. Abdelhay, L.F. Bouzas, L.C.S. Thuler, M.H. Ornellas and H.R. Diamond, 2011 Age-

Related Changes in Natural Killer Cell Receptors from Childhood through Old Age. *Human Immunology*. 72(4): p. 319.

444. Gruver, A.L., L.L. Hudson and G.D. Sempowski, 2007 Immunosenescence of Ageing. *The Journal of pathology*. 211(2): p. 144.

445. Hazeldine, J., P. Hampson and J.M. Lord, 2012 Reduced Release and Binding of Perforin at the Immunological Synapse Underlies the Age-Related Decline in Natural Killer Cell Cytotoxicity. *Aging Cell*. 11(5): p. 751.

446. Ruggieri, A., S. Anticoli, A. D'Ambrosio, L. Giordani and M. Viora, 2016 The Influence of Sex and Gender on Immunity, Infection and Vaccination. *Ann Ist Super Sanita*. 52(2): p. 198.

447. Klein, S.L. and K.L. Flanagan, 2016 Sex Differences in Immune Responses. *Nature Reviews Immunology*. 16: p. 626.

448. Srpan, K., A. Ambrose, A. Karampatzakis, M. Saeed, A.N.R. Cartwright, K. Guldevall, G.D.S.C. De Matos, B. Önfelt and D.M. Davis, 2018 Shedding of Cd16 Disassembles the Nk Cell Immune Synapse and Boosts Serial Engagement of Target Cells. *The Journal of Cell Biology*.

449. Long, E.O. and S. Rajagopalan, 2002 Stress Signals Activate Natural Killer Cells. *The Journal of Experimental Medicine*. 196(11): p. 1399.

450. Zilka, A., G. Landau, O. Hershkovitz, N. Bloushtain, A. Bar-Ilan, F. Benchetrit, E. Fima, T.H. van Kuppevelt, J.T. Gallagher, S. Elgavish and A. Porgador, 2005 Characterization of the Heparin/Heparan Sulfate Binding Site of the Natural Cytotoxicity Receptor Nkp46. *Biochemistry*. 44(44): p. 14477.

451. Bobek, V., M. Boubelik, A. Fiserova, M. L'Uptovcova, L. Vannucci, G. Kacprzak, J. Kolodzej, A.M. Majewski and R.M. Hoffman, 2005 Anticoagulant Drugs Increase Natural Killer Cell Activity in Lung Cancer. *Lung Cancer*. 47(2): p. 215.

452. Naranbhai, V., P. Bartman, D. Ndlovu, P. Ramkalawon, T. Ndung'u, D. Wilson, M. Altfeld and W.H. Carr, 2011 Impact of Blood Processing Variations on Natural Killer Cell Frequency, Activation, Chemokine Receptor Expression and Function. *Journal of immunological methods*. 366(1-2): p. 28.

453. Poggi, A., A.M. Massaro, S. Negrini, P. Contini and M.R. Zocchi, 2005 Tumor-Induced Apoptosis of Human Il-2-Activated Nk Cells: Role of Natural Cytotoxicity Receptors. *J Immunol*. 174(5): p. 2653.

454. Krishnaraj, R., 1997 Senescence and Cytokines Modulate the Nk Cell Expression. *Mech Ageing Dev*. 96(1-3): p. 89.

455. Hayhoe, R.P., S.M. Henson, A.N. Akbar and D.B. Palmer, 2010 Variation of Human Natural Killer Cell Phenotypes with Age: Identification of a Unique Klrg1-Negative Subset. *Hum Immunol*. 71(7): p. 676.

456. Simpson, R.J., C. Cosgrove, L.A. Ingram, G.D. Florida-James, G.P. Whyte, H. Pircher and K. Guy, 2008 Senescent T-Lymphocytes Are Mobilised into the Peripheral Blood Compartment in Young and Older Humans after Exhaustive Exercise. *Brain, Behavior, and Immunity*. 22(4): p. 544.

457. Vyse, A.J., L.M. Hesketh and R.G. Pebody, 2009 The Burden of Infection with Cytomegalovirus in England and Wales: How Many Women Are Infected in Pregnancy? *Epidemiol Infect*. 137(4): p. 526.

458. van Boven, M., J. van de Kassteele, M.J. Korndewal, C.H. van Dorp, M. Kretzschmar, F. van der Klis, H.E. de Melker, A.C. Vossen and D. van Baarle, 2017 Infectious Reactivation of Cytomegalovirus Explaining Age- and Sex-Specific Patterns of Seroprevalence. *PLoS computational biology*. 13(9): p. e1005719.

459. Campos, C., A. Pera, B. Sanchez-Correa, C. Alonso, I. Lopez-Fernandez, S. Morgado, R. Tarazona and R. Solana, 2014 Effect of Age and Cmv on Nk Cell Subpopulations. *Experimental Gerontology*. 54: p. 130.

460. Hutton, A.J., Characterisation of the Human Lung Fibroblasts Ability to Act as an Antigen Presenting Cell for T Helper Cells of the Immune System. 2015. University of Southampton. University of Southampton.

461. Finch, D.K., V.R. Stolberg, J. Ferguson, H. Alikaj, M.R. Kady, B.W. Richmond, V.V. Polosukhin, T.S. Blackwell, L. McCloskey, J.L. Curtis and C.M. Freeman, 2018 Lung Dendritic Cells Drive Nk Cytotoxicity in Chronic Obstructive Pulmonary Disease Via Il-15rα. *American Journal of Respiratory and Critical Care Medicine*. 0(ja): p. null.

462. Hydes, T., Innate and Adaptive Natural Killer Cells in the Liver and the Peripheral Blood. 2017, PhD thesis. University of Southampton. Southampton, UK.

463. Spits, H., D. Artis, M. Colonna, A. Diefenbach, J.P. Di Santo, G. Eberl, S. Koyasu, R.M. Locksley, A.N. McKenzie, R.E. Mebius, F. Powrie and E. Vivier, 2013 Innate Lymphoid Cells--a Proposal for Uniform Nomenclature. *Nat Rev Immunol*. 13(2): p. 145.

464. De Grove, K.C., S. Provoost, F.M. Verhamme, K.R. Bracke, G.F. Joos, T. Maes and G.G. Brusselle, 2016 Characterization and Quantification of Innate Lymphoid Cell Subsets in Human Lung. *PLoS One*. 11(1): p. e0145961.

465. Peng, T. and E.E. Morrisey, 2013 Development of the Pulmonary Vasculature: Current Understanding and Concepts for the Future. *Pulm Circ*. 3(1): p. 176.

466. He, X., V.L. de Oliveira, R. Keijsers, I. Joosten and H.J.P.N. Koenen, 2016 Lymphocyte Isolation from Human Skin for Phenotypic Analysis and Ex Vivo Cell Culture. *Journal of Visualized Experiments : JoVE*, (110): p. 52564.

467. Galli, S.J., N. Borregaard and T.A. Wynn, 2011 Phenotypic and Functional Plasticity of Cells of Innate Immunity: Macrophages, Mast Cells and Neutrophils. *Nature Immunology*. 12: p. 1035.

468. Wu, Y., Z. Tian and H. Wei, 2017 Developmental and Functional Control of Natural Killer Cells by Cytokines. *Frontiers in immunology*. 8: p. 930.

469. Borchers, M.T.*, et al.*, 2009 Sustained Ctl Activation by Murine Pulmonary Epithelial Cells Promotes the Development of Copd-Like Disease. *J Clin Invest*. 119(3): p. 636.

470. Motz, G.T., B.L. Eppert, B.W. Wortham, R.M. Amos-Kroohs, J.L. Flury, S.C. Wesselkamper and M.T. Borchers, 2010 Chronic Cigarette Smoke Exposure Primes Nk Cell Activation in a Mouse Model of Chronic Obstructive Pulmonary Disease. *The Journal of Immunology*. 184(8): p. 4460.

471. Strauch, U.G., R.C. Mueller, X.Y. Li, M. Cernadas, J.M. Higgins, D.G. Binion and C.M. Parker, 2001 Integrin Alpha E(Cd103)Beta 7 Mediates Adhesion to Intestinal Microvascular Endothelial Cell Lines Via an E-Cadherin-Independent Interaction. *J Immunol*. 166(5): p. 3506.

472. Nieto, M., F. Navarro, J.J. Perez-Villar, M.A. del Pozo, R. Gonzalez-Amaro, M. Mellado, J.M. Frade, A.C. Martinez, M. Lopez-Botet and F. Sanchez-Madrid, 1998 Roles of Chemokines and Receptor Polarization in Nk-Target Cell Interactions. *J Immunol*. 161(7): p. 3330.

473. Gregoire, C., L. Chasson, C. Luci, E. Tomasello, F. Geissmann, E. Vivier and T. Walzer, 2007 The Trafficking of Natural Killer Cells. *Immunol Rev*. 220: p. 169.

474. Kohlmeier, J.E., S.C. Miller, J. Smith, B. Lu, C. Gerard, T. Cookenham, A.D. Roberts and D.L. Woodland, 2008 The Chemokine Receptor Ccr5 Plays a Key Role in the Early Memory Cd8+ T Cell Response to Respiratory Virus Infections. *Immunity*. 29(1): p. 101.

475. Lindell, D.M., T.J. Standiford, P. Mancuso, Z.J. Leshen and G.B. Huffnagle, 2001 Macrophage Inflammatory Protein 1alpha/Ccl3 Is Required for Clearance of an Acute Klebsiella Pneumoniae Pulmonary Infection. *Infect Immun*. 69(10): p. 6364.

476. Van de Walle, G.R., K. Sakamoto and N. Osterrieder, 2008 Ccl3 and Viral Chemokine-Binding Protein Gg Modulate Pulmonary Inflammation and Virus Replication During Equine Herpesvirus 1 Infection. *Journal of Virology*. 82(4): p. 1714.

477. Tregoning, J.S., P.K. Pribul, A.M. Pennycook, T. Hussell, B. Wang, N. Lukacs, J. Schwarze, F.J. Culley and P.J. Openshaw, 2010 The Chemokine Mip1alpha/Ccl3 Determines Pathology in Primary Rsv Infection by Regulating the Balance of T Cell Populations in the Murine Lung. *PLoS One*. 5(2): p. e9381.

478. Olszewski, M.A., G.B. Huffnagle, T.R. Traynor, R.A. McDonald, D.N. Cook and G.B. Toews, 2001 Regulatory Effects of Macrophage Inflammatory Protein 1alpha/Ccl3 on the Development of Immunity to Cryptococcus Neoformans Depend on Expression of Early Inflammatory Cytokines. *Infection and immunity*. 69(10): p. 6256.

479. Culley, F.J., A.M. Pennycook, J.S. Tregoning, J.S. Dodd, G. Walzl, T.N. Wells, T. Hussell and P.J. Openshaw, 2006 Role of Ccl5 (Rantes) in Viral Lung Disease. *J Virol*. 80(16): p. 8151.

480. Palaniappan, R., S. Singh, U.P. Singh, R. Singh, E.W. Ades, D.E. Briles, S.K. Hollingshead, W. Royal, 3rd, J.S. Sampson, J.K. Stiles, D.D. Taub and J.W. Lillard, Jr., 2006 Ccl5 Modulates Pneumococcal Immunity and Carriage. *J Immunol*. 176(4): p. 2346.

481. Wu, Y., Y.Y. Li, K. Matsushima, T. Baba and N. Mukaida, 2008 Ccl3-Ccr5 Axis Regulates Intratumoral Accumulation of Leukocytes and Fibroblasts and Promotes Angiogenesis in Murine Lung Metastasis Process. *J Immunol*. 181(9): p. 6384.

482. Borczuk, A.C., N. Papanikolaou, R.L. Toonkel, M. Sole, L.A. Gorenstein, M.E. Ginsburg, J.R. Sonett, R.A. Friedman and C.A. Powell, 2008 Lung Adenocarcinoma Invasion in Tgfbetarii-Deficient Cells Is Mediated by Ccl5/Rantes. *Oncogene*. 27(4): p. 557.

483. Hodge, G., V. Mukaro, M. Holmes, P.N. Reynolds and S. Hodge, 2013 Enhanced Cytotoxic Function of Natural Killer and Natural Killer T-Like Cells Associated with Decreased Cd94 (Kp43) in the Chronic Obstructive Pulmonary Disease Airway. *Respirology*. 18(2): p. 369.

484. Wang, J., R.A. Urbanowicz, P.J. Tighe, I. Todd, J.M. Corne and L.C. Fairclough, 2013 Differential Activation of Killer Cells in the Circulation and the Lung: A Study of Current Smoking Status and Chronic Obstructive Pulmonary Disease (Copd). *PLOS ONE*. 8(3): p. e58556.

485. Kondo, S. and K. Abe, 1991 The Effects of Influenza Virus Infection on Fev1 in Asthmatic Children. The Time-Course Study. *Chest*. 100(5): p. 1235.

486. Kucharski, A.J., J. Lessler, J.M. Read, H. Zhu, C.Q. Jiang, Y. Guan, D.A.T. Cummings and S. Riley, 2015 Estimating the Life Course of Influenza a(H3n2) Antibody Responses from Cross-Sectional Data. *PLOS Biology*. 13(3): p. e1002082.

487. Maestre-Batlle, D., O.M. Pena, J.A. Hirota, E. Gunawan, C.F. Rider, D. Sutherland, N.E. Alexis and C. Carlsten, 2017 Novel Flow Cytometry Approach to Identify Bronchial Epithelial Cells from Healthy Human Airways. *Scientific reports*. 7: p. 42214.

488. Eisfeld, A.J., G. Neumann and Y. Kawaoka, 2015 At the Centre: Influenza a Virus Ribonucleoproteins. *Nat Rev Microbiol*. 13(1): p. 28.

489. Kumar, B.V., T.J. Connors and D.L. Farber, 2018 Human T Cell Development, Localization, and Function Throughout Life. *Immunity*. 48(2): p. 202.

490. Wu, N.-H., W. Yang, A. Beineke, R. Dijkman, M. Matrosovich, W. Baumgärtner, V. Thiel, P. Valentin-Weigand, F. Meng and G. Herrler, 2016 The Differentiated Airway Epithelium Infected by Influenza Viruses Maintains the Barrier Function Despite a Dramatic Loss of Ciliated Cells. *Scientific Reports*. 6: p. 39668.

491. Fujimoto, I., J. Pan, T. Takizawa and Y. Nakanishi, 2000 Virus Clearance through Apoptosis-Dependent Phagocytosis of Influenza a Virus-Infected Cells by Macrophages. *J Virol*. 74(7): p. 3399.

492. Lehmann, C., H. Sprenger, M. Nain, M. Bacher and D. Gemsa, 1996 Infection of Macrophages by Influenza a Virus: Characteristics of Tumour Necrosis Factor-Alpha (Tnf Alpha) Gene Expression. *Res Virol*. 147(2-3): p. 123.

493. Hwang, I., J.M. Scott, T. Kakarla, D.M. Duriancik, S. Choi, C. Cho, T. Lee, H. Park, A.R. French, E. Beli, E. Gardner and S. Kim, 2012 Activation Mechanisms of Natural Killer Cells During Influenza Virus Infection. *PLoS One*. 7(12): p. e51858.

494. Madera, S., M. Rapp, M.A. Firth, J.N. Beilke, L.L. Lanier and J.C. Sun, 2016 Type I Ifn Promotes Nk Cell Expansion During Viral Infection by Protecting Nk Cells against Fratricide. *J Exp Med*. 213(2): p. 225.

495. Hossain, M.J., I. Mori, L. Dong, B. Liu and Y. Kimura, 2008 Fetal Calf Serum Inhibits Virus Genome Expression in Madin-Darby Canine Kidney Cells Persistently Infected with Influenza a Virus. *Med Microbiol Immunol*. 197(1): p. 21.

496. de Vries, E., D.M. Tscherne, M.J. Wienholts, V. Cobos-Jiménez, F. Scholte, A. García-Sastre, P.J.M. Rottier and C.A.M. de Haan, 2011 Dissection of the Influenza a Virus Endocytic Routes Reveals Macropinocytosis as an Alternative Entry Pathway. *PLOS Pathogens*. 7(3): p. e1001329.

497. Hufford, M.M., T.S. Kim, J. Sun and T.J. Braciale, 2015 The Effector T Cell Response to Influenza Infection. *Curr Top Microbiol Immunol*. 386: p. 423.

498. Brodin, P., V. Jojic, T. Gao, S. Bhattacharya, Cesar J.L. Angel, D. Furman, S. Shen-Orr, Cornelia L. Dekker, Gary E. Swan, Atul J. Butte, Holden T. Maecker and Mark M. Davis, 2015 Variation in the Human Immune System Is Largely Driven by Non-Heritable Influences. *Cell*. 160(1): p. 37.

499. Alter, G., J.M. Malenfant and M. Altfeld, 2004 Cd107a as a Functional Marker for the Identification of Natural Killer Cell Activity. *J Immunol Methods*. 294(1-2): p. 15.

500. U. Boehm, T. Klamp, a. M. Groot and J.C. Howard, 1997 Cellular Responses to Interferon-Γ. *Annual Review of Immunology*. 15(1): p. 749.

501. Bade, B., H.E. Boettcher, J. Lohrmann, C. Hink-Schauer, K. Bratke, D.E. Jenne, J.J.C. Virchow and W. Luttmann, 2005 Differential Expression of the Granzymes a, K and M and Perforin in Human Peripheral Blood Lymphocytes. *International Immunology*. 17(11): p. 1419.

502. Bratke, K., M. Kuepper, B. Bade, J.C. Virchow, Jr. and W. Luttmann, 2005 Differential Expression of Human Granzymes a, B, and K in Natural Killer Cells and During Cd8+ T Cell Differentiation in Peripheral Blood. *Eur J Immunol*. 35(9): p. 2608.

503. La Gruta, N.L. and S.J. Turner, 2014 T Cell Mediated Immunity to Influenza: Mechanisms of Viral Control. *Trends in Immunology*. 35(8): p. 396.

504. Topham, D.J. and E.C. Reilly, 2018 Tissue-Resident Memory Cd8+ T Cells: From Phenotype to Function. *Frontiers in Immunology*. 9(515).

505. Cheuk, S.*, et al.*, 2017 Cd49a Expression Defines Tissue-Resident Cd8(+) T Cells Poised for Cytotoxic Function in Human Skin. *Immunity*. 46(2): p. 287.

506. Ray, S.J., S.N. Franki, R.H. Pierce, S. Dimitrova, V. Koteliansky, A.G. Sprague, P.C. Doherty, A.R. de Fougerolles and D.J. Topham, 2004 The Collagen Binding Alpha1beta1 Integrin Vla-1 Regulates Cd8 T Cell-Mediated Immune Protection against Heterologous Influenza Infection. *Immunity*. 20(2): p. 167.

507. Chapman, T.J. and D.J. Topham, 2010 Identification of a Unique Population of Tissue-Memory Cd4+ T Cells in the Airways after Influenza Infection That Is Dependent on the Integrin Vla-1. *J Immunol*. 184(7): p. 3841.

508. Richter, M.V. and D.J. Topham, 2007 The Alpha1beta1 Integrin and Tnf Receptor Ii Protect Airway Cd8+ Effector T Cells from Apoptosis During Influenza Infection. *J Immunol*. 179(8): p. 5054.

509. Dustin, M.L. and A.R. de Fougerolles, 2001 Reprograming T Cells: The Role of Extracellular Matrix in Coordination of T Cell Activation and Migration. *Current Opinion in Immunology*. 13(3): p. 286.

510. Colucci, F., J.P. Di Santo and P.J. Leibson, 2002 Natural Killer Cell Activation in Mice and Men: Different Triggers for Similar Weapons? *Nature Immunology*. 3: p. 807.

511. Ludwig, S., S. Pleschka, O. Planz and T. Wolff, 2006 Ringing the Alarm Bells: Signalling and Apoptosis in Influenza Virus Infected Cells. *Cellular Microbiology*. 8(3): p. 375.

512. Swann, J.B., Y. Hayakawa, N. Zerafa, K.C. Sheehan, B. Scott, R.D. Schreiber, P. Hertzog and M.J. Smyth, 2007 Type I Ifn Contributes to Nk Cell Homeostasis, Activation, and Antitumor Function. *J Immunol*. 178(12): p. 7540.

513. Zwirner, N.W. and C.I. Domaica, 2010 Cytokine Regulation of Natural Killer Cell Effector Functions. *Biofactors*. 36(4): p. 274.

514. Vendrame, E., J. Fukuyama, D.M. Strauss-Albee, S. Holmes and C.A. Blish, 2017 Mass Cytometry Analytical Approaches Reveal Cytokine-Induced Changes in Natural Killer Cells. *Cytometry B Clin Cytom*. 92(1): p. 57.

515. Nakamura, K., M. Nakayama, M. Kawano, R. Amagai, T. Ishii, H. Harigae and K. Ogasawara, 2013 Fratricide of Natural Killer Cells Dressed with Tumor-Derived Nkg2d Ligand. *Proc Natl Acad Sci U S A*. 110(23): p. 9421.

516. Batoni, G., S. Esin, F. Favilli, M. Pardini, D. Bottai, G. Maisetta, W. Florio and M. Campa, 2005 Human Cd56bright and Cd56dim Natural Killer Cell Subsets Respond Differentially to Direct Stimulation with Mycobacterium Bovis Bacillus Calmette-Guerin. *Scand J Immunol*. 62(6): p. 498.

517. Kumar, P., A. Nagarajan and P.D. Uchil, 2018 Analysis of Cell Viability by the Lactate Dehydrogenase Assay. *Cold Spring Harb Protoc*. 2018(6): p. pdb.prot095497.

518. Romero, A.I., F.B. Thorén, M. Brune and K. Hellstrand, 2006 Nkp46 and Nkg2d Receptor Expression in Nk Cells with Cd56dim and Cd56bright Phenotype: Regulation by Histamine and Reactive Oxygen Species. *British Journal of Haematology*. 132(1): p. 91.

519. Seidel, U.J., P. Schlegel and P. Lang, 2013 Natural Killer Cell Mediated Antibody-Dependent Cellular Cytotoxicity in Tumor Immunotherapy with Therapeutic Antibodies. *Front Immunol*. 4: p. 76.

520. Fauriat, C., E.O. Long, H.-G. Ljunggren and Y.T. Bryceson, 2010 Regulation of Human Nk-Cell Cytokine and Chemokine Production by Target Cell Recognition. *Blood*. 115(11): p. 2167.

521. Lunding, L., C. Vock, S. Webering, J. Behrends, C. Hölscher, H. Fehrenbach and M. Wegmann, 2016 The Role of Il-17 Producing Nk Cells and Other Innate Immune Cells in Poly(I:C) Triggered Exacerbation of Experimental Asthma. *European Respiratory Journal*. 48(suppl 60).

522. Vilches, C. and P. Parham, 2002 Kir: Diverse, Rapidly Evolving Receptors of Innate and Adaptive Immunity. *Annual Review of Immunology*. 20(1): p. 217.

523. Ohradanova-Repic, A., C. Machacek, M.B. Fischer and H. Stockinger, 2016 Differentiation of Human Monocytes and Derived Subsets of Macrophages and Dendritic Cells by the Hlda10 Monoclonal Antibody Panel. *Clinical & translational immunology*. 5(1): p. e55.

524. Lacey, D.C., A. Achuthan, A.J. Fleetwood, H. Dinh, J. Roiniotis, G.M. Scholz, M.W. Chang, S.K. Beckman, A.D. Cook and J.A. Hamilton, 2012 Defining Gm-Csf– and Macrophage-Csf–Dependent Macrophage Responses by in Vitro Models. *The Journal of Immunology*. 188(11): p. 5752.

525. Xue, J.*, et al.*, 2014 Transcriptome-Based Network Analysis Reveals a Spectrum Model of Human Macrophage Activation. *Immunity*. 40(2): p. 274.

526. Lescoat, A., A. Ballerie, Y. Augagneur, C. Morzadec, L. Vernhet, O. Fardel, P. Jego, S. Jouneau and V. Lecureur, 2018 Distinct Properties of Human M-Csf and Gm-Csf Monocyte-Derived Macrophages to Simulate Pathological Lung Conditions in Vitro: Application to Systemic and Inflammatory Disorders with Pulmonary Involvement. *Int J Mol Sci*. 19(3).

527. Martinez-Moczygemba, M. and D.P. Huston, 2010 Immune Dysregulation in the Pathogenesis of Pulmonary Alveolar Proteinosis. *Curr Allergy Asthma Rep*. 10(5): p. 320.

528. Souza-Fonseca-Guimaraes, F., A. Young and M.J. Smyth, 2015 Ifn Type Iii: In Vivo Nk Cell Response. *Oncotarget*. 6(24): p. 19960.

529. Ganal, S.C., S.L. Sanos, C. Kallfass, K. Oberle, C. Johner, C. Kirschning, S. Lienenklaus, S. Weiss, P. Staeheli, P. Aichele and A. Diefenbach, 2012 Priming of Natural Killer Cells by Nonmucosal Mononuclear Phagocytes Requires Instructive Signals from Commensal Microbiota. *Immunity*. 37(1): p. 171.

530. Björkström, N.K., P. Riese, F. Heuts, S. Andersson, C. Fauriat, M.A. Ivarsson, A.T. Björklund, M. Flodström-Tullberg, J. Michaëlsson, M.E. Rottenberg, C.A. Guzmán, H.-G. Ljunggren and K.-J. Malmberg, 2010 Expression Patterns of Nkg2a, Kir, and Cd57 Define a Process of $Cd56^{dim}$ Nk Cell Differentiation Uncoupled from Nk Cell Education. *Blood*.

531. Lisovsky, I., G. Isitman, J. Bruneau and N.F. Bernard, 2015 Functional Analysis of Nk Cell Subsets Activated by 721.221 and K562 Hla-Null Cells. *J Leukoc Biol*. 97(4): p. 761.

532. Oyer, J.L., R.Y. Igarashi, A.R. Kulikowski, D.A. Colosimo, M.M. Solh, A. Zakari, Y.A. Khaled, D.A. Altomare and A.J. Copik, 2015 Generation of Highly Cytotoxic Natural Killer Cells for Treatment of Acute Myelogenous Leukemia Using a Feeder-Free, Particle-Based Approach. *Biology of Blood and Marrow Transplantation*. 21(4): p. 632.

533. Nagel, J.E., G.D. Collins and W.H. Adler, 1981 Spontaneous or Natural Killer Cytotoxicity of K562 Erythroleukemic Cells in Normal Patients. *Cancer Res*. 41(6): p. 2284.

534. Holtzman, M.J., D.E. Byers, J. Alexander-Brett and X. Wang, 2014 The Role of Airway Epithelial Cells and Innate Immune Cells in Chronic Respiratory Disease. *Nature reviews. Immunology*. 14(10): p. 686.

535. Nowarski, R., R. Jackson and R.A. Flavell, 2017 The Stromal Intervention: Regulation of Immunity and Inflammation at the Epithelial-Mesenchymal Barrier. *Cell*. 168(3): p. 362.

536. Reefman, E., J.G. Kay, S.M. Wood, C. Offenhauser, D.L. Brown, S. Roy, A.C. Stanley, P.C. Low, A.P. Manderson and J.L. Stow, 2010 Cytokine Secretion Is Distinct from Secretion of Cytotoxic Granules in Nk Cells. *J Immunol*. 184(9): p. 4852.

537. Long, B.R., J. Michaelsson, C.P. Loo, W.M. Ballan, B.A. Vu, F.M. Hecht, L.L. Lanier, J.M. Chapman and D.F. Nixon, 2008 Elevated Frequency of Gamma Interferon-Producing Nk Cells in Healthy Adults Vaccinated against Influenza Virus. *Clin Vaccine Immunol*. 15(1): p. 120.

538. Fotakis, G. and J.A. Timbrell, 2006 In Vitro Cytotoxicity Assays: Comparison of Ldh, Neutral Red, Mtt and Protein Assay in Hepatoma Cell Lines Following Exposure to Cadmium Chloride. *Toxicol Lett*. 160(2): p. 171.

539. Manerba, M., L. Di Ianni, M. Govoni, A. Comparone and G. Di Stefano, 2018 The Activation of Lactate Dehydrogenase Induced by Mtor Drives Neoplastic Change in Breast Epithelial Cells. *PLoS One*. 13(8): p. e0202588.

540. Darzynkiewicz, Z., D. Galkowski and H. Zhao, 2008 Analysis of Apoptosis by Cytometry Using Tunel Assay. *Methods (San Diego, Calif.)*. 44(3): p. 250.

541. Elmore, S., 2007 Apoptosis: A Review of Programmed Cell Death. *Toxicologic pathology*. 35(4): p. 495.

542. Raulet, D.H., S. Gasser, B.G. Gowen, W. Deng and H. Jung, 2013 Regulation of Ligands for the Nkg2d Activating Receptor. *Annu Rev Immunol*. 31: p. 413.

543. Jost, S., H. Quillay, J. Reardon, E. Peterson, R.P. Simmons, B.A. Parry, N.N.P. Bryant, W.D. Binder and M. Altfeld, 2011 Changes in Cytokine Levels and Nk Cell Activation Associated with Influenza. *PLoS ONE*. 6(9): p. e25060.

544. Motz, G.T., B.L. Eppert, B.W. Wortham, R.M. Amos-Kroohs, J.L. Flury, S.C. Wesselkamper and M.T. Borchers, 2010 Chronic Cigarette Smoke Exposure Primes Nk Cell Activation in a Mouse Model of Chronic Obstructive Pulmonary Disease. *J Immunol*. 184(8): p. 4460.

545. Barnes, P.D. and J.E. Grundy, 1992 Down-Regulation of the Class I Hla Heterodimer and Beta 2-Microglobulin on the Surface of Cells Infected with Cytomegalovirus. *J Gen Virol*. 73 (Pt 9): p. 2395.

546. Ende, Z., M.J. Deymier, D.T. Claiborne, J.L. Prince, D.C. Monaco, W. Kilembe, S.A. Allen and E. Hunter, 2018 Hla Class I Downregulation by Hiv-1 Variants from Subtype C Transmission Pairs. *J Virol*.

547. Petersen, J.L., C.R. Morris and J.C. Solheim, 2003 Virus Evasion of Mhc Class I Molecule Presentation. *The Journal of Immunology*. 171(9): p. 4473.

548. Cohen, G.B., R.T. Gandhi, D.M. Davis, O. Mandelboim, B.K. Chen, J.L. Strominger and D. Baltimore, 1999 The Selective Downregulation of Class I Major Histocompatibility Complex Proteins by Hiv-1 Protects Hiv-Infected Cells from Nk Cells. *Immunity*. 10(6): p. 661.

549. Hill, A., P. Jugovic, I. York, G. Russ, J. Bennink, J. Yewdell, H. Ploegh and D. Johnson, 1995 Herpes Simplex Virus Turns Off the Tap to Evade Host Immunity. *Nature*. 375(6530): p. 411.

550. Lin, A., H. Xu and W. Yan, 2007 Modulation of Hla Expression in Human Cytomegalovirus Immune Evasion. *Cell Mol Immunol*. 4(2): p. 91.

551. Glasner, A., E. Oiknine-Djian, Y. Weisblum, M. Diab, A. Panet, D.G. Wolf and O. Mandelboim, 2017 Zika Virus Escapes Nk Cell Detection by Upregulating Major Histocompatibility Complex Class I Molecules. *J Virol*. 91(22).

552. Sakabe, S., K. Iwatsuki-Horimoto, R. Takano, C.A. Nidom, M.t.Q. Le, T. Nagamura-Inoue, T. Horimoto, N. Yamashita and Y. Kawaoka, 2011 Cytokine Production by Primary Human Macrophages Infected with Highly Pathogenic H5n1 or Pandemic H1n1 2009 Influenza Viruses. *The Journal of general virology*. 92(Pt 6): p. 1428.

553. Yu, X., X. Zhang, B. Zhao, J. Wang, Z. Zhu, Z. Teng, J. Shao, J. Shen, Y. Gao, Z. Yuan and F. Wu, 2011 Intensive Cytokine Induction in Pandemic H1n1 Influenza Virus Infection Accompanied by Robust Production of Il-10 and Il-6. *PLOS ONE*. 6(12): p. e28680.

554. Hansson, M., E. Silverpil, A. Linden and P. Glader, 2013 Interleukin-22 Produced by Alveolar Macrophages During Activation of the Innate Immune Response. *Inflamm Res*. 62(6): p. 561.

555. Mack, E.A., L.E. Kallal, D.A. Demers and C.A. Biron, 2011 Type 1 Interferon Induction of Natural Killer Cell Gamma Interferon Production for Defense During Lymphocytic Choriomeningitis Virus Infection. *mBio*. 2(4).

556. Rojas, J.M., M. Avia, V. Martín and N. Sevilla, 2017 Il-10: A Multifunctional Cytokine in Viral Infections. *Journal of immunology research*. 2017: p. 6104054.

557. Herold, S., K. Mayer and J. Lohmeyer, 2011 Acute Lung Injury: How Macrophages Orchestrate Resolution of Inflammation and Tissue Repair. *Frontiers in immunology*. 2: p. 65.

558. De Serres, G., N. Lampron, J. La Forge, I. Rouleau, J. Bourbeau, K. Weiss, B. Barret and G. Boivin, 2009 Importance of Viral and Bacterial Infections in Chronic Obstructive Pulmonary Disease Exacerbations. *J Clin Virol*. 46(2): p. 129.

559. Sawant, K.V., R. Xu, R. Cox, H. Hawkins, E. Sbrana, D. Kolli, R.P. Garofalo and K. Rajarathnam, 2015 Chemokine Cxcl1-Mediated Neutrophil Trafficking in the Lung: Role of Cxcr2 Activation. *Journal of innate immunity*. 7(6): p. 647.

560. Liu, Y., Y. Cai, L. Liu, Y. Wu and X. Xiong, 2018 Crucial Biological Functions of Ccl7 in Cancer. *PeerJ*. 6: p. e4928.

561. Lei, Y. and Y. Takahama, 2012 Xcl1 and Xcr1 in the Immune System. *Microbes and Infection*. 14(3): p. 262.

562. Deshmane, S.L., S. Kremlev, S. Amini and B.E. Sawaya, 2009 Monocyte Chemoattractant Protein-1 (Mcp-1): An Overview. *Journal of interferon & cytokine research : the official journal of the International Society for Interferon and Cytokine Research*. 29(6): p. 313.

563. Bernardini, G., F. Antonangeli, V. Bonanni and A. Santoni, 2016 Dysregulation of Chemokine/Chemokine Receptor Axes and Nk Cell Tissue Localization During Diseases. *Frontiers in immunology*. 7: p. 402.

564. Yamashita, U. and E. Kuroda, 2002 Regulation of Macrophage-Derived Chemokine (Mdc, Ccl22) Production. *Crit Rev Immunol*. 22(2): p. 105.

565. Berger, A., 2000 Th1 and Th2 Responses: What Are They? *BMJ (Clinical research ed.)*. 321(7258): p. 424.

566. Hoves, S., V.R. Sutton, N.M. Haynes, E.D. Hawkins, D. Fernández Ruiz, N. Baschuk, K.A. Sedelies, M. Schnurr, J. Stagg, D.M. Andrews, J.A. Villadangos and J.A. Trapani, 2011 A Critical Role for Granzymes in Antigen Cross-Presentation through Regulating Phagocytosis of Killed Tumor Cells. *The Journal of Immunology*. 187(3): p. 1166.

567. Julkunen, I., K. Melén, M. Nyqvist, J. Pirhonen, T. Sareneva and S. Matikainen, 2000 Inflammatory Responses in Influenza a Virus Infection. *Vaccine*. 19: p. S32.

568. Culley, F.J., 2009 Natural Killer Cells in Infection and Inflammation of the Lung. *Immunology*. 128(2): p. 151.

569. Nielsen, C.M., M.J. White, M.R. Goodier and E.M. Riley, 2013 Functional Significance of Cd57 Expression on Human Nk Cells and Relevance to Disease. *Front Immunol*. 4.

570. Serafini, N., C.A.J. Vosshenrich and J.P. Di Santo, 2015 Transcriptional Regulation of Innate Lymphoid Cell Fate. *Nat Rev Immunol*. 15(7): p. 415.

571. Jiao, Y., N.D. Huntington, G.T. Belz and C. Seillet, 2016 Type 1 Innate Lymphoid Cell Biology: Lessons Learnt from Natural Killer Cells. *Frontiers in immunology*. 7: p. 426.

572. Colonna, M., 2018 Innate Lymphoid Cells: Diversity, Plasticity, and Unique Functions in Immunity. *Immunity*. 48(6): p. 1104.

573. Gao, Y*., et al.*, 2017 Tumor Immunoevasion by the Conversion of Effector Nk Cells into Type 1 Innate Lymphoid Cells. *Nat Immunol*. 18(9): p. 1004.

574. Cortez, V.S., T.K. Ulland, L. Cervantes-Barragan, J.K. Bando, M.L. Robinette, Q. Wang, A.J. White, S. Gilfillan, M. Cella and M. Colonna, 2017 Smad4 Impedes the Conversion of Nk Cells into Ilc1-Like Cells by Curtailing Non-Canonical Tgf-Beta Signaling. *Nat Immunol*. 18(9): p. 995.

575. Frucht, D.M., T. Fukao, C. Bogdan, H. Schindler, J.J. O'Shea and S. Koyasu, 2001 Ifn-Γ Production by Antigen-Presenting Cells: Mechanisms Emerge. *Trends in Immunology*. 22(10): p. 556.

576. Bao, Y., X. Liu, C. Han, S. Xu, B. Xie, Q. Zhang, Y. Gu, J. Hou, L. Qian, C. Qian, H. Han and X. Cao, 2014 Identification of Ifn-Γ-Producing Innate B Cells. *Cell research*. 24(2): p. 161.

577. Tanaka, T., M. Narazaki and T. Kishimoto, 2014 Il-6 in Inflammation, Immunity, and Disease. *Cold Spring Harbor perspectives in biology*. 6(10): p. a016295.

578. Kalliolias, G.D. and L.B. Ivashkiv, 2015 Tnf Biology, Pathogenic Mechanisms and Emerging Therapeutic Strategies. *Nature Reviews Rheumatology*. 12: p. 49.

579. Richmond, J., M. Tuzova, W. Cruikshank and D. Center, 2014 Regulation of Cellular Processes by Interleukin-16 in Homeostasis and Cancer. *J Cell Physiol*. 229(2): p. 139.

580. Owen, R.E., E. Yamada, C.I. Thompson, L.J. Phillipson, C. Thompson, E. Taylor, M. Zambon, H.M.I. Osborn, W.S. Barclay and P. Borrow, 2007 Alterations in Receptor Binding Properties

of Recent Human Influenza H3n2 Viruses Are Associated with Reduced Natural Killer Cell Lysis of Infected Cells. *Journal of virology*. 81(20): p. 11170.

581. Mwimanzi, P., T.J. Markle, T. Ueno and M.A. Brockman, 2012 Human Leukocyte Antigen (Hla) Class I Down-Regulation by Human Immunodeficiency Virus Type 1 Negative Factor (Hiv-1 Nef): What Might We Learn from Natural Sequence Variants? *Viruses*. 4(9): p. 1711.

582. Voskarides, K., E. Christaki and G.K. Nikolopoulos, 2018 Influenza Virus-Host Co-Evolution. A Predator-Prey Relationship? *Frontiers in immunology*. 9: p. 2017.

583. Passos, S.T., J.S. Silver, A.C. O'Hara, D. Sehy, J.S. Stumhofer and C.A. Hunter, 2010 Il-6 Promotes Nk Cell Production of Il-17 During Toxoplasmosis. *Journal of immunology (Baltimore, Md. : 1950)*. 184(4): p. 1776.

584. Ochoa, A.C., G. Gromo, B.J. Alter, P.M. Sondel and F.H. Bach, 1987 Long-Term Growth of Lymphokine-Activated Killer (Lak) Cells: Role of Anti-Cd3, Beta-Il 1, Interferon-Gamma and -Beta. *The Journal of Immunology*. 138(8): p. 2728.

585. Cai, G., R.A. Kastelein and C.A. Hunter, 1999 Il-10 Enhances Nk Cell Proliferation, Cytotoxicity and Production of Ifn-Γ When Combined with Il-18. *European Journal of Immunology*. 29(9): p. 2658.

586. D'Andrea, A., M. Aste-Amezaga, N.M. Valiante, X. Ma, M. Kubin and G. Trinchieri, 1993 Interleukin 10 (Il-10) Inhibits Human Lymphocyte Interferon Gamma-Production by Suppressing Natural Killer Cell Stimulatory Factor/Il-12 Synthesis in Accessory Cells. *The Journal of Experimental Medicine*. 178(3): p. 1041.

587. Peiris, J.S.M., K.P.Y. Hui and H.-L. Yen, 2010 Host Response to Influenza Virus: Protection Versus Immunopathology. *Current Opinion in Immunology*. 22(4): p. 475.

588. Du, N., J. Zhou, X. Lin, Y. Zhang, X. Yang, Y. Wang and Y. Shu, 2010 Differential Activation of Nk Cells by Influenza a Pseudotype H5n1 and 1918 and 2009 Pandemic H1n1 Viruses. *J Virol*. 84(15): p. 7822.

589. Draghi, A., 2nd, J. Bebak, V.L. Popov, A.C. Noble, S.J. Geary, A.B. West, P. Byrne and S. Frasca, Jr., 2007 Characterization of a Neochlamydia-Like Bacterium Associated with Epitheliocystis in Cultured Arctic Charr Salvelinus Alpinus. *Dis Aquat Organ*. 76(1): p. 27.

590. Ni, J., O. Holsken, M. Miller, Q. Hammer, M. Luetke-Eversloh, C. Romagnani and A. Cerwenka, 2016 Adoptively Transferred Natural Killer Cells Maintain Long-Term Antitumor

Activity by Epigenetic Imprinting and Cd4(+) T Cell Help. *Oncoimmunology*. 5(9): p. e1219009.

591. Luetke-Eversloh, M., Q. Hammer, P. Durek, K. Nordstrom, G. Gasparoni, M. Pink, A. Hamann, J. Walter, H.D. Chang, J. Dong and C. Romagnani, 2014 Human Cytomegalovirus Drives Epigenetic Imprinting of the Ifng Locus in Nkg2chi Natural Killer Cells. *PLoS Pathog*. 10(10): p. e1004441.

592. Kapellos, T.S., K. Bassler, A.C. Aschenbrenner, W. Fujii and J.L. Schultze, 2018 Dysregulated Functions of Lung Macrophage Populations in Copd. *J Immunol Res*. 2018: p. 2349045.

593. Sethi, S., 2010 Infection as a Comorbidity of Copd. *European Respiratory Journal*. 35(6): p. 1209.

594. Radigan, K.A., A.V. Misharin, M. Chi and G.S. Budinger, 2015 Modeling Human Influenza Infection in the Laboratory. *Infection and drug resistance*. 8: p. 311.

595. Shin, D.-L., B. Hatesuer, S. Bergmann, T. Nedelko and K. Schughart, 2015 Protection from Severe Influenza Virus Infections in Mice Carrying the Mx1 Influenza Virus Resistance Gene Strongly Depends on Genetic Background. *Journal of virology*. 89(19): p. 9998.

596. Sica, A. and A. Mantovani, 2012 Macrophage Plasticity and Polarization: In Vivo Veritas. *J Clin Invest*. 122(3): p. 787.

597. Li, F., H. Zhu, R. Sun, H. Wei and Z. Tian, 2012 Natural Killer Cells Are Involved in Acute Lung Immune Injury Caused by Respiratory Syncytial Virus Infection. *Journal of Virology*. 86(4): p. 2251.

598. Jayaraman, A*., et al.*, 2014 Il-15 Complexes Induce Nk- and T-Cell Responses Independent of Type I Ifn Signaling During Rhinovirus Infection. *Mucosal Immunol*. 7(5): p. 1151.

599. Roman, M., W.J. Calhoun, K.L. Hinton, L.F. Avendano, V. Simon, A.M. Escobar, A. Gaggero and P.V. Diaz, 1997 Respiratory Syncytial Virus Infection in Infants Is Associated with Predominant Th-2-Like Response. *Am J Respir Crit Care Med*. 156(1): p. 190.

600. McManus, T.E., A.-M. Marley, N. Baxter, S.N. Christie, H.J. O'Neill, J.S. Elborn, P.V. Coyle and J.C. Kidney, 2008 Respiratory Viral Infection in Exacerbations of Copd. *Respiratory Medicine*. 102(11): p. 1575.

601. Rakes, G.P., E. Arruda, J.M. Ingram, G.E. Hoover, J.C. Zambrano, F.G. Hayden, T.A.E. Platts-Mills and P.W. Heymann, 1999 Rhinovirus and Respiratory Syncytial Virus in Wheezing Children Requiring Emergency Care. *American Journal of Respiratory and Critical Care Medicine*. 159(3): p. 785.

602. Osur, S.L., 2002 Viral Respiratory Infections in Association with Asthma and Sinusitis: A Review. *Annals of Allergy, Asthma & Immunology*. 89(6): p. 553.

603. Louie, J.K., A. Roy-Burman, L. Guardia-LaBar, E.J. Boston, D. Kiang, T. Padilla, S. Yagi, S. Messenger, A.M. Petru, C.A. Glaser and D.P. Schnurr, 2009 Rhinovirus Associated with Severe Lower Respiratory Tract Infections in Children. *The Pediatric Infectious Disease Journal*. 28(4): p. 337.

604. Gorska, M.M., 2017 Natural Killer Cells in Asthma. *Current opinion in allergy and clinical immunology*. 17(1): p. 50.